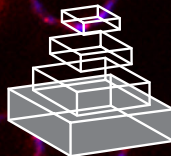


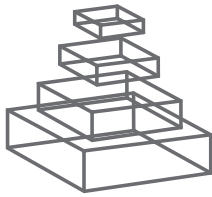
# frontiers RESEARCH TOPICS

AUTOPHAGY IN PLANTS AND  
ALGAE

Topic Editors  
Diane C. Bassham and Jose L. Crespo



frontiers in  
**PLANT SCIENCE**



## FRONTIERS COPYRIGHT STATEMENT

© Copyright 2007-2015  
Frontiers Media SA.  
All rights reserved.

All content included on this site, such as text, graphics, logos, button icons, images, video/audio clips, downloads, data compilations and software, is the property of or is licensed to Frontiers Media SA ("Frontiers") or its licensees and/or subcontractors. The copyright in the text of individual articles is the property of their respective authors, subject to a license granted to Frontiers.

The compilation of articles constituting this e-book, wherever published, as well as the compilation of all other content on this site, is the exclusive property of Frontiers. For the conditions for downloading and copying of e-books from Frontiers' website, please see the Terms for Website Use. If purchasing Frontiers e-books from other websites or sources, the conditions of the website concerned apply.

Images and graphics not forming part of user-contributed materials may not be downloaded or copied without permission.

Individual articles may be downloaded and reproduced in accordance with the principles of the CC-BY licence subject to any copyright or other notices. They may not be re-sold as an e-book.

As author or other contributor you grant a CC-BY licence to others to reproduce your articles, including any graphics and third-party materials supplied by you, in accordance with the Conditions for Website Use and subject to any copyright notices which you include in connection with your articles and materials.

All copyright, and all rights therein, are protected by national and international copyright laws.

The above represents a summary only. For the full conditions see the Conditions for Authors and the Conditions for Website Use.

**ISSN** 1664-8714

**ISBN** 978-2-88919-477-3

**DOI** 10.3389/978-2-88919-477-3

## ABOUT FRONTIERS

Frontiers is more than just an open-access publisher of scholarly articles: it is a pioneering approach to the world of academia, radically improving the way scholarly research is managed. The grand vision of Frontiers is a world where all people have an equal opportunity to seek, share and generate knowledge. Frontiers provides immediate and permanent online open access to all its publications, but this alone is not enough to realize our grand goals.

## FRONTIERS JOURNAL SERIES

The Frontiers Journal Series is a multi-tier and interdisciplinary set of open-access, online journals, promising a paradigm shift from the current review, selection and dissemination processes in academic publishing.

All Frontiers journals are driven by researchers for researchers; therefore, they constitute a service to the scholarly community. At the same time, the Frontiers Journal Series operates on a revolutionary invention, the tiered publishing system, initially addressing specific communities of scholars, and gradually climbing up to broader public understanding, thus serving the interests of the lay society, too.

## DEDICATION TO QUALITY

Each Frontiers article is a landmark of the highest quality, thanks to genuinely collaborative interactions between authors and review editors, who include some of the world's best academicians. Research must be certified by peers before entering a stream of knowledge that may eventually reach the public - and shape society; therefore, Frontiers only applies the most rigorous and unbiased reviews.

Frontiers revolutionizes research publishing by freely delivering the most outstanding research, evaluated with no bias from both the academic and social point of view.

By applying the most advanced information technologies, Frontiers is catapulting scholarly publishing into a new generation.

## WHAT ARE FRONTIERS RESEARCH TOPICS?

Frontiers Research Topics are very popular trademarks of the Frontiers Journals Series: they are collections of at least ten articles, all centered on a particular subject. With their unique mix of varied contributions from Original Research to Review Articles, Frontiers Research Topics unify the most influential researchers, the latest key findings and historical advances in a hot research area!

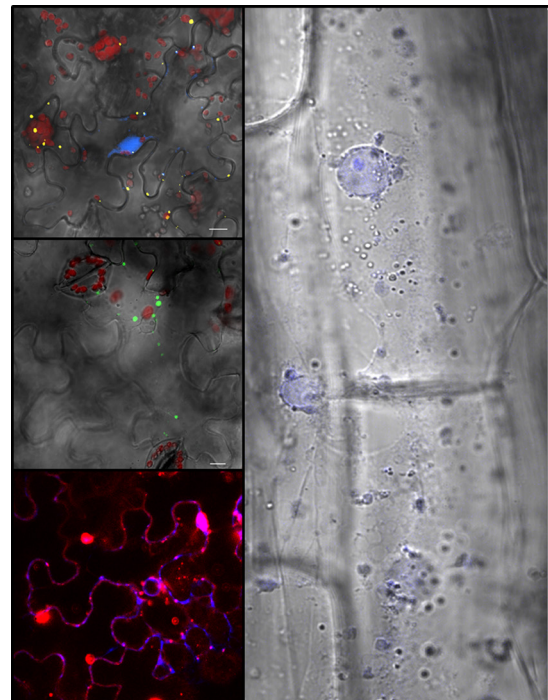
Find out more on how to host your own Frontiers Research Topic or contribute to one as an author by contacting the Frontiers Editorial Office: [researchtopics@frontiersin.org](mailto:researchtopics@frontiersin.org)

# AUTOPHAGY IN PLANTS AND ALGAE

Topic Editors:

**Diane C. Bassham**, Iowa State University, USA

**Jose L. Crespo**, Consejo Superior de Investigaciones Científicas (CSIC), Spain



Description of the cover photos (by dr. Katarzyna Zientara-Rytter)

**Left upper:** Co-localization (white spots) of transiently expressed Joka2-YFP (yellow) and CFP-Atg8f (blue) in epidermal cells of *Nicotiana benthamiana* leaves. Chloroplasts are seen in red. Note CFP-Atg8f is present also in the nucleus. **Left middle:** Bimolecular fluorescent complementation of nYFP-Atg8h2 and Joka2-cYFP (green spots) in epidermal cells of *N. benthamiana* leaves. Chloroplasts are seen in red. **Left lower:** Subcellular localization of transiently expressed RFP-Joka2 (red) and the tonoplast marker based on aquaporin of the vacuolar membrane (gammaTIP-CFP) in epidermal cells of *N. benthamiana* leaves. **Right:** Subcellular localization of Joka2 (blue) in endodermal cells of transgenic tobacco expressing Joka2-CFP.

Autophagy (also known as macroautophagy) is an evolutionarily conserved process by which cytoplasmic components are nonselectively enclosed within a double-membrane vesicle known as the autophagosome and delivered to the vacuole for degradation of toxic components and recycling of needed nutrients. This catabolic process is required for the adequate adaptation and response of the cell, and correspondingly the whole organism, to different types of stress including nutrient starvation or oxidative damage. Autophagy has been extensively investigated in yeasts and mammals but the identification of autophagy-related (ATG) genes in plant and algal genomes together with the characterization of autophagy-deficient mutants in plants have revealed that this process is structurally and functionally conserved in photosynthetic eukaryotes. Recent studies have demonstrated that autophagy is active at a basal level under normal growth in plants and is upregulated during senescence and in response to nutrient limitation, oxidative stress, salt and drought conditions and pathogen attack.

Autophagy was initially considered as a non-selective pathway, but numerous observations mainly obtained in yeasts revealed that autophagy can also selectively eliminate specific proteins, protein complexes and organelles. Interestingly, several types of selective autophagy appear to be also conserved in plants, and the degradation of protein aggregates through specific adaptors or the delivery of chloroplast material to the vacuole via autophagy has been reported.

This research topic aims to gather recent progress on different aspects of autophagy in plants and algae. We welcome all types of articles including original research, methods, opinions and reviews that provide new insights about the autophagy process and its regulation.

# Table of Contents

- 05 Autophagy in Plants and Algae**  
Diane C. Bassham and Jose L. Crespo
- 07 Significant Role of PB1 and UBA Domains in Multimerization of Joka2, a Selective Autophagy Cargo Receptor from Tobacco**  
Katarzyna Zientara-Rytter and Agnieszka Sirko
- 20 Role and Regulation of Autophagy in Heat Stress Responses of Tomato Plants**  
Jie Zhou, Jian Wang, Jing-Quan Yu and Zhixiang Chen
- 32 Monitoring Protein Turnover During Phosphate Starvation-Dependent Autophagic Degradation Using a Photoconvertible Fluorescent Protein Aggregate in Tobacco BY-2 Cells**  
Maiko Tasaki, Satoru Asatsuma and Ken Matsuoka
- 41 Degradation of Plant Peroxisomes by Autophagy**  
Han Nim Lee, Jimi Kim and Taijoon Chung
- 45 Plant Peroxisomes are Degraded by Starvation-Induced and Constitutive Autophagy in Tobacco BY-2 Suspension Cultured-Cells**  
Olga V. Voitsekhoukaja, Andreas Schiermeyer and Sigrun Reumann
- 59 The Emerging Role of Autophagy in Peroxisome Dynamics and Lipid Metabolism of Phyllosphere Microorganisms**  
Masahide Oku, Yoshitaka Takano and Yasuyoshi Sakai
- 63 Involvement of Autophagy in the Direct ER to Vacuole Protein Trafficking Route in Plants**  
Simon Michaeli, Tamar Avin-Wittenberg and Gad Galili
- 68 Selective Autophagy of Non-Ubiquitylated Targets in Plants: Looking for Cognate Receptor/Adaptor Proteins**  
Vasko Veljanovski and Henri Batoko
- 74 When RNA and Protein Degradation Pathways Meet**  
Benoît Derrien and Pascal Genschik
- 80 Autophagy-Like Processes are Involved in Lipid Droplet Degradation in *Auxenochlorella Protothecoides* During the Heterotrophy-Autotrophy Transition**  
Li Zhao, Junbiao Dai and Qingyu Wu
- 92 Roles of Autophagy in Male Reproductive Development in Plants**  
Shigeru Hanamata, Takamitsu Kurusu and Kazuyuki Kuchitsu
- 98 Functions of Autophagy in Plant Carbon and Nitrogen Metabolism**  
Chenxia Ren, Jingfang Liu and Qingqiu Gong



# Autophagy in plants and algae

Diane C. Bassham<sup>1\*</sup> and Jose L. Crespo<sup>2\*</sup>

<sup>1</sup> Department of Genetics, Development and Cell Biology, Iowa State University, Ames, IA, USA

<sup>2</sup> Instituto de Bioquímica Vegetal y Fotosíntesis, Consejo Superior de Investigaciones Científicas-Universidad de Sevilla, Seville, Spain

\*Correspondence: bassham@iastate.edu; crespo@ibvf.csic.es

**Edited and reviewed by:**

Simon Gilroy, University of Wisconsin - Madison, USA

**Keywords:** selective autophagy, lipid degradation, plants, algae, pexophagy

Autophagy is a major cellular degradation pathway in which materials are delivered to the vacuole in double-membrane vesicles known as autophagosomes, broken down, and recycled (Li and Vierstra, 2012; Liu and Bassham, 2012). In photosynthetic organisms, the pathway is strongly activated by biotic and abiotic stresses, including nutrient limitation, oxidative, salt and drought stress and pathogen infection, and during senescence (Perez-Perez et al., 2012; Lv et al., 2014). Mutation of genes required for autophagy causes hypersensitivity to stress, indicating that autophagy is important for tolerance of multiple stresses. While autophagy is often non-selective, a growing number of examples of selectivity are now evident, in which specific cargos are recruited into autophagosomes via cargo receptors (Floyd et al., 2012; Li and Vierstra, 2012). In this Research Topic, a series of original research articles and reviews highlight areas of current focus in plant and algal autophagy research, including mechanisms and cargos of selective autophagy, lipid degradation, and metabolic and physiological consequences of the autophagy pathway.

Several contributions to the Research Topic address the emerging concept of selective autophagy, well established in animal cells but only described recently in plants. Zientara-Rytter and Sirko (2014) in a research article follow up on previous work describing a potential selective autophagy receptor in tobacco, Joka2, identified as possibly functioning in responses to sulfur deficiency (Zientara-Rytter et al., 2011). They perform a functional analysis of protein domains within Joka2, identifying domains responsible for homodimerization and for the sequestration of cargo, tagged with ubiquitin, into aggregates within the cytoplasm. Zhou et al. (2014) address a potential function of the tomato Joka2 homolog, NBR1, in heat stress. They demonstrate that heat stress in tomato leads to activation of autophagy and that silencing of the core autophagy machinery, or of NBR1, leads to hypersensitivity to heat stress. In addition, silencing of tomato WRKY33 transcription factors causes heat sensitivity and reduced autophagy, suggesting that WRKY33 proteins are involved in the regulation of autophagy under these conditions. A likely cargo for Joka2/NBR1 is cytoplasmic protein aggregates, and Tasaki et al. (2014) describe a novel method for monitoring protein aggregate turnover by autophagy. They generate a fusion protein, Cyt b5-KikGR, which forms cytoplasmic aggregates and contains a photoconvertible fluorescent protein. Upon starvation of tobacco suspension cells for sucrose, phosphate, or nitrogen, the fluorescence is seen inside the vacuole after transfer of the aggregates

by autophagy. Illumination of the aggregates with purple light converts the green fluorescence to red, enabling the authors to track autophagic transport of pre-existing vs. newly synthesized protein, thus allowing an assessment of autophagic flux.

Articles also discuss the selective autophagy of cellular organelles. Lee et al. (2014) review recent progress in the understanding of plant pexophagy, the selective degradation of peroxisomes by autophagy. Peroxisomal proteins are degraded in the developmental transition from glyoxysomes in seedlings to leaf peroxisomes and also as a quality control mechanism. Several groups have now demonstrated that this occurs by autophagy. The pathway for degradation of peroxisomes in tobacco suspension cells, both during sucrose starvation and under normal growth conditions, is described in a research article by Voitsekhoukaja et al. (2014). They demonstrate that peroxisomes are degraded in the vacuole by a mechanism that is sensitive to the autophagy inhibitor 3-methyladenine, suggesting a pexophagy pathway. Oku et al. (2014) describe interesting recent examples of pexophagy in plant-associated microorganisms, including a phytopathogenic fungus in which pexophagy is required for infection and a methylotrophic yeast residing on plant leaves, in which pexophagy is required for growth. Michaeli et al. (2014) review direct ER-to-vacuole transport pathways, including the transport of seed storage proteins and cysteine proteases by autophagy-related mechanisms. They discuss the recently identified ATI1 and 2 proteins, which bind to the autophagosome protein ATG8, are found in the endoplasmic reticulum under normal conditions, and are transported to the vacuole during starvation, features consistent with a selective autophagy mechanism. A review by Veljanovski and Batoko (2014) describes the potential selective autophagy of mitochondria, peroxisomes and endoplasmic reticulum.

Veljanovski and Batoko (2014) also discuss the mechanism by which individual proteins and other molecules can be degraded by autophagy. TSPO is a protein that can scavenge free heme, preventing its accumulation to toxic levels. TSPO binds to heme and causes its incorporation into autophagosomes, leading to vacuole delivery by autophagy. Another example that has recently come to light is the degradation of RNA silencing components by autophagy, discussed by Derrien and Genschik (2014). This pathway was originally discovered in the context of viral infection, but also occurs in mutants that are defective in RISC assembly, and possible physiological roles are discussed.

The degradation of lipid droplets by autophagy-related mechanisms is also a theme of the Research Topic. Zhao et al.

(2014) study the transition from heterotrophic to autotrophic growth in the green microalga *Auxenochlorella protothecoides* in a research article. They analyze lipid droplet degradation and show that while macroautophagy is induced during the heterotrophic to autotrophic transition, lipid bodies are degraded in the vacuole by a microautophagy-like mechanism. Hanamata et al. (2014) discuss autophagy during male reproductive development in a review article. Rice autophagy mutants, unlike those of Arabidopsis, are male sterile, as pollen does not mature due to defects in the tapetum. Autophagy in tapetal cells is required for lipid body degradation, which in turn is involved in pollen maturation, highlighting an important difference between plant species. Lipophagy in phytopathogenic fungi is also discussed by Oku et al. (2014), as breakdown of lipid droplets is required for efficient infection but the mechanism is not well understood.

Finally, Ren et al. (2014) review the relationship of autophagy to carbon and nitrogen metabolism. Autophagy is known to function in starch degradation during the night and also to degrade chloroplast components during carbon deficiency. It is also involved in nitrogen remobilization from leaves during senescence, and autophagy mutants have lower nitrogen use efficiency. Transcriptome analysis indicates that several autophagy genes are found as hubs in transcriptional networks, an intriguing observation that should lead to interesting future experiments analyzing the role of these networks.

This collection highlights some of the recent advances in our understanding of plant autophagy and its role in numerous physiological processes and we hope that it will stimulate further discussion and research into this exciting topic.

## REFERENCES

- Derrien, B., and Genschik, P. (2014). When RNA and protein degradation pathways meet. *Front. Plant Sci.* 5:161. doi: 10.3389/fpls.2014.00161
- Floyd, B. E., Morriss, S. C., Macintosh, G. C., and Bassham, D. C. (2012). What to eat: evidence for selective autophagy in plants. *J. Integr. Plant Biol.* 54, 907–920. doi: 10.1111/j.1744-7909.2012.01178.x
- Hanamata, S., Kurusu, T., and Kuchitsu, K. (2014). Roles of autophagy in male reproductive development in plants. *Front. Plant Sci.* 5:457. doi: 10.3389/fpls.2014.00457
- Lee, H. N., Kim, J., and Chung, T. (2014). Degradation of plant peroxisomes by autophagy. *Front. Plant Sci.* 5:139. doi: 10.3389/fpls.2014.00139
- Li, F., and Vierstra, R. D. (2012). Autophagy: a multifaceted intracellular system for bulk and selective recycling. *Trends Plant Sci.* 17, 526–537. doi: 10.1016/j.tplants.2012.05.006
- Liu, Y., and Bassham, D. C. (2012). Autophagy: pathways for self-eating in plant cells. *Annu. Rev. Plant Biol.* 63, 215–237. doi: 10.1146/annurev-arplant-042811-105441
- Lv, X., Pu, X., Qin, G., Zhu, T., and Lin, H. (2014). The roles of autophagy in development and stress responses in *Arabidopsis thaliana*. *Apoptosis* 19, 905–921. doi: 10.1007/s10495-014-0981-4
- Michaeli, S., Avin-Wittenberg, T., and Galili, G. (2014). Involvement of autophagy in the direct ER to vacuole protein trafficking route in plants. *Front. Plant Sci.* 5:134. doi: 10.3389/fpls.2014.00134
- Oku, M., Takano, Y., and Sakai, Y. (2014). The emerging role of autophagy in peroxisome dynamics and lipid metabolism of phyllosphere microorganisms. *Front. Plant Sci.* 5:81. doi: 10.3389/fpls.2014.00081
- Perez-Perez, M. E., Lemaire, S. D., and Crespo, J. L. (2012). Reactive oxygen species and autophagy in plants and algae. *Plant Physiol.* 160, 156–164. doi: 10.1104/pp.112.199992
- Ren, C., Liu, J., and Gong, Q. (2014). Functions of autophagy in plant carbon and nitrogen metabolism. *Front. Plant Sci.* 5:301. doi: 10.3389/fpls.2014.00301
- Tasaki, M., Asatsuma, S., and Matsuoka, K. (2014). Monitoring protein turnover during phosphate starvation-dependent autophagic degradation using a photoconvertible fluorescent protein aggregate in tobacco BY-2 cells. *Front. Plant Sci.* 5:172. doi: 10.3389/fpls.2014.00172
- Veljanovski, V., and Batoko, H. (2014). Selective autophagy of non-ubiquitylated targets in plants: looking for cognate receptor/adaptor proteins. *Front. Plant Sci.* 5:308. doi: 10.3389/fpls.2014.00308
- Voitsekhovskaja, O. V., Schiermeyer, A., and Reumann, S. (2014). Plant peroxisomes are degraded by starvation-induced and constitutive autophagy in tobacco BY-2 suspension cultured cells. *Front. Plant Sci.* 5:629. doi: 10.3389/fpls.2014.00629
- Zhao, L., Dai, J., and Wu, Q. (2014). Autophagy-like processes are involved in lipid droplet degradation in *Auxenochlorella protothecoides* during the heterotrophy-autotrophy transition. *Front. Plant Sci.* 5:400. doi: 10.3389/fpls.2014.00400
- Zhou, J., Wang, J., Yu, J. Q., and Chen, Z. (2014). Role and regulation of autophagy in heat stress responses of tomato plants. *Front. Plant Sci.* 5:174. doi: 10.3389/fpls.2014.00174
- Zientara-Rytter, K., Lukomska, J., Moniuszko, G., Gwozdecki, R., Surowiecki, P., Lewandowska, M., et al. (2011). Identification and functional analysis of Joka2, a tobacco member of the family of selective autophagy cargo receptors. *Autophagy* 7, 1145–1158. doi: 10.4161/auto.7.10.16617
- Zientara-Rytter, K., and Sirko, A. (2014). Significant role of PB1 and UBA domains in multimerization of Joka2, a selective autophagy cargo receptor from tobacco. *Front. Plant Sci.* 5:13. doi: 10.3389/fpls.2014.00013

**Conflict of Interest Statement:** The authors declare that the research was conducted in the absence of any commercial or financial relationships that could be construed as a potential conflict of interest.

**Received:** 11 November 2014; **accepted:** 13 November 2014; **published online:** 01 December 2014.

**Citation:** Bassham DC and Crespo JL (2014) Autophagy in plants and algae. *Front. Plant Sci.* 5:679. doi: 10.3389/fpls.2014.00679

*This article was submitted to Plant Cell Biology, a section of the journal Frontiers in Plant Science.*

*Copyright © 2014 Bassham and Crespo. This is an open-access article distributed under the terms of the Creative Commons Attribution License (CC BY). The use, distribution or reproduction in other forums is permitted, provided the original author(s) or licensor are credited and that the original publication in this journal is cited, in accordance with accepted academic practice. No use, distribution or reproduction is permitted which does not comply with these terms.*



# Significant role of PB1 and UBA domains in multimerization of Joka2, a selective autophagy cargo receptor from tobacco

Katarzyna Zientara-Rytter and Agnieszka Sirk \*

Department of Plant Biochemistry, Institute of Biochemistry and Biophysics, Polish Academy of Sciences, Warsaw, Poland

**Edited by:**

Diane C. Bassham, Iowa State University, USA

**Reviewed by:**

Gian P. Di Sansebastiano, Università del Salento, Italy

Georgia Drakakaki, University of California Davis, USA

**\*Correspondence:**

Agnieszka Sirk, Department of Plant Biochemistry, Institute of Biochemistry and Biophysics, Polish Academy of Sciences, ul. Pawinskiego 5A, 02-106 Warsaw, Poland  
e-mail: asirko@ibb.waw.pl

Tobacco Joka2 protein is a hybrid homolog of two mammalian selective autophagy cargo receptors, p62 and NBR1. These proteins can directly interact with the members of ATG8 family and the polyubiquitinated cargoes designed for degradation. Function of the selective autophagy cargo receptors relies on their ability to form protein aggregates. It has been shown that the N-terminal PB1 domain of p62 is involved in formation of aggregates, while the UBA domains of p62 and NBR1 have been associated mainly with cargo binding. Here we focus on roles of PB1 and UBA domains in localization and aggregation of Joka2 in plant cells. We show that Joka2 can homodimerize not only through its N-terminal PB1-PB1 interactions but also via interaction between N-terminal PB1 and C-terminal UBA domains. We also demonstrate that Joka2 co-localizes with recombinant ubiquitin and sequesters it into aggregates and that C-terminal part (containing UBA domains) is sufficient for this effect. Our results indicate that Joka2 accumulates in cytoplasmic aggregates and suggest that in addition to these multimeric forms it also exists in the nucleus and cytoplasm in a monomeric form.

**Keywords:** Joka2, PB1, UBA, autophagy, proteasome, ubiquitin, selective autophagy cargo receptor, NBR1

## INTRODUCTION

Autophagy is a highly evolutionary conserved process among all eukaryotic organisms. It is responsible for degradation of cellular components in ubiquitin-proteasome system (UPS) independent manner (Yoshimori, 2004). The cellular components could be degraded by autophagy in unselective or selective manner. In the latter case the specific proteins, so called selective autophagy receptors, capable of the selective recognition of the cargos are needed (Weidberg et al., 2011). Soluble proteins, protein aggregates, or other cellular components assigned for degradation in the selective manner are usually marked by a polyubiquitin tail (Hershko and Ciechanover, 1998) which is recognized by the selective autophagy cargo receptors as a signal for degradation (Wilkinson et al., 2001). The selective autophagy cargo receptors control selectivity of autophagy flux. Similarly to other proteins involved in signaling and regulatory pathways they have modular domains responsible for specific interactions with variety of proteins (Pawson and Nash, 2003). Such form of regulation guarantees interconnections with the wide range of pathways and provides exact control of the appropriate process.

Both the N-terminal PB1 (Phox and Bem1) domains and the C-terminal UBA (ubiquitin associated) domains of p62 and NBR1 as well as of their homologs from animals, fungi, and plants are recognized as modules mediating protein-protein interaction (Geetha and Wooten, 2002; Kirkin et al., 2009a,b). Interestingly, p62 contains only one UBA domain, while NBR1 and plant selective autophagy cargo receptors, such as tobacco Joka2 and Arabidopsis AtNBR1 have two non-identical UBA domains. The animal proteins contain JUBA and UBA, while the plant proteins

contain UBA1 and UBA2 domains. It has been shown that only UBA2 of AtNBR1 (NBR1 from *Arabidopsis*) can bind ubiquitin *in vitro* (Svenning et al., 2011). Both PB1 and UBA domains of p62 appeared absolutely crucial for its ability to form characteristic cytoplasmic bodies and for its function as a factor driving polyubiquitinated cargos to the autophagic degradation machinery. Therefore, specific degradation of polyubiquitinated cargos is highly dependent on two features of p62, its polymerization via the N-terminal PB1 domain and its ability to bind polyubiquitin via the C-terminal UBA domain (Bjorkoy et al., 2005).

PB1 domain is a protein interaction module conserved in animals, fungi, amoebas, and plants (Sumimoto et al., 2007). It was first found in phagocyte oxidase activator p67<sup>phox</sup> and the yeast polarity protein Bem1p (Ito et al., 2001). According to the recent data, in all eukaryotes there are nearly 200 proteins containing the PB1 domain (Letunic et al., 2002). It is about 80 amino acids long and possesses an ubiquitin-like β-grasp fold containing two alpha helices and mixed five-stranded β-sheets. Additionally, it can harbor an OPCA (OPC/PC/AID) motif composed of about 20-amino acid with highly conserved acidic and hydrophobic residues and/or lysine residue conserved on the first β-strand (Ponting, 1996; Nakamura et al., 1998; Moscat and Diaz-Meco, 2000; Terasawa et al., 2001; Ponting et al., 2002). The PB1 domain present in mammalian p62 possesses both, the acidic OPCA motif and the conserved lysine (a residue of basic charge). It enables specific PB1-PB1 dimerization due to salt bridges formation between the OPCA from one PB1 and the lysine from the other PB1 (Gong et al., 1999; Sanz et al., 1999, 2000; Avila et al., 2002; Cariou et al., 2002; Lamark et al., 2003). The PB1 domain

of p62 is responsible not only for homo-dimerization but also for interaction with other proteins. Conversely, the PB1 domain of mammalian NBR1 harbors only the OPCA motif and lacks the lysine residue what enables hetero-dimerization but is not sufficient for NBR1-NBR1 homo-dimers formation via PB1. Thus, additional CC motifs are involved in homo-dimerization of NBR1 proteins (Lamark et al., 2003). Interestingly, an ubiquitin fold of the PB1 domain is structurally similar to the ubiquitin and to the UbL (ubiquitin-like) domain and (Hirano et al., 2004). Although much weaker than the conventional ubiquitin-UBA binding, an apparent interaction between UbL and UBA domains of Dsk2 protein was indicated (Lowe et al., 2006). For those reasons it was postulated that the PB1 domain of p62 could be recognized by its UBA domain.

The UBA domain was initially identified by bioinformatic analysis (Hofmann and Bucher, 1996). It is about 45 residues long domain formed by three alpha helices and a hydrophobic patch mediating protein–protein interaction (Dieckmann et al., 1998). The UBA domain is found in many proteins involved in the degradation pathways engaging ubiquitin-like proteins, for example in Dsk2 or Rad23 involved in UPS or in p62 and NBR1 involved in autophagy-lysosomal machinery. Most UBA domains, but not all of them (Davies et al., 2004), are able to bind various ubiquitin forms, such as monoubiquitin or the K48- or K63-chains of polyubiquitin (Vadlamudi et al., 1996; Bertolaet et al., 2001a,b; Wilkinson et al., 2001; Funakoshi et al., 2002; Rao and Sastry, 2002). For instance, the UBA domain of p62 shows a preference for K63-polyubiquitinated substrates (Seibenhenner et al., 2004; Long et al., 2008).

Although the mammalian p62 and NBR1 proteins were extensively studied, their plant homologs are far less characterized. Previously, it has been shown by us that Joka2, a selective autophagy cargo receptor from tobacco, is a functional and structural hybrid of mammalian selective autophagy cargo receptors by sharing some features of p62 and some of NBR1 (Zientara-Rytter et al., 2011). In this study we focused on two regions of Joka2, the N-terminal PB1 domain and the C-terminal region containing UBA domains. Our results pointed out their significant role in oligomerization and aggregation of Joka2 in plant cells.

## MATERIALS AND METHODS

### DNA CLONING AND PLASMID CONSTRUCTION

Plasmids used in this study are listed in **Table 1**. Details of their construction are available upon request. Sequences encoding recombinant unstable ubiquitin ( $\text{Ub}^{\text{G76V}}$ ) linked to YFP were designed based on previous results (Heessen et al., 2003). Gateway entry vectors were created by cDNA cloning into pENTR™/D-TOPO vector. Gateway LR recombination reactions were done as described in the Gateway® Technology—manual (Invitrogen, 12535-019 and 12535-027, respectively). Oligonucleotides for PCR and DNA sequencing are listed in **Table 2**. All plasmids were checked by DNA sequencing and/or by digestion by restriction enzymes. Conventional techniques were used for *Escherichia coli* or *Agrobacterium tumefaciens* transformation.

### YEAST TWO HYBRID ASSAY

Yeast cells transformation was performed by the LiAc/ss carrier DNA/PEG method (Gietz and Woods, 2002) following the

“Quick and Easy TRAFO Protocol.” After the transformation cells were placed on the appropriate synthetic dropout (SD) medium, prepared according to Invitrogen Handbook (PT3024-1), for transformants selection and, later, for testing of the possible protein-protein interactions. Plates were incubated at 30°C for up to 7 days.

### PLANT MATERIAL AND GROWTH CONDITIONS

*Nicotiana benthamiana* plants were grown in soil in growth chamber under the conditions of 60% relative humidity, with a day/night regime of 16 h light 300  $\mu\text{mol}$  photons  $\text{m}^{-2} \text{s}^{-1}$  at 23°C and 8 h dark at 19°C.

### TRANSIENT PROTEIN EXPRESSION

For transient co-expression of proteins in *N. benthamiana* leaves fresh overnight cultures of *A. tumefaciens* containing appropriate binary plasmids were spun down and washed twice. Next, cells were re-suspended in sterile water and brought to a final cell density  $2 \times 10^8$  cfu/ml (OD600 ~ 0.2). For bimolecular fluorescent complementation (BiFC) experiments the cell suspensions were adjusted to  $4 \times 10^8$  cfu/ml and mixed 1:1 before infiltration. Young *N. benthamiana* plants with fully expanded leaves of about 5 cm in diameter were infiltrated by bacterial suspension using a needless syringe. Leaves were harvested and analyzed under confocal microscope 3 days after agroinfiltration.

### CONFOCAL MICROSCOPE ANALYSIS

For staining of nuclei, prior the microscope analysis, agroinfiltrated leaves were incubated with a fluorescent dye DAPI (1  $\mu\text{g}/\text{ml}$ ) for 15 min in the darkness at room temperature. After the treatment, plant material was washed in water (3 times, 5 min each) and immediately observed in a confocal microscope. For LMB treatment plant material was incubated with leptomycin B (20 ng/ml) up to 24 h before observation. All images were obtained in the Laboratory of Confocal and Fluorescence Microscopy at IBB PAS using a Nicon confocal microscope, Eclipse TE2000-E and processed using EZ-C1 3.60 FreeViewer software. For GFP/YFP the 488-nm line from an Argon-Ion Laser (40 mW) was used for excitation, and a 500–530 nm band pass filter for detection of emission. For RFP the 543 nm line of a Green He-Ne Laser (1.0 mW) was used for excitation and the 565–640 nm filter was used for detection. The same 543 nm line of a Green He-Ne Laser (1.0 mW) but with a 650 nm long pass filter was used for chlorophyll emission and detection, respectively. The blue fluorescence of DAPI or CFP was imaged using 404 nm Violet-Diode Laser MOD (44.8 mW) for excitation and 430–465 nm or 435–485 nm bands pass filter for emission.

## RESULTS

### JOKA2 LOCALIZATION AND INTERACTIONS IN PLANT CELLS

Joka2 protein is a homolog of two human receptors of selective autophagy, p62 and NBR1. Similarly to these proteins, Joka2 not only forms small cytosolic, punctuated bodies which are imported to the central vacuole by autophagy machinery but also creates larger cytoplasmic aggregates. Also alike p62, Joka2 has been observed by us in a nucleus in stably transformed *Nicotiana tabacum* plants (Zientara-Rytter et al., 2011). To understand the phenomenon of this variable localization of

**Table 1 | Plasmids used in this study.**

Plasmid	Description	References
<b>GATEWAY ENTRY VECTOR</b>		
pENTR-D TOPO	Entry vector for subcloning in gateway technology	Invitrogen
<b>GATEWAY DESTINATION VECTORS</b>		
pSITE-nEYFP-C1	Binary vector for BiFC	Chakrabarty et al., 2007; Martin et al., 2009
pSITE-cEYFP-C1	Binary vector for BiFC	Chakrabarty et al., 2007; Martin et al., 2009
pSITE-nEYFP-N1	Binary vector for BiFC	Chakrabarty et al., 2007; Martin et al., 2009
pSITE-cEYFP-N1	Binary vector for BiFC	Chakrabarty et al., 2007; Martin et al., 2009
pSITE-2CA	Binary vector for <i>gfp</i> fusion at N-terminus of cDNA	Chakrabarty et al., 2007
pSITE-4CA	Binary vector for <i>rfp</i> fusion at N-terminus of cDNA	Chakrabarty et al., 2007
pSITE-4NB	Binary vector for <i>rfp</i> fusion at C-terminus of cDNA	Chakrabarty et al., 2007
pH7CWG2	Binary vector for <i>cfp</i> fusion at C-terminus of cDNA	Karimi et al., 2005
pK7WGY2	Binary vector for <i>yfp</i> fusion at N-terminus of cDNA	Karimi et al., 2005
pH7YWG2	Binary vector for <i>yfp</i> fusion at C-terminus of cDNA	Karimi et al., 2005
pK7CWG2	Binary vector for <i>cfp</i> fusion at C-terminus of cDNA	Karimi et al., 2005
pH7WGC2	Binary vector for <i>cfp</i> fusion at N-terminus of cDNA	Karimi et al., 2005
pDEST22	"Prey" vector for Y2H with AD domain of GAL4 protein fused to cDNA N-terminus	Invitrogen
pDEST32	"Bait" vector for Y2H with BD domain of GAL4 protein fused to cDNA N-terminus	Invitrogen
<b>CONSTRUCTED GATEWAY ENTRY VECTORS FOR SUBCLONING</b>		
pEntrUBA	UBA domains (1444–2526 bp/482–842 aa) from NtJoka2 in pENTR-D TOPO	This study
pEntrUb-VV	NtUb <sup>G76V</sup> in pENTR-D TOPO	This study
pEntrPB1	PB1 domain (1–1266 bp/1–422 aa) from NtJoka2 in pENTR-D TOPO	Zientara-Rytter et al., 2011
pEntrPB1ZZ	PB1ZZ domain (1–2253 bp/1–751 aa) from NtJoka2 in pENTR-D TOPO	Zientara-Rytter et al., 2011
pEntrZZ	ZZ domain (316–2253 bp/106–751 aa) from NtJoka2 in pENTR-D TOPO	Zientara-Rytter et al., 2011
pEntrZZUBA	ZZUBA domain (316–2526 bp/106–842 aa) from NtJoka2 in pENTR-D TOPO	Zientara-Rytter et al., 2011
pEntrATG8f	NtATG8f cDNA in pENTR-D TOPO	Zientara-Rytter et al., 2011
pEntrJ	Full-length NtJoka2 in pDONR221	Zientara-Rytter et al., 2011
U17036	ORF cDNA of AtNBR1 in vector pENTR/SD-TOPO for subcloning and direct expression	<a href="http://www.arabidopsis.org">www.arabidopsis.org</a>
<b>CONSTRUCTED PLANT EXPRESSION VECTORS</b>		
PB1-YFP	PB1 domain (1–1266 bp/1–422 aa) of NtJoka2 from pEntrPB1 in pH7YWG2	This study
PB1-CFP	PB1 domain (1–1266 bp/1–422 aa) of NtJoka2 from pEntrPB1 in pH7CWG2	This study
PB1ZZ-YFP	PB1-ZZ domains (1–2253 bp/1–751 aa) of NtJoka2 from pEntrPB1ZZ in pH7YWG2	This study
PB1ZZ-CFP	PB1-ZZ domains (1–2253 bp/1–751 aa) of NtJoka2 from pEntrPB1ZZ in pK7CWG2	This study
INT1-YFP	First interdomain region (316–1266 bp/106–422 aa) of NtJoka2 from pEntrINT1 in pH7YWG2	This study
INT2-YFP	Second interdomain region (–2253 bp/–751 aa) of NtJoka2 from pEntrINT2 in pH7YWG2	This study
ZZ-YFP	ZZ domain (316–2253 bp/106–751 aa) of NtJoka2 from pEntrZZ in pH7YWG2	This study
ZZUBA-YFP	ZZ-UBA domains (316–2526 bp/106–842 aa) of NtJoka2 from pEntrZZUBA in pH7YWG2	This study
ZZUBA-CFP	ZZ-UBA domains (316–2526 bp/106–842 aa) of NtJoka2 from pEntrZZUBA in pH7CWG2	This study
CFP-ZZUBA	ZZ-UBA domains (316–2526 bp/106–842 aa) of NtJoka2 from pEntrZZUBA in pH7WGC2	This study
UBA-YFP	UBA domains (1444–2526 bp/482–842 aa) of NtJoka2 from pEntrUBA in pH7YWG2	This study
UBA-CFP	UBA domains (1444–2526 bp/482–842 aa) of NtJoka2 from pEntrUBA in pH7CWG2	This study
Joka2-YFP	Full-length NtJoka2 from pEntrJ in pH7YWG2	This study
YN-ATG8f	Full-length NtATG8f from pEntrATG8f in pSITE-nEYFP-C1	This study
Joka2-YC	Full-length NtJoka2 from pEntrJ in pSITE-cEYFP-N1	This study
Joka2-YN	Full-length NtJoka2 from pEntrJ in pSITE-nEYFP-N1	This study
YC-Joka2	Full-length NtJoka2 from pEntrJ in pSITE-cEYFP-C1	This study
YN-Joka2	Full-length NtJoka2 from pEntrJ in pSITE-nEYFP-C1	This study

(Continued)

**Table 1 | Continued**

Plasmid	Description	References
PB1ZZ-YN	PB1-ZZ domains (1–2253 bp/1–751 aa) of NtJoka2 from pEntrPB1ZZ in pSITE-nEYFP-N1	This study
PB1ZZ-YC	PB1-ZZ domains (1–2253 bp/1–751 aa) of NtJoka2 from pEntrPB1ZZ in pSITE-cEYFP-N1	This study
PB1-YC	PB1 domain (1–1266 bp/1–422 aa) of NtJoka2 from pEntrPB1 in pSITE-cEYFP-N1	This study
PB1-YN	PB1 domain (1–1266 bp/1–422 aa) of NtJoka2 from pEntrPB1 in pSITE-nEYFP-N1	This study
YC-PB1	PB1 domain (1–1266 bp/1–422 aa) of NtJoka2 from pEntrPB1 in pSITE-cEYFP-C1	This study
YN-PB1	PB1 domain (1–1266 bp/1–422 aa) of NtJoka2 from pEntrPB1 in pSITE-nEYFP-C1	This study
UBA-YC	UBA domains (~2526 bp/–842 aa) of NtJoka2 from pEntrUBA in pSITE-cEYFP-N1	This study
UBA-YN	UBA domains (~2526 bp/–842 aa) of NtJoka2 from pEntrUBA in pSITE-nEYFP-N1	This study
YC-UBA	UBA domains (~2526 bp/–842 aa) of NtJoka2 from pEntrUBA in pSITE-cEYFP-C1	This study
YN-UBA	UBA domains (~2526 bp/–842 aa) of NtJoka2 from pEntrUBA in pSITE-nEYFP-C1	This study
YC-NBR1	Full-length NtJoka2 from pEntrJ in pSITE-cEYFP-C1	This study
YN-NBR1	Full-length NtJoka2 from pEntrJ in pSITE-nEYFP-C1	This study
Joka2-RFP	Full-length NtJoka2 from pEntrJ in pSITE-4NB	This study
GFP-NBR1	Full-length NtJoka2 from pEntrJ in pSITE-2CA	This study
RFP-NBR1	Full-length NtJoka2 from pEntrJ in pSITE-4CA	This study
Ub-VV-YFP	NtUb from pEntrUb-VV in pH7YWG2	This study
<b>CONSTRUCTED YEAST EXPRESSION VECTORS</b>		
AD-UBA	UBA domains (1444–2526 bp/482–842 aa) of NtJoka2 from pEntrUBA in pDEST22	This study
BD-UBA	UBA domains (1444–2526 bp/482–842 aa) of NtJoka2 from pEntrUBA in pDEST32	This study
AD-PB1	PB1 domain (1–1266 bp/1–422 aa) of NtJoka2 from pEntrPB1 in pDEST22	Zientara-Rytter et al., 2011
BD-PB1	PB1 domain (1–1266 bp/1–422 aa) of NtJoka2 from pEntrPB1 in pDEST32	Zientara-Rytter et al., 2011
AD-PB1ZZ	PB1-ZZ domains (1–2253 bp/1–751 aa) of NtJoka2 from pEntrPB1ZZ in pDEST22	Zientara-Rytter et al., 2011
BD-PB1ZZ	PB1-ZZ domains (1–2253 bp/1–751 aa) of NtJoka2 from pEntrPB1ZZ in pDEST32	Zientara-Rytter et al., 2011
AD-ZZUBA	ZZ-UBA domains (316–2526 bp/106–842 aa) of NtJoka2 from pEntrZZUBA in pDEST22	Zientara-Rytter et al., 2011
BD-ZZUBA	ZZ-UBA domains (316–2526 bp/106–842 aa) of NtJoka2 from pEntrZZUBA in pDEST32	Zientara-Rytter et al., 2011
<b>YEAST EXPRESSION VECTORS USED AS A CONTROLS</b>		
pEXP32/Krev1	Yeast expression vector to use as a “bait” for interaction strength controls	Invitrogen
pEXP22/RalGDS-wt	Yeast expression “prey” vector for strong interaction control	Invitrogen
pEXP22/RalGDS-m1	Yeast expression “prey” vector for weak interaction control	Invitrogen
pEXP22/RalGDS-m2	Yeast expression “prey” vector for negative interaction control	Invitrogen
<b>PLANT EXPRESSION VECTORS USED AS A LOCALIZATION CONTROLS</b>		
vac-crk CD3-969	Tonoplast marker—binary plasmid with a CFP fuses to the C-terminus of γ-TIP, an aquaporin of the vacuolar membrane	Nelson et al., 2007

**Table 2 | Oligonucleotides used for PCR and DNA sequencing.**

Name	Sequence	Description
Joka2-F3	caccatgaagggtttacatgatct	For cloning UBA domains with second interdomain region of Joka2
Joka2-R3	ctctccagcaataagatccatg	
Joka2-F2	caccatgtctactcccttacgatc	For cloning first interdomain region of Joka2
Joka2-R1	aatagtcccagtcccatactg	
Joka2-F3	caccatgaagggtttacatgatct	For cloning second interdomain region of Joka2
Joka2-R2	ctggggtggtgcctgcg	
ubq-F	caccatgcagatcttcgtgaa	For cloning tobacco ubiquitin cDNA
ubq-R-VV	cttaccaacaacaccacggagacggaggac	
att-L2	gtacaagaagctgggtcg	For sequencing destination vectors from 3' end
CaM35S-F	gatatccactgacgtaaaggatg	For sequencing binary vectors from 5' end

Joka2 several plasmids encoding truncated variants of the protein were prepared (**Figure S1**). A series of co-localization experiments in leaves of *N. benthamiana* plants transiently transformed with the plasmids containing plant expression cassettes encoding various combinations of the fusion proteins were performed (**Figures 1–3**). Previously, localization of Joka2 in acidic speckles and co-localization of Joka2 with NtATG8f was established in our laboratory (Zientara-Rytter et al., 2011). The BiFC method, used in this study, confirmed not only the autophagosomal localization of Joka2 but also its direct *in vivo* interaction with NtATG8f (**Figure 1A**). Moreover, the vacuolar localization of Joka2 fused to RFP (**Figures 1C,D**) and the partial co-localization of the GFP-AtNBR1 and RFP-AtNBR1 proteins used as a localization control (**Figure 1B**) are in agreement with results reported previously for EGFP-mCherry-AtNBR1 suggesting that AtNBR1 is transported to the vacuole (Svenning et al., 2011). Additionally, the nuclear localization of Joka2 in stably transformed Joka2-YFP seedlings was confirmed by DAPI staining (**Figure 2B**) and the functionality of the nuclear export sequence (NES) located in the first interdomain region (INT1), between PB1 and ZZ domains was demonstrated (**Figure 2A**). The treatment with nuclear export inhibitor (LMB) enclosed the truncated PB1-YFP protein in the

nucleus but did not change the cytoplasmic localization of the INT1 protein nor the localization of the INT2 protein, each fused to YFP (**Figure 2A**). The observed subcellular localization of INT1 and PB1 truncated proteins in the absence of LMB strongly suggests that the nuclear localization signal (NLS) is located in PB1 domain and not in INT1 region. The subcellular location of the truncated PB1-YFP protein is affected by LMB treatment similarly as the subcellular location of the full length Joka2 (Zientara-Rytter et al., 2011 and **Figure S2**), however LMB does not change intracellular distribution of the free green fluorescent protein (GFP) in stably transformed plants (**Figure S3**).

Finally, co-localization of Joka2-CFP with unstable recombinant ubiquitin linked to YFP (Ub-VV-YFP) indicated that Joka2 is present in ubiquitin-containing protein aggregates (**Figure 3**). It could be assumed that at least one of UBA domains of Joka2 is involved in recognition of ubiquitin-containing proteins and in sequestration of poly-ubiquitinated proteins into aggregates. To verify this assumption, the cassettes: PB1-CFP, PB1ZZ-CFP, ZZUBA-CFP, CFP-ZZUBA, UBA-CFP were transiently co-expressed in *N. benthamiana* leaves with the cassette for Ub-VV-YFP. This experiment showed that the C-terminal part of Joka2 possessing UBA domains was necessary for co-localization

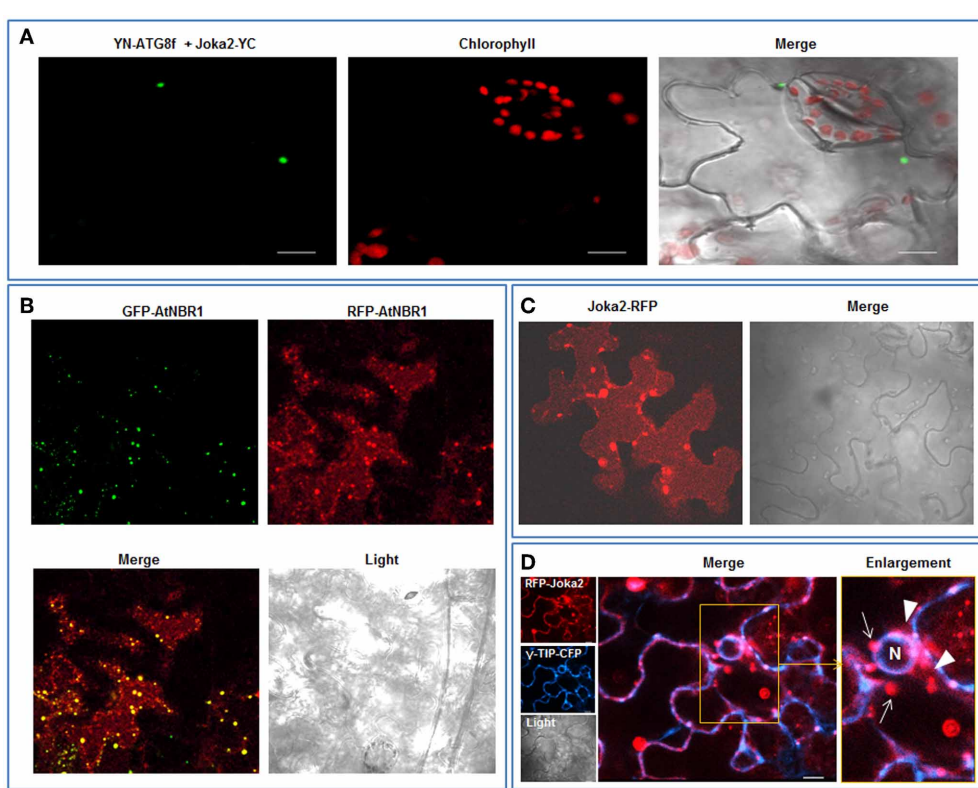
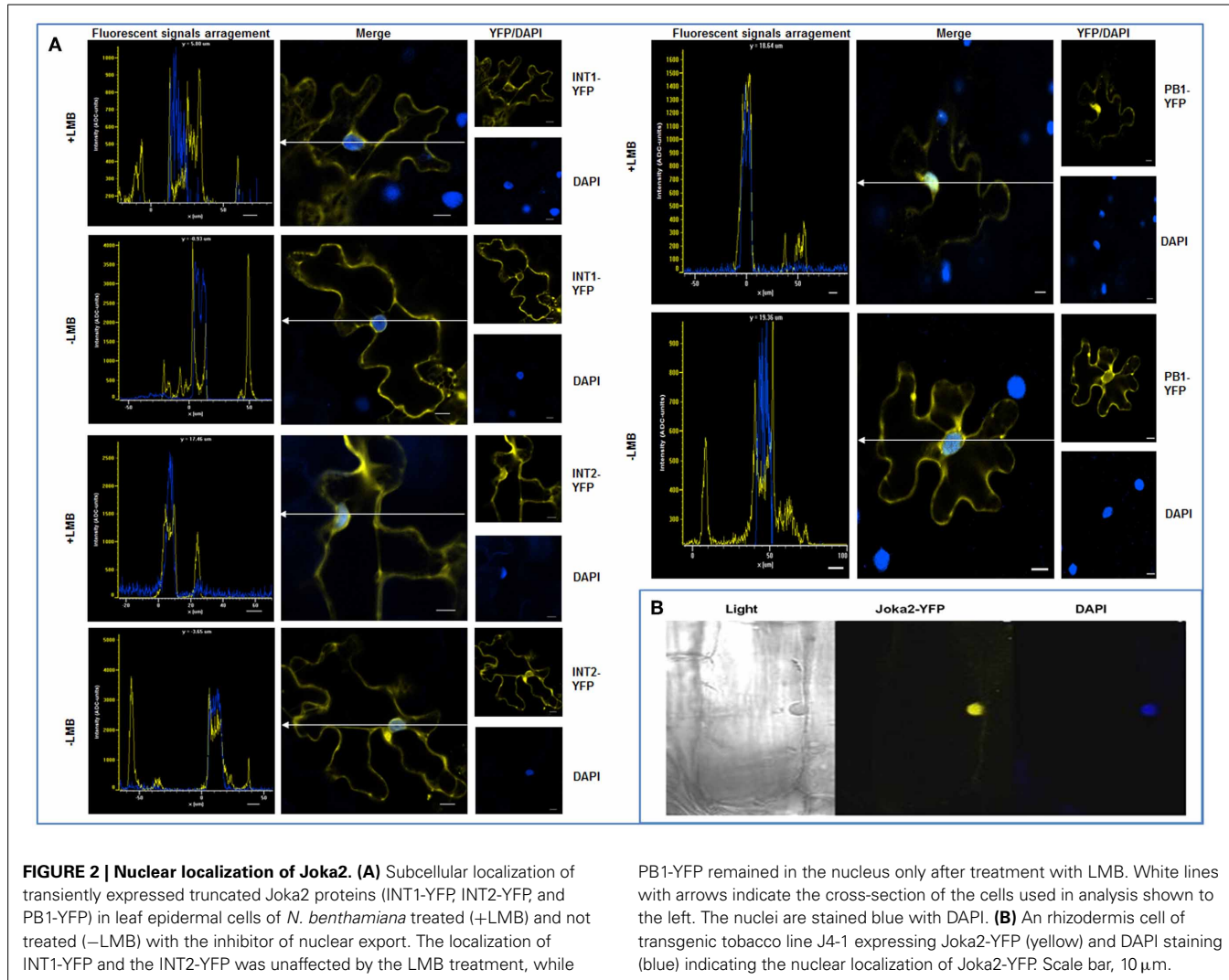


**FIGURE 1 | Cytoplasmic and vacuolar localization of transiently expressed Joka2 and AtNBR1 in leaf epidermal cells of *N. benthamiana*.** **(A)** BiFC assay of interaction between Joka2 and NtATG8f using randomly chosen combination (YN-NtATG8f+Joka2-YC) of the vectors. **(B)** Co-localization of co-expressed GFP-AtNBR1 and RFP-AtNBR1 (AtNBR1 fused to two variants of fluorescent protein). **(C)** Localization of Joka2-RFP in the vacuole. **(D)** Subcellular

localization of co-expressed RFP-Joka2 and  $\gamma$ -TIP-CFP—a tonoplast marker based on an aquaporin of the vacuolar membrane fused to CFP. The enlarged part of the picture visualizes tonoplast (the blue fluorescence signal) of the central vacuole which surrounds the nucleus (N) and red fluorescence of RFP-Joka2 fusion protein observed mainly inside the vacuole close to the tonoplast as a smear (arrowheads) or in spots (arrows). Scale bar, 10  $\mu$ m.



of Joka2 with Ub-VV-YFP. Moreover, the sequestration of Ub-VV-YFP into aggregates took place only in the presence of C-terminal UBA domains of Joka2, whereas N-terminal PB1 domain of Joka2 had no effect on its localization. Moreover, truncated Joka2 with ZZUBA or UBA domains were always co-localized with Ub-VV-YFP.

#### Joka2 EXISTS IN PLANTA IN MONOMERIC AND IN OLIGOMERIC FORMS

Due to a structural similarity between Phox/Bem1p (PB1) domain and ubiquitin-like (UbL) domain, selective autophagy cargo receptors (Joka2, p62, and NBR1) might be included into a family of ubiquitin receptor proteins containing both UbL and ubiquitin-associated (UBA) domains (Figures 4B,D). Moreover, p62 possess many properties that are similar to the UbL-UBA proteins, such as direct interaction with proteasome by PB1 domain (Babu et al., 2005; Geetha et al., 2008) and ability to deliver polyubiquitinated proteins to UPS (Seibenheuer et al., 2004; Babu et al., 2005). It was shown by us previously in yeast two hybrid (Y2H) experiments that Joka2 can form homodimers (Zientara-Rytter et al., 2011). Here, Joka2 dimerization

is confirmed *in planta* using the BiFC method in which fusion proteins linking Joka2 with either N- or C-terminal part of YFP (YN or YC, respectively; see Figure S4) were generated by transient co-expression in *N. benthamiana* leaves using all four possible combinations, namely YN-Joka2 with YC-Joka2, YN-Joka2 with Joka2-YC, Joka2-YN with Joka2-YC, and Joka2-YN with YC-Joka2 (Figure 5 and Figure S5). Additionally, self-interaction of AtNBR1, an Arabidopsis homolog of Joka2, was verified using one randomly selected combination, namely YN-AtNBR1 and YC-AtNBR1 (Figure 5). The BiFC assay confirmed that both cargo receptors, Joka2 and AtNBR1, were able to make multimeric forms *in planta*. Interestingly, for both proteins the fluorescence of the restored YFP was observed only in aggregates what suggests that Joka2 and AtNBR1 are present in oligomeric forms only in aggresomes, while outside of aggresomes, in the cytoplasm and the nucleus they rather exist in monomeric forms.

#### PB1-PB1 INTERACTIONS ARE SUFFICIENT FOR AGGREGATES FORMATION

It is obvious that aggregation of selective autophagy cargo receptors is possible due to their ability to polymerize. Molecular

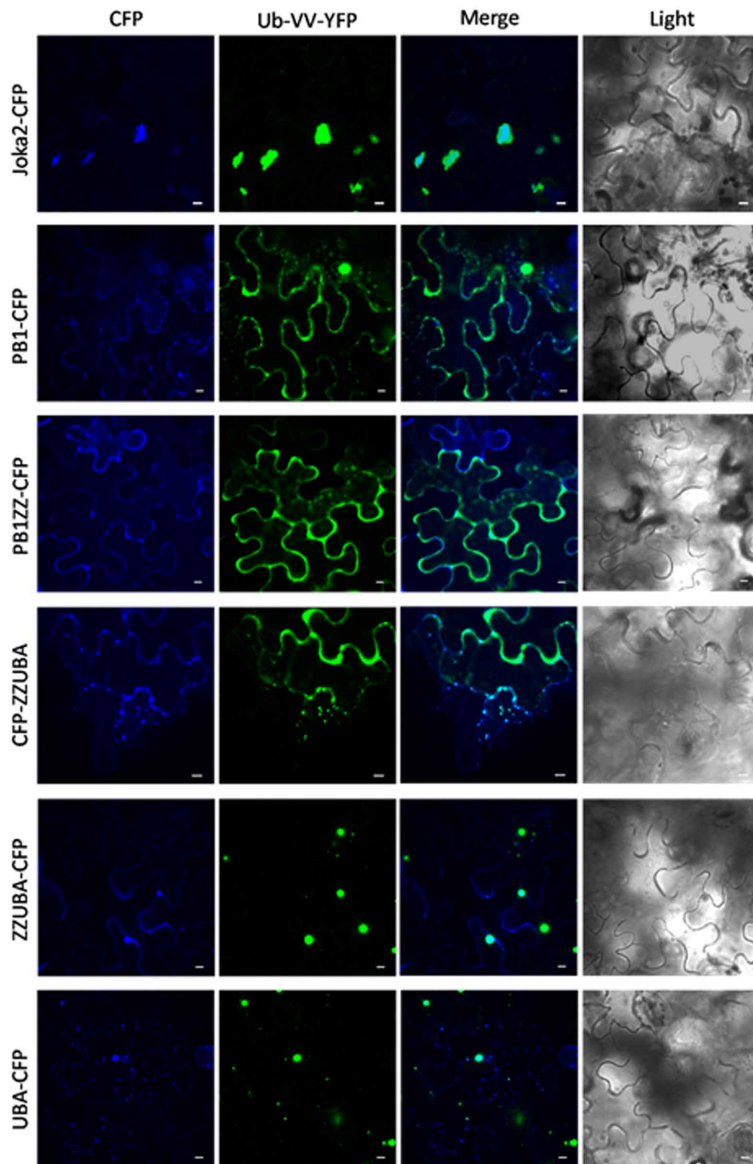


**FIGURE 3 | Truncated Joka2 containing only UBA domains co-localizes with ubiquitin linked to YFP (Ub-VV-YFP).** Truncated Joka2 proteins lacking PB1, PB1, and ZZ, ZZ, and UBA or UBA domains were transiently co-expressed in *N. benthamiana* leaves with unstable ubiquitin linked to YFP

(Ub-VV-YFP). The overlapping fluorescent signals were observed only in the case of co-expression of Ub-VV-YFP with the following versions of the recombinant proteins: full-length Joka2-CFP, ZZUBA-CFP, CFP-ZZUBA, UBA-CFP. Scale bar, 10  $\mu$ m.

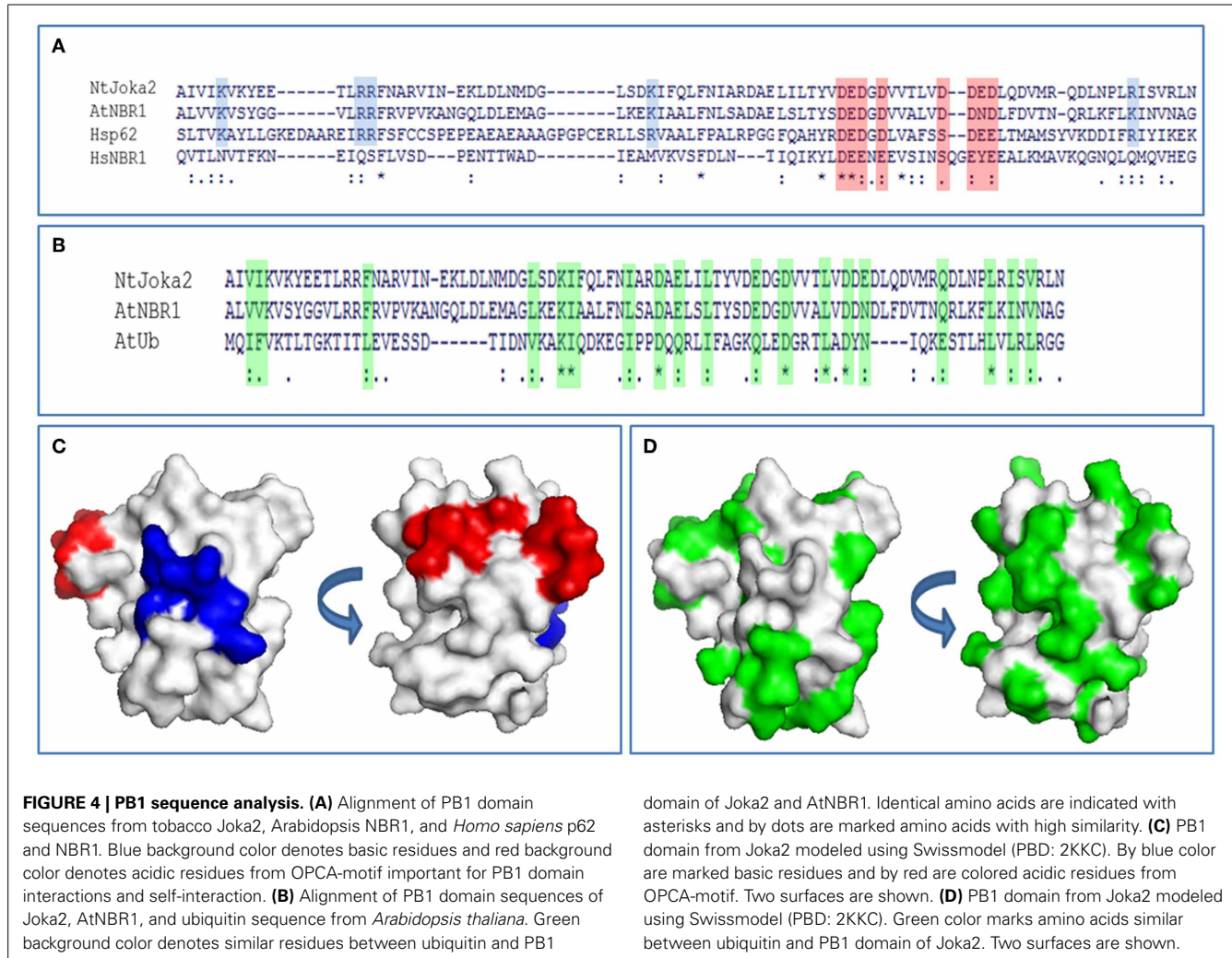
modeling of PB1 domain of Joka2 revealed that it has a basic/acidic surface structure, which is similar to PB1 domain of p62 which, in turn, has the ability to polymerize (Svenning et al., 2011). In the PB1 domain, both proteins harbor the N-terminal basic charge cluster and the C-terminal, acidic OPCA motif (Figures 4A,C).

Previously, it has been shown by us in Y2H experiments that the N-terminal PB1 domain of Joka2 is involved in dimers formation (Zientara-Rytter et al., 2011). We decided to confirm this result *in planta* by BiFC. The constructs encoding the PB1ZZ and PB1 fragments of Joka2 were used in this experiment. The fusion proteins were generated by linking PB1ZZ or PB1 with

either N- or C-terminal parts of YFP and fluorescence of YFP was observed in several combinations of the fusions. For PB1ZZ only one combination was tested (PB1ZZ-YC+PB1ZZ-YN), while for PB1 all four combinations were used. The fluorescence was observed in all analyzed combinations except PB1-YC+YN-PB1 (Figure 6) and the negative controls (not shown). These results indicate that PB1 domain of Joka2 protein can form homo-dimers *in planta*.

#### UBA DOMAINS ARE ALSO INVOLVED IN AGGREGASOMES FORMATION

During subsequent analysis, various Joka2 fragments linked to YFP or CFP were tested for their subcellular localization and



ability to form cytoplasmic aggregates. Cassettes encoding the respective fusion proteins were transiently expressed in *N. benthamiana* leaves and the recombinant proteins were analyzed under confocal microscopy (**Figure 7**). Interestingly, somewhat diffused distribution was observed in each of the tested deletion constructs, namely PB1, PB1ZZ, INT1, ZZ, INT2, ZZUBA, UBA. Such distribution was similar to K11A/D60A mutant with disturbed acidic/basic surface described by the Johansen's group (Svenning et al., 2011). The truncated proteins containing PB1 domain (PB1, PB1ZZ) were able to create aggregates *in planta*, but this tendency was weaker (e.g., smaller and less aggregates and more apparent "diffused" distribution in the cytoplasm) than in the case of full Joka2 containing all three domains, PB1, ZZ, and double UBA (**Figure 7A**). In summary, this experiment indicated (i) necessity of PB1 domain for protein multimerization *in vivo* and (ii) contribution of UBA domains to the process of aggregates formation (or stabilization).

This problem was investigated further by transient co-production of the full length Joka2 (Joka2-YFP) with truncated versions (PB1 or PB1ZZ, ZZUBA, UBA) linked to CFP, what enabled monitoring of both types of the proteins in one cell

(**Figure 7B**). Interestingly, full-length Joka2 co-expressed with some truncated forms (PB1 or PB1ZZ) was observed not only in aggregates but also a weak fluorescence was present in the nucleus and cytoplasm (**Figure 7B**). Such dual localization was not observed when Joka2 was co-produced with ZZUBA or UBA domains or with full-length Joka2 (**Figure 7B**). This result is in agreement with the results shown in **Figures 3, 7A** and indicates that UBA domains are also involved in cytoplasmic bodies formation. Moreover, this result strongly suggested a possibility of PB1-UBA interaction.

#### PB1-UBA INTERACTIONS IN AGGREGASOMES

It is known that PB1 domains are also able to interact with other domains. For example, PB1 domain from p62 can directly interact with PB1 domain from NBR1 protein or with the Rpt1 subunit of 26S proteasome (Seibenbener et al., 2004; Babu et al., 2005; Geetha et al., 2008). The NMR studies of PB1 domain has shown that it creates an ubiquitin-like,  $\beta$ -grasp fold, similar to the well-characterized UbL domain (Hirano et al., 2004). Therefore, it was postulated that PB1 domain can also directly interact with UBA (Su and Lau, 2009; Isogai et al.,

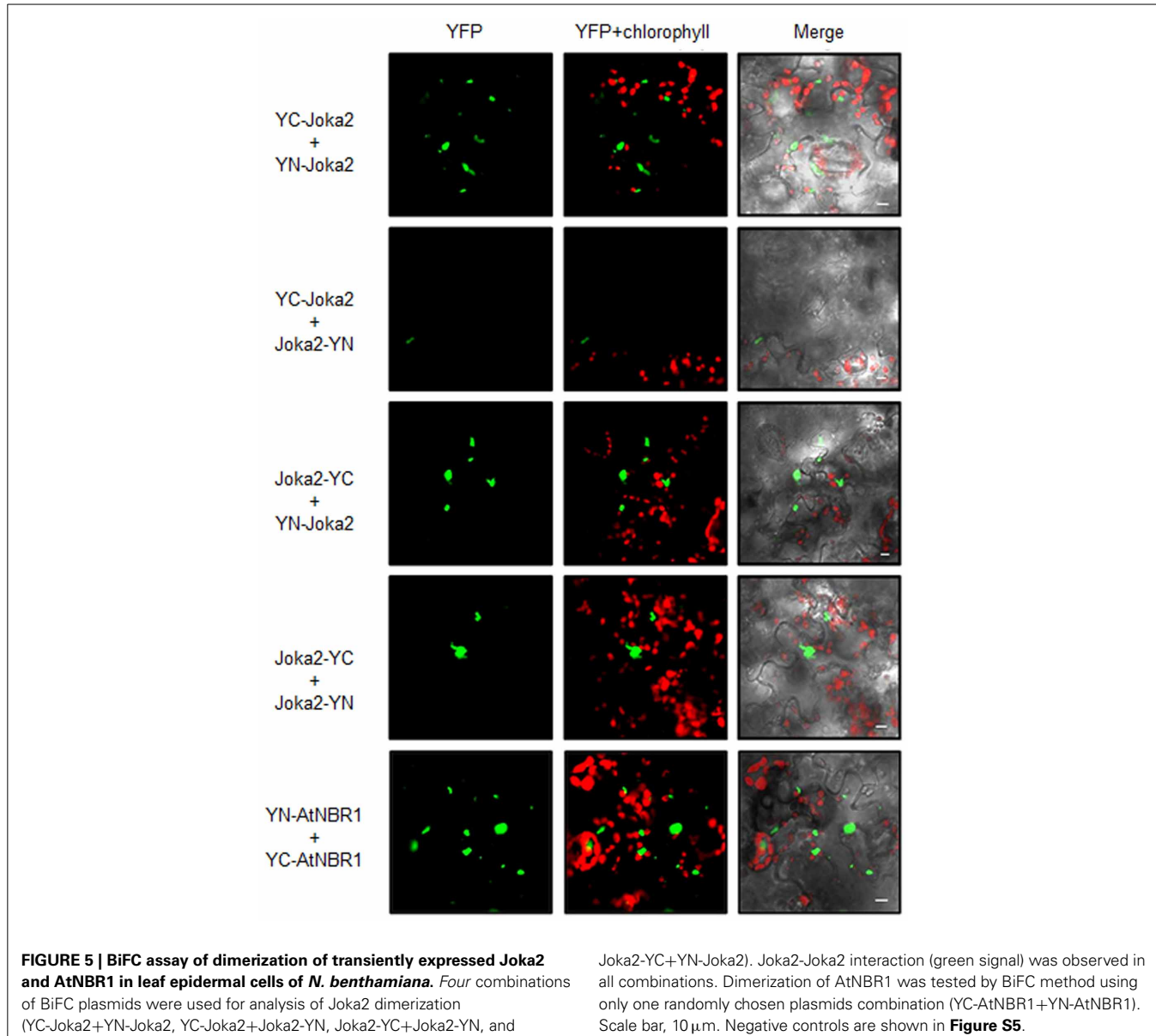


**FIGURE 5 | BiFC assay of dimerization of transiently expressed Joka2 and AtNBR1 in leaf epidermal cells of *N. benthamiana*.** Four combinations of BiFC plasmids were used for analysis of Joka2 dimerization (YC-Joka2+YN-Joka2, YC-Joka2+Joka2-YN, Joka2-YC+Joka2-YN, and

Joka2-YC+YN-Joka2). Joka2-Joka2 interaction (green signal) was observed in all combinations. Dimerization of AtNBR1 was tested by BiFC method using only one randomly chosen plasmids combination (YC-AtNBR1+YN-AtNBR1). Scale bar, 10 μm. Negative controls are shown in **Figure S5**.

2011). A similar interaction was reported for the UbL and UBA family of ubiquitin binding proteins involved in proteasomal degradation of ubiquitinated substrates, like Dsk2 protein (Lowe et al., 2006). Despite the fact that UBA domains were not crucial for multimerization of the selective autophagy cargo receptors, we decided to test if a direct interaction between PB1 and UBA domains from Joka2 is possible. The screening performed in Y2H system indicated that the interaction between these domains could take place *in vivo* (**Figure 8A**). The strongest interaction was observed when the truncated PB1ZZ protein was fused to AD domain of GAL4, while the truncated ZZUBA protein was fused to BD domain of GAL4. Nevertheless, it was still moderate interaction in comparison to the positive control and the other previously described by us interactions using Y2H system, namely PB1-PB1. Nevertheless, the PB1-UBA interaction was also confirmed by BiFC experiment *in planta*. Interestingly, the fluorescent signal from YFP (obtained

as a consequence of a direct binding of UBA and PB1) was observed only in aggregates (**Figure 8B**) despite the fact that both fusion proteins share diffuse localization in *N. benthamiana* cells (see **Figures 3, 7B**).

## DISCUSSION

The main focus of this study was on characterization of the role of PB1 and UBA domains in multimerization and aggregation of Joka2 in plant cells. The results are shown in a form of a model summarizing and explaining detected interactions (**Figure 8**). It has been shown by us that Joka2 has multiple cellular localizations. We have observed Joka2 in autophagosomes, where its interaction with ATG8 proteins is possible; in vacuole where it is presumably degraded; in cytosolic aggregates (aggregasomes) and in the nucleus. The nuclear location was especially apparent after treatment with LMB, an inhibitor of nuclear export. We were able to localize the functional NES (nuclear export sequence),

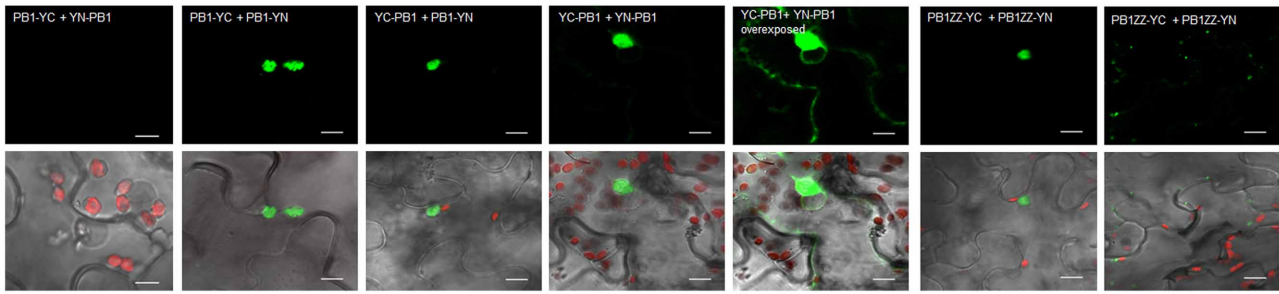


**FIGURE 6 | BiFC assay of dimerization of PB1 in planta.** The combinations of plasmids (PB1-YC+YN-PB1, PB1-YC+PB1-YN, YC-PB1+PB1-YN, YC-PB1+YN-PB1, and PB1ZZ-YC+PB1ZZ-YN) were used for BiFC analysis in leaf epidermal cells of *N. benthamiana*. The interaction (green signal) was mainly observed in cytosolic aggregates.

For the combination of PB1-YC+YN-PB1 no fluorescence signal was observed in plant cells. For the combination of YC-PB1+YN-PB1 the weak fluorescence in cytoplasm was also present. Two independent representative pictures are shown for the combination of YC-PB1ZZ+YN-PB1ZZ. Scale bar, 10  $\mu$ m.

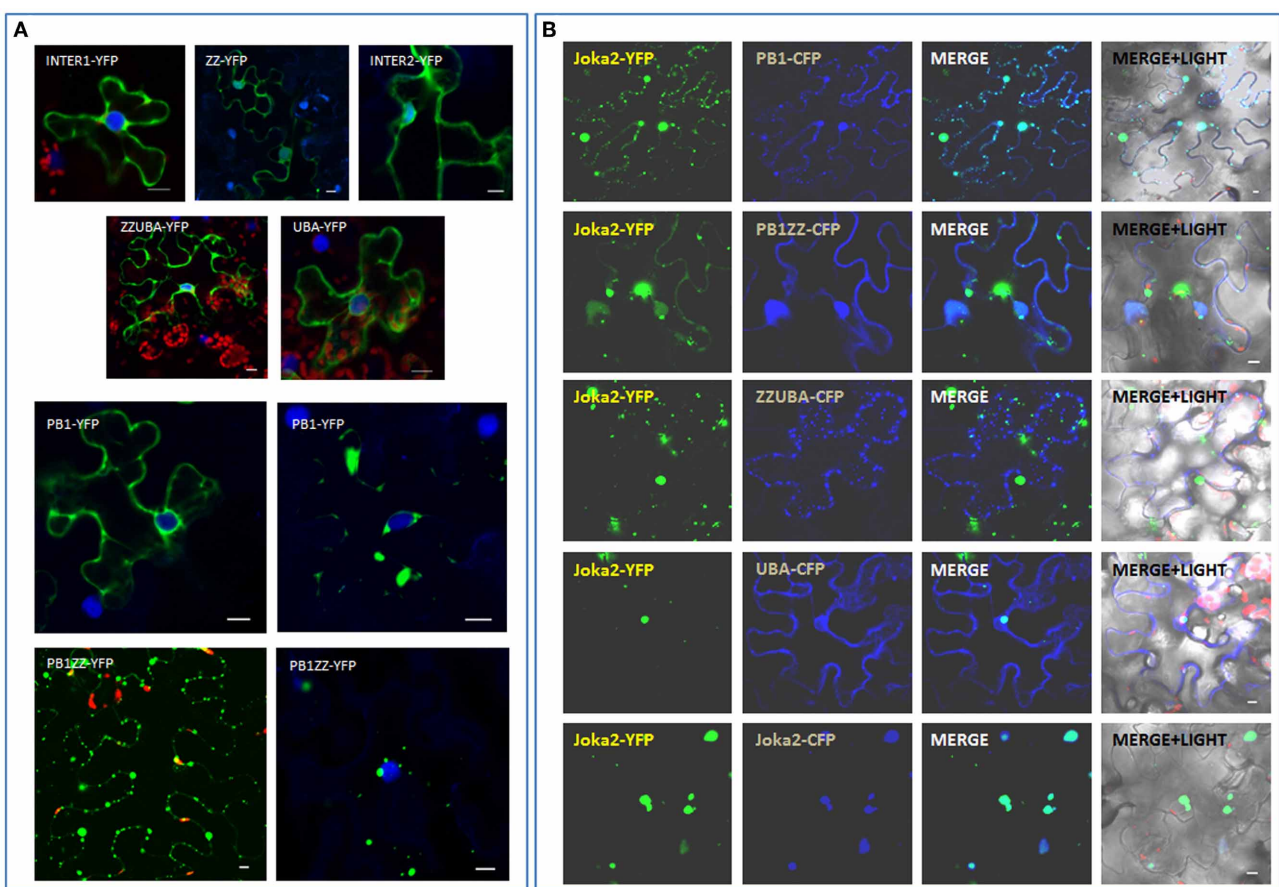
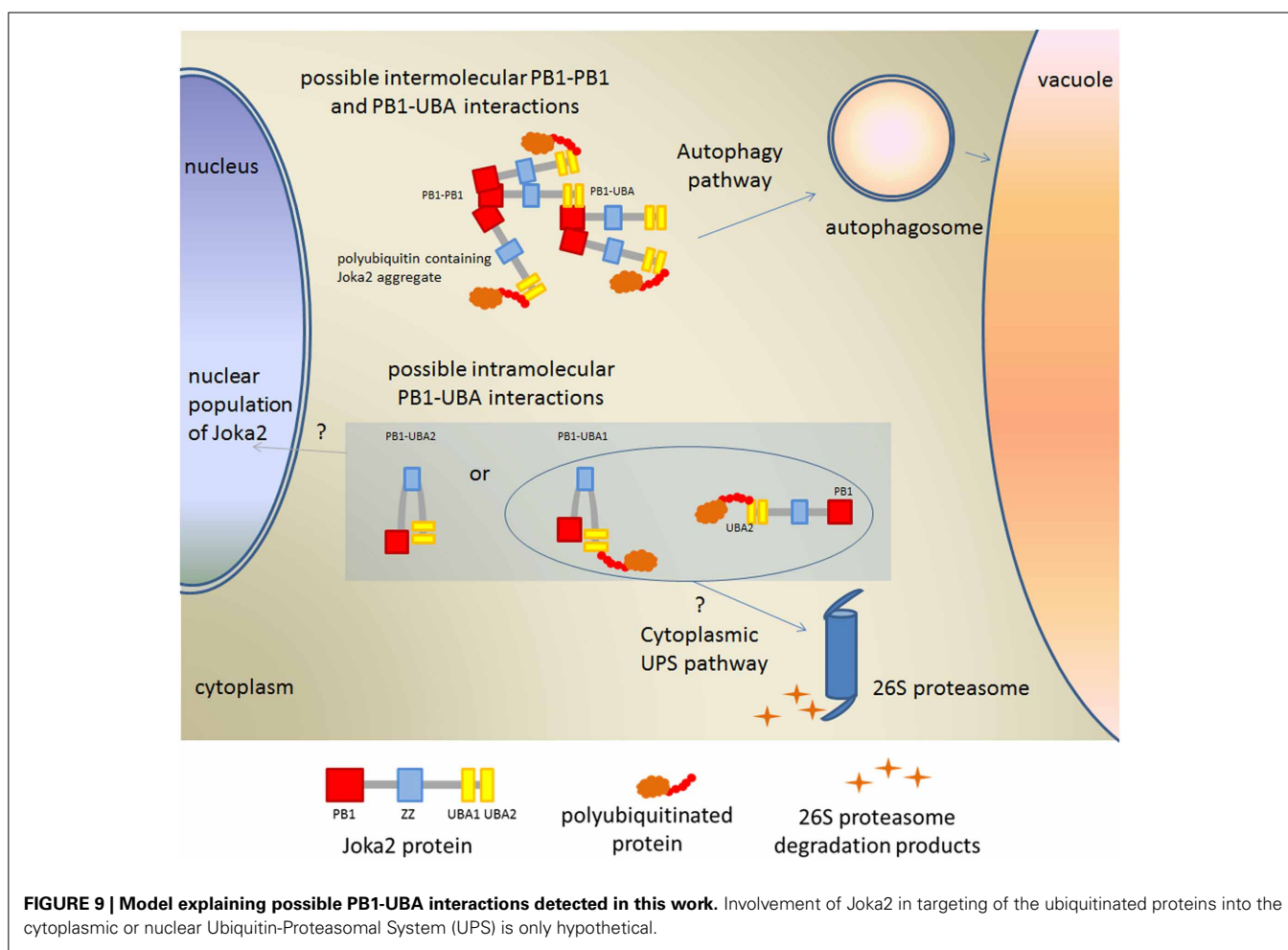
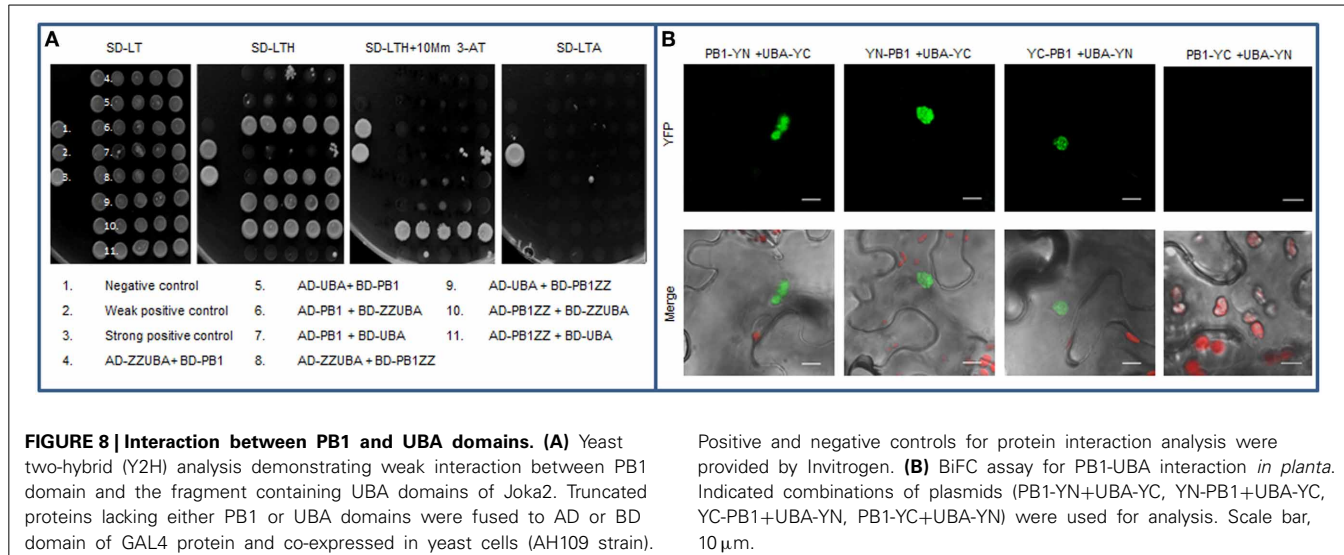


**FIGURE 7 | Involvement of PB1 and UBA domains in formation of Joka2-Joka2 aggregates in planta.** (A) Localization of truncated forms of Joka2 in *N. benthamiana* epidermal cells. (B) Joka2 subcellular

localization analysis after co-expression of Joka2-YFP with various truncated forms of Joka2 linked to CFP in *N. benthamiana* leaves. Scale bar, 10  $\mu$ m.

however, localization of NLS (nuclear localization sequence) was not yet done. Several positions might be considered since several NLS consensuses were detected within Joka2. Nonetheless, the results shown in Figure 2A suggest that NLS must be present in the INT2 region. The function of Joka2 in nucleus is still

unknown. It is possible that Joka2, similarly to ATG8 proteins, accumulates in the nucleus to prevent activation of autophagy by the excess of Joka2 in the cytoplasm or, since UPS is the main degradation pathway in the nucleus, Joka2 could be involved in shuttling of the protein cargos to the nuclear proteasomes as it is



postulated for p62 (Pankiv et al., 2010). Such role of Joka2 is plausible due to the strong structural similarity of Phox/Bem1p (PB1) domain to the ubiquitin-like (UBL) domain directly interacting with proteasome compounds (Hirano et al., 2004).

Joka2 is a strongly aggregating protein. PB1 domain of Joka2 has similar basic/acidic surface to PB1 of p62 protein (Svenning et al., 2011; Zientara-Rytter et al., 2011). It is known that the N-terminal basic charge cluster is able to bind non-covalently to

the C-terminal acidic OPCA motif. Our results indicate that PB1 domain is sufficient for Joka2 oligomerization *in planta* and that the C-terminal region containing UBA1 and UBA2 domains additionally promotes Joka2 aggregation. Moreover, the aggregates formed by the truncated proteins lacking the fragment with UBA domains are mostly not co-localized with ubiquitin aggregates (**Figure 3**), what is in agreement with previously proved involvement of UBA domains in recognition of poly-ubiquitinated proteins (Seibenhener et al., 2004). We noticed that small aggregates formed by the truncated ZZUBA or UBA proteins co-localized with the aggregates formed by recombinant ubiquitin linked to YFP (Ub-VV-YFP). Such co-localization was not observed for truncated Joka2 lacking UBA but possessing PB1 domain. Our data proved that co-localization of Joka2 with ubiquitin linked to YFP is dependent upon the presence of C-terminal UBA domains but not the N-terminal PB1 domain. Therefore, we conclude that at least one of UBA domains of Joka2 (presumably UBA2) is necessary of binding of polyubiquitin aggregates.

We have demonstrated that the specific protein-protein interaction between PB1 and at least one of UBA domain of Joka2 is possible. Such interaction was only hypothesized for other selective autophagy cargo receptors due to the high similarity in domain architecture between, for example, p62 and Dsk2 or Rad23 (Su and Lau, 2009). Our data indicated that interaction between PB1 and at least one of UBA domains takes place *in vivo* and that it is much weaker than PB1-PB1 interaction. Interestingly, such PB1-UBA interaction was only observed in aggregates despite the fact that both truncated proteins were spread in the whole cytoplasm. Also for PB1-PB1 interaction the fluorescent signal was observed mostly in aggregates. This conclusion is supported by the observation that detection of the PB1-PB1 interaction in the cytoplasmic non-aggregated fractions of PB1 proteins was possible only in one combination of the vectors. Therefore, we conclude that PB1-PB1 and PB1-UBA interactions take place mainly in aggregates. Aggregates formation is a consequence of self oligomerization of Joka2 and both types of interactions are necessary for multimerization of Joka2 in poly-ubiquitin-containing aggregates (**Figure 9**).

Interestingly, since the aggregates of p62 have been reported to contain proteasomal components (Seibenhener et al., 2004), it is worth to speculate that Joka2 may interact with proteasomal subunits. Such interaction was previously determined for p62 (Babu et al., 2005; Geetha et al., 2008). The structural similarity of the PB1 domain from Joka2 to the PB1 domain from p62 as well as to the UbL domain, let us hypothesize that Joka2 upon binding of poly-ubiquitinated substrates via one of its C-terminally located UBA domains could bring them directly to proteasome by the presumed direct contact of N-terminal PB1 domain with proteasomal subunits. Thus, it is tempting to speculate that Joka2, similarly to p62 (Seibenhener et al., 2004; Babu et al., 2005; Geetha et al., 2008), could be involved in shuttling of substrates for degradation between UPS and autophagy machinery (**Figure 9**).

## ACKNOWLEDGMENTS

This work was supported by the Polish Ministry of Science and Higher Education (grant No W16/7.PR/2011) and the National Science Centre (grant No 2012/05/N/NZ1/00699).

## SUPPLEMENTARY MATERIAL

The Supplementary Material for this article can be found online at: <http://www.frontiersin.org/journal/10.3389/fpls.2014.00013/abstract>

**Figure S1 | Graphical illustration of Joka2 and its truncated forms used in this study.** The proteins and domains are drawn to scale. See text for details and domains description.

**Figure S2 | Cycling of Joka2-YFP and PB1-YFP between cytoplasm and nucleus is inhibited by LMB treatment.**

**Figure S3 | Subcellular localization analysis of fluorescent signal in cells of transgenic tobacco line AB5 expressing free GFP protein treated (+LMB) and not treated (-LMB) with the inhibitor of nuclear export.** No change in fluorescent protein localization could be noticed regardless from LMB treatment. Arrows indicate nuclei.

**Figure S4 | Schematic illustration of binary vectors used for BiFC assay.**

**Figure S5 | The typical examples of negative controls for BiFC assay.**

## REFERENCES

- Avila, A., Silverman, N., Diaz-Meco, M. T., and Moscat, J. (2002). The Drosophila atypical protein kinase C-ref(2)p complex constitutes a conserved module for signaling in the toll pathway. *Mol. Cell. Biol.* 22, 8787–8795. doi: 10.1128/MCB.22.24.8787-8795.2002
- Babu, J. R., Geetha, T., and Wooten, M. W. (2005). Sequestosome 1/p62 shuttles polyubiquitinated tau for proteasomal degradation. *J. Neurochem.* 94, 192–203. doi: 10.1111/j.1471-4159.2005.03181.x
- Bertolaet, B. L., Clarke, D. J., Wolff, M., Watson, M. H., Henze, M., Divita, G., et al. (2001a). UBA domains mediate protein-protein interactions between two DNA damage-inducible proteins. *J. Mol. Biol.* 313, 955–963. doi: 10.1006/jmbi.2001.5105
- Bertolaet, B. L., Clarke, D. J., Wolff, M., Watson, M. H., Henze, M., Divita, G., et al. (2001b). UBA domains of DNA damage-inducible proteins interact with ubiquitin. *Nat. Struct. Biol.* 8, 417–422. doi: 10.1038/87575
- Bjorkoy, G., Lamark, T., Brech, A., Outzen, H., Perander, M., Overvatn, A., et al. (2005). p62/SQSTM1 forms protein aggregates degraded by autophagy and has a protective effect on huntingtin-induced cell death. *J. Cell Biol.* 171, 603–614. doi: 10.1083/jcb.200507002
- Cariou, B., Perdereau, D., Cailliau, K., Browaeys-Poly, E., Bereziat, V., Vasseur-Cognet, M., et al. (2002). The adapter protein ZIP binds Grb14 and regulates its inhibitory action on insulin signaling by recruiting protein kinase Czeta. *Mol. Cell. Biol.* 22, 6959–6970. doi: 10.1128/MCB.22.20.6959-6970.2002
- Chakrabarty, R., Banerjee, R., Chung, S. M., Farman, M., Citovsky, V., Hogenhout, S. A., et al. (2007). PSITE vectors for stable integration or transient expression of autofluorescent protein fusions in plants: probing *Nicotiana benthamiana*-virus interactions. *Mol. Plant Microbe Interact.* 20, 740–750. doi: 10.1094/MPMI-20-7-0740
- Davies, G. C., Ettenberg, S. A., Coats, A. O., Mussante, M., Ravichandran, S., Collins, J., et al. (2004). Cbl-b interacts with ubiquitinated proteins; differential functions of the UBA domains of c-Cbl and Cbl-b. *Oncogene* 23, 7104–7115. doi: 10.1038/sj.onc.1207952
- Dieckmann, T., Withers-Ward, E. S., Jarosinski, M. A., Liu, C. F., Chen, I. S., and Feigon, J. (1998). Structure of a human DNA repair protein UBA domain that interacts with HIV-1 Vpr. *Nat. Struct. Biol.* 5, 1042–1047. doi: 10.1038/4220
- Funakoshi, M., Sasaki, T., Nishimoto, T., and Kobayashi, H. (2002). Budding yeast Dsk2p is a polyubiquitin-binding protein that can interact with the proteasome. *Proc. Natl. Acad. Sci. U.S.A.* 99, 745–750. doi: 10.1073/pnas.012585199
- Geetha, T., Seibenhener, M. L., Chen, L., Madura, K., and Wooten, M. W. (2008). p62 serves as a shuttling factor for TrkA interaction with the proteasome. *Biochem. Biophys. Res. Commun.* 374, 33–37. doi: 10.1016/j.bbrc.2008.06.082
- Geetha, T., and Wooten, M. W. (2002). Structure and functional properties of the ubiquitin binding protein p62. *FEBS Lett.* 512, 19–24. doi: 10.1016/S0014-5793(02)02286-X
- Gietz, R. D., and Woods, R. A. (2002). Transformation of yeast by lithium acetate/single-stranded carrier DNA/polyethylene glycol method. *Methods Enzymol.* 350, 87–96. doi: 10.1016/S0076-6879(02)50957-5

- Gong, J., Xu, J., Bezanilla, M., Van Huizen, R., Derin, R., and Li, M. (1999). Differential stimulation of PKC phosphorylation of potassium channels by ZIP1 and ZIP2. *Science* 285, 1565–1569. doi: 10.1126/science.285.5433.1565
- Heessen, S., Dantuma, N. P., Tessarz, P., Jellne, M., and Masucci, M. G. (2003). Inhibition of ubiquitin/proteasome-dependent proteolysis in *Saccharomyces cerevisiae* by a Gly-Ala repeat. *FEBS Lett.* 555, 397–404. doi: 10.1016/S0014-5793(03)01296-1
- Hershko, A., and Ciechanover, A. (1998). The ubiquitin system. *Annu. Rev. Biochem.* 67, 425–479. doi: 10.1146/annurev.biochem.67.1.425
- Hirano, Y., Yoshinaga, S., Ogura, K., Yokochi, M., Noda, Y., Sumimoto, H., et al. (2004). Solution structure of atypical protein kinase C PB1 domain and its mode of interaction with ZIP/p62 and MEK5. *J. Biol. Chem.* 279, 31883–31890. doi: 10.1074/jbc.M403092200
- Hofmann, K., and Bucher, P. (1996). The UBA domain: a sequence motif present in multiple enzyme classes of the ubiquitination pathway. *Trends Biochem. Sci.* 21, 172–173. doi: 10.1016/S0968-0004(96)30015-7
- Isogai, S., Morimoto, D., Arita, K., Unzai, S., Tenno, T., Hasegawa, J., et al. (2011). Crystal structure of the ubiquitin-associated (UBA) domain of p62 and its interaction with ubiquitin. *J. Biol. Chem.* 286, 31864–31874. doi: 10.1074/jbc.M111.259630
- Ito, T., Matsui, Y., Ago, T., Ota, K., and Sumimoto, H. (2001). Novel modular domain PB1 recognizes PC motif to mediate functional protein-protein interactions. *EMBO J.* 20, 3938–3946. doi: 10.1093/emboj/20.15.3938
- Karimi, M., De Meyer, B., and Hilson, P. (2005). Modular cloning in plant cells. *Trends Plant Sci.* 10, 103–105. doi: 10.1016/j.tplants.2005.01.008
- Kirkin, V., Lamark, T., Sou, Y. S., Bjorkoy, G., Nunn, J. L., Bruun, J. A., et al. (2009a). A role for NBR1 in autophagosomal degradation of ubiquitinated substrates. *Mol. Cell* 33, 505–516. doi: 10.1016/j.molcel.2009.01.020
- Kirkin, V., McEwan, D. G., Novak, I., and Dikic, I. (2009b). A role for ubiquitin in selective autophagy. *Mol. Cell* 34, 259–269. doi: 10.1016/j.molcel.2009.04.026
- Lamark, T., Perander, M., Outzen, H., Kristiansen, K., Overvatn, A., Michaelsen, E., et al. (2003). Interaction codes within the family of mammalian Phox and Bem1p domain-containing proteins. *J. Biol. Chem.* 278, 34568–34581. doi: 10.1074/jbc.M303221200
- Letunic, I., Goodstadt, L., Dickens, N. J., Doerks, T., Schultz, J., Mott, R., et al. (2002). Recent improvements to the SMART domain-based sequence annotation resource. *Nucleic Acids Res.* 30, 242–244. doi: 10.1093/nar/30.1.242
- Long, J., Gallagher, T. R., Cavey, J. R., Sheppard, P. W., Ralston, S. H., Layfield, R., et al. (2008). Ubiquitin recognition by the ubiquitin-associated domain of p62 involves a novel conformational switch. *J. Biol. Chem.* 283, 5427–5440. doi: 10.1074/jbc.M704973200
- Lowe, E. D., Hasan, N., Trempe, J. F., Fonso, L., Noble, M. E., Endicott, J. A., et al. (2006). Structures of the Dsk2 UBL and UBA domains and their complex. *Acta Crystallogr. D Biol. Crystallogr.* 62, 177–188. doi: 10.1107/S0907444905037777
- Martin, K., Kopperud, K., Chakrabarty, R., Banerjee, R., Brooks, R., and Goodin, M. M. (2009). Transient expression in *Nicotiana benthamiana* fluorescent marker lines provides enhanced definition of protein localization, movement and interactions in planta. *Plant J.* 59, 150–162. doi: 10.1111/j.1365-313X.2009.03850.x
- Moscat, J., and Diaz-Meco, M. T. (2000). The atypical protein kinase Cs. Functional specificity mediated by specific protein adapters. *EMBO Rep.* 1, 399–403. doi: 10.1093/embo-reports/kvd098
- Nakamura, R., Sumimoto, H., Mizuki, K., Hata, K., Ago, T., Kitajima, S., et al. (1998). The PC motif: a novel and evolutionarily conserved sequence involved in interaction between p40phox and p67phox, SH3 domain-containing cytosolic factors of the phagocyte NADPH oxidase. *Eur. J. Biochem.* 251, 583–589. doi: 10.1046/j.1432-1327.1998.2510583.x
- Nelson, B. K., Cai, X., and Nebenfuhr, A. (2007). A multicolored set of *in vivo* organelle markers for co-localization studies in Arabidopsis and other plants. *Plant J.* 51, 1126–1136. doi: 10.1111/j.1365-313X.2007.03212.x
- Pankiv, S., Lamark, T., Bruun, J. A., Overvatn, A., Bjorkoy, G., and Johansen, T. (2010). Nucleocytoplasmic shuttling of p62/SQSTM1 and its role in recruitment of nuclear polyubiquitinated proteins to promyelocytic leukemia bodies. *J. Biol. Chem.* 285, 5941–5953. doi: 10.1074/jbc.M109.039925
- Pawson, T., and Nash, P. (2003). Assembly of cell regulatory systems through protein interaction domains. *Science* 300, 445–452. doi: 10.1126/science.1083653
- Ponting, C. P. (1996). Novel domains in NADPH oxidase subunits, sorting nexins, and PtdIns 3-kinases: binding partners of SH3 domains? *Protein Sci.* 5, 2353–2357. doi: 10.1002/pro.5560051122
- Ponting, C. P., Ito, T., Moscat, J., Diaz-Meco, M. T., Inagaki, F., and Sumimoto, H. (2002). OPR, PC and AID: all in the PB1 family. *Trends Biochem. Sci.* 27, 10. doi: 10.1016/S0968-0004(01)02006-0
- Rao, H., and Sastry, A. (2002). Recognition of specific ubiquitin conjugates is important for the proteolytic functions of the ubiquitin-associated domain proteins Dsk2 and Rad23. *J. Biol. Chem.* 277, 11691–11695. doi: 10.1074/jbc.M200245200
- Sanz, L., Diaz-Meco, M. T., Nakano, H., and Moscat, J. (2000). The atypical PKC-interacting protein p62 channels NF-kappaB activation by the IL-1-TRAF6 pathway. *EMBO J.* 19, 1576–1586. doi: 10.1093/emboj/19.7.1576
- Sanz, L., Sanchez, P., Lallena, M. J., Diaz-Meco, M. T., and Moscat, J. (1999). The interaction of p62 with RIP links the atypical PKCs to NF-kappaB activation. *EMBO J.* 18, 3044–3053. doi: 10.1093/emboj/18.11.3044
- Seibenhener, M. L., Babu, J. R., Geetha, T., Wong, H. C., Krishna, N. R., and Wooten, M. W. (2004). Sequestosome 1/p62 is a polyubiquitin chain binding protein involved in ubiquitin proteasome degradation. *Mol. Cell. Biol.* 24, 8055–8068. doi: 10.1128/MCB.24.18.8055-8068.2004
- Su, V., and Lau, A. F. (2009). Ubiquitin-like and ubiquitin-associated domain proteins: significance in proteasomal degradation. *Cell. Mol. Life Sci.* 66, 2819–2833. doi: 10.1007/s00018-009-0048-9
- Sumimoto, H., Kamakura, S., and Ito, T. (2007). Structure and function of the PB1 domain, a protein interaction module conserved in animals, fungi, amoebas, and plants. *Sci. STKE* 2007:re6. doi: 10.1126/stke.4012007re6
- Svenning, S., Lamark, T., Krause, K., and Johansen, T. (2011). Plant NBR1 is a selective autophagy substrate and a functional hybrid of the mammalian autophagic adaptors NBR1 and p62/SQSTM1. *Autophagy* 7, 993–1010. doi: 10.4161/auto.7.9.16389
- Terasawa, H., Noda, Y., Ito, T., Hatanaka, H., Ichikawa, S., Ogura, K., et al. (2001). Structure and ligand recognition of the PB1 domain: a novel protein module binding to the PC motif. *EMBO J.* 20, 3947–3956. doi: 10.1093/emboj/20.15.3947
- Vadlamudi, R. K., Joung, I., Strominger, J. L., and Shin, J. (1996). p62, a phosphotyrosine-independent ligand of the SH2 domain of p56lck, belongs to a new class of ubiquitin-binding proteins. *J. Biol. Chem.* 271, 20235–20237. doi: 10.1074/jbc.271.34.20235
- Weidberg, H., Shvets, E., and Elazar, Z. (2011). Biogenesis and cargo selectivity of autophagosomes. *Annu. Rev. Biochem.* 80, 125–156. doi: 10.1146/annurev-biochem-052709-094552
- Wilkinson, C. R., Seeger, M., Hartmann-Petersen, R., Stone, M., Wallace, M., Semple, C., et al. (2001). Proteins containing the UBA domain are able to bind to multi-ubiquitin chains. *Nat. Cell Biol.* 3, 939–943. doi: 10.1038/ncb1001-939
- Yoshimori, T. (2004). Autophagy: a regulated bulk degradation process inside cells. *Biochem. Biophys. Res. Commun.* 313, 453–458. doi: 10.1016/j.bbrc.2003.07.023
- Zientara-Rytter, K., Lukomska, J., Moniuszko, G., Gwozdecki, R., Surowiecki, P., Lewandowska, M., et al. (2011). Identification and functional analysis of Joka2, a tobacco member of the family of selective autophagy cargo receptors. *Autophagy* 7, 1145–1158. doi: 10.4161/auto.7.10.16617

**Conflict of Interest Statement:** The authors declare that the research was conducted in the absence of any commercial or financial relationships that could be construed as a potential conflict of interest.

Received: 30 October 2013; accepted: 12 January 2014; published online: 31 January 2014.

Citation: Zientara-Rytter K and Sirko A (2014) Significant role of PB1 and UBA domains in multimerization of Joka2, a selective autophagy cargo receptor from tobacco. *Front. Plant Sci.* 5:13. doi: 10.3389/fpls.2014.00013

This article was submitted to Plant Cell Biology, a section of the journal Frontiers in Plant Science.

Copyright © 2014 Zientara-Rytter and Sirko. This is an open-access article distributed under the terms of the Creative Commons Attribution License (CC BY). The use, distribution or reproduction in other forums is permitted, provided the original author(s) or licensor are credited and that the original publication in this journal is cited, in accordance with accepted academic practice. No use, distribution or reproduction is permitted which does not comply with these terms.



# Role and regulation of autophagy in heat stress responses of tomato plants

Jie Zhou<sup>1,2†</sup>, Jian Wang<sup>1†</sup>, Jing-Quan Yu<sup>1</sup> and Zhixiang Chen<sup>1,2\*</sup>

<sup>1</sup> Department of Horticulture, Zhejiang University, Hangzhou, China

<sup>2</sup> Department of Botany and Plant Pathology, Purdue University, West Lafayette, IN, USA

**Edited by:**

Diane C. Bassham, Iowa State University, USA

**Reviewed by:**

Viktor Zarsky, Charles University, Czech Republic

Allan Caplan, University of Idaho, USA

**\*Correspondence:**

Zhixiang Chen, Department of Botany and Plant Pathology, Purdue University, 915 W. State Street, West Lafayette, IN 47907-2054, USA  
e-mail: zhixiang@purdue.edu

<sup>†</sup>These authors have contributed equally to this work.

As sessile organisms, plants are constantly exposed to a wide spectrum of stress conditions such as high temperature, which causes protein misfolding. Misfolded proteins are highly toxic and must be efficiently removed to reduce cellular proteotoxic stress if restoration of native conformations is unsuccessful. Although selective autophagy is known to function in protein quality control by targeting degradation of misfolded and potentially toxic proteins, its role and regulation in heat stress responses have not been analyzed in crop plants. In the present study, we found that heat stress induced expression of autophagy-related (ATG) genes and accumulation of autophagosomes in tomato plants. Virus-induced gene silencing (VIGS) of tomato ATG5 and ATG7 genes resulted in increased sensitivity of tomato plants to heat stress based on both increased development of heat stress symptoms and compromised photosynthetic parameters of heat-stressed leaf tissues. Silencing of tomato homologs for the selective autophagy receptor NBR1, which targets ubiquitinated protein aggregates, also compromised tomato heat tolerance. To better understand the regulation of heat-induced autophagy, we found that silencing of tomato ATG5, ATG7, or NBR1 compromised heat-induced expression of not only the targeted genes but also other autophagy-related genes. Furthermore, we identified two tomato genes encoding proteins highly homologous to Arabidopsis WRKY33 transcription factor, which has been previously shown to interact physically with an autophagy protein. Silencing of tomato WRKY33 genes compromised tomato heat tolerance and reduced heat-induced ATG gene expression and autophagosome accumulation. Based on these results, we propose that heat-induced autophagy in tomato is subject to cooperative regulation by both WRKY33 and ATG proteins and plays a critical role in tomato heat tolerance, mostly likely through selective removal of heat-induced protein aggregates.

**Keywords:** autophagy, heat tolerance, tomato, WRKY33, NBR1, ATG5, ATG7

## INTRODUCTION

Autophagy is a highly conserved intracellular degradation system in eukaryotes for removal and recycling of cytoplasmic components including damaged proteins and organelles (Klionsky, 2005). Central to autophagy is the formation of autophagosomes resulting from the dynamic membrane reorganization. In yeast, more than 30 autophagy-related (ATG) genes have been identified and their products often form functional groups that cooperate to perform the physiologically continuous but mechanistically distinct processes of autophagy including the induction of autophagy, autophagosome nucleation, elongation, maturation, and fusion with vacuoles (He and Klionsky, 2009). Autophagy is active at very low levels but is highly inducible in responses to stress and extracellular cues (He and Klionsky, 2009). In yeast and animal systems, the serine/threonine protein kinase TOR (target of rapamycin) functions as a central inhibitor of autophagosome formation. In yeast, inhibition of TOR leads to activation of ATG1, which can then bind ATG13 and ATG17 with increased affinities to promote assembly of the ATG1-ATG13-ATG17 scaffold and initiation of autophagosome formation through recruitment of multiple ATG proteins (He and Klionsky, 2009). The

rapid increase in the autophagic flux during the early minutes or hours of exposure to stress conditions is mostly mediated by post-translational modifications of the core machinery of autophagy (He and Klionsky, 2009). A delayed and protracted autophagic response, however, also relies on activation of specific transcription programs involving stress-responsive transcription factors.

Over the past two decades or so, more than 30 ATG genes have been identified in Arabidopsis and other plants including tobacco, rice, and maize. Functional analysis of the ATG genes has shown that autophagy plays an important role in nutrient recycling and utilization in plants (Bassham et al., 2006; Liu and Bassham, 2012). Autophagy is also involved in the regulation of plant senescence, which may be considered a process of nutrient redistribution. In addition, autophagy shapes plant innate immune responses (Zhou et al., 2014b). Autophagy is also induced by a wide spectrum of abiotic stresses including oxidative, high salt, osmotic stress and heat conditions (Slavikova et al., 2008; Liu et al., 2009). Autophagy-defective mutants or transgenic plants are hypersensitive to reactive oxygen species (ROS), salt, drought, and heat conditions (Xiong et al., 2007a,b;

Liu et al., 2009; Zhou et al., 2013, 2014c). As in other organisms, formation of autophagosomes and expression of ATG genes are induced by a variety of stresses and environmental cues in plants. TOR is also a negative regulator of autophagy in plants (Liu and Bassham, 2010). Furthermore, a NADPH oxidase inhibitor blocks autophagy induction upon nutrient starvation and salt stress, but not during osmotic stress (Liu and Bassham, 2010). Thus, ROS may mediate induction of autophagy during some, but not all stress conditions. There is, however, little information available about the transcriptional regulation of plant autophagy-associated genes under stress conditions.

In the present study, we analyze the role and regulation of autophagy in heat stress tolerance of tomato plants (*Solanum lycopersicum*). Heat is an important abiotic stress condition that can cause misfolding and denaturation of proteins. As an important protein quality control mechanism, autophagy could play a critical role in removal of those misfolded/denatured and potentially highly toxic proteins or protein aggregates that fail to be reestablished for normal protein conformations (Kraft et al., 2010; Johansen and Lamark, 2011; Shaid et al., 2013). Tomato is one of the most important vegetable plants closely related to many commercially important plants including potato, eggplant, peppers, tobacco, and petunias and an important model plant because it has a number of interesting features such as fleshy fruits not shared by other model plants (e.g., *Arabidopsis* and rice) and has many recognized wild species. The tomato genome has been sequenced (Consortium, 2012) and its genes can be functionally analyzed through a number of complementary approaches including virus-induced gene silencing (VIGS) (Liu et al., 2002). From the sequenced tomato genome, we have identified tomato homologs for ATG5 and ATG7, two important autophagy-related proteins that have been subjected to functional analysis in *Arabidopsis* (Yoshimoto, 2010; Lai et al., 2011b; Zhou et al., 2013). We have also identified tomato homologs for NBR1, a plant selective autophagy receptor (Svenning et al., 2011; Zhou et al., 2013, 2014c), and WRKY33, a transcription factor that physically interacts with ATG18a in *Arabidopsis* (Lai et al., 2011b). Using a variety of molecular approaches including VIGS, we analyzed the roles of these genes in heat-induced autophagy and heat stress tolerance. These experiments not only support the critical role of autophagy in plant heat tolerance but also provide new important insights into the regulation of autophagy during plant stress responses.

## MATERIALS AND METHODS

### PLANT MATERIALS AND GROWTH CONDITIONS

Tomato (*Solanum lycopersicum* L. cv. Ailsa Craig) seeds were germinated in a growth medium filled with a mixture of peat and vermiculite (7:3, v/v) in trays in a growth chamber. When the first true leaf was fully expanded, seedlings were transplanted into plastic pots containing the same medium. The growth conditions were as follows: light/dark cycle, 22/20°C, and photosynthetic photon flux density (PPFD), 600  $\mu\text{mol m}^{-2} \text{s}^{-1}$ .

### QUANTITATIVE RT-PCR (qRT-PCR)

Total RNA was isolated from tomato leaves using Trizol reagent (Sangon Co., Shanghai, China), according to the manufacturer's

recommendations. Genomic DNA was removed with the RNeasy Mini Kit (Qiagen Co., Hilden, Germany). 1  $\mu\text{g}$  RNA was reverse-transcribed using the ReverTra Ace qPCR RT Kit (Toyobo Co., Osaka, Japan), following the manufacturer's instructions. Gene-specific RT-PCR primers were designed based on their cDNA sequences (Supplemental Table S1).

The quantitative real-time PCR was performed using the iCycleri QTM real-time PCR detection system (Bio-Rad Co., Hercules, CA, USA). Each reaction (25  $\mu\text{L}$ ) consisted 12.5  $\mu\text{L}$  of SYBR Green PCR Master Mix (Takara Co., Chiga, Japan), 1  $\mu\text{L}$  of diluted cDNA and 0.1  $\mu\text{mol}$  forward and reserve primers. The PCR cycling conditions and the calculation of relative gene expression were as previously described. The tomato *ACTIN* gene was used as internal control as previously described (Zhou et al., 2014a).

### VIRUS-INDUCED GENE SILENCING (VIGS)

The tobacco rattle virus (TRV) VIGS constructs for silencing of tomato *ATG5*, *ATG7*, *NBR1a*, *NBR1b*, *WRKY33a*, and *WRKY33b* genes were generated by PCR amplification using gene-specific primers (Supplemental Table S2), digested with appropriate restriction enzymes and ligated into the same sites of pTRV2. The resulting plasmids were transformed into *Agrobacterium tumefaciens* GV3101. *Agrobacterium*-mediated virus infection was performed as previously described (Ekengren et al., 2003). Plants were then kept at 22/20°C under 150  $\mu\text{mol m}^{-2} \text{s}^{-1}$  PPFD for 30 days before they were used for the experiments (Kandoth et al., 2007). Leaflets in the terminal of the fifth fully expanded leaves, which showed 20–30% transcript levels of control plants, were used. Each replicate had 12 plants.

### ASSESSMENT OF HEAT TOLERANCE

To evaluate the role of autophagy in heat stress responses of tomato plants, tomato plants at the five-leaf stage were transferred to a growth chamber for heat stress treatment (45°C, 400  $\mu\text{mol m}^{-2} \text{s}^{-1}$  PPFD, 8 h).

For determination of electrolyte leakage (EL) caused by high temperature, the leaflets in the terminal of the fifth fully expanded leaves were measured after heat stress as previous described (Huang et al., 2010). Chlorophyll fluorescence was measured using an Imaging-PAM Chlorophyll Fluorometer equipped with a computer-operated PAM-control unit (IMAG-MAXI; Heinz Walz, Effeltrich, Germany). The plants were maintained in the dark for more than 30 min before the measurements were performed. The intensities of the actinic light and saturating light were 280 and 2500  $\mu\text{mol mol}^{-2} \text{s}^{-1}$  PPFD, respectively. The maximum quantum yield of PSII (Fv/Fm) was measured and calculated as previous described (Zhou et al., 2014a). Three replicates for each treatment were used with 12 plants for each replicate.

The light-saturated CO<sub>2</sub> assimilation (Asat), stomatal conductance (Gs), and intracellular CO<sub>2</sub> concentration (Ci) were determined in the silenced and pTRV plants with an infrared gas analyzer-based potable photosynthesis system (LI-6400; LI-COR, Lincoln, NE, USA). The air temperature, relative humidity, CO<sub>2</sub> concentration, and PPFD were maintained at 22°C, 85%, 380  $\mu\text{mol mol}^{-1}$ , and 1000  $\mu\text{mol m}^{-2} \text{s}^{-1}$ , respectively.

## SEPARATION AND MEASUREMENTS OF TOTAL AND INSOLUBLE PROTEINS

Tomato leaves were collected before and after heat treatment, ground in liquid nitrogen and homogenized in a detergent containing extraction buffer (100 mM Tris/HCl, pH 8.0, 10 mM NaCl, 1 mM EDTA, 1% Triton X-100, 0.2%  $\beta$ -mercaptoethanol). Soluble and detergent-resistant insoluble proteins were separated through low-speed centrifugation and measured as previously described (Zhou et al., 2013).

## VISUALIZATION OF INDUCTION OF AUTOPHAGY

For visualization of autophagosomes, tomato leaves were vacuum-infiltrated with 1  $\mu$ M of the fluorescence dye Lysotracker Green DND-26 (Cell Signaling Technology, Danvers, MA, USA) or 500  $\mu$ M of monodansylcadaverine (MDC) (Sigma-Aldrich, St. Louis, MO, USA). Fluorescence was visualized using a Zeiss LSM510 UVMeta laser scanning confocal microscope (Zeiss Co., Munchen, Germany) and images were superimposed using Zeiss LSM510 software.

## RESULTS

### IDENTIFICATION OF TOMATO ATG5, ATG7, AND NBR1 GENES

To analyze the role of autophagy in tomato heat tolerance, we chose first to focus on tomato *ATG5* and *ATG7* as potential targets for gene silencing as their products are required for the core process of autophagy and mutants of their Arabidopsis homologs, which are single-copy genes, have been widely used for functional analysis of autophagy (Yoshimoto, 2010; Lai et al., 2011b; Zhou et al., 2013). From the sequenced tomato genome, we identified two tomato *ATG5* genes, *ATG5a* (Sl02g038380) and *ATG5b* (Sl06g043140). Based on its genomic and full-length cDNA sequences, *ATG5a* has an intron-exon structure similar to that of Arabidopsis *ATG5* with eight exons and seven introns (**Supplemental Figure 1A**). *ATG5a* encodes a protein containing 369 amino acid residues and sharing approximately 60% sequence identity with Arabidopsis *ATG5*. The genomic sequence of tomato *ATG5b* is 97% identical to the coding sequence of tomato *ATG5a* (**Supplemental Figure 1B**). The lack of introns in tomato *ATG5b* indicates that the gene was copied from mRNA of tomato *ATG5a* and incorporated into the tomato genome. Further sequence analysis revealed multiple mutations in tomato *ATG5b*, including a G to A transition at nucleotide position 246 that changes a tryptophan to a stop codon, resulting in a predicted loss of the last 277 amino acids (77%) of the polypeptide if the mutation is not removed by alternative splicing (**Supplemental Figure 2**). Thus, tomato *ATG5b* likely encodes a nonfunctional protein even if it is expressed in tomato tissues. Like Arabidopsis, tomato contains a single *ATG7* gene (Sl11g068930) that encodes a protein of 715 amino acid residues. Tomato *ATG7* shares approximately 70% sequence identity with Arabidopsis *ATG7*.

There is a mounting body of evidence that selective autophagy of dysfunctional organelles and toxic macromolecules mediated by selective autophagy receptors play a critical role in protein/organelle quality control and in responses to adverse environmental and physiological conditions (Kraft et al., 2010; Johansen and Lamark, 2011; Floyd et al., 2012; Shaid et al., 2013). Previously Arabidopsis *NBR1*, homolog of the mammalian

autophagy receptors P62 and *NBR1*, has been analyzed and found to play a critical role in plant responses to a spectrum of abiotic stresses by targeting stress-induced cytosolic protein aggregates (Zhou et al., 2013). Unlike in Arabidopsis, which contains a single *NBR1* gene, tomato contains two *NBR1* genes, *NBR1a* (Sl03g112230), and *NBR1b* (Sl06g071770), with intron-exon structures similar to each other and to that of Arabidopsis *NBR1*. Tomato *NBR1a* and *NBR1b* encodes proteins of 864 and 737 amino acids, respectively (**Supplemental Figure 3**), which share approximately 50% sequence identify with each other and with that of Arabidopsis *NBR1*. Like Arabidopsis *NBR1*, both tomato *NBR1a* and *NBR1b* contain two highly conserved ubiquitin-associated (UBA) domains and a WxxI ATG8-interacting motif at their respective C-terminus (**Supplemental Figure 3**).

### HEAT INDUCTION OF AUTOPHAGY-RELATED GENES IN TOMATO

To determine the role of autophagy in tomato heat tolerance, we firstly analyzed the effect of heat stress on expression of tomato *ATG5*, *ATG7*, and *NBR1* genes. Tomato seedlings were placed in the 22 and 45°C chambers, and the *ATG* and *NBR1* gene transcripts were analyzed by qRT-PCR using total RNA isolated from the leaflets of the fifth fully expanded leaves. As shown in **Figure 1**, the levels of tomato *ATG5*, *ATG7* and *NBR1* transcripts remained unchanged at 22°C throughout the 8-h period of the experiments. In contrast, transcript levels of the autophagy genes were elevated after 2–4 h of heat stress (45°C) and displayed large increases after 6 h of heat stress (**Figure 1**). After 6-h heat stress, the transcript levels of the *ATG* and *NBR1* genes started to decline and reduced to basal levels by 8 h at 45°C, when the leaves of seedlings started to show symptoms of dehydration (**Figure 1**). Thus, heat stress induced the expression of autophagy-related genes.

### SILENCING OF TOMATO ATG5, ATG7, AND NBR1 GENES

To determine directly the role of autophagy in tomato responses to heat stress, we used VIGS to assess the impact of down-regulated expression of tomato *ATG5*, *ATG7*, *NBR1a*, and *NBR1b* on tomato heat tolerance. Gene-specific DNA fragments were cloned into the pTRV vector and *Agrobacterium* cells harboring the VIGS vectors were infiltrated into tomato cotyledons. We used qRT-PCR to compare the transcript levels for tomato *ATG5*, *ATG7*, *NBR1a*, and *NBR1b* in tomato plants infiltrated with the pTRV empty vector or infiltrated with the pTRV-*ATG5*, pTRV-*ATG7*, pTRV-*NBR1a*, or pTRV-*NBR1b* silencing vector. As shown in **Figure 2**, the basal transcript levels of *ATG5*, *ATG7*, *NBR1a*, and *NBR1b* were unchanged in tomato plants after infiltration with the pTRV empty vector but decreased 70–80% in the leaves of plants after infiltration with their respective silencing vectors (**Figure 2**). No significant alteration in growth or development was observed upon silencing of the *ATG5*, *ATG7*, *NBR1a*, or *NBR1b* gene.

Abiotic stress including high temperature induces both *ATG* gene expression and formation of autophagosomes. To further assess the effect of silencing of tomato *ATG5* and *ATG7* on heat-induced autophagy, we used Lysotracker Green dye as a probe to detect autolysosome-like structures. The Lysotracker dye has been widely used as a probe for detecting autophagic activity in a variety of organisms including plants (Otegui et al.,

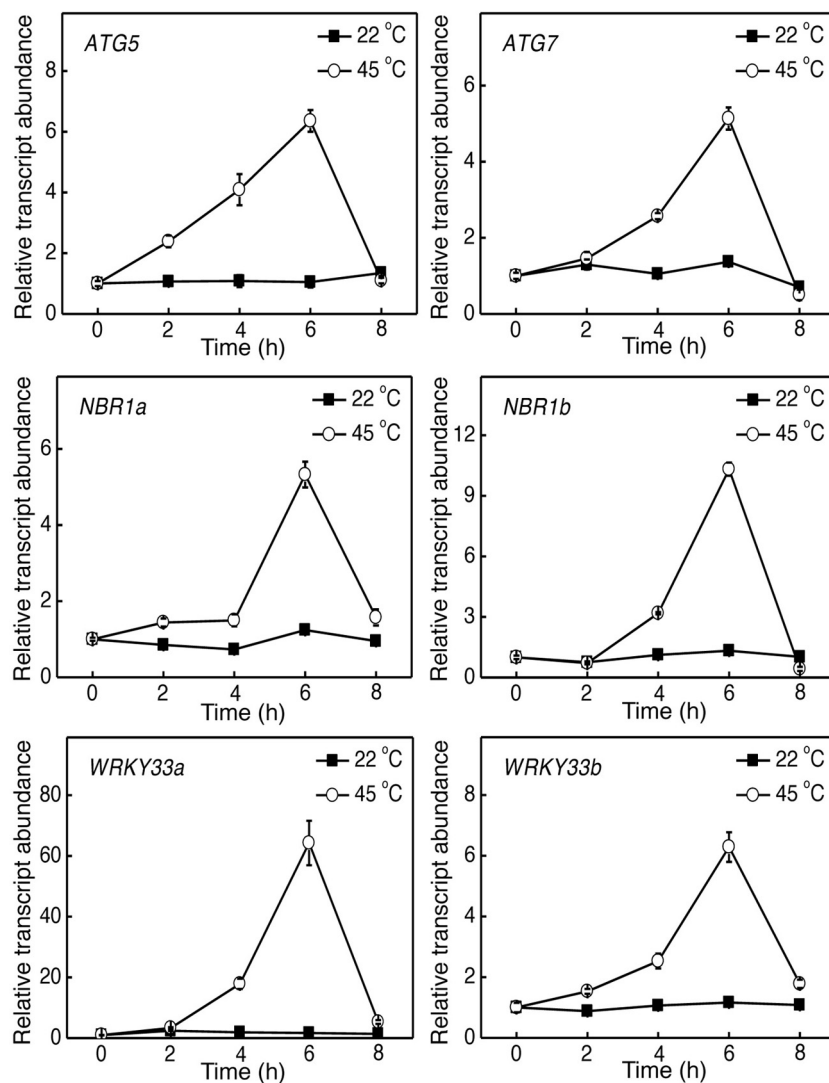


**FIGURE 1 | Induction of tomato *ATG5*, *ATG7*, *NBR1*, and *WRKY33* genes by heat stress.** Six weeks-old tomato plants were placed in the 22 and 45°C growth chambers and total

RNA was isolated from leaf samples collected at indicated times. Transcript levels were determined using real-time qRT-PCR. Error bars indicate SE ( $n = 3$ ).

2005). Comparative studies with other autophagosome makers such as ATG8 have shown that although Lysotracker dyes stain acidic organelles, including autophagosomes, up-regulated Lysotracker-stained structures are biologically characteristic of induced autophagic activity (Phadwal et al., 2012; Chikte et al., 2014). Under the normal temperature (22°C), we observed low numbers of punctate green fluorescent signals in both pTRV and gene silenced plants (Figure 3). After 6-h heat stress, however, the numbers of punctate green fluorescent signals increased by more than 10 fold in the control plants infiltrated with the pTRV empty vector (Figure 3). Importantly, in the plants infiltrated with the pTRV-*ATG5* or pTRV-*ATG7* silencing vector, there was only a 2–3-fold increase in the numbers of the punctate fluorescence signals after 6-h heat stress (Figure 3).

We also used MDC as a probe for detection of autophagic activity in tomato leaves. MDC is an autofluorescent dye that stains autophagosomes in mammals and plants (Biederbick et al., 1995; Munafó and Colombo, 2001; Contento et al., 2005; Liu and Bassham, 2010). Under the normal temperature (22°C), again, we observed low numbers of punctate fluorescent signals in both control (pTRV) and *ATG5*- or *ATG7*-silenced plants (Figure 4). After treatment with dithiothreitol (DTT), a known inducer of autophagy (Liu et al., 2012), the numbers of punctate fluorescent signals increased by more than 8 fold in control plants infiltrated with the pTRV empty vector (Figure 4). After 6-h heat treatment, the numbers of punctate fluorescent signals also increased by about 6 fold in control plants infiltrated with the pTRV empty vector (Figure 4). In the plants infiltrated with the pTRV-*ATG5* or pTRV-*ATG7*

silencing vector, the numbers of the punctate fluorescence signals after DTT or heat stress were substantially reduced when compared to those in DTT- or heat-treated control plants (**Figure 4**). These observations confirmed that heat-induced autophagy was

partially blocked by silencing of the tomato *ATG5* and *ATG7* genes.

### COMPROMISED HEAT TOLERANCE OF AUTOPHAGY-SILENCED TOMATO PLANTS

For comparison of heat tolerance of pTRV, pTRV-*ATG5*, pTRV-*ATG7*, pTRV-*NBR1a*, and pTRV-*NBR1b* plants, they were placed in a 45°C growth chamber for 8 h and then moved to room temperature for 3-day recovery. For heat-treated pTRV control plants, only patches of old leaves displayed symptoms of dehydration while a majority of the leaves remained green and viable after recovery (**Figure 5A**). On the other hand, a majority of fully expanded leaves from the pTRV-*ATG5*, pTRV-*ATG7*, pTRV-*NBR1a*, and pTRV-*NBR1b* plants exhibited wilting after the recovery (**Figure 5A**). The more severe symptoms in autophagy-suppressed tomato plants after heat stress were confirmed by increased EL in the silenced plants relative to that in the pTRV control plants (**Figure 5B**).

Heat has a harmful effect on various biology processes including photosynthesis. To further investigate responses of *ATG5*, *ATG7*, and *NBR1*-silenced tomato plants to heat stress, we compared these tomato plants with the pTRV control tomato plants for the effects of heat stress on the maximum quantum yield of photosystem II (PSII) (*Fv/Fm*) of leaves immediately after heat treatment and light-saturated CO<sub>2</sub> assimilation rate (*Asat*) following 1-day recovery after heat stress. As shown in **Figure 6**, after 8-h at 45°C, *Fv/Fm* values for silencing plants were 22–37% lower than those of control pTRV plants. Likewise, the *Asat* values for the silenced plants were 35–68% lower than those of

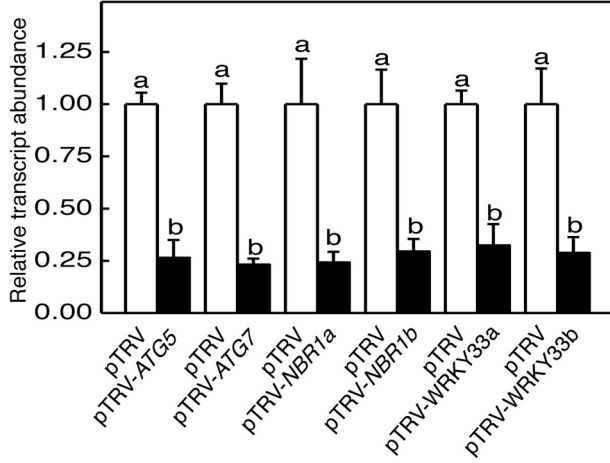


**FIGURE 2 | TRV-mediated silencing of tomato *ATG5*, *ATG7*, *NBR1*, and *WRKY33* genes.** Transcript levels for each silenced gene in tomato plants infiltrated with *Agrobacterium* cells harboring the empty pTRV vector or the corresponding silencing vector were determined by qRT-PCR analysis using total RNA isolated from the terminal leaflets of the fifth leaves of *Agrobacterium*-infiltrated tomato plants. Error bars indicate SE ( $n = 3$ ). According to Duncan's multiple range test ( $P = 0.05$ ), means of lesion areas do not differ significantly if they are indicated with the same letter.

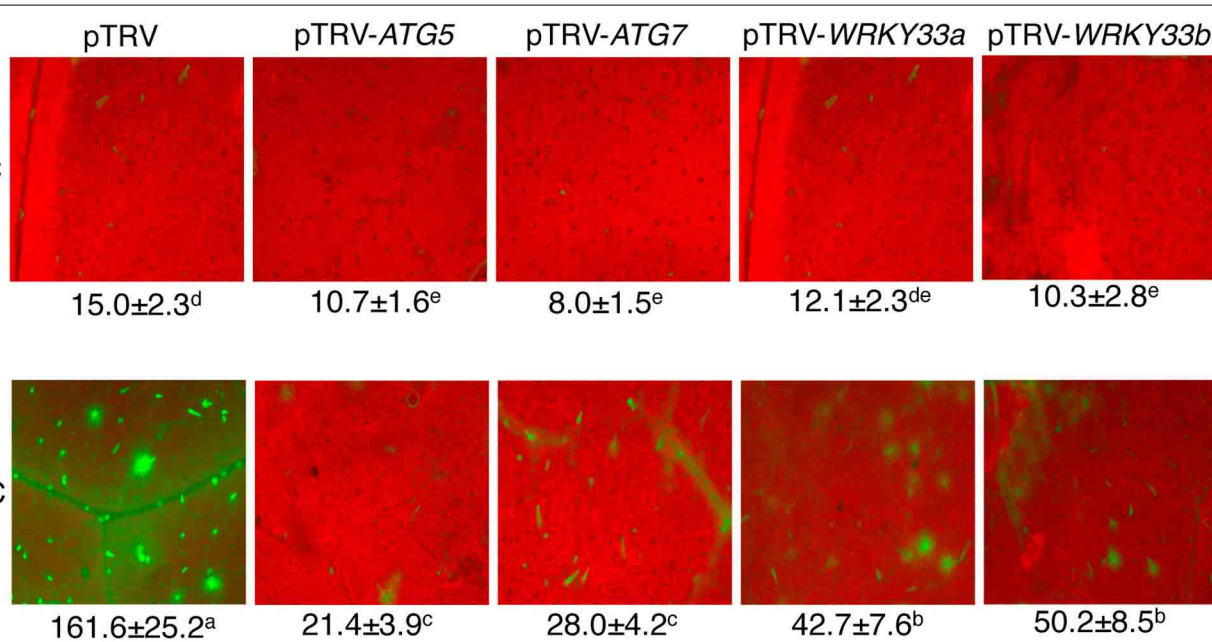
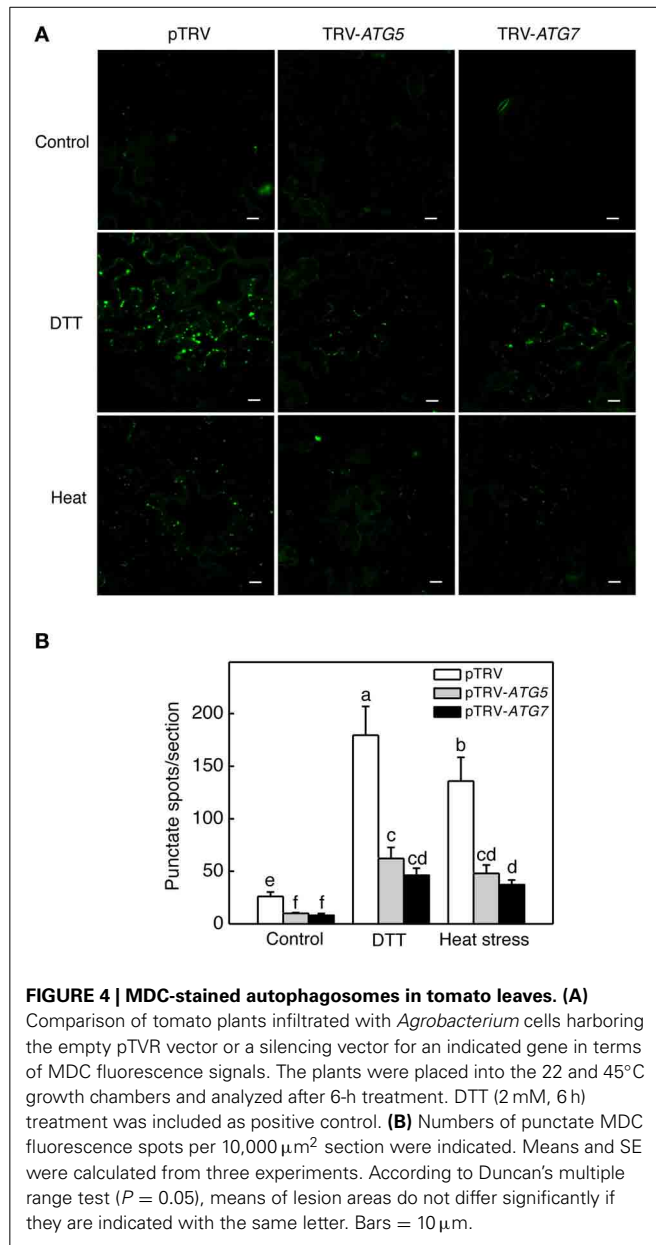


**FIGURE 3 | Detection of autophagic activity using Lysotracker Green.**

Comparison of tomato plants infiltrated with *Agrobacterium* cells harboring the empty pTRV vector or a silencing vector for an indicated gene in terms of Lysotracker Green fluorescence signals. The plants were placed into the 22 and 45°C growth chambers and analyzed after 6-h treatment. Numbers of

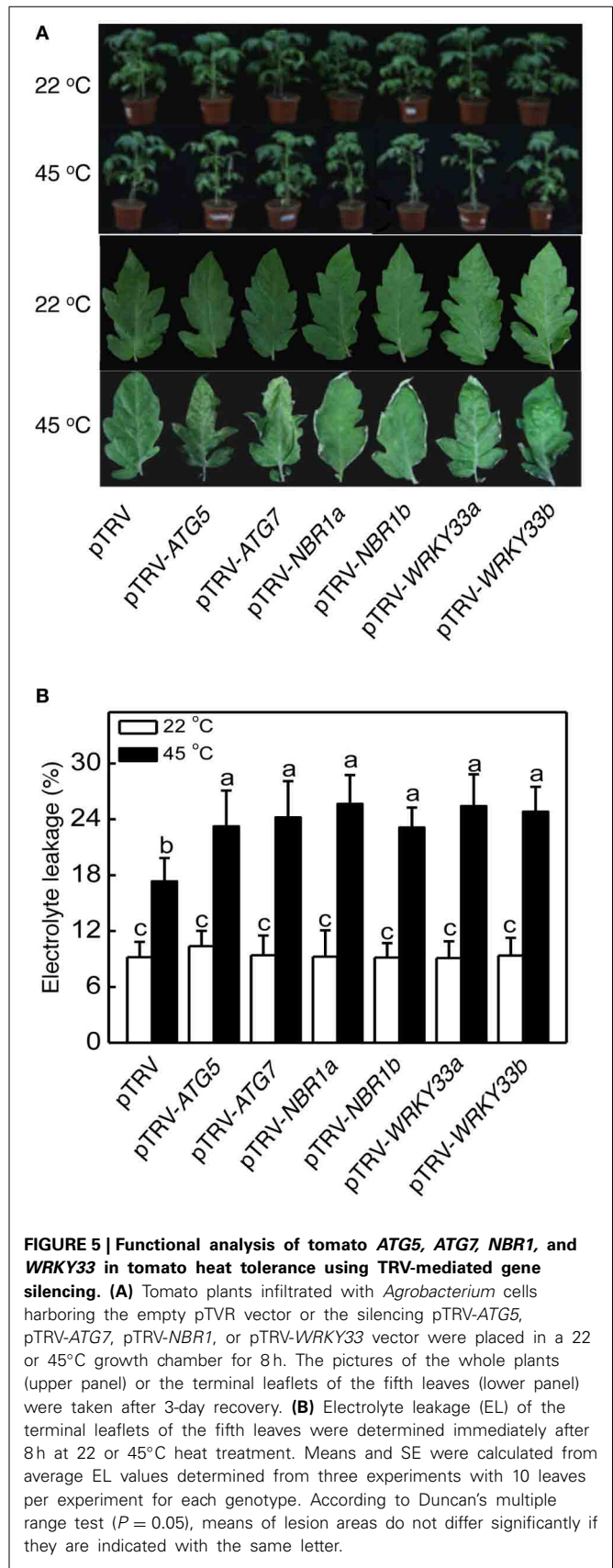
punctate Lysotracker Green fluorescence spots per 10,000  $\mu\text{m}^2$  section from the cells in the central areas of the terminal leaflets of the fifth leaves were indicated below the images. Means and SE were calculated from three experiments. According to Duncan's multiple range test ( $P = 0.05$ ), means of lesion areas do not differ significantly if they are indicated with the same letter.



pTRV control plants when assayed after 1-day recovery following heat stress (Figure 7). In addition, *ATG5*-, *ATG7*-, and *NBR1*-silenced tomato plants had reduced stomatal conductance ( $G_s$ ) and intracellular  $\text{CO}_2$  concentration ( $C_i$ ) compared to the unsilenced pTRV control plants after heat stress (Figure 7). Thus, photosynthetic efficiency and capacity were more compromised by heat stress in the autophagy-suppressed tomato plants than in the control plants.

#### INCREASED ACCUMULATION OF INSOLUBLE PROTEINS IN AUTOPHAGY-SILENCED PLANTS

Heat stress causes protein misfolding and denaturation, which can result in formation of protein aggregates and proteotoxic



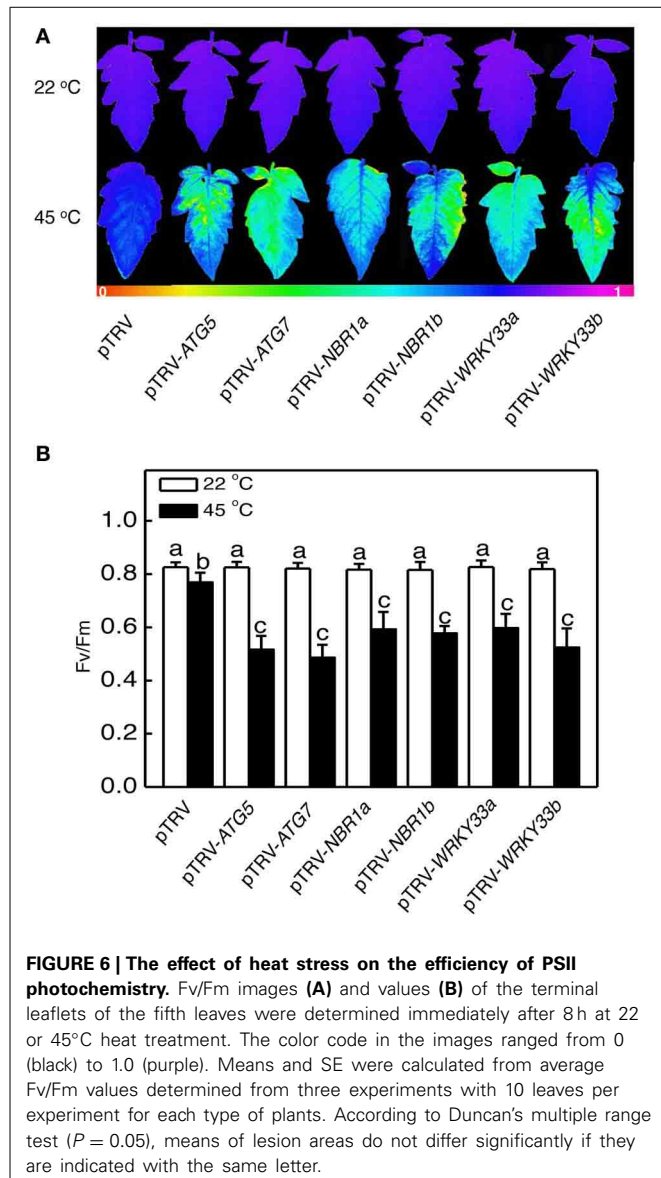


**FIGURE 6 |** The effect of heat stress on the efficiency of PSII photochemistry. Fv/Fm images (**A**) and values (**B**) of the terminal leaflets of the fifth leaves were determined immediately after 8 h at 22 or 45°C heat treatment. The color code in the images ranged from 0 (black) to 1.0 (purple). Means and SE were calculated from average Fv/Fm values determined from three experiments with 10 leaves per experiment for each type of plants. According to Duncan's multiple range test ( $P = 0.05$ ), means of lesion areas do not differ significantly if they are indicated with the same letter.

stress. To analyze the role of autophagy in protection against heat-induced proteotoxic stress, we investigated the accumulation of insoluble, detergent-resistant proteins in the pTRV, pTRV-ATG5, pTRV-ATG7, pTRV-NBR1a, and pTRV-NBR1b plants after 8 h heat treatment. Total proteins were first isolated and insoluble proteins were separated by low speed centrifugation. As shown in **Figure 8**, the percentages of insoluble to total proteins were similar in all plants when they were grown at 22°C. After 8-h heat stress, insoluble proteins as percentages to total proteins increased only by 40% in unsilenced pTRV control plants but increased by 138–154% in the pTRV-ATG5, pTRV-ATG7, pTRV-NBR1a, and pTRV-NBR1b plants (**Figure 8**). By the end of the heat stress, the levels of insoluble proteins in the ATG5-, ATG7-, and NBR1-silenced tomato plants were more than two times higher than those in the unsilenced control plants (**Figure 8**).

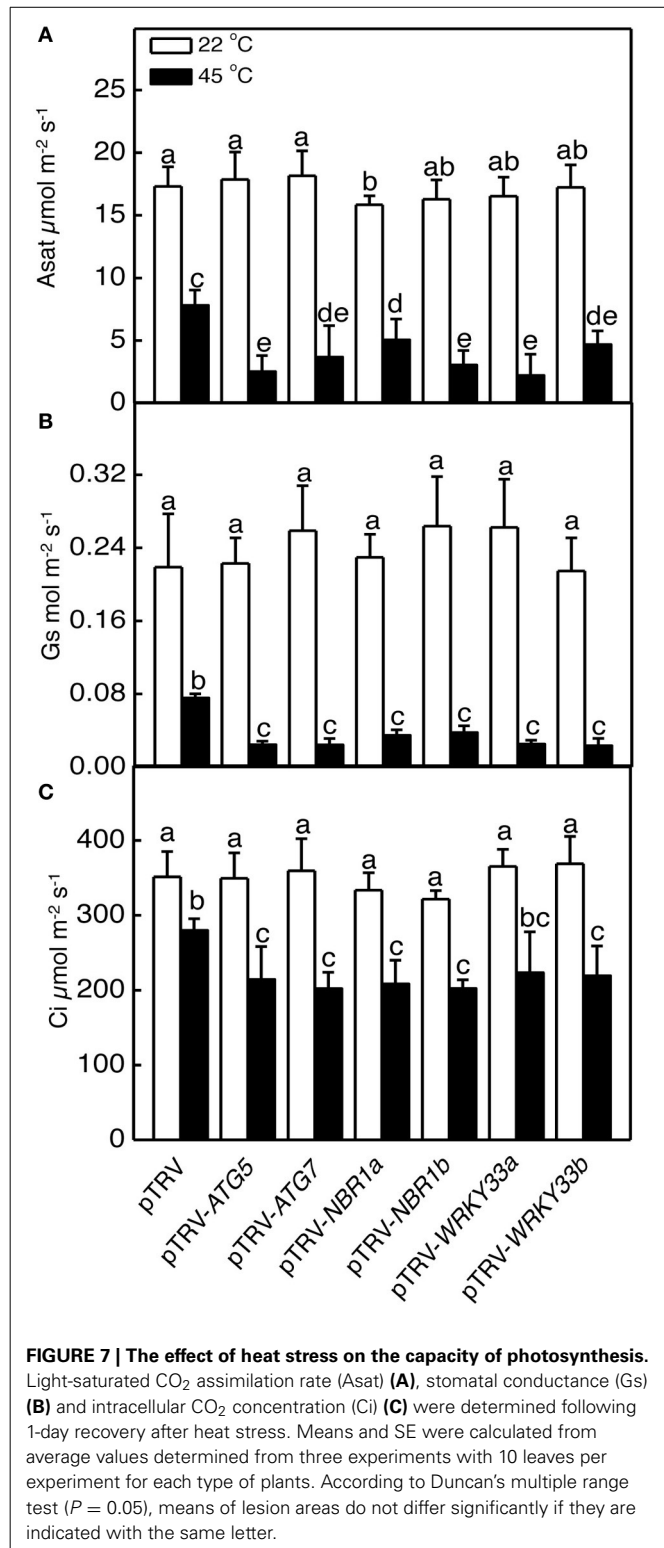


**FIGURE 7 |** The effect of heat stress on the capacity of photosynthesis. Light-saturated CO<sub>2</sub> assimilation rate (Asat) (**A**), stomatal conductance (Gs) (**B**) and intracellular CO<sub>2</sub> concentration (Ci) (**C**) were determined following 1-day recovery after heat stress. Means and SE were calculated from average values determined from three experiments with 10 leaves per experiment for each type of plants. According to Duncan's multiple range test ( $P = 0.05$ ), means of lesion areas do not differ significantly if they are indicated with the same letter.

#### IDENTIFICATION AND FUNCTIONAL ANALYSIS OF TOMATO WRKY33 IN HEAT TOLERANCE

*Arabidopsis* WRKY33 is a transcription factor important for plant resistance to necrotrophic fungal pathogens and for plant

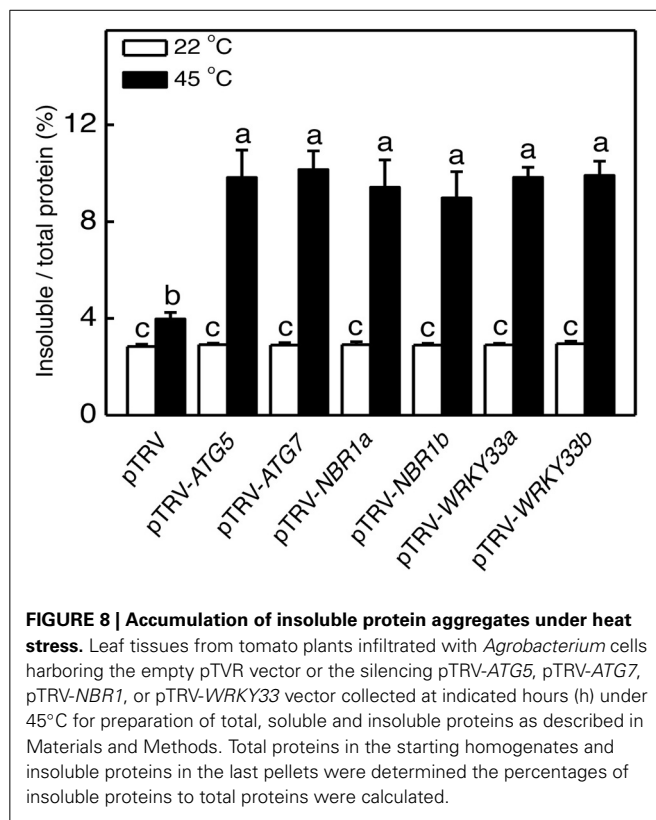


**FIGURE 8 | Accumulation of insoluble protein aggregates under heat stress.** Leaf tissues from tomato plants infiltrated with *Agrobacterium* cells harboring the empty pTRV vector or the silencing pTRV-ATG5, pTRV-ATG7, pTRV-NBR1, or pTRV-WRKY33 vector collected at indicated hours (h) under 45°C for preparation of total, soluble and insoluble proteins as described in Materials and Methods. Total proteins in the starting homogenates and insoluble proteins in the last pellets were determined the percentages of insoluble proteins to total proteins were calculated.

heat tolerance (Zheng et al., 2006; Li et al., 2011). Arabidopsis WRKY33 interacts with Arabidopsis ATG18a, a critical component of autophagy, and plays a positive role in pathogen-induced *ATG18a* expression and autophagosome formation (Lai et al., 2011a). These results suggest that the critical role of WRKY33 in plant responses to biotic and abiotic stresses may be at least in part mediated through its positive regulation of pathogen/stress-induced autophagy. To investigate whether tomato contains similar WRKY transcription factor(s) with a critical role in heat tolerance and regulation of stress-induced autophagy, we searched the sequenced tomato genomes and identified two close WRKY33 homologs, WRKY33a (Sl09g014990) and WRKY33b (Sl06g066370). As shown in **Supplemental Figure 4**, Arabidopsis WRKY33, tomato WRKY33a and WRKY33b all belong to Group I WRKY transcription factors containing two WRKY domains with highly conserved amino acid sequences. High sequence similarities are also found in the N-terminal domains including the highly conserved SP clusters as putative MAPK phosphorylation sites and the intervening sequences between the two WRKY domains (**Supplemental Figure 4**). Furthermore, both tomato WRKY33a and WRKY33b contain a segment of about 100 amino acid residues on the C-terminal side of the second WRKY domain with substantial sequence homology with Arabidopsis WRKY33, which are absent in other related Group I WRKY transcription factors such as Arabidopsis WRKY25 and WRKY26 (**Supplemental Figure 4**) (Lai et al., 2011a).

To analyze heat-induced expression of tomato WRKY33 genes, we analyzed their transcripts in the tomato seedlings grown

at 22 or 45°C. As shown in **Figure 1**, the transcript levels of both tomato WRKY33a and WRKY33b remained low throughout the 8-h period of the experiments at 22°C. At 45°C, however, the transcript levels of tomato WRKY33a and WRKY33b were elevated with similar kinetics (**Figure 1**). Transcript levels for both genes displayed substantial increases after 4-h exposure to 45°C and peaked after 6-h heat stress (**Figure 1**). Like those of other analyzed autophagy-related genes, the transcript levels for both WRKY33a and WRKY33b declined after 6-h heat exposure and approached those of control plants by 8-h heat exposure (**Figure 1**).

To determine directly the roles of tomato WRKY33 genes, we used VIGS technology to assess the impact of their down-regulated expression on tomato heat tolerance. Tomato WRKY33-specific DNA fragments were cloned into the pTRV vector and *Agrobacterium* cells harboring the VIGS vectors were infiltrated into tomato leaves. As shown in **Figure 2**, basal expression of WRKY33a or WRKY33b was observed in the tomato plants infiltrated with the pTRV empty vector. By contrast, infiltration with either pTRV-SI/WRKY33a or pTRV-SI/WRKY33b silencing vector resulted in approximately 5–7-fold reduction in the transcript levels for both tomato WRKY33a and WRKY33b (**Figure 2**). The cross silencing likely resulted from the high sequence homology between the two genes, which share more than 75% nucleotide sequence identity. The tomato plants silenced for WRKY33a and WRKY33b were normal in growth and development and displayed no detectable morphological phenotype.

We analyzed the impact of silencing of WRKY33 genes on tomato heat tolerance. Both control and silenced plants were placed in a 45°C growth chamber for 8 h and then moved to room temperature for 3-day recovery. Unlike heat-treated pTRV control plants, which had only some patches of old leaves that displayed symptoms of dehydration, a majority of leaves from the pTRV-WRKY33a and pTRV-WRKY33b plants exhibited extensive wilting or even bleaching after the recovery (**Figure 5**). Thus, silencing tomato WRKY33 genes caused increased sensitivity to heat stress. Assays of EL, the maximum quantum yield of PSII (Fv/Fm), light-saturated CO<sub>2</sub> assimilation rate (Asat), stomatal conductance (Gs), and intracellular CO<sub>2</sub> concentration (Ci) confirmed that silencing of tomato WRKY33a and WRKY33b compromised tomato heat tolerance (**Figures 5–7**). Furthermore, silencing of tomato WRKY33a and WRKY33b led to increased accumulation of insoluble proteins under heat stress (**Figure 8**).

#### REGULATION OF HEAT-INDUCED AUTOPHAGY BY WRKY33 AND AUTOPHAGY PROTEINS

To investigate whether the critical role of tomato WRKY33 genes in heat tolerance is associated with their positive roles in regulation of heat-induced autophagy, we analyzed whether silencing the WRKY33 genes in tomato compromised heat-induced autophagosome formation. As shown in **Figure 3**, while there was a more than 10 fold increase in the numbers of punctate green fluorescent signals after 6-h heat stress in the pTRV control plants, there was only 3–5-fold increase in the pTRV-WRKY33a and pTRV-WRKY33b plants. As a result of combined reduction of both basal and induced autophagosome formation, the levels of autophagosomes in the WRKY33-silenced plants were only about

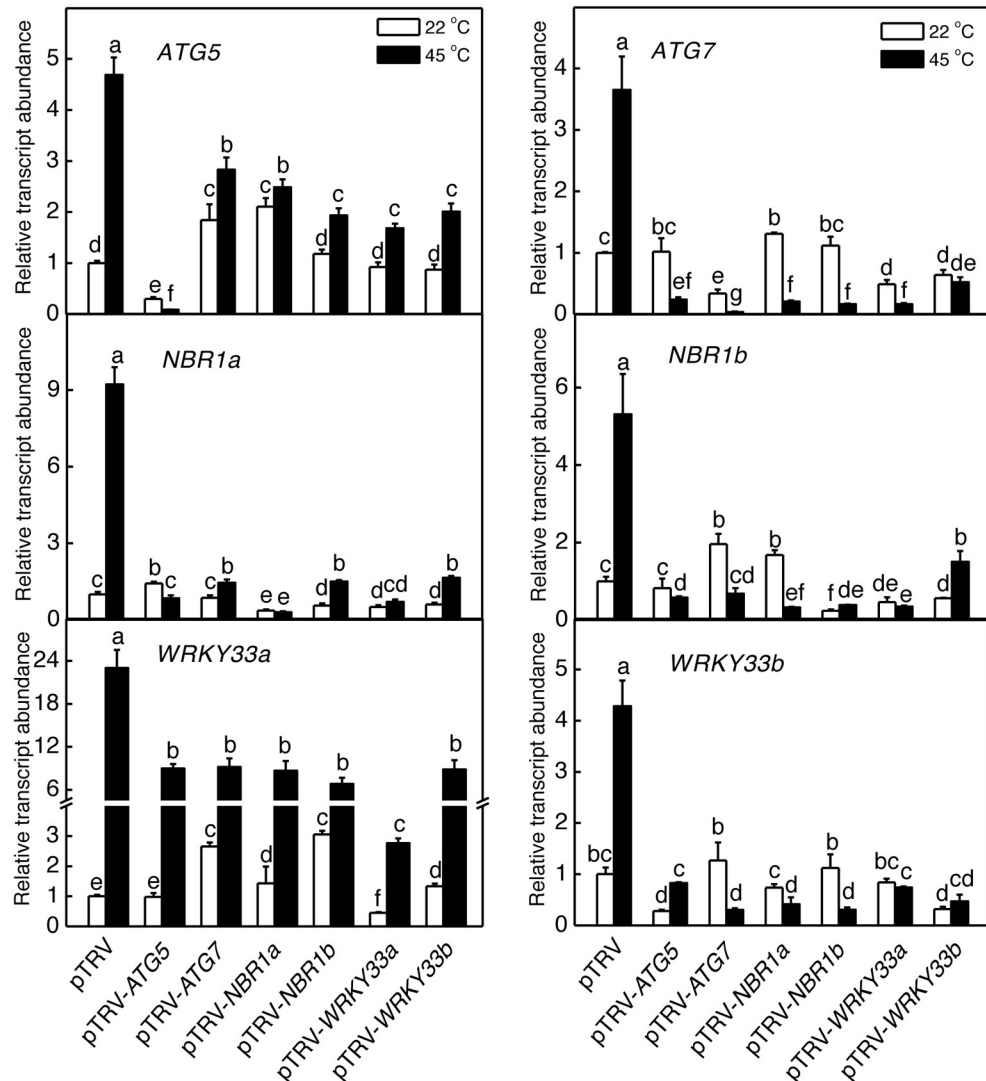
25–30% of those in the control plants after 6-h heat stress. Thus, tomato WRKY33 proteins play a positive role in heat-induced autophagosome formation.

We also analyzed the mutual regulation among the silencing tomato *ATG5*, *ATG7*, *NBR1*, and WRKY33 genes during plant responses to heat stress. For this purpose, we analyzed the transcript levels of *ATG5*, *ATG7*, *NBR1a*, *NBR1b*, *WRKY33a*, and *WRKY33b* in the silencing plants after 6-h heat stress. In pTRV control plants, as expected, the transcript levels for *ATG5*, *ATG7*, *NBR1a*, *NBR1b*, *WRKY33a*, and *WRKY33b* were elevated under heat stress. However, induction of these genes was all reduced not only in the plants harboring their respective silencing vectors but also in the plants harboring silencing vectors for the other genes (Figure 9). Induction of three heat

shock proteins (*HSP17.6*, *HSP20*, and *HSP100*) in *ATG5*-, *ATG7*-, *NBR1*-, or WRKY33-silencing plants or pTRV plants was almost as strong as that in the pTRV control plants after 6-h heat stress (Figure 10). However, induction of a tomato *HSP40* gene was significantly compromised by silencing of the autophagy-related or WRKY33 genes (Figure 10). These results indicated that ATG and WRKY33 proteins have a positive role in heat-induced expression of autophagy-related genes.

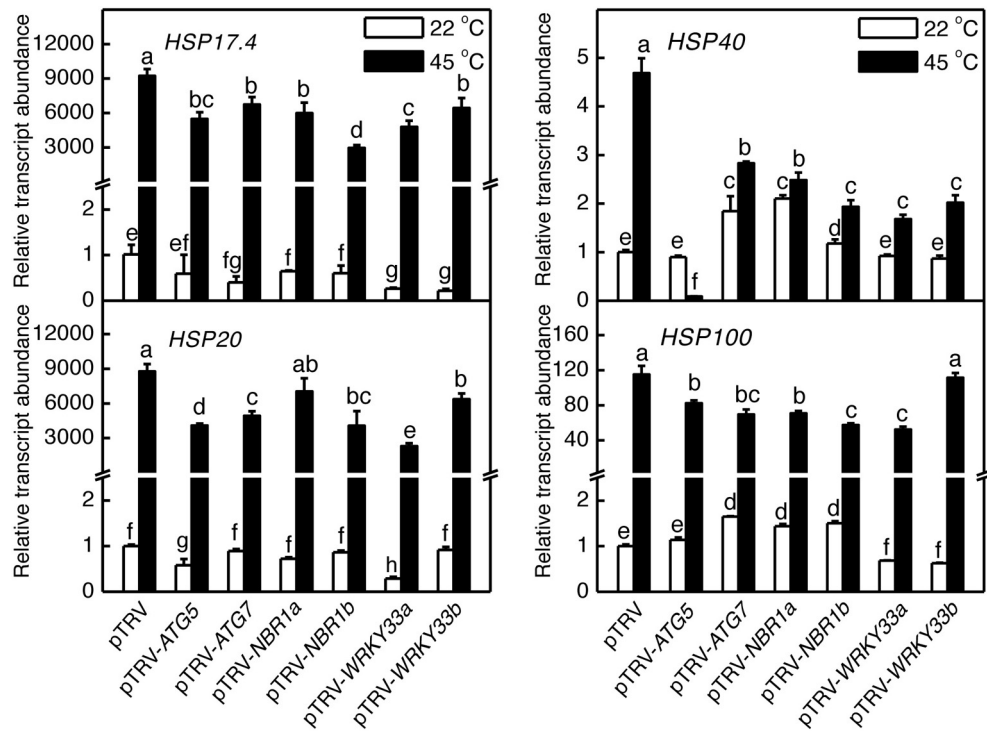
## DISCUSSION

In the present study, we analyzed the role of autophagy in responses to heat stress in tomato, an important horticultural crop. Both the expression of *ATG5* and *ATG7* genes and formation of autophagosomes were induced in heat-stressed tomato plants



**FIGURE 9 | Regulation of heat-induced expression of tomato *ATG5*, *ATG7*, *NBR1*, and *WRKY33* genes.** Tomato plants infiltrated with *Agrobacterium* cells harboring the empty pTRV vector or the silencing pTRV-ATG5, pTRV-ATG7, pTRV-NBR1, or pTRV-WRKY33 vector were placed in a 45°C growth chamber and total RNA was isolated from

leaf samples collected after 6-h heat stress for determination of transcript levels of indicated genes by qRT-PCR. Error bars indicate SE ( $n = 3$ ). According to Duncan's multiple range test ( $P = 0.05$ ), means of lesion areas do not differ significantly if they are indicated with the same letter.

**FIGURE 10 | Regulation of heat-induced expression of tomato HSP genes.**

Tomato plants infiltrated with *Agrobacterium* cells harboring the empty pTRV vector or the silencing pTRV-ATG5, pTRV-ATG7, pTRV-NBR1, or pTRV-WRKY33 vector were placed in a 45°C growth chamber and total RNA was isolated

from leaf samples collected after 6-h heat stress for determination of transcript levels of indicated genes by qRT-PCR. Error bars indicate SE ( $n = 3$ ). According to Duncan's multiple range test ( $P = 0.05$ ), means of lesion areas do not differ significantly if they are indicated with the same letter.

(Figures 1, 3, 4). The heat tolerance of autophagy-suppressed tomato plants due to silencing of *ATG5* and *ATG7* genes was compromised based on their increased morphological symptoms associated with enhanced defects in the efficiency and capacity of photosynthesis after heat stress (Figures 5–7). These results indicate that autophagy plays an important role in tomato heat tolerance.

Heat stress causes protein misfolding and denaturation. Misfolded/denatured proteins are highly toxic due to nonspecific binding to a variety of cellular constituent and, therefore, must be efficiently removed to prevent proteotoxic stresses (Hightower, 1991). Extensive studies in yeast and animal organisms have revealed that misfolded proteins are recognized by the protein quality control system, ubiquitinated by chaperone-dependent E3 ubiquitin ligases such as the C-terminus of Hsc70-interacting protein (CHIP) and subjected to degradation by the ubiquitin proteasome system (UPS) (Kraft et al., 2010; Shaid et al., 2013). Very recently we have conducted comprehensive genetic analysis of Arabidopsis CHIP E3 ubiquitin ligase and discovered its critical role in plant responses to a spectrum of abiotic stresses including heat stress (Zhou et al., 2014c). Previously, it has also been reported that Arabidopsis CHIP E3 ubiquitin ligase and Hsc70-4 mediate plastid-destination precursor degradation through UPS when the import of the precursors are blocked in a plastid-import mutant (Lee et al., 2009). In the present study, we demonstrated that silencing of tomato genes encoding *NBR1a* and *NBR1b*,

two close homologs of mammalian ubiquitin-binding autophagy receptors P62 and NBR1, also compromised tomato heat tolerance (Figures 5–7). Thus, NBR1-mediated selective autophagy is critical in tomato heat tolerance most likely through its activity in removing heat-induced misfolded proteins. For degradation by UPS, proteins must be unfolded to enter the narrow central cavity of its barrel-shaped 20S proteolytic core since the steric conditions of a folded protein would not be able to pass through the entrance channel. Under heat stress, misfolded, or denatured proteins may form protein aggregates that are difficult to dissociate or unfold. These protein aggregates are likely to be targeted by NBR1-mediated selective autophagy if they fail to be processed by UPS. Consistent with this interpretation, compromised heat tolerance of NBR1-silenced tomato plants was associated with increased accumulation of protein aggregates under heat stress (Figure 8). These results provide further support that UPS and NBR1-mediated selective autophagy function in cooperation in the removal of misfolded proteins for protection against proteotoxic stress under adverse environmental and physiological conditions (Zhou et al., 2014c).

Heat stress induced both LysoTracker or MDC-stained autolysosome-like structures (Figures 3, 4) and expression of *ATG* and *NBR1* genes (Figure 1). Interestingly, silencing of an *ATG* or *NBR1* gene in tomato plants led to down regulation of not only the silenced gene but also other sequence-unrelated autophagy genes (Figure 9). Since *ATG5*, *ATG7*, and *NBR1*

proteins are not known to be regulators of gene transcription, their effect on the expression of other genes is probably indirect and most likely related to induced autophagy under heat stress. It is possible that induced autophagy under heat and perhaps other stress conditions as well has a positive role in the upregulation of autophagy genes. Consistent with the potential signaling role of autophagy, silencing of *Arabidopsis TOR* gene leads to not only constitutive formation of autophagosomes but also induced expression of some *ATG* genes (Liu and Bassham, 2010). We have also previously observed that in autophagy-deficient mutants, induction of jasmonate-regulated *PDF1.2* gene by *Botrytis* infection was compromised (Lai et al., 2011b). Likewise, in the *ATG5*- or *ATG7*-silenced tomato mutants, induction of a gene encoding a *HSP40* was significantly reduced (**Figure 10**), indicating that induced autophagy, perhaps through formation and turnover of autophagosomes, has a positive role in up-regulation of not only autophagy genes but also other genes associated with defense and stress responses. We have previously shown that in *Arabidopsis atg5* and *atg7* mutants, the protein levels of *NBR1* increased greatly under heat stress (Zhou et al., 2013). Other studies have also showed that some of the autophagy-related proteins and *NBR1* are themselves autophagy substrates (Svenning et al., 2011) that undergo rapid turnover and must be replenished through increased synthesis for sustained autophagy. On the other hand, when autophagy is suppressed or blocked as in the *ATG5*- and *ATG7*-silenced plants, there would be no need for increased transcription of the *ATG* or *NBR1* genes since their degradation by autophagy is inhibited.

*Arabidopsis WRKY33* transcription factor plays a critical role in plant resistance to necrotrophic fungal pathogens and in plant tolerance to heat stress (Zheng et al., 2006; Li et al., 2011). Autophagy is induced by necrotrophic pathogens, heat, and salt stresses and plays an important role in plant responses to these biotic and abiotic stresses as well. We have previously shown that in the *Arabidopsis wrky33* mutants, increased formation of autophagosomes was observed in *Botrytis*-infected lesion areas but not in the areas surrounding the lesions found in wild-type plants (Lai et al., 2011b). In addition, induction of *ATG18a* was normal at 1 day post *Botrytis* infection (dpi) but was severely compromised at 2, 3, and 4 dpi in *wrky33* (Lai et al., 2011b). Thus, *WRKY33* is dispensable for early induction of autophagy but necessary for sustained induction of autophagy in *Botrytis*-infected plants. Likewise, silencing of tomato *WRKY33* compromised heat-induced autophagy gene expression and reduced autophagosome formation (**Figures 3, 8**). Thus, it is likely that the critical role of *WRKY33* in plant disease resistance and stress tolerance is, at least in part, mediated by its critical role in induction of autophagy.

In *Arabidopsis*, *WRKY33* is subjected to dual-level regulation by the mitogen protein kinase 3 and 6 (MPK3/6) cascade (Mao et al., 2011). Upon pathogen infection, *WRKY33* is phosphorylated by the pathogen/stress-induced MPK3/MPK6 and phosphorylation of *WRKY33* is likely to promote the transcription activity of *WRKY33*, which can bind to the W boxes in its promoter and turning on its own expression (Mao et al., 2011). Expression of *Arabidopsis WRKY33* is also induced by abiotic stress conditions and by paraquat, which generates ROS in exposed plant cells

(Zheng et al., 2006). In plants, autophagy is also induced by a variety of stresses, including nutrient deprivation, drought, salt stress, ROS, and pathogen infection (Liu and Bassham, 2010; Lai et al., 2011b; Zhou et al., 2013). It has also been shown that NADPH oxidase inhibitors block autophagy induction by nutrient starvation and salt stress, indicating that ROS may also function as a signal in induction of autophagy by some environmental stresses (Liu and Bassham, 2010). It is tempting to speculate that multiple stress-initiated pathways may converge to the activation and induction of *WRKY33* for induction of some autophagy- and other stress-related genes. Although autophagy is highly conserved in eukaryotic organisms, *WRKY* transcription factors are mostly plant-specific (Zhang and Wang, 2005). A critical role of *WRKY33* in the regulation of plant autophagy genes would strongly indicate that the regulatory mechanisms of autophagy in plants have diverged from those in other eukaryotic organisms.

## ACKNOWLEDGMENTS

This work is, in part, supported by the National Basic Research Program of China (2009CB119000), Natural Science Foundation of China (2013C150203), and the U.S. National Science Foundation (IOS0958066).

## SUPPLEMENTARY MATERIAL

The Supplementary Material for this article can be found online at: <http://www.frontiersin.org/journal/10.3389/fpls.2014.00174/abstract>

**Supplemental Figure 1 | Gene structures and coding sequences of tomato *ATG5a* and *ATG5b*.** **(A)** Gene structures of tomato *ATG5a* and *ATG5b*. **(B)** Comparison of tomato *ATG5a* and *ATG5b* nucleotide sequences. Identical nucleotides are in red.

**Supplemental Figure 2 | Protein sequence comparison of tomato *ATG5a* and *ATG5b*.** Identical amino acid residues between tomato *ATG5a* and *ATG5b* are in red.

**Supplemental Figure 3 | Protein sequence comparison of tomato *NBR1a* and *NBR1b*.** Identical amino acid residues between tomato *NBR1a* and *NBR1b* are in red.

**Supplemental Figure 4 | Protein sequence comparison of *Arabidopsis WRKY33*, tomato *WRKY33a* (SI06g066370), and *WRKY33b* (SI09g014990).** Amino acid residues of tomato *WRKY33a* or *WRKY33b* identical to those of *Arabidopsis WRKY33* are in red. The highly conserved *WRKYGQK* sequences and the residues forming the C<sub>2</sub>H<sub>2</sub> zinc fingers are in blue.

## REFERENCES

- Bassham, D. C., Laporte, M., Marty, F., Moriyasu, Y., Ohsumi, Y., Olsen, L. J., et al. (2006). Autophagy in development and stress responses of plants. *Autophagy* 2, 2–11.
- Biederbick, A., Kern, H. F., and Elsasser, H. P. (1995). Monodansylcadaverine (MDC) is a specific *in vivo* marker for autophagic vacuoles. *Eur. J. Cell Biol.* 66, 3–14.
- Chikte, S., Panchal, N., and Warnes, G. (2014). Use of LysoTracker dyes: a flow cytometric study of autophagy. *Cytometry A* 85, 169–178. doi: 10.1002/cyto.a.22312
- Consortium, T. T. G. (2012). The tomato genome sequence provides insights into fleshy fruit evolution. *Nature* 485, 635–641. doi: 10.1038/nature11119
- Contento, A. L., Xiong, Y., and Bassham, D. C. (2005). Visualization of autophagy in *Arabidopsis* using the fluorescent dye monodansylcadaverine

- and a GFP-AtATG8e fusion protein. *Plant J.* 42, 598–608. doi: 10.1111/j.1365-313X.2005.02396.x
- Ekengren, S. K., Liu, Y. L., Schiff, M., Dinesh-Kumar, S. P., and Martin, G. B. (2003). Two MAPK cascades, NPR1, and TGA transcription factors play a role in Pto-mediated disease resistance in tomato. *Plant J.* 36, 905–917. doi: 10.1046/j.j.1365-313X.2003.01944.x
- Floyd, B. E., Morrissey, S. C., Macintosh, G. C., and Bassham, D. C. (2012). What to eat: evidence for selective autophagy in plants. *J. Integr. Plant Biol.* 54, 907–920. doi: 10.1111/j.1744-7909.2012.01178.x
- He, C., and Klionsky, D. J. (2009). Regulation mechanisms and signaling pathways of autophagy. *Annu. Rev. Genet.* 43, 67–93. doi: 10.1146/annurev-genet-102808-114910
- Hightower, L. E. (1991). Heat shock, stress proteins, chaperones, and proteotoxicity. *Cell* 66, 191–197. doi: 10.1016/0092-8674(91)90611-2
- Huang, J. L., Gu, M., Lai, Z. B., Fan, B. F., Shi, K., Zhou, Y. H., et al. (2010). Functional analysis of the *Arabidopsis PAL* gene family in plant growth, development, and response to environmental stress. *Plant Physiol.* 153, 1526–1538. doi: 10.1104/pp.110.157370
- Johansen, T., and Lamark, T. (2011). Selective autophagy mediated by autophagic adapter proteins. *Autophagy* 7, 279–296. doi: 10.4161/auto.7.3.14487
- Kandoth, P. K., Ranf, S., Pancholi, S. S., Jayanty, S., Walla, M. D., Miller, W., et al. (2007). Tomato MAPKs LeMPK1, LeMPK2, and LeMPK3 function in the systemin-mediated defense response against herbivorous insects. *Proc. Natl. Acad. Sci. U.S.A.* 104, 12205–12210. doi: 10.1073/pnas.0700344104
- Klionsky, D. J. (2005). Autophagy. *Curr. Biol.* 15, R282–R283. doi: 10.1016/j.cub.2005.04.013
- Kraft, C., Peter, M., and Hofmann, K. (2010). Selective autophagy: ubiquitin-mediated recognition and beyond. *Nat. Cell Biol.* 12, 836–841. doi: 10.1038/ncb0910-836
- Lai, Z., Li, Y., Wang, F., Cheng, Y., Fan, B., Yu, J. Q., et al. (2011a). Arabidopsis sigma factor binding proteins are activators of the WRKY33 transcription factor in plant defense. *Plant Cell* 23, 3824–3841. doi: 10.1105/tpc.111.090571
- Lai, Z., Wang, F., Zheng, Z., Fan, B., and Chen, Z. (2011b). A critical role of autophagy in plant resistance to necrotrophic fungal pathogens. *Plant J.* 66, 953–968. doi: 10.1111/j.1365-313X.2011.04553.x
- Lee, S., Lee, D. W., Lee, Y., Mayer, U., Stierhof, Y. D., Jurgens, G., et al. (2009). Heat shock protein cognate 70-4 and an E3 ubiquitin ligase, CHIP, mediate plastid-destined precursor degradation through the ubiquitin-26S proteasome system in *Arabidopsis*. *Plant Cell* 21, 3984–4001. doi: 10.1105/tpc.109.071548
- Li, S., Fu, Q., Chen, L., Huang, W., and Yu, D. (2011). *Arabidopsis thaliana* WRKY25, WRKY26, and WRKY33 coordinate induction of plant thermotolerance. *Planta* 233, 1237–1252. doi: 10.1007/s00425-011-1375-2
- Liu, Y., and Bassham, D. C. (2010). TOR is a negative regulator of autophagy in *Arabidopsis thaliana*. *PLoS ONE* 5:e11883. doi: 10.1371/journal.pone.0011883
- Liu, Y., and Bassham, D. C. (2012). Autophagy: pathways for self-eating in plant cells. *Annu. Rev. Plant Biol.* 63, 215–237. doi: 10.1146/annurev-arplant-042811-105441
- Liu, Y., Burgos, J. S., Deng, Y., Srivastava, R., Howell, S. H., and Bassham, D. C. (2012). Degradation of the endoplasmic reticulum by autophagy during endoplasmic reticulum stress in *Arabidopsis*. *Plant Cell* 24, 4635–4651. doi: 10.1105/tpc.112.101535
- Liu, Y., Schiff, M., and Dinesh-Kumar, S. P. (2002). Virus-induced gene silencing in tomato. *Plant J.* 31, 777–786. doi: 10.1046/j.1365-313X.2002.01394.x
- Liu, Y., Xiong, Y., and Bassham, D. C. (2009). Autophagy is required for tolerance of drought and salt stress in plants. *Autophagy* 5, 954–963. doi: 10.4161/auto.5.7.9290
- Mao, G., Meng, X., Liu, Y., Zheng, Z., Chen, Z., and Zhang, S. (2011). Phosphorylation of a WRKY transcription factor by two pathogen-responsive MAPKs drives phytoalexin biosynthesis in *Arabidopsis*. *Plant Cell* 23, 1639–1653. doi: 10.1105/tpc.111.084996
- Munafò, D. B., and Colombo, M. I. (2001). A novel assay to study autophagy: regulation of autophagosome vacuole size by amino acid deprivation. *J. Cell Sci.* 114, 3619–3629.
- Otegui, M. S., Noh, Y. S., Martinez, D. E., Vila Petroff, M. G., Staehelin, L. A., Amasino, R. M., et al. (2005). Senescence-associated vacuoles with intense proteolytic activity develop in leaves of *Arabidopsis* and soybean. *Plant J.* 41, 831–844. doi: 10.1111/j.1365-313X.2005.02346.x
- Phadwal, K., Alegre-Abarrategui, J., Watson, A. S., Pike, L., Anbalagan, S., Hammond, E. M., et al. (2012). A novel method for autophagy detection in primary cells: impaired levels of macroautophagy in immunosenescent T cells. *Autophagy* 8, 677–689. doi: 10.4161/auto.18935
- Shaid, S., Brandts, C. H., Serve, H., and Dikic, I. (2013). Ubiquitination and selective autophagy. *Cell Death Differ.* 20, 21–30. doi: 10.1038/cdd.2012.72
- Slavikova, S., Ufaz, S., Avin-Wittenberg, T., Levanony, H., and Galili, G. (2008). An autophagy-associated Atg8 protein is involved in the responses of *Arabidopsis* seedlings to hormonal controls and abiotic stresses. *J. Exp. Bot.* 59, 4029–4043. doi: 10.1093/jxb/ern244
- Svenning, S., Lamark, T., Krause, K., and Johansen, T. (2011). Plant NBR1 is a selective autophagy substrate and a functional hybrid of the mammalian autophagic adapters NBR1 and p62/SQSTM1. *Autophagy* 7, 993–1010. doi: 10.4161/auto.7.9.16389
- Xiong, Y., Contento, A. L., and Bassham, D. C. (2007a). Disruption of autophagy results in constitutive oxidative stress in *Arabidopsis*. *Autophagy* 3, 257–258.
- Xiong, Y., Contento, A. L., Nguyen, P. Q., and Bassham, D. C. (2007b). Degradation of oxidized proteins by autophagy during oxidative stress in *Arabidopsis*. *Plant Physiol.* 143, 291–299. doi: 10.1104/pp.106.092106
- Yoshimoto, K. (2010). Plant autophagy puts the brakes on cell death by controlling salicylic acid signaling. *Autophagy* 6, 192–193. doi: 10.4161/auto.6.1.10843
- Zhang, Y., and Wang, L. (2005). The WRKY transcription factor superfamily: its origin in eukaryotes and expansion in plants. *BMC Evol. Biol.* 5:1. doi: 10.1186/1471-2148-5-1
- Zheng, Z., Qamar, S. A., Chen, Z., and Mengiste, T. (2006). *Arabidopsis* WRKY33 transcription factor is required for resistance to necrotrophic fungal pathogens. *Plant J.* 48, 592–605. doi: 10.1111/j.1365-313X.2006.02901.x
- Zhou, J., Wang, J., Cheng, Y., Chi, Y. J., Fan, B., Yu, J. Q., and Chen, Z. (2013). NBR1-Mediated selective autophagy targets insoluble ubiquitinated protein aggregates in plant stress responses. *PLoS Genet.* 9:e1003196. doi: 10.1371/journal.pgen.1003196
- Zhou, J., Xia, X. J., Zhou, Y. H., Shi, K., Chen, Z., and Yu, J. Q. (2014a). RBOH1-dependent H<sub>2</sub>O<sub>2</sub> production and subsequent activation of MPK1/2 play an important role in acclimation-induced cross-tolerance in tomato. *J. Exp. Bot.* 65, 595–607. doi: 10.1093/jxb/ert404
- Zhou, J., Yu, J. Q., and Chen, Z. (2014b). The perplexing role of autophagy in plant innate immune responses. *Mol. Plant Pathol.* doi: 10.1111/mpp.12118. [Epub ahead of print].
- Zhou, J., Zhang, Y., Qi, J., Chi, Y., Fan, B., Yu, J. Q., et al. (2014c). E3 ubiquitin ligase CHIP and NBR1-mediated selective autophagy protect additively against proteotoxicity in plant stress responses. *PLoS Genet.* 10:e1004116. doi: 10.1371/journal.pgen.1004116
- Conflict of Interest Statement:** The authors declare that the research was conducted in the absence of any commercial or financial relationships that could be construed as a potential conflict of interest.
- Received:** 22 January 2014; **accepted:** 11 April 2014; **published online:** 30 April 2014.
- Citation:** Zhou J, Wang J, Yu J-Q and Chen Z (2014) Role and regulation of autophagy in heat stress responses of tomato plants. *Front. Plant Sci.* 5:174. doi: 10.3389/fpls.2014.00174
- This article was submitted to Plant Cell Biology, a section of the journal *Frontiers in Plant Science*.
- Copyright © 2014 Zhou, Wang, Yu and Chen. This is an open-access article distributed under the terms of the Creative Commons Attribution License (CC BY). The use, distribution or reproduction in other forums is permitted, provided the original author(s) or licensor are credited and that the original publication in this journal is cited, in accordance with accepted academic practice. No use, distribution or reproduction is permitted which does not comply with these terms.



# Monitoring protein turnover during phosphate starvation-dependent autophagic degradation using a photoconvertible fluorescent protein aggregate in tobacco BY-2 cells

Maiko Tasaki<sup>1</sup>, Satoru Asatsuma<sup>2</sup> and Ken Matsuoka<sup>1,2,3,4\*</sup>

<sup>1</sup> Graduate School of Bioscience and Biotechnology, Kyushu University, Fukuoka, Japan

<sup>2</sup> Faculty of Agriculture, Kyushu University, Fukuoka, Japan

<sup>3</sup> Biotron Application Center, Kyushu University, Fukuoka, Japan

<sup>4</sup> Research Center for Organelle Homeostasis, Kyushu University, Fukuoka, Japan

**Edited by:**

Diane C. Bassham, Iowa State University, USA

**Reviewed by:**

Marie-Theres Hauser, BOKU - University of Natural Resources and Life Sciences, Vienna, Austria  
Yuji Moriyasu, Saitama University, Japan

**\*Correspondence:**

Ken Matsuoka, Faculty of Agriculture, Graduate School of Bioscience and Biotechnology, Kyushu University, 6-10-1 Hakozaki, Higashi-ku, Fukuoka 812-8581, Japan  
e-mail: kenmat@agr.kyushu-u.ac.jp

We have developed a system for quantitative monitoring of autophagic degradation in transformed tobacco BY-2 cells using an aggregate-prone protein comprised of cytochrome b5 (Cyt b5) and a tetrameric red fluorescent protein (RFP). Unfortunately, this system is of limited use for monitoring the kinetics of autophagic degradation because the proteins synthesized before and after induction of autophagy cannot be distinguished. To overcome this problem, we developed a system using kikume green-red (KikGR), a photoconvertible and tetrameric fluorescent protein that changes its fluorescence from green to red upon irradiation with purple light. Using the fusion protein of Cyt b5 and KikGR together with a method for the bulk conversion of KikGR, which we had previously used to convert the Golgi-localized monomeric KikGR fusion protein, we were able to monitor both the growth and *de novo* formation of aggregates. Using this system, we found that tobacco cells do not cease protein synthesis under conditions of phosphate (Pi)-starvation. Induction of autophagy under Pi-starvation, but not under sugar- or nitrogen-starvation, was specifically inhibited by phosphite, which is an analog of Pi with a different oxidation number. Therefore, the mechanism by which BY-2 cells can sense Pi-starvation and induce autophagy does not involve sensing a general decrease in energy supply and a specific Pi sensor might be involved in the induction of autophagy under Pi-starvation.

**Keywords:** autophagy, phosphate, phosphite, photoconvertible fluorescent protein, tobacco BY-2 cells, chase experiment, protein aggregate, turnover

## INTRODUCTION

Plants have various ways of responding to limitations in their nutrient supply to ensure their survival. One such response is the induction of autophagy, which is the digestion by a cell of its own intracellular contents. It has been shown that this reaction occurs at the cellular level because autophagy can be induced in cultured cells by changing the regular medium to a nutrient-deficient one. In the case of tobacco BY-2 cells, autophagy is induced when there are restricted supplies of sugar, nitrogen, or phosphate (Pi) in the medium (Moriyasu and Ohsumi, 1996; Toyooka et al., 2006).

The *in planta* responses to Pi-starvation have been linked to sugar-signaling pathways (Rouached et al., 2010). In contrast to the *in planta* responses that require days after exposure to Pi-starvation, the induction of autophagy of BY-2 cells under nutrient-depleted conditions including Pi-starvation requires less than 12 h (Toyooka et al., 2006). The loss of Pi in the medium not only induces autophagy (Toyooka et al., 2006), but also causes cell cycle arrest of BY-2 cells at the G1 phase (Sano et al., 2004). Thus, information regarding a low extracellular level of Pi is transmitted not only to induce autophagy, but also to prevent progression of the cell cycle. In contrast to Pi-starvation, the deprivation of

other major nutrients does not stop the cell cycle at a specific phase, although cell growth is arrested as in the case of Pi depletion (Sano et al., 2004). Therefore, in the present study we tested whether the induction of autophagy under conditions of deprivation of different nutrients would also interact with each other early in the process, or whether there are specific sensing steps for each nutrient in the cell.

We showed previously that a protein aggregate formed of the fusion protein of Cyt b5 and RFP (Cyt b5-RFP) was a good substrate for autophagy in tobacco BY-2 cells (Toyooka et al., 2006). Because the intact and processed forms of Cyt b5-RFP can be distinguished easily after the separation of proteins by SDS-PAGE, quantification of the fluorescent intensities of RFP-related polypeptides can be used to calculate the efficiency of autophagy (Toyooka et al., 2006). However, this method of quantification has a limitation in that the reporter proteins produced before the induction of autophagy cannot be distinguished from those produced afterwards. In other words, this method cannot distinguish whether the small amounts of intact Cyt b5-RFP that can be detected in cells undergoing induced autophagy arise from the *de novo* synthesis of the reporter protein or via

inefficient degradation of the protein. To overcome this problem, we improved the previously reported method by using a photoconvertible and tetrameric fluorescent protein, kikume green-red (KikGR; Tsutsui et al., 2005) as a substitute for RFP, and the results of the analysis of Pi-starvation-induced autophagy using this new reporter protein are described below.

## MATERIALS AND METHODS

The culture of tobacco BY-2 cells and transformation of this cell line were performed as described previously (<http://mrg.psc.riken.go.jp/strc/BY-2tran.htm>). The induction of autophagy using a medium deficient in Pi, nitrogen, or sugar was carried out as described previously (Toyooka et al., 2006). In some cases, dipotassium hydrogen phosphite (Phi; Kanto Kagaku Co. Inc., Tokyo, Japan) was included at a final concentration of 2.6 mM.

Construction of pMAT137-Cytb5-cKikGR, which is an expression plasmid for the Cyt b5-KikGR fusion protein under the enhancer-duplicated CaMV35S promoter, was done as follows. A fragment containing restriction enzyme digestion sites for KpnI at the 5' terminus and for ClaI at the 3' terminus of the KikGR-coding region was amplified by polymerase chain reaction (PCR) using pKikGR1-MC1 (MBL, Nagoya, Japan) as a template and TTTAGGTACCCATGGTGAGTGTGATTACAT and TTATATCGATTACTGCCAGCCTGGCA as primers. The resulting DNA fragment was digested with ClaI and KpnI and cloned into the corresponding sites of a binary expression plasmid pMAT137 (Yuasa et al., 2005) to yield pMAT137-cKikume. A DNA fragment encoding *Arabidopsis* Cyt b5 (At5g48810) was amplified by PCR using GCGGAGATCTGTCACCAGCAGATC ATCGGAGATGGG and GGCGGTACCAAGAAGAAGGAGGCC TTGGTCTTAGTGTAGT as primers and a plasmid for the expression of Cyt b5-RFP (Toyooka et al., 2006) as a template. The resulting DNA fragment was digested using BglII and KpnI, and subcloned into the corresponding sites of pMAT137-cKikume to yield pMAT137-Cyt b5-cKikGR. Expression of NtAtg8-YFP in cells expressing Cyt b5-KikGR was carried out by transforming the Cyt b5-KikGR-expressing cells with *Agrobacterium* harboring the expression plasmid for NtAtg8-YFP (Toyooka et al., 2006).

Conversion of the fluorescence of Cyt b5-KikGR was carried out essentially as described previously (Abiodun and Matsuoka, 2013a) with a minor modification. In brief, a 100 ml aliquot of the cultured transformed cells at the exponential phase of growth in a 300 ml Erlenmeyer flask was exposed to purple light from a 100 W black light bulb (H100BL-L; Toshiba, Tokyo, Japan), which emits line spectra at wavelengths of 334, 365, and 404 nm, with shaking at room temperature for appropriate times.

Proteins were extracted from the cells as follows. After incubation in various media, cells were collected from cell suspension by centrifugation at 360 × g for 1 min in a 1.5 ml microfuge tube. Precipitated cells were suspended into approximately 10 volumes of phosphate-buffered saline (PBS; 4.3 mM Na<sub>2</sub>HPO<sub>4</sub>, 1.4 mM KH<sub>2</sub>PO<sub>4</sub>, 2.7 mM KCl, 137 mM NaCl, pH 7.4) and centrifuged as above. The resulting cell pellet was suspended with an equal volume of PBS and disrupted by sonication in an ice-cold water bath using a Bioruptor UCD-200TM sonicator (Cosmo Bio. Co. Ltd. Tokyo, Japan) at an M power setting for 1 min with 30 s interval 10 times. After centrifuging the microfuge tube at 360 × g for

5 min, the supernatant was collected and used for total protein fraction. Proteins were quantified using Bio-Rad Protein Assay kits (Bio-Rad Co., Hercules, CA, USA) as indicated by the manufacturer's instructions, using bovine serum albumin as a standard. To estimate the cell volume in culture, a 10-ml aliquot was centrifuged in a conical tube with graduations at 360 × g for 5 min and the volumes of cell precipitates were recorded. To weigh the cells, a 100 ml aliquot of the culture was filtered through a filter paper attached to a Buchner funnel with vacuum applied, and the weights of trapped cells were measured using a balance.

For detecting red and green fluorescence, aliquots of total protein fractions were mixed with 0.25 volumes of 5 × SDS sample buffer (250 mM Tris-HCl, pH 6.8, 50% (w/v) glycerol, 10% (w/v) SDS, 0.2 M dithiothreitol (DTT), 1% (w/v) bromophenol blue), and subjected directly to 9% SDS-PAGE without heating. After the separation of proteins by electrophoresis, the green and red fluorescence of proteins in the gels were recorded using a Typhoon 9400 image analyzer (GE Healthcare) with the following conditions: a 526 SP Cy2 filter set with a 488 nm laser running at 650 V was used for the recording of green fluorescence and a 580 BP30 Cy3 filter set with 532 nm laser running at 650 V was used for the recording of red fluorescence. The intensity of fluorescence was quantified using Image Quant Software (GE Healthcare).

For collecting epifluorescence images, an Olympus IX50 microscope equipped with DP70 color CCD camera (Olympus, Tokyo, Japan) was used. All the images were collected using a 20 × LC PLAN FL lens (Olympus). For the observation of green fluorescence, WIB filter/dichroic mirror cube (Olympus) was used. An RFP filter/dichroic mirror cube (Olympus) was used for detecting red fluorescence.

For collecting confocal images, a Leica TCS SP8 confocal microscope system (Leica Microsystems, Mannheim, Germany) equipped with a white light laser and HyD detectors was used. Images were captured using an HCPL APO CS2 40 × 1.30 oil lens with a pinhole of 44.1 μm of the confocal unit at an image resolution of 1024 × 1024 pixels at 100 Hz. For detecting green fluorescence, the excitation wavelength was 505 nm and signals of 514–546 nm were recorded using a HyD detector at a gain of 100. For detecting red fluorescence, the excitation wavelength was 555 nm and signals of 610–653 nm were recorded using a HyD detector at gain 101. At the same time, transmission images were recorded using a photomultiplier tube (PMT)-type detector. Only a single scan of each color using the line scan mode was used to collect each image.

The isolation of vacuole-enriched fractions from BY-2 cells and *in vitro* processing of reporter proteins were carried out essentially as described previously (Toyooka et al., 2006), except that the buffer conditions were changed as follows: the pH 6.6 and 6.0 buffers consisted of 8:2 and 6:4 mixtures of 50 mM Hepes-KOH pH 7.4 and citrate-Na pH 5.0, respectively.

## RESULTS

### GENERATION OF PROTEIN AGGREGATES WITH A PHOTOCOVERTIBLE FLUORESCENT PROTEIN IN TOBACCO BY-2 CELLS AND DEGRADATION UNDER NUTRIENT-STARVATION CONDITIONS

Transformed BY-2 cells expressing a fusion protein of Cyt b5 and KikGR (Cyt b5-KikGR) at the log-phase of growth contained protein aggregates of green fluorescence, but with little

fluorescence in vacuoles. Many of the aggregates were spherical at 0.5–2 μm in diameter, similar to what we observed for Cyt b5-RFP aggregates (Toyooka et al., 2006). After the incubation of such cells in a normal medium for 24 h, the patterns of fluorescence were not changed significantly and only green puncta were found in the cells (Figure 1A). When cells in the log phase of growth were incubated in medium devoid of either sucrose, Pi, or nitrogen sources for 24 h, they showed strong fluorescence in the vacuoles (Figures 1B–D). Time-course analyses of the processing of the fusion protein under such starvation conditions revealed that the migration position of the fusion protein in SDS-PAGE changed from the intact form of approximately 160 kDa to a smaller form of approximately 100 kDa (Figures 1E–H). These behaviors of Cyt b5-KikGR in tobacco BY-2 cells were essentially identical to that of Cyt b5-RFP in the same cell line (Toyooka et al., 2006). Therefore, we concluded that the protein aggregates generated by Cyt b5-KikGR behave as suitable substrates for autophagy, as in the case of Cyt b5-RFP in tobacco BY-2 cells.

#### COLOR CONVERSION OF THE Cyt B5-KikGR AGGREGATE

We have reported that fluorescence of a Golgi-targeted fusion protein comprising of a prolyl-hydroxylase NtP4H1.1 and monomeric KikGR could be converted under illumination by purple light, and this conversion allowed us to monitor the proliferation of the Golgi apparatus in tobacco BY-2 cells (Abiodun and Matsuoka, 2013a,b). We used the same conversion apparatus (Abiodun and Matsuoka, 2013a) to convert the fluorescence of the color of the aggregate from green to red. Three-day-old (mid-log phase) cells were illuminated with purple light and the fluorescence was monitored using an epifluorescence microscope. Within 1 h of illumination, nearly all the aggregates of Cyt b5-KikGR emitted red fluorescence (Figure 2A). Proteins extracted from the cells before and after illumination were separated by SDS-PAGE and their green and red fluorescence were recorded (Figure 2B). Before illumination with purple light, a major band of the intact-size Cyt b5-KikGR and a weak band of the processed form were detected by recording the green fluorescence. The red fluorescence recording allowed us to detect a faint band corresponding to intact Cyt b5-KikGR. After illumination, the green bands disappeared almost completely and bands with red fluorescence appeared. Time-course analysis of the fluorescence of aggregates in the cell indicated that the green fluorescence disappeared almost completely within 1 h of illumination (Figure 2C). These observations indicated that 1 h was sufficient for a near-complete conversion of the fluorescence color of Cyt b5-KikGR expressed in tobacco BY-2 cells.

Next, we analyzed whether the newly synthesized Cyt b5-KikGR protein would be incorporated into preexisting aggregates. We recorded both green and red fluorescence confocal images before and after color conversion. The color-converted cells were further grown for 24 h and confocal images of both green and red fluorescence were recorded. The merged images of the green and red fluorescence after 24 h incubation showed ring, dot, and line structures of varied colors from reddish orange to yellow and green (Figure 2D). Colors of many aggregates were not uniform and some parts of such aggregates were redder than others. These observations suggested that some of the newly synthesized

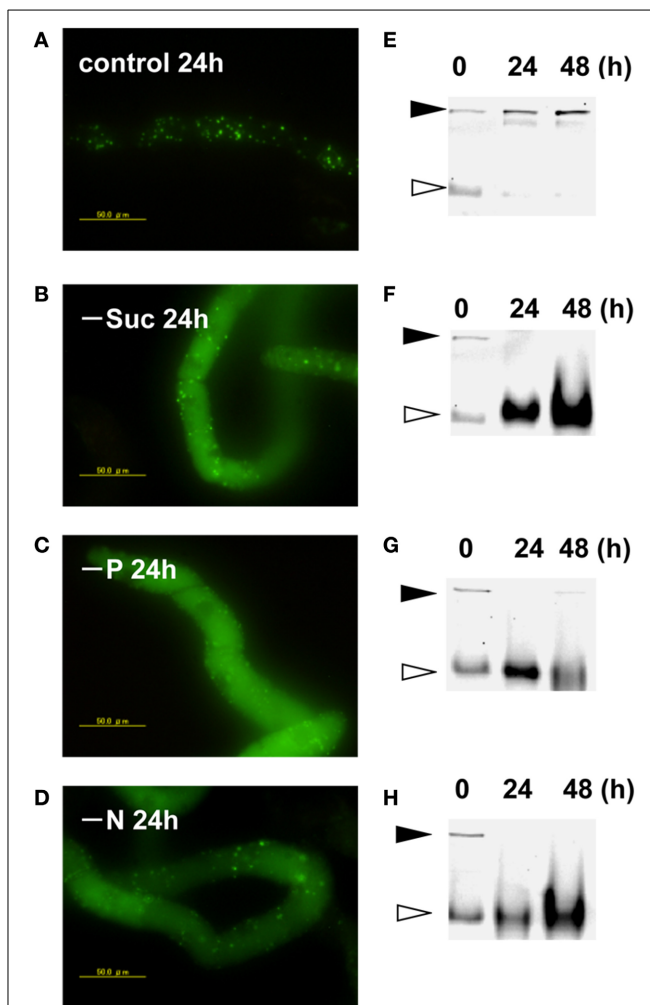
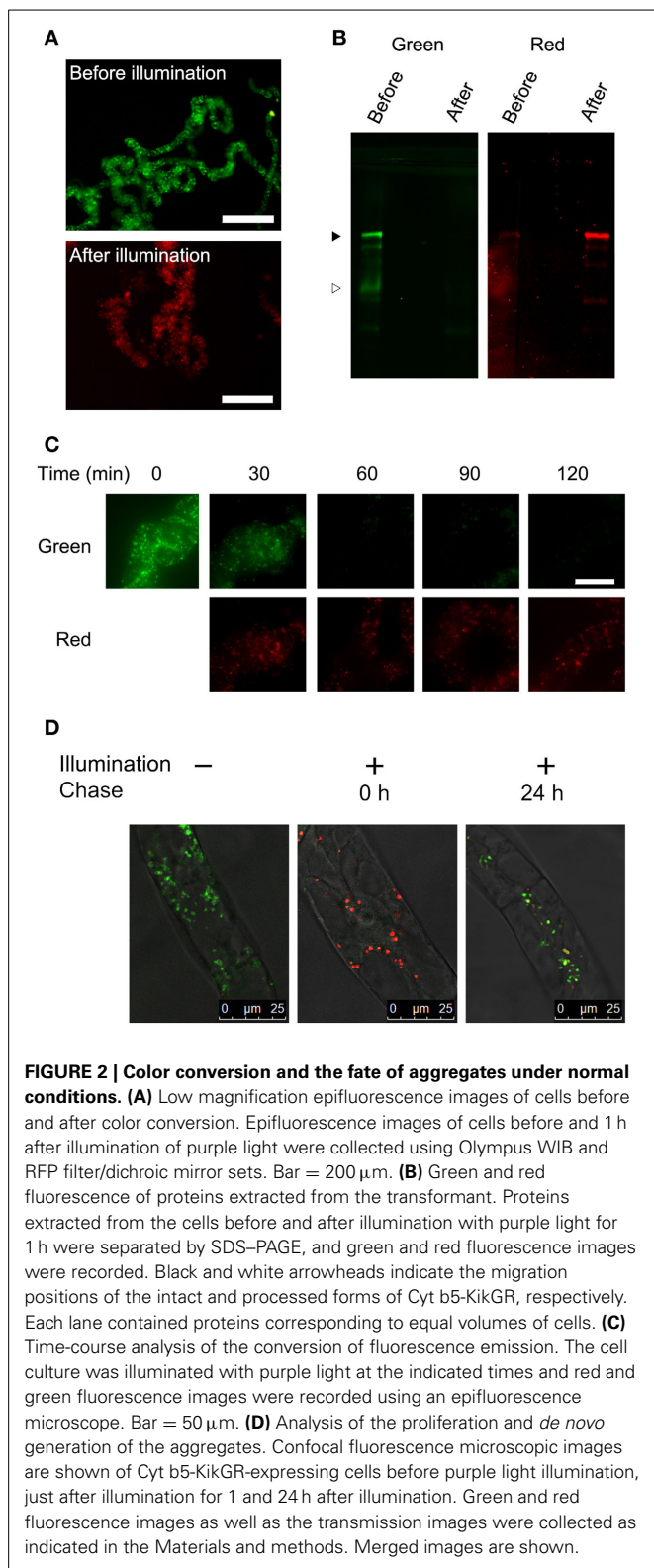


**FIGURE 1 |** Cytb5-KikGR aggregates were degraded by nutrient deprivation-induced autophagy in tobacco BY-2 cells. Transformed tobacco BY-2 cells expressing Cyt b5-KikGR at the exponential growth phase were incubated with normal control medium (A,E), sucrose-free medium (B,F), phosphate (Pi)-free medium (C,G), or nitrogen-free medium (D,H) and further cultured for 24 or 48 h. The epifluorescence image at 24 h (A–D) and migration pattern of KikGR fluorescent proteins on SDS-PAGE (E–H) at 0, 24, and 48 h of culture are shown. Each lane contains 5 μg of protein from cell extracts. Black and white arrowheads indicate the migration positions of the intact and processed forms of Cyt b5-KikGR, respectively.

Cyt b5-KikGR was incorporated into preexisting aggregates and that some other fraction contributed to formation of the new aggregate during the 24 h incubation period.

#### PROTEIN SYNTHESIS DURING STARVATION-INDUCED AUTOPHAGY

After conversion of the fluorescence color of the aggregates, cells were washed and suspended in fresh medium with or without Pi and incubated further. The cells were harvested from an aliquot of the culture and proteins were extracted from the cells. Then, equal amounts of the proteins were separated by SDS-PAGE and the green and red fluorescence bands were recorded. Within 3 h after the start of incubation in normal medium, a green band



of intact Cyt b5-KikGR was observed, and further incubation for up to 24 h increased its intensity (**Figure 3A**). In contrast, both intact and processed polypeptides emitting green fluorescence were detected after 3 h of incubation in cells under Pi-free

conditions (**Figure 3A**). The intensity of the red fluorescence of the intact Cyt b5-KikGR decreased 24 h after color conversion in both media. No clear processed form of red fluorescence was observed in either case. The decrease in red fluorescence bands in cells after incubation might have arisen either from the dilution of preexisting protein during cell growth or degradation by autophagy, or both. To determine which of these systems contributed to the decrease, we carried out quantitative time-course analysis up to 48 h by measuring both the decrease in red fluorescence as well as cell growth, and estimated the relative amount of red-converted intact Cyt b5-KikGR in the net culture over time (**Figure 3B**). In the presence of Pi, the net amount of red-converted Cyt b5-KikGR per culture volume did not decrease up to 48 h of incubation. In the absence of Pi, the protein decreased almost completely after 24 h. This observation, as well as the formation of the green processed form under Pi-starvation, suggested that both preexisting and newly synthesized Cyt b5-KikGR were degraded by autophagy during the incubation.

Unlike the nonconverted (green) Cyt b5-KikGR, red-converted Cyt b5-KikGR did not yield clear processed bands under this starvation condition. To test whether this was the result of transport to the vacuoles, we analyzed whether processing by proteases in the vacuoles would eliminate the fluorescence of the red-converted processed form. We prepared sediment fractions from cell lysates of both native and photoconverted tobacco cells expressing Cyt b5-KikGR, and used them as a source of non-processed Cyt b5-KikGR protein aggregates. These fractions were incubated with buffers at either pH 6.6 or 6.0 with or without a vacuole-enriched fraction, which was prepared from nontransformed tobacco cells cultured in Pi-free medium. Thereafter, the proteins were separated by SDS-PAGE and the fluorescence was recorded (**Figure 3C**). In the presence of vacuoles, almost all the nonconverted Cyt b5-KikGR was converted into the fast-migrating form. However, such conversion was not detectable in the absence of the vacuole fraction, although a partially processed form that migrated to a slightly distant position from the sample well was observed, as in the case of Cyt b5-RFP (Toyooka et al., 2006). The green fluorescence of all bands was weaker at pH 6.0 than that at pH 6.6. When incubation was carried out using the sediment fraction from illuminated cells, the processing pattern at pH 6.6 was almost identical to that of the nonconverted one. In contrast, only a very slight amount of red fluorescence signal was observed at pH 6.0, regardless of the presence or absence of the vacuole fraction. These observations indicate that the red-converted fluorescence of Cyt b5-KikGR is more sensitive to acidic pH than that of the nonconverted one and suggest that our failure to detect the processed red fluorescent bands under Pi-free conditions was the result of autophagy-dependent vacuolar delivery of Cyt b5-KikGR, which caused denaturation of the fluorescence-converted KikGR protein under an acidic environment in the vacuoles.

#### Phi RETARDED THE INDUCTION OF AUTOPHAGY UNDER PI-STARVATION

The Phi ion is a less oxidized form of phosphorous than the Pi ion and sometimes acts as a negative regulator of Pi deficiency-dependent gene expression in plants. Therefore, we

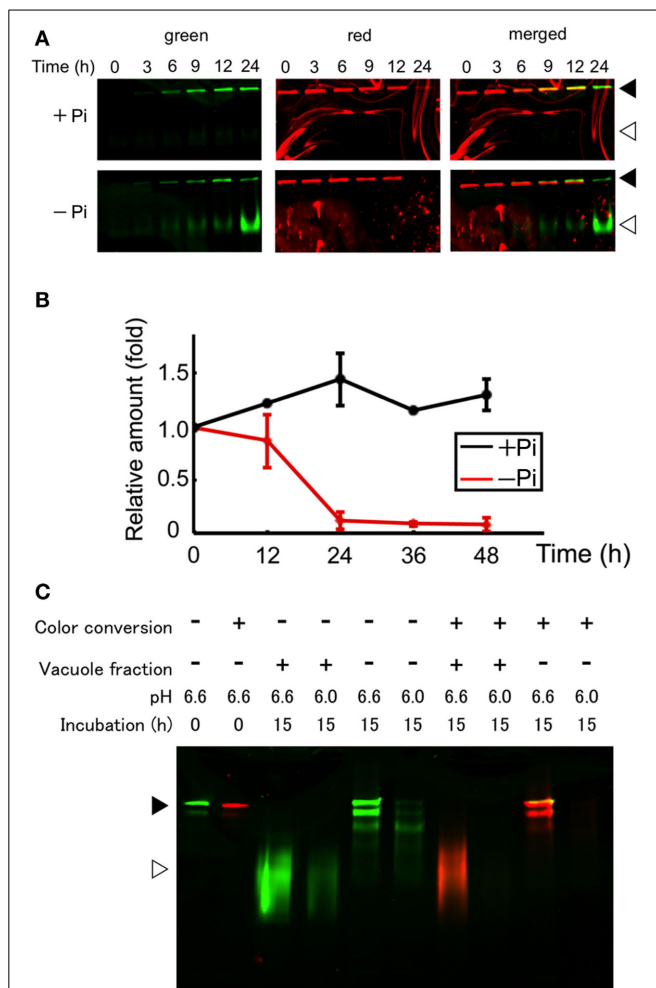


**FIGURE 3 | Protein synthesis and autophagic degradation under phosphate-limited conditions. (A)** Short time-course analysis.

Color-converted cells were re-suspended into normal (+Pi) and Pi-free (-Pi) medium and further cultured up to 24 h. Equal amounts of proteins (5 µg) from the cells were separated by SDS-PAGE and fluorescence in the gel was recorded. Black and white arrowheads indicate the migration position of intact and processed forms of Cyt b5-KikGR, respectively. **(B)** Decrease of red-converted intact-size Cyt b5-KikGR during incubation. Cells were treated as described for panel **(A)**, and at each time point, the volume of cells in culture was measured. After the extraction of proteins from cells at the indicated time points, an equal amount (5 µg) of protein was loaded to 9% SDS-PAGE and the intensity of the red-converted intact forms of Cyt b5-KikGR was quantified from the scanned image of the gel. Thereafter the amount of red-converted protein relative to that at the start of the experiment was calculated using the cell volume, the concentration of extracted protein, the volume of the extract, and the intensity of the protein band. The average of triplicated experiments is shown. The bar represents the SD. **(C)** *In vitro* fluorescence loss and processing with vacuole proteins of nonconverted and color-converted Cyt b5-KikGR under different pH conditions. Pellets of cell lysates from nonconverted or color-converted cells after 1000 × g centrifugation were used as the source of Cyt b5-KikGR aggregates. After incubation for the indicated times with buffers at the indicated pH, with or without vacuole-enriched fractions prepared from nontransformed cells cultured in Pi-deficient medium, the proteins were separated by SDS-PAGE and their emissions of green or red fluorescence were recorded. A merged image of the green and red fluorescence is shown. Black and white arrowheads indicate the migration position of the intact and processed forms of Cyt b5-KikGR, respectively.

tested whether Phi would prevent the induction of autophagy under Pi-starvation. Cells containing red-converted Cyt b5-KikGR aggregates were incubated in Pi-free medium with or without 2.6 mM Phi and cultured for up to 72 h. As shown in **Figure 4A**, the formation of the green processed form was prevented for up to 48 h in the presence of Phi. Decreases in red Cyt b5-KikGR were also prevented in the presence of Phi for up to 48 h. Under the same conditions, the Pi-starvation-dependent formation of the slow-migrating form of YFP-Atg8 as well as a decrease in YFP-Atg8 was also suppressed in the presence of Phi.

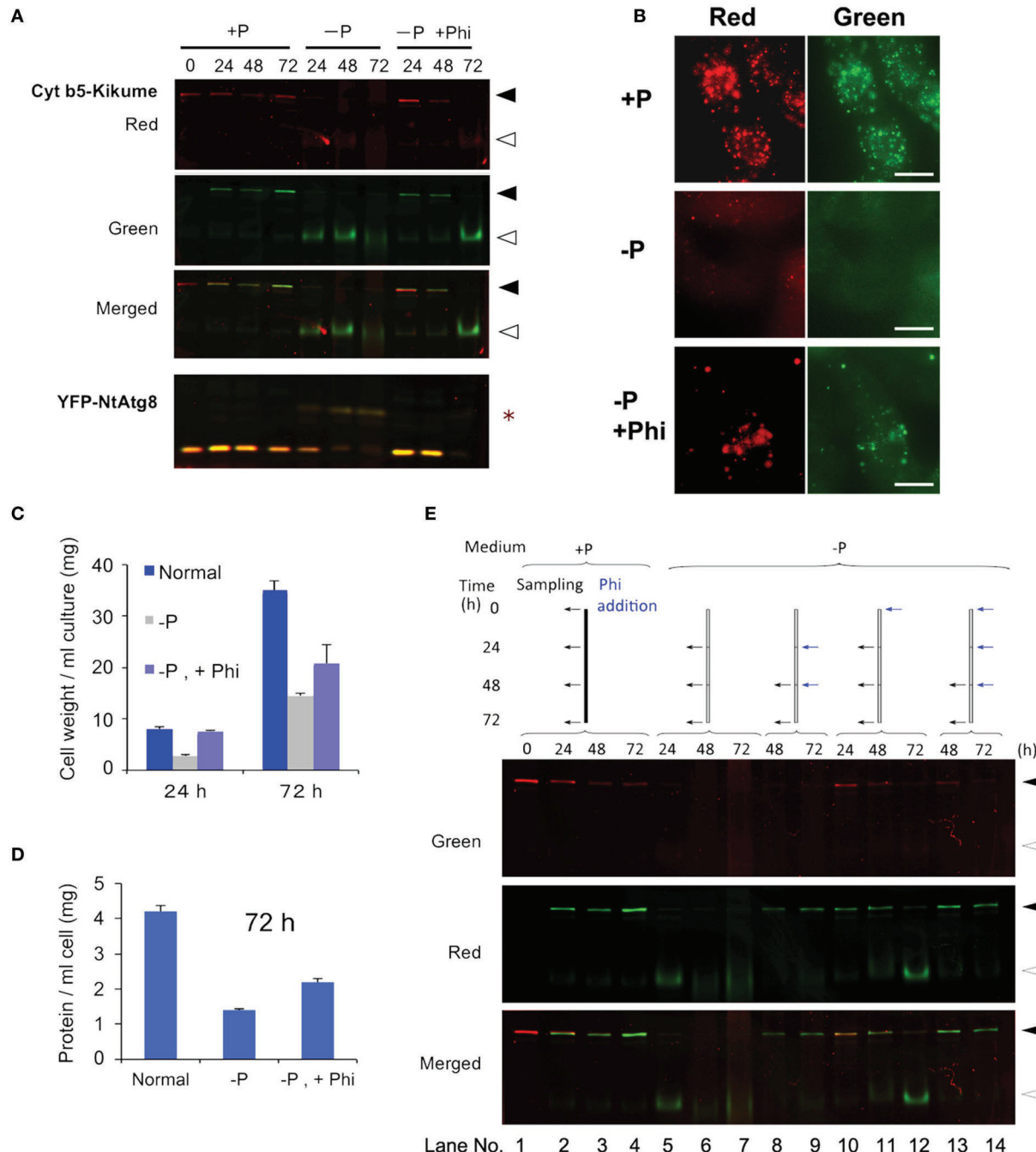
Microscopy of cells incubated under Pi-starvation for 24 h showed that vacuoles emitted faint red and green fluorescence with weak red fluorescence of aggregates (**Figure 4B**, -P). In the presence of Phi, red fluorescence in the vacuoles was not apparent and protein aggregates emit both red and green fluorescence (**Figure 4B**, -P, +P). This observation confirmed that the presence of Phi retarded the degradation of both preexisting and newly synthesized aggregates whereas newly synthesized Cyt b5-KikGR aggregates were degraded efficiently in the absence of Phi under Pi-starvation.

We also tested whether the suppression of cell growth subjected to Pi-starvation was restored by adding Phi. As shown in **Figure 4C**, an increase in cell volume was prevented under the Pi-starvation, and this was partially prevented by Phi. Likewise, the decreases in the concentrations of proteins in the cells subjected to Pi-starvation were partially prevented by Phi (**Figure 4D**). These observations suggest that Phi prevents several responses to Pi-starvation including the induction of autophagy in tobacco BY-2 cells.

Interestingly, the suppressive effect of Phi on the induction of autophagy did not continue to 72 h because the processed form of the nonconverted Cyt b5-KikGR was detectable at this time (**Figure 4A**, -P, +Phi, 72 h). In a previous study, it was reported that Phi was sequestered into the vacuoles of tobacco BY-2 cells within 48 h of its addition to the medium (Danova-Alt et al., 2008). Therefore, we tested whether the timing of the addition of Phi would affect the suppression of autophagy and the stability of preexisting (red) and newly synthesized (green) Cyt b5-KikGR (**Figure 4E**). When Phi was added 24 h after the shift to Pi-free medium and then the incubation was continued for 24 h (**Figure 4E**, lane 8), the level of intact Cyt b5-KikGR with red fluorescence was below the detection level and only green fluorescence was observed in the cells. Further addition of Phi and incubation for another 24 h did not change these results (**Figure 4E**, lane 9). In contrast, when Phi was included in the medium from the start and also augmented every 24 h, the preexisting Cyt b5-KikGR was still detectable after 72 h of incubation (**Figure 4E**, lane 14). This observation and the previous findings (Danova-Alt et al., 2008) suggest that the presence of Phi in the cytoplasm is necessary to suppress the induction of autophagy in tobacco BY-2 cells under Pi-starvation.

#### Phi DID NOT PREVENT INDUCTION OF AUTOPHAGY UNDER SUGAR- OR NITROGEN-STARVATION

Starvation of carbon and nitrogen sources induces autophagy in tobacco BY-2 cells (Moriyasu and Ohsumi, 1996; Toyooka et al., 2006). It was also reported that, in some cases, the signaling

**FIGURE 4 | Phosphate prevented Pi-starvation-induced autophagy.**

(A) Time-course analysis of the effects of the presence or absence of Phi under Pi-free conditions. Cells expressing both Cyt b5-KikGR and YFP-NtAtg8 (Toyooka et al., 2006) were exposed to purple light, incubated in Pi-free medium with or without 2.6 mM Phi and cultured for the indicated times. Proteins extracted from the cells were analyzed as in the legend to Figure 3A. Black and white arrowheads indicate the migration positions of the intact and processed forms of Cyt b5-KikGR, respectively. Asterisk indicate the slow-migrating form of YFP-NtAtg8. (B) Epifluorescence images of cells incubated in normal (+P) or Pi-free (-P) medium with (+Phi) or without Phi for 24 h. (C) Effect of Phi on the growth of transformed tobacco cells under Pi-starvation. Transformed tobacco cells were incubated for the indicated times as described in panel (A) above, and the weights of cells were measured after removal of the culture medium by filtration. The average of triplicate experiments is

shown and the bar represents the standard deviation (SD). (D) Effect of Phi on the amount of proteins in transformed tobacco cells under Pi-starvation. Transformed tobacco cells were incubated for 72 h as described in panel (A) above, and the amount of protein was measured after extraction. The mean of triplicate experiments is shown and the bar represents the SD. (E) Continued addition of Phi prevented the induction of autophagy. Color-converted cells expressing Cyt b5-KikGR were incubated in medium with or without Pi, and Phi was added to the culture to a final concentration of 2.6 mM. When multiple additions of Phi were carried out, the concentration of Phi at each time corresponded to an additional 2.6 mM in the medium. Culture conditions and the times of addition of extra lots of Phi were carried out as indicated at the top of the figure. Proteins extracted from the cells were analyzed as in the legend to Figure 3A. Black and white arrowheads indicate the migration positions of the intact and processed forms of Cyt b5-KikGR, respectively.

pathways related to sugar- and Pi-responses interact with each other in plants (Rouached et al., 2010). Therefore, we tested whether Phi would also affect the induction of autophagy in the absence of these nutrients (**Figure 5**). We found that the presence of Phi did not prevent a decrease in the intact form of both red-converted and green Cyt b5-KikGR, and allowed the formation of processed green Cyt b5-KikGR. Thus, treatment with Phi had no effect on the induction of autophagy under sugar- or nitrogen-starvation.

## DISCUSSION

We observed that the fusion protein of Cyt b5 and KikGR forms aggregates as in the case of the Cyt b5 and RFP fusion protein (**Figure 1**). The protein aggregates are able to change their fluorescence color after illumination with purple light, as in the case of the intact KikGR protein. The color-converted aggregates change color from red to orange, yellow or both red and green after the incubation of cells in normal medium (**Figure 2D**). This observation suggests that the aggregates are not static structures and can incorporate newly synthesized proteins. However, we cannot rule out the possibility that the formation of the aggregates with both green and red fluorescence were the result of *de novo* formation of newly synthesized (green) Cyt b5-KikGR and the preexisting (red-converted) Cyt b5-KikGR that had not contributed to generate aggregates. We also cannot rule out the possibility that some of the images of aggregates with both green and red colors (**Figure 4D**) were the result of close association of aggregates of two different colors because the resolution of our fluorescence microscope was not high enough. Future time-course analyses chasing one aggregate will be necessary to determine whether these aggregates with both colors were derived from color-converted aggregates.

Our observations here and our recent analysis of Golgi proliferation using a monomeric KikGR-tagged reporter protein (Abiodun and Matsuoka, 2013a,b) indicate that bulk conversion of the reporter fluorescence color and subsequent analysis is a method that can be applied to analyze the synthesis and/or turnover of distinct intracellular structures. However, this

method has a limitation when used for the quantitative comparison of preexisting and newly synthesized proteins. The fluorescence of the red-converted KikGR is more sensitive to acidic pH than that of the nonconverted KikGR (**Figure 3C**). Despite this limitation, the method could be used successfully for the analysis of inducible protein turnover and/or intracellular movements. Analysis of protein turnover after separating the proteins by SDS-PAGE and subsequent scanning of both red and green fluorescence allowed the quantification of preexisting and newly synthesized proteins (**Figure 3**). However, such protein samples should be handled as quickly as possible because both sunlight and light from regular fluorescent lamps contain wavelengths that can cause the conversion of the fluorescence color of KikGR. The presence of faint red signals in nonconverted samples (**Figure 2B**) could have arisen from the conversion of fluorescence during sample processing.

The depletion of extracellular nutrients such as sugar, nitrogen, or Pi induced degradation of the aggregate. Thus, both the degradation of preexisting (red-converted) Cyt b5-KikGR and the synthesis of green-fluorescent Cyt b5-KikGR were observed in color-converted cells (**Figure 3**). The kinetics of the increase in green Cyt b5-KikGR were not significantly different from the Pi-limited and normal conditions up to 12 h (**Figure 3A**). Autophagic degradation was not observed early after the change in medium, and only a small decrease in color-converted protein was observed at 12 h after the shift to nutrient-starved medium. This suggested that the induction of autophagy under Pi-starvation was not a result of the sensing of the level of extracellular Pi, but rather that some intracellular events might be required. Protein synthesis was not attenuated at the time when autophagy was already induced (**Figure 3A**, at 24 and 48 h). This suggests that *de novo* protein synthesis might be taking place under Pi-starvation and autophagic degradation of the cellular constituents might supply energy and building blocks for protein synthesis.

Under Pi-starvation, we observed a decrease in a form of YFP-NtAtg8A found in nonstarved cells, and an increase in the slowly migrating form of YFP-NtAtg8 (**Figure 3A**). The formation of the slow-migrating form was suppressed in the presence of Phi when autophagic degradation of the aggregates was not occurring (**Figure 3A**). Although the nature of this form is unknown, similar slowly migrating forms of the Atg8 protein have been observed in *Arabidopsis*, especially in mutants deficient in Atg8/12 conjugation systems (Thompson et al., 2005; Chung et al., 2010). Interestingly, such forms were not found in maize (Chung et al., 2009). Therefore, it will be interesting to characterize this in terms of whether multiple orthologs of Atg8s in *Arabidopsis* and tobacco (Thompson et al., 2005; Toyooka and Matsuoka, 2006) generate such forms under different conditions of autophagic induction. It will also be interesting to investigate whether such processing is related to a plant-specific autophagy-related compartment that is generated under carbon-starvation (Honig et al., 2012).

The induction of autophagy was retarded when Phi was included in the Pi-deficient medium (**Figure 3**). Phi is a nonmetabolizable analog of Pi that does not support the growth of plants (Thao and Yamakawa, 2009). However, it has been shown to affect multiple events related to Pi metabolism. Thus, Phi attenuates

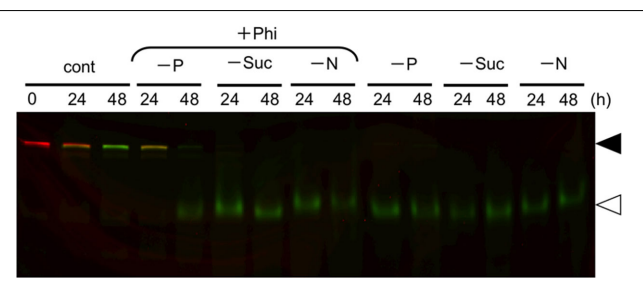


**FIGURE 5 | Phosphate did not prevent the induction of autophagy under sucrose—or nitrogen-starvation.** Color-converted cells expressing Cyt b5-KikGR were incubated in medium with or without one of the nutrients as described in the legend to **Figure 1A** with or without 2.6 mM Phi for the indicated times, and analyzed as in the legend to **Figure 3A**. Only a color-merged image is shown. Black and white arrowheads indicate the migration positions of the intact and processed forms of Cyt b5-KikGR, respectively.

several, but not all, *in planta* responses to Pi-starvation (Ticconi et al., 2001, 2004; Varadarajan et al., 2002; Kobayashi et al., 2006; Stefanovic et al., 2007; Ribot et al., 2008; Li et al., 2010; Berkowitz et al., 2013). Moreover, Phi mimics Pi in terms of the inducible degradation of Pi-deficient inducible phosphatase (Bozzo et al., 2004), and Phi accelerates programmed cell death induced by Pi-starvation in cultured brassica cells (Singh et al., 2003). Our observations indicate that not only the *in planta* response to Pi deficiency, but also the induction of autophagy are prevented by Phi (**Figure 4**). However, the effect was lost at 72 h after incubation in Pi-free medium when Phi was included from the start. This limited effect can be explained by the observation that Phi rapidly absorbed from the medium is slowly sequestered into the vacuoles in tobacco BY-2 cells (Danova-Alt et al., 2008). In fact, subsequent addition of Phi under the Pi-deficient induction condition continued to prevent the induction of autophagy (**Figure 4E**). Thus, cytosolic Phi might mimic Pi and prevent the induction of autophagy.

Some of the signal transduction pathways induced by Pi deficiency merge with sugar-signaling pathways (Rouached et al., 2010 and references therein). However, our observation that Phi did not prevent the induction of autophagy in sugar-starved medium (**Figure 5**) suggests that the sensing mechanism for Pi-starvation that induces autophagy is independent of sugar signaling. Likewise, Phi did not prevent the induction of autophagy under nitrogen-starvation (**Figure 5**). In the case of sugar starvation-dependent induction of autophagy, it was reported in sycamore maple cells that the level of energy supply is crucial, and that the inclusion of pyruvate, which is a good substrate for the mitochondrial energy supply system, could suppress sugar starvation-inducible autophagy (Aubert et al., 1996). In mammalian and yeast systems, the target of rapamycin (TOR) protein kinase has been shown as a key negative regulator for nutrient limitation-induced autophagy (Díaz-Troya et al., 2008). It was also shown in *Arabidopsis* that constitutive autophagy is negatively regulated by TOR using an interfering RNA (RNAi)-based suppression approach (Liu and Bassham, 2010). Therefore, it would be interesting to apply the present approach, along with pyruvate and/or respiratory inhibitors or downregulation of the expression of TOR, to analyze whether the cellular mechanisms used to sense limitations in the supply of different nutrients and in the induction of autophagy might be associated.

## ACKNOWLEDGMENTS

This work was supported in part by grants from the Japan Society for the Promotion of Science (Nos 19380045 and 21380208 to Ken Matsuoka) and by a grant from the Ministry of Education, Culture, Sports, Science and Technology, Japan (No. 17078009 to Ken Matsuoka).

## REFERENCES

- Abiodun, M. O., and Matsuoka, K. (2013a). Evidence that proliferation of Golgi apparatus depends on both *de novo* generation from the endoplasmic reticulum and formation from pre-existing stacks during the growth of tobacco BY-2 cells. *Plant Cell Physiol.* 54, 541–554. doi: 10.1093/pcp/pct014
- Abiodun, M. O., and Matsuoka, K. (2013b). Proliferation of the Golgi apparatus in tobacco BY-2 cells during cell proliferation after release from the stationary phase of growth. *Plant Signal. Behav.* 8, pii:e25027. doi: 10.4161/psb.25027
- Aubert, S., Gout, E., Bligny, R., Marty-Mazars, D., Barrieu, F., Alabouvette, J., et al. (1996). Ultrastructural and biochemical characterization of autophagy in higher plant cells subjected to carbon deprivation: control by the supply of mitochondria with respiratory substrates. *J. Cell Biol.* 133, 1251–1263.
- Berkowitz, O., Jost, R., Kollehn, D. O., Fenske, R., Finnegan, P. M., O'Brien, P. A., et al. (2013). Acclimation responses of *Arabidopsis thaliana* to sustained phosphate treatments. *J. Exp. Bot.* 64, 1731–1743. doi: 10.1093/jxb/ert037
- Bozzo, G. G., Singh, V. K., and Plaxton, W. C. (2004). Phosphate or phosphate addition promotes the proteolytic turnover of phosphate-starvation inducible tomato purple acid phosphatase isozymes. *FEBS Lett.* 573, 51–54. doi: 10.1016/j.febslet.2004.07.051
- Chung, T., Phillips, A. R., and Vierstra, R. D. (2010). ATG8 lipidation and ATG8-mediated autophagy in *Arabidopsis* require ATG12 expressed from the differentially controlled ATG12A and ATG12B loci. *Plant J.* 62, 483–493. doi: 10.1111/j.1365-313X.2010.04166.x
- Chung, T., Suttangkakul, A., and Vierstra, R. D. (2009). The ATG autophagic conjugation system in maize: ATG transcripts and abundance of the ATG8-lipid adduct are regulated by development and nutrient availability. *Plant Physiol.* 149, 220–234. doi: 10.1104/pp.108.126714
- Danova-Alt, R., Dijkema, C., De Waard, P., and Köck, M. (2008). Transport and compartmentation of phosphate in higher plant cells—kinetic and p nuclear magnetic resonance studies. *Plant Cell Environ.* 31, 1510–1521. doi: 10.1111/j.1365-3040.2008.01861.x
- Díaz-Troya, S., Pérez-Pérez, M. E., Florencio, F. J., and Crespo, J. L. (2008). The role of TOR in autophagy regulation from yeast to plants and mammals. *Autophagy* 4, 851–865.
- Honig, A., Avin-Wittenberg, T., Ufaz, S., and Galili, G. (2012). A new type of compartment, defined by plant-specific Atg8-interacting proteins, is induced upon exposure of *Arabidopsis* plants to carbon starvation. *Plant Cell* 24, 288–303. doi: 10.1105/tpc.111.093112
- Kobayashi, K., Masuda, T., Takamiya, K., and Ohta, H. (2006). Membrane lipid alteration during phosphate starvation is regulated by phosphate signaling and auxin/cytokinin cross-talk. *Plant J.* 47, 238–248. doi: 10.1111/j.1365-313X.2006.02778.x
- Li, W. F., Perry, P. J., Prafulla, N. N., and Schmidt, W. (2010). Ubiquitin-specific protease 14 (UBP14) is involved in root responses to phosphate deficiency in *Arabidopsis*. *Mol. Plant* 3, 212–223. doi: 10.1093/mp/ssp086
- Liu, Y., and Bassham, D. C. (2010). TOR is a negative regulator of autophagy in *Arabidopsis thaliana*. *PLoS ONE*. 5:e11883. doi: 10.1371/journal.pone.0011883
- Moriyasu, Y., and Ohsumi, Y. (1996). Autophagy in tobacco suspension-cultured cells in response to sucrose starvation. *Plant Physiol.* 111, 1233–1241.
- Ribot, C., Wang, Y., and Poirier, Y. (2008). Expression analyses of three members of the AtPHO1 family reveal differential interactions between signaling pathways involved in phosphate deficiency and the responses to auxin, cytokinin, and abscisic acid. *Planta*, 227, 1025–1036. doi: 10.1007/s00425-007-0677-x
- Rouached, H., Arpat, A. B., and Poirier, Y. (2010). Regulation of phosphate starvation responses in plants: signaling players and cross-talks. *Mol. Plant* 3, 288–299. doi: 10.1093/mp/ssp120
- Sano, T., Shimizu, T., Sakamoto, K., and Nagata, T. (2004). “Block points in the cell cycle progression of plant cells: deduced lesson from tobacco BY-2 cells,” in *Biotechnology in Agriculture and Forestry*. Vol. 53, *Tobacco BY-2 Cells*, eds T. Nagata, S. Hasezawa, and D. Inze (Berlin, Heidelberg: Springer-Verlag), 149–158.
- Singh, V. K., Wood, S. M., Knowles, V. L., and Plaxton, W. C. (2003). Phosphate accelerates programmed cell death in phosphate-starved oilseed rape (*Brassica napus*) suspension cell cultures. *Planta* 218, 233–239. doi: 10.1007/s00425-003-1088-2
- Stefanovic, A., Ribot, C., Rouached, H., Wang, Y., Chong, J., Belbahri, L., et al. (2007). Members of the *PHO1* gene family show limited functional redundancy in phosphate transfer to the shoot, and are regulated by phosphate deficiency via distinct pathways. *Plant J.* 50, 982–994. doi: 10.1111/j.1365-313X.2007.03108.x
- Thao, H. T. B., and Yamakawa, T. (2009). Phosphate (phosphorous acid): fungicide, fertilizer or bio-stimulator? *Soil Sci. Plant Nutr.* 55, 228–234. doi: 10.1111/j.1747-0765.2009.00365.x
- Thompson, A. R., Doelling, J. H., Suttangkakul, A., and Vierstra, R. D. (2005). Autophagic nutrient recycling in *Arabidopsis* directed by the ATG8 and ATG12 conjugation pathways. *Plant Physiol.* 138, 2097–2110. doi: 10.1104/pp.105.060673

- Ticconi, C. A., Delatorre, C. A., and Abel, S. (2001). Attenuation of phosphate starvation responses by phosphite in *Arabidopsis*. *Plant Physiol.* 127, 963–972. doi: 10.1104/pp.010396
- Ticconi, C. A., Delatorre, C. A., Lahner, B., Salt, D. E., and Abel, S. (2004). *Arabidopsis pdr2* reveals a phosphate-sensitive checkpoint in root development. *Plant J.* 37, 801–814. doi: 10.1111/j.1365-313X.2004.02005.x
- Toyooka, K., and Matsuoka, K. (2006). “Autophagy and non-classical vacuolar targeting in tobacco BY-2 cells,” in *Biotechnology in Agriculture and Forestry. Vol. 58, Tobacco BY-2 Cells: From Cellular Dynamics to Omics*, eds T. Nagata, K. Matsuoka, and D. Inze (Berlin, Heidelberg: Springer-Verlag), 167–180.
- Toyooka, K., Takeuchi, M., Moriyasu, Y., Fukuda, H., and Matsuoka, K. (2006). Protein aggregates are transported to vacuoles by macroautophagic mechanism in nutrient-starved plant cells. *Autophagy* 2, 91–106.
- Tsutsui, H., Karasawa, S., Shimizu, H., Nukina, N., and Miyawaki, A. (2005). Semirational engineering of a coral fluorescent protein into an efficient highlighter. *EMBO Rep.* 6, 233–238. doi: 10.1038/sj.emboj.7400361
- Varadarajan, D. K., Karthikeyan, A. S., Matilda, P. D., and Raghothama, K. G. (2002). Phosphite, an analog of phosphate, suppresses the coordinated expression of genes under phosphate starvation. *Plant Physiol.* 129, 1232–1240. doi: 10.1104/pp.010835
- Yuasa, K., Toyooka, K., Fukuda, H., and Matsuoka, K. (2005). Membrane-anchored prolyl hydroxylase with an export signal from the endoplasmic reticulum. *Plant J.* 41, 81–94. doi: 10.1111/j.1365-313X.2004.02279.x

**Conflict of Interest Statement:** The authors declare that the research was conducted in the absence of any commercial or financial relationships that could be construed as a potential conflict of interest.

Received: 30 January 2014; accepted: 10 April 2014; published online: 30 April 2014.

Citation: Tasaki M, Asatsuma S and Matsuoka K (2014) Monitoring protein turnover during phosphate starvation-dependent autophagic degradation using a photoconvertible fluorescent protein aggregate in tobacco BY-2 cells. *Front. Plant Sci.* 5:172. doi: 10.3389/fpls.2014.00172

This article was submitted to Plant Cell Biology, a section of the journal *Frontiers in Plant Science*.

Copyright © 2014 Tasaki, Asatsuma and Matsuoka. This is an open-access article distributed under the terms of the Creative Commons Attribution License (CC BY). The use, distribution or reproduction in other forums is permitted, provided the original author(s) or licensor are credited and that the original publication in this journal is cited, in accordance with accepted academic practice. No use, distribution or reproduction is permitted which does not comply with these terms.



# Degradation of plant peroxisomes by autophagy

Han Nim Lee, Jimi Kim and Taijoon Chung\*

Department of Biological Sciences, Pusan National University, Busan, South Korea

**Edited by:**

Diane C. Bassham, Iowa State University, USA

**Reviewed by:**

Jianping Hu, Michigan State University, USA

Sigrun Reumann, University of Stavanger, Norway

**\*Correspondence:**

Taijoon Chung, Department of Biological Sciences, Pusan National University, 63 Beon-gil2, Busandaehag-ro, Geumjeong-gu, Busan 609-735, South Korea  
e-mail: taijoon@pusan.ac.kr

Peroxisomes play a critical role in many metabolic pathways during the plant life cycle. It has been proposed that the transition between different types of peroxisomes involves the degradation of obsolete peroxisomal enzymes via proteolytic activities in the peroxisome matrix, the cytosol, or the vacuole. Forward and reverse genetic studies recently provided evidence for autophagic degradation of peroxisomes in the vacuole of *Arabidopsis* seedlings. Here, we briefly review a model of pexophagy, or selective autophagy of peroxisomes, in plant cells.

**Keywords:** autophagy-related, Atg, peroxisome-associated protein degradation, hydrogen peroxide, glyoxylate cycle enzymes

## PLANT PEROXISOMES: TYPES, TRANSITION, AND PROTEIN DEGRADATION

Plant peroxisomes are versatile organelles that participate in many metabolic pathways such as fatty acid  $\beta$ -oxidation and photorespiration (reviewed by Hu et al., 2012). In addition to the enzymes needed for these pathways, peroxisomes contain antioxidant enzymes, for example, catalase, to protect plants from oxidative damage, since hydrogen peroxide is generated from fatty acid  $\beta$ -oxidation and photorespiration and other oxidation reactions in the peroxisome.

Peroxisomes are dynamic organelles with the capacity to change their appearance, their association with other organelles, and their enzyme composition. These changes depend on the developmental program and metabolic needs of the cell. For example, when oil-storing seeds such as cucumber (*Cucumis sativus*) and *Arabidopsis* (*Arabidopsis thaliana*) germinate, peroxisomes contain the glyoxylate cycle enzymes. The enzymes are needed for the consumption of acetyl-CoA (the product of fatty acid  $\beta$ -oxidation) for synthesis of organic acids that can be used to generate sugars by gluconeogenesis (reviewed by Pracharoenwattana and Smith, 2008). These seedling peroxisomes, formerly called glyoxysomes, are closely associated with lipid bodies supplying fatty acids (Trelease et al., 1971). When the seedlings are exposed to light, peroxisomal glyoxylate cycle enzymes, such as isocitrate lyase (ICL) and malate synthase (MLS), are rapidly degraded and enzymes involved in photorespiration accumulate. These peroxisomes are referred to as leaf peroxisomes. The change in peroxisomal enzyme composition may result from the transition of seedling peroxisomes to leaf peroxisomes (the “one-population model”), rather than from the degradation of seedling peroxisomes and the formation of new leaf peroxisomes (the “two-population model”; Beevers, 1979; Nishimura et al., 1996). Light also triggers changes in the position of peroxisomes. Seedling peroxisomes are associated with lipid bodies, while leaf peroxisomes are positioned near chloroplasts (Trelease et al., 1971; Gruber et al., 1973) from which glycolate, a photorespiration intermediate, enters the

peroxisome for oxidation. Interestingly, a reverse transition from leaf peroxisomes to peroxisomes containing ICL may occur during starvation and organ senescence (reviewed by Nishimura et al., 1996; Pracharoenwattana and Smith, 2008).

When seedling peroxisomes are transformed to leaf peroxisomes, obsolete ICL and MLS must be degraded. In recent studies, three mechanisms have been proposed for the degradation of these proteins during post-germinative growth of *Arabidopsis* seedlings (Figure 1). In one mechanism [herein designated intraperoxisomal degradation (IPD)], it is proposed that peroxisomal proteins are degraded by resident proteases. However, known peroxisomal proteases, which include Lon-related protease 2 (LON2), have not been implicated in full degradation of peroxisomal matrix proteins (Lingard and Bartel, 2009). This argument was mainly based on the observation that ICL and MLS levels in *lon2* mutant were not higher than those in wild-type (Lingard and Bartel, 2009; Burkhart et al., 2013). According to a second mechanism, obsolete proteins are retranslocated from peroxisomes and degraded in the cytosol by the 26S proteasome. During this process, called peroxisome-associated protein degradation (PexAD), the proteins are polyubiquitylated before they are recognized by the proteasome, analogous to ER-associated protein degradation (ERAD; reviewed by Smith et al., 2012). The possibility of polyubiquitylation is supported by a survey of *Arabidopsis* ubiquitylome, in which ICL was identified as a ubiquitylated protein (Kim et al., 2013a). Furthermore, the *PEROXIN4* (*PEX4*) gene, which may be involved in ubiquitylation, is necessary for the degradation of ICL and MLS (Zolman et al., 2005; Lingard et al., 2009). A third mechanism for peroxisomal degradation is pexophagy, a selective type of autophagy in which peroxisomes are targeted to the vacuole.

Pexophagy and its mechanism are well described in methylotrophic yeast and to a lesser extent in mammalian cells (reviewed by Till et al., 2012). Pexophagy typically removes obsolete or damaged peroxisomes. For example, peroxisomes are proliferated when methylotrophic yeast is grown in methanol, and excess peroxisomes are eliminated by pexophagy when methanol is replaced

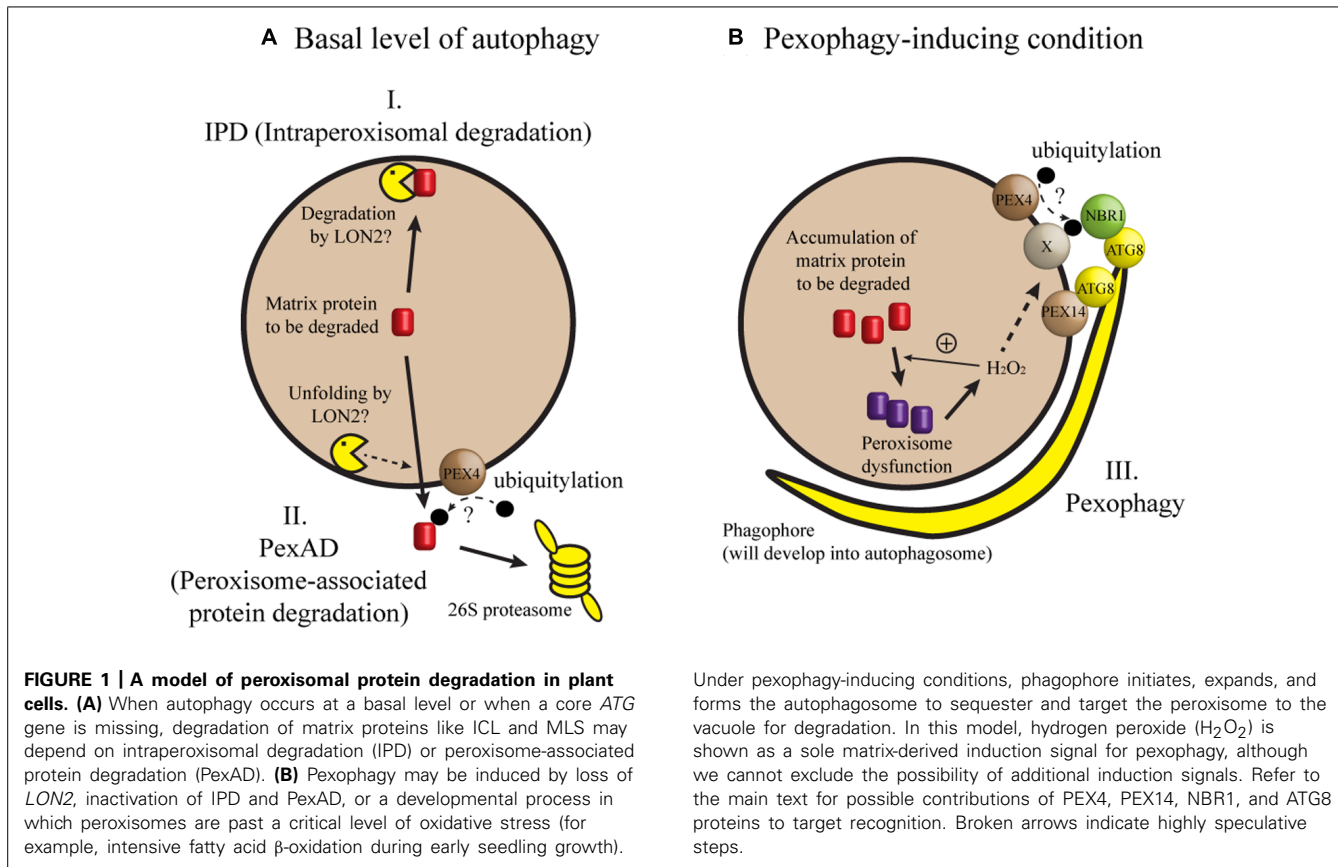


**FIGURE 1 | A model of peroxisomal protein degradation in plant cells.** (A) When autophagy occurs at a basal level or when a core ATG gene is missing, degradation of matrix proteins like ICL and MLS may depend on intraperoxisomal degradation (IPD) or peroxisome-associated protein degradation (PexAD). (B) Pexophagy may be induced by loss of *LON2*, inactivation of IPD and PexAD, or a developmental process in which peroxisomes are past a critical level of oxidative stress (for example, intensive fatty acid  $\beta$ -oxidation during early seedling growth).

Under pexophagy-inducing conditions, phagophore initiates, expands, and forms the autophagosome to sequester and target the peroxisome to the vacuole. In this model, hydrogen peroxide ( $H_2O_2$ ) is shown as a sole matrix-derived induction signal for pexophagy, although we cannot exclude the possibility of additional induction signals. Refer to the main text for possible contributions of PEX4, PEX14, NBR1, and ATG8 proteins to target recognition. Broken arrows indicate highly speculative steps.

by other carbon source. Two types of pexophagy are known in yeast: in macropexophagy, peroxisomes are sequestered by the phagophore (Figure 1) and subsequently targeted to the vacuole, and micropexophagy occurs when peroxisomes are directly engulfed by the vacuolar membrane (Till et al., 2012). It was found that many core *Autophagy-related* (Atg) genes are required for pexophagy in yeast and mouse. Despite significant progress in our understanding of plant autophagy (reviewed by Floyd et al., 2012; Li and Vierstra, 2012), direct evidence for pexophagy in plant cells has not been available until recently and will be discussed herein.

## DEGRADATION OF PEROXISOMES BY AUTOPHAGY IN ARABIDOPSIS

Early electron microscopy studies rarely include snapshots of autophagic degradation of peroxisomes in plant cells. However, there is a published example of autophagic vacuoles located near peroxisomes in castor bean endosperm, taken approximately 6 days after germination (Vigil, 1970). These snapshots alone were not sufficient for definitive evidence of plant pexophagy and required confirmation by immunoelectron microscopy and three-dimensional electron tomography.

A recent study employing a genetic suppressor screen provides evidence for pexophagy in plants. This was done by Dr. Bonnie Bartel's group at Rice University in an attempt to identify the molecular function and targets of the LON2 protease (Farmer et al., 2013). The investigators screened for mutations suppressing

*lon2* phenotypes of defective  $\beta$ -oxidation activity and incomplete processing of peroxisome targeting signal (PTS) 2. In addition to the phenotypes, *lon2* mutant cells had abnormally large spherical structures labeled by green fluorescent protein tagged with PTS (GFP-PTS), a widely used peroxisomal matrix marker. In contrast, the wild-type cells had small GFP-PTS puncta. Cloning of mutant genes that code for the *lon2* suppressors resulted in the identification of several alleles of *atg* genes, specifically *atg2*, *atg3*, and *atg7*, two of which had been previously shown to cause defective autophagy (Doelling et al., 2002; Inoue et al., 2006). Double mutants of *lon2 atg2*, *lon2 atg3*, and *lon2 atg7* all had normal  $\beta$ -oxidation and PTS2 processing, and had small GFP-PTS puncta. Moreover, endogenous ICL and MLS were stabilized in the double mutants, but not significantly in *atg* single-mutant seedlings. Farmer et al. (2013) presented a model in which autophagy removes a fraction of peroxisomes in wild-type *Arabidopsis* seedlings, while peroxisomal defects in *lon2* mutation induce pexophagy (Figure 1B). Similar results were obtained by Dr. Mikio Nishimura's group at National Institute for Basic Biology, Japan (Goto-Yamada et al., 2014). Lack of autophagy in the *lon2* background appears to prevent the double-mutant seedlings from losing small peroxisomes, leading to the suppression of *lon2* phenotypes (Bartel et al., 2014; Goto-Yamada et al., 2014). Although the precise function of LON2 in ICL and MLS degradation has yet to be defined, data described in Farmer et al. (2013), Goto-Yamada et al. (2014) indicate that LON2 protease plays a pivotal role in the IPD,

unfolding, and/or translocation of misfolded peroxisomal proteins (**Figure 1**).

A role for pexophagy in ICL and MLS degradation was also demonstrated in a reverse genetics study performed in our laboratory (Kim et al., 2013b). 5-day-old wild-type hypocotyls had approximately 50% fewer peroxisomes than 3-day-old hypocotyls, while the reduction was about 20% in *atg7* hypocotyls. Degradation of ICL and MLS was delayed in *atg7* hypocotyls, but this stabilization effect was not obvious at the whole-seedling scale. Consistent with the observation that phenotypes were more obvious in hypocotyls than in the whole seedling, *ATG7* transcription appeared to be induced preferentially in hypocotyls (Kim et al., 2013b). Thus, autophagy during seedling growth may be spatiotemporally controlled to promote degradation of peroxisomes. A relatively low level of autophagic activity in cotyledons and roots would explain why Farmer et al. (2013), Goto-Yamada et al. (2014) failed to detect stabilization of ICL and MLS in *atg7* and *atg2* single mutant seedlings. Finally, Kim et al. (2013b) reported *ATG7*-dependent degradation of peroxisomes in the central vacuole and observed autophagic puncta overlapping with peroxisomal markers.

As seedlings mature, pexophagy may have a role in peroxisomal quality control. This suggestion is supported by the results from another forward genetic screen performed by Dr. Mikio Nishimura's group (Shibata et al., 2013). These authors identified mutants with aggregated peroxisomes and showed that the *atg2*, *atg7*, and *atg18a* mutations were responsible for aggregation. In line with the findings of Farmer et al. (2013), the *atg2* mutation did not affect peroxisome function. However, leaves from 3-week-old *atg2* mutant plants accumulated more peroxisomal proteins than the wild-type control, but had the same amount of mitochondrial and chloroplast proteins as leaves from wild-type plants, suggesting selective degradation of peroxisomal proteins by autophagy. Shibata et al. (2013) found that exogenously supplied hydrogen peroxide induced peroxisome aggregation. The aggregated peroxisomes in *atg2* mutants were highly oxidized and contained a high level of inactive catalase. More recently, Yoshimoto et al. (2014) observed a phagophore-like structure that formed near the aggregated peroxisomes in *atg2* leaves. These observations suggest that hydrogen peroxide is an induction signal for pexophagy, a process that aids in the disposal of damaged peroxisomes in the cell (**Figure 1B**).

## FUTURE RESEARCH PERSPECTIVES

We can identify several questions concerning pexophagy in plant cells. First, why have there been few ultrastructure images suggestive of pexophagy in plant cells? The scarcity may be due to rapid targeting of autophagic vesicles to the vacuole (Zhuang et al., 2013). This possibility is supported by the observation of the phagophore-like structures in *atg2*, where autophagosome formation may not be completed (Yoshimoto et al., 2014). In addition, the scarcity may result from a small developmental window in which seedling peroxisomes are rapidly transformed to leaf peroxisomes, as our study suggested (Kim et al., 2013b).

Another important question concerns the selectivity of autophagy. While autophagy in mature leaves may be selective for peroxisomes over mitochondria or plastids (Shibata et al., 2013),

such selectivity was not clearly demonstrated in hypocotyls. A more quantitative tool to assess selectivity of autophagy in plant cells will be useful, and would apply to other types of selective autophagy, too.

Three of the studies mentioned here (Farmer et al., 2013; Kim et al., 2013b; Goto-Yamada et al., 2014) focused on peroxisome transition in young seedlings, while mature plants were used for the analysis of leaf peroxisomes in two other papers (Shibata et al., 2013; Yoshimoto et al., 2014). Nevertheless, these studies all underscore a role for autophagy in homeostasis of peroxisome number. Is there any unifying concept from the studies? It seems that the transition of seedling peroxisomes to leaf peroxisomes involves aggregation of small, highly oxidized peroxisomes that contain damaged or misfolded enzymes. In fact, aggregated peroxisomes were accumulated in the mesophyll cells of young *atg2* seedlings (Goto-Yamada et al., 2014) and possibly in *atg7* hypocotyl cells (Kim et al., 2013b). Hydrogen peroxide has been proposed as a signal for autophagy in plants (reviewed by Pérez-Pérez et al., 2012; Hackenberg et al., 2013). In support of this proposal, *cat2* seedlings lacking a detectable level of catalase showed accelerated degradation of ICL and MLS (Lingard et al., 2009; see **Figure 1B**) compared to wild-type seedlings. Future work should clarify whether hydrogen peroxide acts as an upstream signal for both general and selective autophagy.

What proteins are necessary for recognizing peroxisomes targeted for autophagy? In methylotrophic yeast, a pexophagy receptor Atg30 bridges the molecular interaction between an autophagic complex and the peroxisomal proteins Pex3 and Pex14 (Farré et al., 2008; Zutphen et al., 2008). In mammalian cells, Pex14 interacts with LC3, an Atg8 homolog (Hara-Kuge and Fujiki, 2008). In addition, p62 and Neighbor of BRCA1 gene 1 (NBR1) may form a bridge between an ubiquitylated peroxisomal protein and LC3 (Kim et al., 2008; Deosaran et al., 2013). Intriguingly, an *Arabidopsis* ortholog of yeast Pex14 was identified from a genetic screen for mutants that showed stabilization of peroxisomal markers (Burkhart et al., 2013). It remains to be seen whether molecular interaction leading to pexophagy is conserved among distant eukaryotes (**Figure 1**).

## ACKNOWLEDGMENTS

We apologize to colleagues whose work has not been mentioned because of space limitations. This work is supported by the Basic Science Research Program through the National Research Foundation of Korea funded by the Ministry of Science, ICT and Future Planning (2011-0010683) and by a grant from the Next-Generation BioGreen 21 Program (No. PJ009004), Rural Development Administration, South Korea.

## REFERENCES

- Bartel, B., Farmer, L. M., Rinaldi, M. A., Young, P. G., Danan, C. H., and Burkhart, S. E. (2014). Mutation of the *Arabidopsis* LON2 peroxisomal protease enhances pexophagy. *Autophagy* 10, 518–519. doi: 10.4161/auto.27565
- Beevere, H. (1979). Microbodies in higher plants. *Annu. Rev. Plant Physiol.* 30, 159–193. doi: 10.1146/annurev.pp.30.060179.001111
- Burkhart, S. E., Lingard, M. J., and Bartel, B. (2013). Genetic dissection of peroxisome-associated matrix protein degradation in *Arabidopsis thaliana*. *Genetics* 193, 125–141. doi: 10.1534/genetics.112.146100

- Deosaran, E., Larsen, K. B., Hua, R., Sargent, G., Wang, Y., Kim, S., et al. (2013). NBR1 acts as an autophagy receptor for peroxisomes. *J. Cell Sci.* 126, 939–952. doi: 10.1242/jcs.114819
- Doelling, J. H., Walker, J. M., Friedman, E. M., Thompson, A. R., and Vierstra, R. D. (2002). The APG8/12-activating enzyme APG7 is required for proper nutrient recycling and senescence in *Arabidopsis thaliana*. *J. Biol. Chem.* 277, 33105–33114. doi: 10.1074/jbc.M204630200
- Farmer, L. M., Rinaldi, M. A., Young, P. G., Danan, C. H., Burkhardt, S. E., and Bartel, B. (2013). Disrupting autophagy restores peroxisome function to an *Arabidopsis* lon2 mutant and reveals a role for the LON2 protease in peroxisomal matrix protein degradation. *Plant Cell* 25, 4085–4100. doi: 10.1105/tpc.113.113407
- Farré, J. C., Manjithaya, R., Mathewson, R. D., and Subramani, S. (2008). PpAtg30 tags peroxisomes for turnover by selective autophagy. *Dev. Cell* 14, 365–376. doi: 10.1016/j.devcel.2007.12.011
- Floyd, B. E., Morris, S. C., MacIntosh, G. C., and Bassham, D. C. (2012). What to eat: evidence for selective autophagy in plants. *J. Integr. Plant Biol.* 54, 907–920. doi: 10.1093/jip/pcu017
- Goto-Yamada, S., Mano, S., Nakamori, C., Kondo, M., Yamawaki, R., Kato, A., et al. (2014). Chaperone and protease functions of LON protease 2 modulate the peroxisomal transition and degradation with autophagy. *Plant Cell Physiol.* 55, 482–496. doi: 10.1093/pcp/pcu017
- Gruber, P. J., Becker, W. M., and Newcomb, E. H. (1973). The development of microbodies and peroxisomal enzymes in greening bean leaves. *J. Cell Biol.* 56, 500–518. doi: 10.1083/jcb.56.2.500
- Hackenberg, T., Juul, T., Auzina, A., Gwizdz, S., Malolepszy, A., van der Kelen, K., et al. (2013). Catalase and NO CATALASE ACTIVITY1 promote autophagy-dependent cell death in *Arabidopsis*. *Plant Cell* 25, 4616–4626. doi: 10.1105/tpc.113.117192
- Hara-Kuge, S., and Fujiki, Y. (2008). The peroxin Pex14p is involved in LC3-dependent degradation of mammalian peroxisomes. *Exp. Cell Res.* 314, 3531–3541. doi: 10.1016/j.yexcr.2008.09.015
- Hu, J., Baker, A., Bartel, B., Linka, N., Mullen, R. T., Reumann, S., et al. (2012). Plant peroxisomes: biogenesis and function. *Plant Cell* 24, 2279–2303. doi: 10.1105/tpc.112.096586
- Inoue, Y., Suzuki, T., Hattori, M., Yoshimoto, K., Ohsumi, Y., and Moriyasu, Y. (2006). AtATG genes, homologs of yeast autophagy genes, are involved in constitutive autophagy in *Arabidopsis* root tip cells. *Plant Cell Physiol.* 47, 1641–1652. doi: 10.1093/pcp/pcl031
- Kim, D. Y., Scalf, M., Smith, L. M., and Vierstra, R. D. (2013a). Advanced proteomic analyses yield a deep catalog of ubiquitylation targets in *Arabidopsis*. *Plant Cell* 25, 1523–1540. doi: 10.1105/tpc.112.108613
- Kim, J., Lee, H., Lee, H. N., Kim, S., Shin, K., and Chung, T. (2013b). Autophagy-related proteins are required for degradation of peroxisomes in *Arabidopsis* hypocotyls during seedling growth. *Plant Cell* 25, 4956–4966. doi: 10.1105/tpc.113.117960
- Kim, P. K., Hailey, D. W., Mullen, R. T., and Lippincott-Schwartz, J. (2008). Ubiquitin signals autophagic degradation of cytosolic proteins and peroxisomes. *Proc. Natl. Acad. Sci. U.S.A.* 105, 20567–20574. doi: 10.1073/pnas.0810611105
- Li, F., and Vierstra, R. D. (2012). Autophagy: a multifaceted intracellular system for bulk and selective recycling. *Trends Plant Sci.* 17, 526–537. doi: 10.1016/j.tplants.2012.05.006
- Lingard, M. J., and Bartel, B. (2009). *Arabidopsis* LON2 is necessary for peroxisomal function and sustained matrix protein import. *Plant Physiol.* 151, 1354–1365. doi: 10.1104/pp.109.142505
- Lingard, M. J., Monroe-Augustus, M., and Bartel, B. (2009). Peroxisome-associated matrix protein degradation in *Arabidopsis*. *Proc. Natl. Acad. Sci. U.S.A.* 106, 4561–4566. doi: 10.1073/pnas.0811329106
- Nishimura, M., Hayashi, M., Kato, A., Yamaguchi, K., and Mano, S. (1996). Functional transformation of microbodies in higher plant cells. *Cell Struct. Funct.* 21, 387–393. doi: 10.1247/csf.21.387
- Pérez-Pérez, M. E., Lemaire, S. D., and Crespo, J. L. (2012). Reactive oxygen species and autophagy in plants and algae. *Plant Physiol.* 160, 156–164. doi: 10.1104/pp.112.199992
- Pracharoenwattana, I., and Smith, S. M. (2008). When is a peroxisome not a peroxisome? *Trends Plant Sci.* 13, 522–525. doi: 10.1016/j.tplants.2008.07.003
- Shibata, M., Oikawa, K., Yoshimoto, K., Kondo, M., Mano, S., Yamada, K., et al. (2013). Highly oxidized peroxisomes are selectively degraded via autophagy in *Arabidopsis*. *Plant Cell* 25, 4967–4983. doi: 10.1105/tpc.113.116947
- Smith, M. H., Ploegh, H. L., and Weissman, J. S. (2012). Road to ruin: targeting proteins for degradation in the endoplasmic reticulum. *Science* 334, 1086–1090. doi: 10.1126/science.1209235
- Till, A., Lakhani, R., Burnett, S. F., and Subramani, S. (2012). Pexophagy: the selective degradation of peroxisomes. *Int. J. Cell Biol.* 2012, 18. doi: 10.1155/2012/512721
- Trelease, R. N., Becker, W. M., Gruber, P. J., and Newcomb, E. H. (1971). Microbodies (glyoxysomes and peroxisomes) in cucumber cotyledons. *Plant Physiol.* 48, 461–475. doi: 10.1104/pp.48.4.461
- Vigil, E. L. (1970). Cytochemical and developmental changes in microbodies (glyoxysomes) and related organelles of castor bean endosperm. *J. Cell Biol.* 46, 435–454. doi: 10.1083/jcb.46.3.435
- Yoshimoto, K., Shibata, M., Oikawa, K., Sato, M., Toyooka, K., et al. (2014). Quality control of plant peroxisomes in organ specific manner via autophagy. *J. Cell Sci.* 127, 1161–1168. doi: 10.1242/jcs.139709
- Zhuang, X., Wang, H., Lam, S. K., Gao, C., Wang, X., Cai, Y., et al. (2013). A BAR-domain protein SH3P2, which binds to phosphatidylinositol 3-phosphate and ATG8, regulates autophagosome formation in *Arabidopsis*. *Plant Cell* 25, 4596–4615. doi: 10.1105/tpc.113.118307
- Zolman, B. K., Monroe-Augustus, M., Silva, I. D., and Bartel, B. (2005). Identification and functional characterization of *Arabidopsis* PEROXIN4 and the interacting protein PEROXIN22. *Plant Cell* 17, 3422–3435. doi: 10.1105/tpc.105.035691
- Zutphen, T., Veenhuis, M., and van der Klei, I. J. (2008). Pex14 is the sole component of the peroxisomal translocon that is required for pexophagy. *Autophagy* 4, 63–66.

**Conflict of Interest Statement:** The authors declare that the research was conducted in the absence of any commercial or financial relationships that could be construed as a potential conflict of interest.

**Received:** 21 January 2014; **paper pending published:** 19 February 2014; **accepted:** 24 March 2014; **published online:** 08 April 2014.

**Citation:** Lee HN, Kim J and Chung T (2014) Degradation of plant peroxisomes by autophagy. *Front. Plant Sci.* 5:139. doi: 10.3389/fpls.2014.00139

*This article was submitted to Plant Cell Biology, a section of the journal Frontiers in Plant Science.*

*Copyright © 2014 Lee, Kim and Chung. This is an open-access article distributed under the terms of the Creative Commons Attribution License (CC BY). The use, distribution or reproduction in other forums is permitted, provided the original author(s) or licensor are credited and that the original publication in this journal is cited, in accordance with accepted academic practice. No use, distribution or reproduction is permitted which does not comply with these terms.*



# Plant peroxisomes are degraded by starvation-induced and constitutive autophagy in tobacco BY-2 suspension-cultured cells

Olga V. Voitsekhovskaja<sup>1,2</sup>, Andreas Schiermeyer<sup>3</sup> and Sigrun Reumann<sup>1,4,5 \*</sup>

<sup>1</sup> Department of Plant Biochemistry, Albrecht-von-Haller-Institute for Plant Sciences, Georg-August-Universität Göttingen, Göttingen, Germany

<sup>2</sup> Komarov Botanical Institute, Russian Academy of Sciences, Laboratory of Plant Ecological Physiology, Saint Petersburg, Russia

<sup>3</sup> Abteilung Pflanzenbiotechnologie, Fraunhofer-Institut für Molekularbiologie und Angewandte Ökologie, Aachen, Germany

<sup>4</sup> Institute for Mathematics and Natural Sciences, Faculty of Science and Technology, Centre for Organelle Research, University of Stavanger, Stavanger, Norway

<sup>5</sup> Faculty of Mathematics, Informatics and Natural Sciences, Biocentre Klein Flottbek, University of Hamburg, Hamburg, Germany

**Edited by:**

Jose Luis Crespo, Consejo Superior de Investigaciones Científicas, Spain

**Reviewed by:**

Taijoon Chung, Pusan National University, South Korea

Shino Yamada Goto, Kyoto University, Japan

**\*Correspondence:**

Sigrun Reumann, Faculty of Mathematics, Informatics and Natural Sciences, Biocentre Klein Flottbek, University of Hamburg, Ohnhorststrasse 18, 22609 Hamburg, Germany  
e-mail: sigrun.reumann@uni-hamburg.de

Very recently, autophagy has been recognized as an important degradation pathway for quality control of peroxisomes in *Arabidopsis* plants. To further characterize the role of autophagy in plant peroxisome degradation, we generated stable transgenic suspension-cultured cell lines of heterotrophic *Nicotiana tabacum* L. cv. Bright Yellow 2 expressing a peroxisome-targeted version of enhanced yellow fluorescent protein. Indeed, this cell line model system proved advantageous for detailed cytological analyses of autophagy stages and for quantification of cellular peroxisome pools under different culturing conditions and upon inhibitor applications. Complementary biochemical, cytological, and pharmacological analyses provided convincing evidence for peroxisome degradation by bulk autophagy during carbohydrate starvation. This degradation was slowed down by the inhibitor of autophagy, 3-methyladenine (3-MA), but the 3-MA effect ceased at advanced stages of starvation, indicating that another degradation mechanism for peroxisomes might have taken over. 3-MA also caused an increase particularly in peroxisomal proteins and cellular peroxisome numbers when applied under nutrient-rich conditions in the logarithmic growth phase, suggesting a high turnover rate for peroxisomes by basal autophagy under non-stress conditions. Together, our data demonstrate that a great fraction of the peroxisome pool is subject to extensive autophagy-mediated turnover under both nutrient starvation and optimal growth conditions. Our analyses of the cellular pool size of peroxisomes provide a new tool for quantitative investigations of the role of plant peroxisomes in reactive oxygen species metabolism.

**Keywords:** peroxisome, autophagy, pexophagy, tobacco BY-2 cells, organelle degradation, cellular peroxisome pool

## INTRODUCTION

Plant peroxisomes perform many important functions including metabolism of reactive oxygen species (ROS), photorespiration, lipid metabolism, synthesis of plant hormones, polyamine metabolism, and ureate catabolism (Hayashi and Nishimura, 2003; del Rio et al., 2006; Reumann and Weber, 2006; Graham, 2008; Moschou et al., 2008; Kaur et al., 2009; Palma et al., 2009). Proteomic methodology recently allowed the recognition of additional metabolic functions, including, for instance, in the biosynthesis of phylloquinone (Babujee et al., 2010). Plant peroxisomes also play essential roles in photomorphogenesis, embryogenesis, and seed germination and in plant pathogen defense mechanisms

(Kaur et al., 2009; Hu et al., 2012). Peroxisome biogenesis has been studied in considerable detail both mechanistically and at the molecular level. More than 30 PEXs have been cloned and functionally characterized in fungi, mammals, and plants (for review, see Kaur et al., 2009; Ma and Subramani, 2009; Ma et al., 2011; Hu et al., 2012). Contrary to plant peroxisome biogenesis, our knowledge about mechanisms of peroxisome degradation in plant cells has remained scarce.

Studies in fungi and mammals demonstrated that peroxisomes are degraded by autophagy (Farre and Subramani, 2004; Dunn et al., 2005). Autophagy is a catabolic process for cellular remodeling and macromolecule recycling to tolerate extensive phases of nutrient starvation and to eliminate superfluous and dysfunctional cell organelles. Autophagy ultimately leads to degradation of cytoplasmic structures such as single proteins, protein complexes, and entire organelles in the acidic central vacuole (yeast, plants) or lysosome (mammals). Two major autophagic pathways have been described, macro- and microautophagy (Bassham, 2007, 2009). Macroautophagy, which is the major and best characterized mechanism, is initiated in the cytoplasm with the formation of

**Abbreviations:** Ab, autophagic body; Al, autolysosome; ATG, autophagy-related gene; BY-2, *Nicotiana tabacum* L. cv. Bright Yellow 2; CaMV, cauliflower mosaic virus; CAT, catalase; CLSM, confocal laser scanning microscopy; Concanamycin A; DEHP, di(2-ethylhexyl) phthalate; DIC, differential interference contrast; DMSO, dimethylsulfoxide; EYFP, enhanced yellow fluorescent protein; FW, fresh weight; ICL, isocitrate lyase; LTR, Lysotracker Red; MDC, monodansylcadaverine; 3-MA, 3-methyladenine; MS, Murashige and Skoog; OD, optical density; PEX, peroxisomal biogenesis protein; PEPCx, phosphoenolpyruvate carboxylase; RT, room temperature; ROS, reactive oxygen species.

cup-shaped membranes termed the preautophagosomal structure. The elongating membranes enclose the material to be degraded in double-membrane autophagosomes that subsequently fuse with the vacuole. The outer membrane of the autophagosome fuses with the tonoplast and releases its content, referred to as the autophagic body, into the vacuolar lumen (Li and Vierstra, 2012; Liu and Bassham, 2012). By contrast, in microautophagy, cytosolic proteins or entire cell organelles are directly engulfed by the vacuole through invagination of the tonoplast.

Macroautophagy, hereafter referred to as autophagy, has been also reported to exist in plants, where the mechanism is involved in various developmental processes, including the formation of the vegetative and protein storage vacuoles and senescence (Moriyasu and Hillmer, 2000). Plant autophagy is induced by various types of nutrient starvation. Degradation of non-essential cellular components liberates energy and catabolic intermediates that can be recycled to maintain basal levels of cellular metabolism. Plant autophagy is also important to cope with adverse environmental stress conditions by removal of damaged dysfunctional structures. During senescence in individually darkened leaves, chloroplasts were shown to be degraded by autophagy (Wada et al., 2009). *Arabidopsis* loss-of-function mutants of genes homologous to yeast Autophagy-related (Atg) genes are generally viable but exhibit early senescence (for review, see Thompson and Vierstra, 2005; Bassham, 2007, 2009; Reumann et al., 2010; Li and Vierstra, 2012).

Very recently, the first reports on plant pexophagy, or selective degradation of peroxisomes by autophagy have been published. As deduced from pharmacological studies inhibiting autophagy and genetic experiments using *atg7* mutants, peroxisomes in *Arabidopsis thaliana* hypocotyls are turned over by autophagy during seedling growth (Kim et al., 2013, 2014). In leaves of *atg5* gene knockout *Arabidopsis thaliana* mutants, peroxisomes accumulated and contained elevated levels of insoluble inactive catalase (CAT) (Yoshimoto et al., 2014). In a forward genetic screen for *Arabidopsis* mutants altered in peroxisomal positioning, Shibata et al. (2013) identified three *Arabidopsis thaliana* mutants that contained aggregated peroxisomes and whose gene defects were identical to autophagy mutants (*atg2*, *atg18a*, and *atg7*). The number of peroxisomes was increased, and the aggregated peroxisomes, which co-localized with the autophagosome marker, ATG8, contained high levels of inactive CAT indicative of damaged peroxisomes. Hence, the most recent data provided evidence that autophagy is crucial for quality control mechanisms for peroxisomes in *Arabidopsis* (Kim et al., 2013, 2014; Shibata et al., 2013; Yoshimoto et al., 2014).

Contrary to whole plants, suspension-cultured tobacco (*Nicotiana tabacum*) BY-2 cells offer several advantages for autophagic studies, including their accessibility to inhibitors and small fluorescent molecules and the ability to induce autophagy by sucrose starvation. For instance, autophagy can be blocked by 3-MA in BY-2 cells (Takatsuka et al., 2004). To establish suspension-cultured BY-2 cells as a model system for studies of plant pexophagy and characterize the degradation mechanism in greater detail, we labeled peroxisomes in tobacco BY-2 cells with EYFP-SKL. By comprehensive biochemical and cytological analyses we demonstrate in this study that peroxisomes in BY-2 cells are degraded by autophagy under nutrient starvation. We furthermore show

that even under optimal, nutrient-sufficient growth conditions and in exponential growth phase, peroxisomes are subjected to autophagy-mediated turnover, indicating a major physiological need for replacement of most likely dysfunctional peroxisomes in plants.

## MATERIALS AND METHODS

### PLANT MATERIAL AND GENERATION OF STABLE TRANSGENIC BY-2 CELL LINES

Tobacco (*N. tabacum*) BY-2 suspension cells were stably transformed by *Agrobacterium*-mediated transformation (An, 1985) to express a peroxisome-targeted version of EYFP from the CaMV 35S promoter. For peroxisome targeting the reporter protein was extended C-terminally by the last ten amino acid residues (KALGLPVSKL) of *Arabidopsis* hydroxypyruvate reductase (Genbank reference sequence NP\_176968, At1g68010) using the primers EYFP-for (*Nco*I, 5'-A AGTCCATGGTGAGCAAGGGCGAGGA-3') and EYFP-PTD<sub>HPR</sub>-rev (*Xba*I, 5'-TATATCTAGATCATAGCTTCGAAACAGGCAATC CTAAGGCCCTTCTGTACAGCTCGTCCATGCC-3') and subcloned first into pCAT (Ma and Reumann, 2008). The insert, EYFP-SKL was then, via pUC18ENTR2, further transferred into the plant expression vector pCAMBIA3300 via LR reaction for gene expression in BY-2 cells from the CaMV 35S promoter. pCAMBIA-EYFP-SKL was transformed into *Agrobacterium tumefaciens* GV3101::pMP90 (Hellens et al., 2000) by electroporation and kanamycin resistant clones were analyzed for the presence of the recombinant plasmid by restriction enzyme digest of the isolated plasmid DNA. Tobacco BY-2 cells were co-cultivated with the transgenic agrobacteria for 3 days and then spread out on blotting papers (MN 218 B, Macherey-Nagel, Düren, Germany) layered on top of MSMO medium (Sigma-Aldrich, Taufkirchen, Germany) agar plates containing 100 mg/l cefotaxim (Duchefa, Haarlem, The Netherlands). After 8 days the blotting papers with the cells were transferred to MSMO selection plates containing 100 mg/L cefotaxim and 0.3 mg/L bialaphos (Duchefa). Bialaphos resistant calli appeared after a 14-day incubation period on the selection plates. From these calli, suspension cell cultures were established and maintained as described (Schiermeyer et al., 2005). Consistent with previous reports, EYFP-SKL was efficiently targeted to peroxisomes with hardly any detectable cytosolic background staining (see Figure 1). One cell line with high EYFP expression level was selected for autophagy studies.

BY-2 transformants were cultured in MS growth medium at 25 ± 1°C with orbital shaking of 120 rpm in the dark. The medium consisted of MS basal salts with minimal organics (4.33 g/l), 3% (w/v) sucrose, 0.01% (w/v) myo-inositol, 0.2 mg/l 2,4-D, 1 mg/l thiamine hydrochloride, and 255 mg/l KH<sub>2</sub>PO<sub>4</sub>, pH 5.8. Under these culture conditions, the BY-2 cells reached the stationary phase after 6 days and were weekly sub-cultured (dilution 1:35 in 70 ml).

### AUTOPHAGY ANALYSIS DURING SUCROSE STARVATION

250 ml MS medium containing 3% sucrose was inoculated in duplicates with 4-day-old cells (1:25 dilution) and grown for 4 days. The cells were sedimented by centrifugation (100 × g for

5 min), washed twice with MS medium lacking sucrose and re-suspended in MS medium lacking sucrose  $\pm$  5 mM 3-MA. The cultures were incubated at 25  $\pm$  1°C under rotation (120 rpm) in the darkness. During the 12-day period of analysis, three 1-ml aliquots (for determination of cell viability and EYFP fluorescence in living cells and for cytological observations) and one 15-ml aliquot [for determination of fresh weight (FW), protein content, and enzymatic activities] were taken from each culture daily.

#### AUTOPHAGY ANALYSIS UNDER STANDARD GROWTH CONDITIONS

BY-2 cells were grown in MS medium containing 3% sucrose  $\pm$  5 mM 3-MA for 3 days. After sedimentation and washing, the cells were transferred back to standard MS medium (3% sucrose) lacking 3-MA and observed for additional 6 days (for 9 days altogether). 1-ml aliquots were taken daily for determination of cell viability and EYFP fluorescence in living cells and for light microscopy observations.

#### PROTEIN EXTRACTION AND ANALYSIS OF PROTEIN CONTENT AND OF ENZYMATIC ACTIVITIES

The cells were sedimented by centrifugation, the residual MS medium was removed with a syringe, and the FW was determined. The cells were frozen in liquid N<sub>2</sub>, lyophilized and stored at -80°C. For extraction, the cells were supplemented with glass beads (800  $\mu$ l beads Ø 0.25–0.50 mm and four beads Ø 0.4 cm) and 3 ml of extraction buffer [50 mM Hepes-KOH (pH 7.4), 5 mM MgCl<sub>2</sub>, 5 mM DTT, 2 mM benzamidin, 2 mM  $\epsilon$ -amino-caproic acid, 1 mM Na<sub>2</sub>-EDTA, 1 mM EGTA, 0.5 mM PMSF, 0.1% (v/v) Triton-X-100, 10% (v/v) glycerol], vortexed (1 min) and incubated on ice (1 min). This procedure was repeated six times. After centrifugation (16000 g, 15 min, 4°C) the supernatant was frozen in small aliquots. The protein concentration was measured according to Lowry using bovine serum albumin as standard (Lowry et al., 1951). The activity of CAT was measured in 100 mM potassium phosphate buffer (pH 7.0) and 3% (v/v) H<sub>2</sub>O<sub>2</sub> by monitoring H<sub>2</sub>O<sub>2</sub> disproportionation at 240 nm (see Figure S1). The activities of fumarase and phosphoenolpyruvate carboxylase (PEPCx) were determined as described elsewhere (Stitt et al., 1978; Stitt, 1984). To investigate complete quenching of proteolytic activities in sucrose-starved BY-2 cells by protease inhibitors, proteins were extracted from BY-2 cells subjected to sucrose starvation for 0 and 6 days and the activities of two representative compartment-specific marker enzymes, PEPCx and CAT, were determined in separate and combined extract (mixed at a ratio of 1:1) after incubation on ice for 60 min. For the combined extract, theoretical activity values were calculated based on the data obtained from single extracts. For neither PEPCx nor CAT the measured enzymatic activities were significantly reduced (data not shown), indicating complete quenching of autophagy-induced proteolytic activities in protein extracts.

#### CELL DEATH ASSAY

Accumulation of Evans' blue in dead BY2 cells (living cells actively extrude the dye) was determined as in Takatsuka et al. (2004) and calculated as A<sub>600</sub> per gram FW. 0% cell death was attributed to sucrose-supplied cells in the middle of logarithmic growth. To

define 100% cell death, cells were killed by two cycles of freezing and thawing.

#### INHIBITOR APPLICATION FOR CYTOLOGICAL STUDIES

3-MA and E-64 were applied as described by Takatsuka et al. (2004). Concanavalin A was prepared as a 100  $\mu$ M stock solution in DMSO and used at final concentration 1  $\mu$ M. The cells supplied with inhibitors were cultured at 25  $\pm$  1°C with rotation of 120 rpm. Aliquots were washed with 100 mM potassium phosphate buffer (pH 7.4) and analyzed by light microscopy.

#### IMMUNOLocalization of CATALASE

BY-2 transformants (200  $\mu$ l of culture) were re-suspended in 600  $\mu$ l 1% glutaraldehyde in MS medium, shaken vigorously for 15 min at room temperature (RT) and washed twice with MS medium. 400  $\mu$ l solution containing 5 U/ml cellulase Onozuka R-10 (Serva), a mixture of 0.5 U/mg pectinase, 0.1 U/mg cellulase, 0.25 U/mg hemicellulase (Macerozyme R-10, Serva) and 5 U/ml pectinase (Fluka) dissolved in osmoticum (0.5% BSA, 0.01%  $\beta$ -mercaptoethanol, 50 mM CaCl<sub>2</sub>, 250 mM sorbitol, 100 mM Na acetate, pH 5.0) were added to the cells. Cells were incubated for 1 h at 28°C while shaking, washed three times with 600  $\mu$ l PBS, then 600  $\mu$ l of 0.3% Triton-X-100 in PBS were added and the cells were incubated for 15 min while shaking. After washing with 600  $\mu$ l of 5% (w/v) BSA dissolved in PBS, cells were incubated in a new portion of 600  $\mu$ l of 5% BSA solution for 1 h at RT (shaking). The cells were re-dissolved in 100  $\mu$ l of anti-CAT antiserum (gift by Prof. Feierabend, University of Frankfurt, polyclonal rabbit antiserum against barley CAT) diluted 1:400 with 1% (w/v) BSA in PBS. Control cells were re-dissolved in 1% BSA solution. The cells were incubated at 4°C overnight, washed four times with PBS and incubated with Alexa 568-conjugated secondary antibody diluted 1:100 with 1% (w/v) BSA in PBS for 4 h in the dark at RT while shaking. The cells were washed four times with PBS and observed by confocal laser scanning microscopy (CLSM).

#### WESTERN BLOTTING

After denaturation in Laemmli buffer, proteins were separated by SDS-PAGE and blotted to nitrocellulose membranes. After blocking of unspecific binding sites (1% dry milk powder in TBS buffer) the membranes were incubated in primary antiserum followed by secondary antibody. Primary antisera were kindly provided by Prof. Feierabend (University of Frankfurt, Germany, anti-CAT, polyclonal rabbit antiserum against barley CAT), Prof. Keegstra (MSU-DOE Plant Research Laboratory, East Lansing, MI, USA, anti-Toc75, polyclonal rabbit antiserum against pea Toc75), Prof. Feussner (University of Göttingen, Germany, polyclonal rabbit antiserum against cucumber isocitrate lyase, ICL), and Prof. Erdmann (University of Bochum, Germany, polyclonal rabbit antiserum against *Saccharomyces cerevisiae* Tom40). For detection of denatured EYFP a commercial monoclonal anti-GFP antiserum was used (Invitrogen). Protein dynamics were investigated by loading proteins from equal cell culture volumes. Western blot analysis by constant protein essentially showed the same dynamics as that relative to culture volume, but protein concentrations appeared to be overestimated at later stages of sucrose starvation, as shown by Coomassie Brilliant Blue staining (data not shown).

## QUANTIFICATION OF CELLULAR PEROXISOME NUMBERS

Individual BY-2 cells were separated from cell chains by addition of a similar volume of a mixture of cell wall-hydrolyzing enzymes dissolved in osmoticum as used in CAT immunolocalization protocol and incubation for 40 min at RT while shaking. The cells were fixed with 3.7% paraformaldehyde in 100 mM potassium phosphate buffer pH 7.4 and shaken at RT for 2 h to remove residual cell wall-hydrolyzing enzymatic activities. The cells were observed in potassium phosphate buffer by CLSM and cellular peroxisome numbers determined as described below.

## LIGHT AND CONFOCAL MICROSCOPY

A BX51 microscope (Olympus Deutschland GmbH, Hamburg, Germany) equipped with fluorescence and Nomarski DIC optics was used. Images were captured using a ColorView II digital camera and DP-Soft image-analytical software (Olympus Soft Imaging Solutions, Muenster, Germany). Peroxisomes were visualized by EYFP fluorescence using BP 450–480, DM 500, BA 515 filter. To visualize (auto)lysosomes, cells were incubated in 100 mM potassium phosphate buffer (pH 6.5) containing 1  $\mu$ M Lysotracker Red (LTR, Invitrogen, Molecular Probes) at RT for about 5 min, spun down for 5 min, washed twice and re-suspended in the same buffer and observed using BP 545–580, DM 600, BA 610-IF filter. To visualize autophagosomes, cells were incubated in 100 mM potassium phosphate buffer (pH 6.5) containing 5 mM monodansylcadaverine (MDC, Sigma Aldrich) at RT for about 5 min, spun down for 5 min, washed twice and re-suspended in the same buffer and observed using BP 330–385, DM 400, BA 420 filter. In control (i.e., sucrose-supplied) cells, (auto)lysosomes (Figures S2A–D) were not detected.

Cellular peroxisome numbers were quantified by CLSM (Zeiss LSM 510, Carl Zeiss, Göttingen, Germany) using a 488/568-nm ArKr laser in combination with a 505- to 550-nm band-pass filter set. Z-stacks of optical sections were obtained throughout the individual cells. 3D projections were obtained for every Z-stack corresponding to a single cell using either ImageJ 1.37v software (NIH, USA), or AxioVision 4.7.2. software (Carl Zeiss, Germany) using ramp 50, maximum opacity 50, brightness 1 and threshold 10%. Peroxisomes were counted manually using cell counter tool. For immunolocalization of CAT, a 488/561-nm ArKr laser in combination with a 505- to 530-nm band-pass and 575-nm filter set was used.

## STATISTICS

The experiments were repeated at least three times each with similar results. The figures show data from a typical experiment if not otherwise indicated. The quantification of peroxisomes per cell was made for two sucrose starvation experiments and for two experiments with the growth of cells upon addition of 3-MA, respectively. For each variant, 10–18 individual cells were worked up, and mean numbers of peroxisomes per cell  $\pm$  SE are shown. The significance of differences between cellular numbers of peroxisomes with vs. without addition of 3-MA at every time point of the experiments was analyzed using Student's *t*-test.

## RESULTS

### STARVATION-INDUCED AUTOPHAGY REDUCES STEADY-STATE LEVELS OF PEROXISOMAL PROTEINS

To address peroxisome degradation by autophagy in tobacco BY-2 cells, we created stable transgenic lines expressing the peroxisome marker EYFP-SKL from the constitutive *CaMV 35S* promoter. The peroxisome marker was created by extending the fluorophore C-terminally by the C-terminal decapeptide (KALGLPVSKL) of the *Arabidopsis* photorespiratory enzyme, hydroxypyruvate reductase. EYFP fluorescence was detected in numerous punctate subcellular structures (Figures 1A–D) that moved quickly within the cytosol. Organelle identity with peroxisomes was verified by immunocytochemical co-localization using a polyclonal antiserum against CAT (Figures 1E–G). CLSM confirmed that the strong targeting signal of hydroxypyruvate reductase EYFP-SKL (Ser-Lys-Leu) directed the fluorophore to peroxisomes with high efficiency, without any cytosolic background fluorescence when grown under nutrient-sufficient culturing conditions (Figures 1E,F). The EYFP-SKL lines did not show any growth phenotype compared to wild-type (WT) BY-2 cells, neither under sucrose-sufficient culturing conditions nor during sucrose starvation (data not shown).

Since autophagy is reported being induced in BY-2 cells upon nutrient starvation (Moriyasu and Ohsumi, 1996), we first investigated whether peroxisomes are degraded by autophagy under sucrose starvation. When cultured to mid-log phase under nutrient-sufficient conditions and thereafter deprived of sucrose, the BY-2 cells largely stopped cell growth and proliferation, as indicated by constant FW (Figure 2A). Despite nutrient starvation, the cells remained viable for about 6 days, as determined by Evans' Blue dye exclusion assay, indicating the activity of an efficient endogenous mechanism for cell remodeling and nutrient recycling such as autophagy. Subsequently, the cells slowly started dying (>day 8), coinciding with a drastic decline in FW (Figures 2A,B). Hence, heterotrophic BY-2 cells cultured without external carbon source can survive for nearly 1 week by using endogenous energy resources such as internal stores and/or autophagic recycling mechanisms. Application of the autophagy inhibitor 3-MA dramatically accelerated cell death (Figure 2B), consistent with the reported function of autophagy in cellular remodeling and survival during nutrient starvation in BY-2 cells (e.g., Takatsuka et al., 2004; Toyooka et al., 2006). Hence, the overexpressor lines with EYFP labeled peroxisomes showed similar growth characteristics and responses to sucrose starvation compared to WT, thereby allowing autophagic degradation studies of peroxisomes *in vivo*.

We first investigated peroxisome dynamics by biochemical means, applying immunoblotting with polyclonal antibodies against two endogenous and one recombinant soluble peroxisomal matrix proteins, CAT, ICL, and EYFP-SKL. Upon sucrose starvation the levels of the three peroxisomal matrix proteins decreased during the following 6 days, indicating proteolytic degradation of peroxisomal matrix protein (Figures 2C,D). In the presence of 3-MA, the three matrix proteins showed higher protein levels compared to culturing conditions in inhibitor absence. This effect was most pronounced for the native peroxisomal matrix proteins (CAT and ICL) at various time points and for the recombinant protein (EYFP-SKL) after 4 days of sucrose starvation (Figures 2C,D).

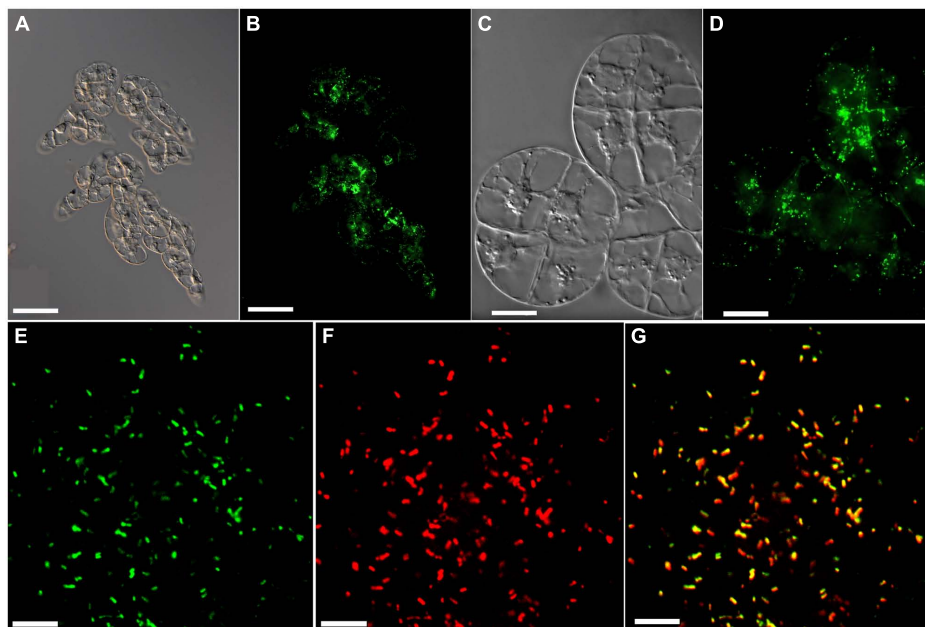


**FIGURE 1 | Fluorescent labeling of peroxisomes by EYFP-SKL.**

(A–D) Live-cell imaging of BY-2 transformants expressing *CaMV35S::EYFP-SKL* with Nomarski optics (A,C) or epifluorescence showing peroxisomes labeled by EYFP-SKL (B,D). CLSM imaging of EYFP (E), CAT immunofluorescence (F), and the merge of both (G). Scale bar 100  $\mu\text{m}$  (A,B), 20  $\mu\text{m}$  (C,D), and 4  $\mu\text{m}$  (E–G). CLSM confirmed that the strong targeting signal of the

*Arabidopsis* photorespiratory enzyme, hydroxypyruvate reductase (SKL), directed the fluorophore to peroxisomes with high efficiency, without any cytosolic background fluorescence when grown under nutrient-sufficient culturing conditions (E,F compare with images on B,D obtained by epifluorescence microscopy where some “cytosolic” background represents the EYFP fluorescence emitted by out-of-focus peroxisomes).

Interestingly, the chosen marker proteins for plastids (Toc75) and mitochondria (Tom40) showed a similar trend but only a marginal effect of 3-MA (Figures 2C,D), indicating that chloroplasts and mitochondria were degraded by starvation-induced autophagy to much lesser extent.

We complemented the analyses of organelle dynamics by activity analyses of compartment-specific marker enzymes such as CAT, fumarase (mitochondria), and PEP carboxylase (cytosol). Of several starvation experiments showing the same trend, one representative example is shown. The activities of all marker enzymes declined during sucrose starvation with minor differences in kinetics (Figure S1). In the presence of 3-MA the activities of the organelle marker enzymes remained higher and the starvation-induced loss of enzymatic activity was delayed (Figures S1B–D). The simplest explanation for the higher marker activities of 3-MA samples in Figures S1B–D is that they likely resulted from higher levels of enzyme protein in 3-MA-treated cells (Figure S1A). Along the same line, the total cellular protein content declined during sucrose starvation, and this effect was inhibited by 3-MA (Figure S1A). Control experiments verified that the decrease in protein content and enzymatic activities was not reduced *in vitro* by high proteolytic activities of sucrose-starved cells (data not shown; see Materials and Methods).

#### MICROSCOPIC ANALYSIS OF PEROXISOMES AND AUTOPHAGIC ORGANELLES

Consistent with the biochemical data (see above), the cellular abundance of peroxisomes gradually declined with the duration

of sucrose starvation. For instance, after 2 days of sucrose starvation the cellular number of peroxisomes was visibly reduced as compared to sucrose-supplied cells (Figures 3A,B; compare to Figures 1B,D), indicative of peroxisome turnover. Interestingly, also the shape and subcellular localization of EYFP-labeled peroxisomes changed. While the peroxisomes of BY2 cells cultured under nutrient-rich conditions were rather evenly distributed in the cytosol (Figures 1B,D), those of sucrose-starved cells tended to cluster around the nucleus (Figures 3A,B). In the presence of 3-MA, the cellular number of peroxisomes was visibly higher, further supporting the conclusion that peroxisomes are degraded by autophagy. Interestingly, peroxisome clustering around the nucleus was not observed in 3-MA-treated cells (Figures 3C,D), suggesting that the change in subcellular peroxisome localization preceded autophagic peroxisome degradation and was triggered by the signal transduction cascade inducing autophagy.

In tobacco cells treated with protease inhibitors, cytosolic structures to be degraded by autophagy are sequestered in autophagosomes that are subsequently converted to autolysosomes and release their content as autophagic bodies into the vacuole (Bassham, 2007, 2009). The results above suggested an analogous mechanism for autophagic peroxisome degradation in tobacco BY2 cells (Figure 4). Autophagy can be analyzed by staining with the acidotropic fluorescent dye monodansylcadaverine (MDC), which labels autolysosomes and possibly other acidic organelles (Figure 4; Contento et al., 2005). Due to their short half-life in the absence of inhibitors, autolysosomes can generally

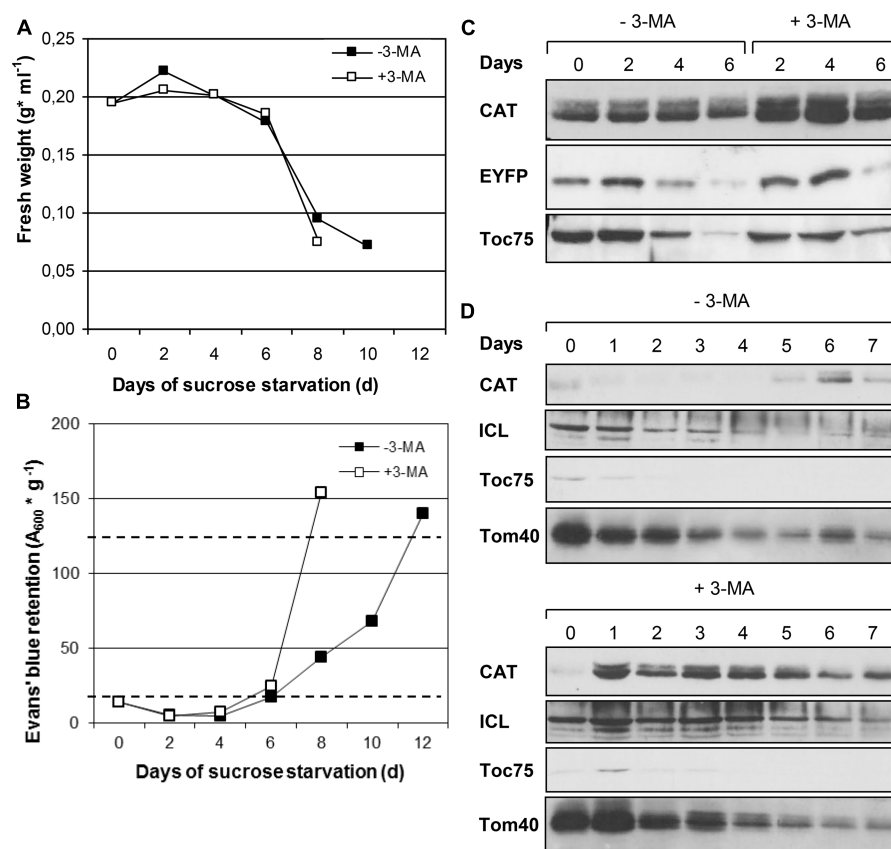


**FIGURE 2 |** Time course analysis of cell growth and organelle degradation in BY-2 transformants expressing *CaMV35S::EYFP-SKL* during sucrose starvation in the absence or presence of 3-MA. Data from one representative experiment are shown. (A) Fresh weight. (B) Cell viability estimated as  $A_{600\text{ nm}}$  of Evans' blue retained in dead BY-2 cells relative to gram fresh weight. Full cell viability (0% cell death) and complete cell death (100%) corresponded to 20 OD units  $\text{g}^{-1}$  and 125 units  $\text{g}^{-1}$ , respectively

(dotted lines). (C) Protein levels of compartment-specific marker proteins CAT and EYFP (peroxisomes) and Toc75 (plastids) as determined by immunoblotting. The amounts of protein loaded in each lane corresponded to equal cell culture volumes (C) or protein amount (50  $\mu\text{g}$ , D). The immunoblots of (D) stem from 3 large SDS-gels run, transferred, incubated and developed in parallel. Due to cutting of the large membranes into two halves for control and 3-MA-treated cells, the lanes are not presented continuously.

only be observed in the presence of inhibitors that block downstream steps of autophagic organelle processing (Bassham, 2007, 2009). Indeed, when staining sucrose-starved BY-2 cells with MDC (in the absence of 3-MA and E-64), only very few punctate structures could be visualized (Figure 3F). Likewise, only few Lysotracker Red (LTR)-positive organelles, which might represent (auto-)lysosomes (Al), could be visualized in sucrose-starved BY-2 cells (in the absence of 3-MA and E-64, Figure 3H). This result is consistent with the high turnover rate of autolysosomes.

To provide further evidence that peroxisomes are degraded by autophagy and to investigate a possible accumulation of autophagic vesicles, we applied the cysteine protease inhibitor, E-64, which blocks the transfer of autolysosomes to the central vacuole (Figure 4) and leads to pronounced accumulation of autolysosomes in the cytosol (Moriyasu and Inoue, 2008). Indeed, E-64 caused a drastic increase in the cellular abundance of LTR-stained organelles, particularly in the initial phase of sucrose starvation (32 h, Figure 3J). Interestingly, the LTR-positive organelles often formed large subcellular clusters in close proximity to the nucleus (Figures 3I,J). In parallel, the peroxisomes

clustered in the same cell areas as the LTR-stained organelle aggregates, suggesting that peroxisomes were degraded inside autolysosomes (Figures 3K,L). After 5 days of sucrose starvation, E-64 no longer caused accumulation of autolysosomes, even upon prolonged application time (48 h, data not shown). The data suggested that autophagy ceased after about 4 days of starvation in our experimental system and was replaced by a yet unknown mechanism of cell death.

When vacuolar degradation of autophagic bodies was blocked by the vacuolar V-ATPase inhibitor, ConcA, the central vacuole became filled with small particles (Figure 3M). As concluded previously (Thompson et al., 2005), the vacuolar structures most likely represented autophagic bodies (Ab). If this were the case, the accumulation of these bodies in the central vacuole should depend on the induction of autophagy and be abolished when blocking the signal transduction pathway inducing autophagy by 3-MA. As expected, the simultaneous application of both ConcA and 3-MA prevented the accumulation of particles in the vacuole, strengthening the idea that these organelles represented autophagic bodies (Figures 3O,P). The ConcA-dependent accumulation of vacuolar

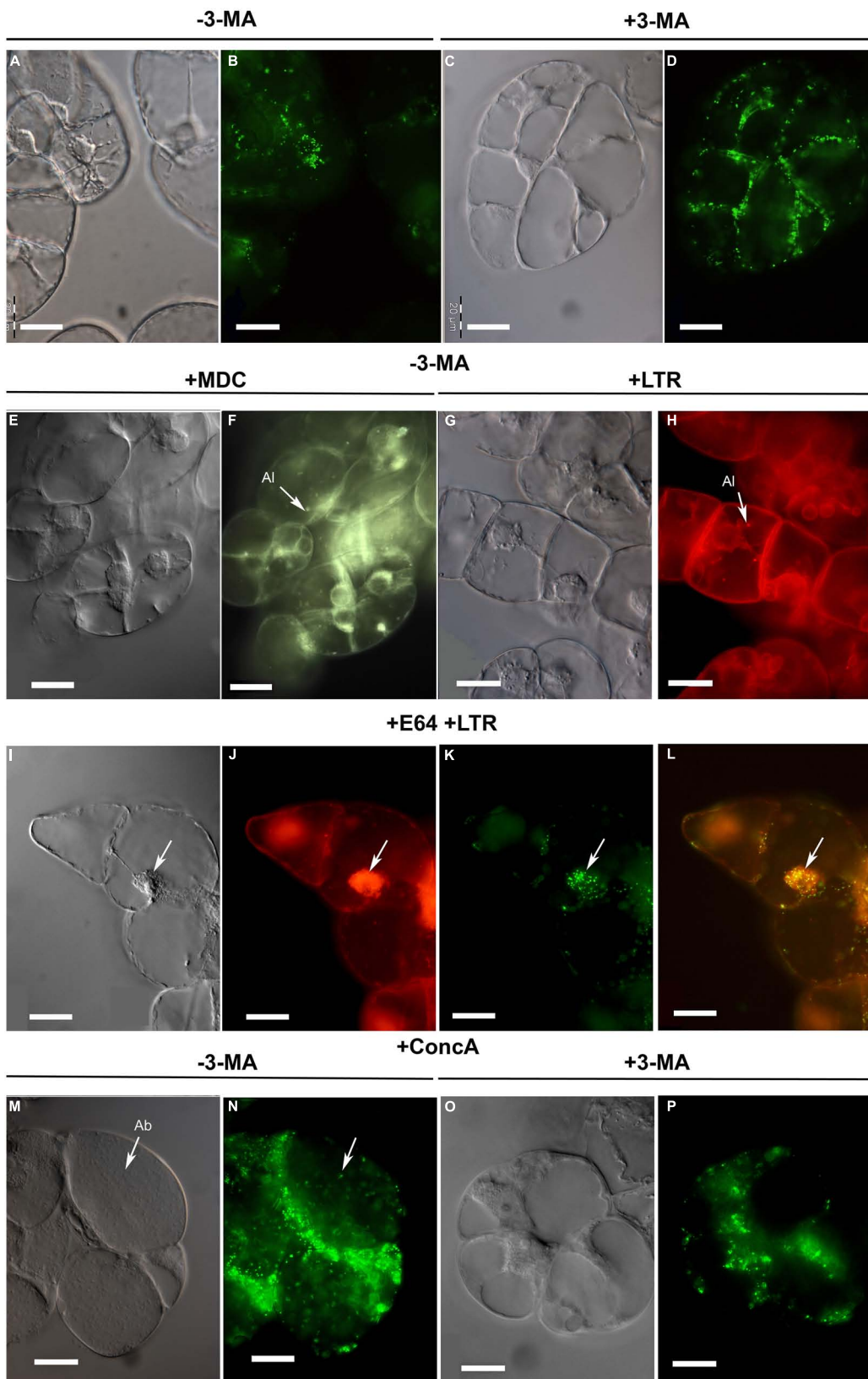


FIGURE 3 | Continued

**FIGURE 3 | Continued**

**Microscopic analysis of peroxisome dynamics during sucrose starvation.** (A–D) BY-2 cells were subjected to sucrose starvation for 2 days in the absence (A,B; –3-MA) or presence of 3-MA (C,D; +3-MA). Note peroxisome clustering around the cell nucleus in the absence of 3-MA (at this magnification seen as green clots in the cell center). (E–H) Monodansylcadaverine (MDC)-positive organelles (E,F) and Lysotracker red (LTR)-positive organelles (G,H), both indicative of autolysosomes (AI), appeared in the cells and were detected by staining after sucrose starvation (32 h) in the absence of 3-MA. (I–L) To achieve autolysosome accumulation, BY-2 cells were subjected to sucrose starvation alone for 8 h and in the presence of E-64 for an additional 24 h. The arrow points to a subcellular aggregate of putative autolysosomes (I,J) around the cell nucleus and peroxisomes (K) with image overlay (L = J+K). (M–P) After 2 days of sucrose starvation and in the presence of ConcA autophagic bodies (Ab, in M) and EYFP fluorescent structures (N) were detected in the central vacuole (M,N). (O,P) Application of 3-MA inhibited ConcA-dependent autophagic body formation (O) and the appearance of EYFP fluorescent structures in the central vacuole (P). Images were taken with Nomarski optic (A,C,E,G,I,M,O) and epifluorescence (B,D,F,H,J,K,N,P). Scale bar: 20  $\mu$ m.

autophagic bodies was paralleled by the appearance of yellow fluorescent punctate structures in the central vacuole (Figure 3N), suggesting that some vacuolar autophagic bodies contained peroxisomes and their remnant matrix proteins including EYFP-SKL. A certain degree of uniform background fluorescence of the vacuolar lumen was also observed, consistent with execution of the subsequent steps of autophagy when autophagic bodies and their organellar content become dissolved (Figure 4). Similar to E-64, ConcA ceased causing detectable accumulation of autophagic bodies in the vacuoles of the cells at advanced stages of starvation (data not shown).

#### REDUCTION OF CELLULAR PEROXISOME NUMBERS BY STARVATION-INDUCED AUTOPHAGY

To investigate the effect of starvation-induced autophagy on BY2 cell peroxisomes in greater details, we determined cellular

peroxisome numbers quantitatively by CLSM in a time course experiment in the absence and presence of 3-MA. BY-2 cells grown to mid logarithmic phase in nutrient-rich conditions (3% sucrose) contained on average about 350 peroxisomes per cell (day 0, Figure 5). Upon autophagy induction by sucrose starvation, the average cellular peroxisome number of control cells (i.e., in the absence of 3-MA) decreased by ~40% (to about 200, day 2) within the first 2 days and by ~70% (to 120 peroxisomes per cell) by day 6. The cellular steady-state number of peroxisomes is determined by the rates of peroxisome biogenesis and degradation and cell division. The results suggest that at least 70% of cellular peroxisomes were degraded, and even more if peroxisome proliferation continued.

When starvation-induced autophagy was blocked by 3-MA, the cellular number of peroxisomes first increased from 350 (day 0) to ~440 (day 2) and declined thereafter. Hence, peroxisome proliferation continued (possibly at lower pace compared to nutrient-sufficient conditions) in the first days of starvation in the presence of 3-MA. Compared to sucrose-starved control cells, the blockage of autophagy led to a ~2-fold increase in cellular peroxisome number (day 2). Similarly, at later stages of sucrose starvation (e.g., 4 and 6 days) the cellular peroxisome number was ~2-fold higher in cells treated with 3-MA as compared to the controls. Taken together, the decreasing steady-state levels of cellular peroxisomes in sucrose-starved BY2 cells and the 2-fold accumulation of peroxisomes in cells unable to execute starvation-induced autophagy further supported the previous pharmacological, biochemical, and microscopic data that whole tobacco BY2 cell peroxisomes are degraded by starvation-induced autophagy.

Interestingly, in the presence of 3-MA the cellular peroxisome number did not remain constant but decreased steadily (day 2: 440, day 4: 360, day 4: 250, Figure 4). Since the cells remained fully viable (Figure 2B), the data indicate that either starvation-induced

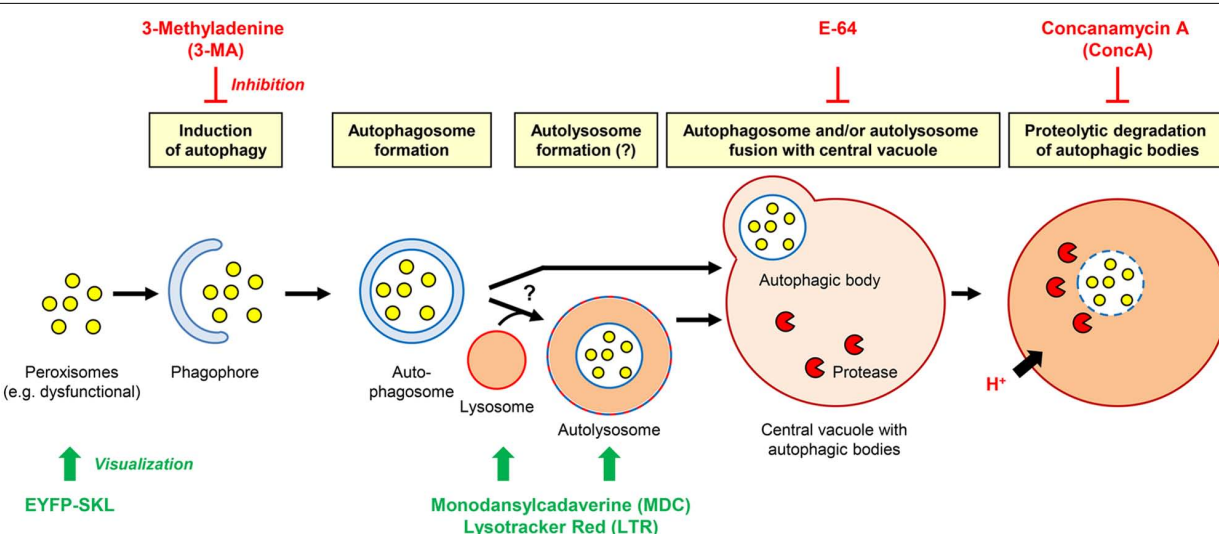


**FIGURE 4 | Hypothetical working model of the degradation of plant peroxisomes in tobacco by autophagy.** The effect of inhibitors and method of organelle visualization are indicated.

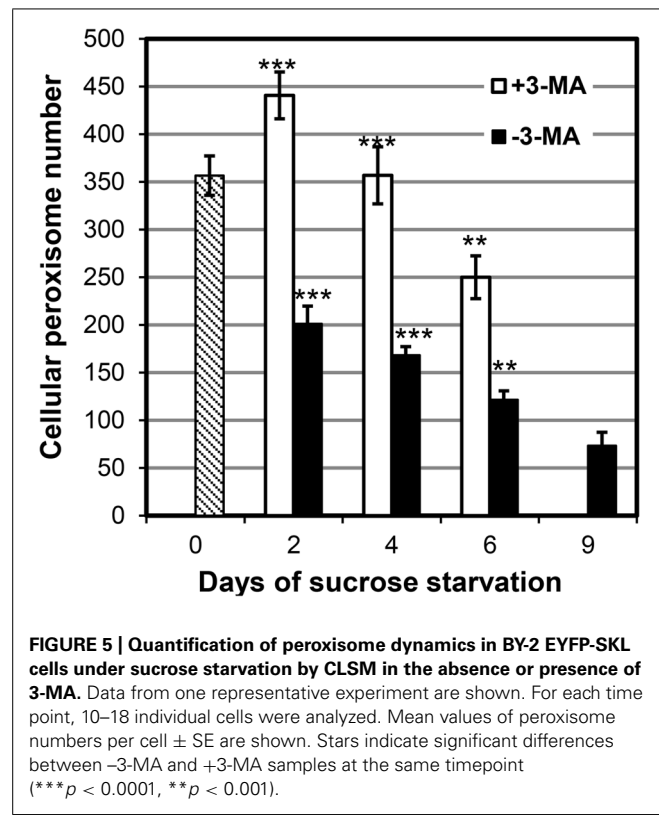


**FIGURE 5 | Quantification of peroxisome dynamics in BY-2 EYFP-SKL cells under sucrose starvation by CLSM in the absence or presence of 3-MA.** Data from one representative experiment are shown. For each time point, 10–18 individual cells were analyzed. Mean values of peroxisome numbers per cell  $\pm$  SE are shown. Stars indicate significant differences between –3-MA and +3-MA samples at the same timepoint ( $***p < 0.0001$ ,  $**p < 0.001$ ).

peroxisome degradation was incompletely blocked or that it was complemented by another mechanism different from autophagy. The latter explanation is in line with the observations that autophagy-specific structures could no longer be detected after the fourth day of starvation (see above). This second mechanism for peroxisome degradation might be induced on top of autophagy at late stage of sucrose starvation.

#### PEROXISOME DEGRADATION BY CONSTITUTIVE AUTOPHAGY

Given that peroxisomes are a major site of cellular ROS production, their matrix proteins are prone to oxidative damage, and efficient elimination of dysfunctional plant peroxisomes might be required under standard growth conditions. Recent plant autophagy studies in *Arabidopsis* support this idea (Shibata et al., 2013; Yoshimoto et al., 2014). To address constitutive peroxisome turnover in BY-2 cells, we investigated peroxisome degradation under nutrient-rich conditions. Tobacco BY-2 cells were first grown to mid-log phase and low cell density in the presence of sucrose (3%), then the medium was removed by gentle centrifugation, and the cells were re-suspended in a similar volume of fresh medium (day 0), either in the absence or presence of 3-MA. After 3 days the inhibitor was removed by multiple cell washes and the cells were transferred to new nutrient-rich MS medium (3% sucrose) lacking 3-MA (day 3) and analyzed after additional three to 6 days (day 6 and day 9, respectively). Control cells grown in the absence of 3-MA were sub-cultured identically except for the omission of 3-MA. As shown by FW analysis, BY-2 cells not exposed to 3-MA grew at exponential rate in sucrose-containing growth medium and reached stationary phase approximately at day 6, when

minimal signs of cell death became detectable (Figures 6A,B). The blockage of (constitutive) autophagy by 3-MA negatively affected BY-2 cell proliferation (FW, Figure 6A). Cell proliferation largely stagnated but after inhibitor removal (day 3), the cells recovered, as indicated by nearly 2-fold daily increase in FW (Figures 6A,B). In the representative experiment shown (Figure 6B), the rate of cell death 3 days after 3-MA addition was 8%; in other experiments, however, it was reaching  $\sim$ 20% (data not shown).

To investigate peroxisome dynamics under nutrient-rich conditions, we determined cellular peroxisome numbers as described above. The data yielded two major results. First, steady-state levels of cellular peroxisome numbers decreased with culture age and progressing cell senescence, i.e., from early exponential to late stationary phase. While BY-2 cells contained on average about 400 peroxisomes per cells at early exponential growth phase (day 3), the number decreased to about 300 at early (day 6) and 250 at late stationary phase (day 9). Notably, the extent of cell death was only marginal under these conditions (<10%, Figure 6).

Second, 3-MA caused a clearly visible increase in the cellular number of peroxisomes which was statistically significant after three and 6 days of recovery (Figures 6C,D). The average cellular peroxisome number was about 1.7 (after 3 days of recovery) to 2.0-fold higher (after 6 days of recovery) in BY-2 cells exposed transiently to 3-MA, even though grown under nutrient-rich conditions, as compared to control cells. Since control and treated cells were affected differently with respect to cell proliferation in this experiment (contrary to sucrose starvation), as indicated by exponentially increasing FW (for control cells) and stagnant FW (for 3-MA treated cells), not only the blockage of peroxisome degradation but also continuous of peroxisome proliferation might have affected the 2-fold higher cell numbers of peroxisomes in MA-treated cells (see Discussion).

The inhibitory effect of 3-MA on peroxisome degradation was supported by immuno-biochemical analysis of CAT protein levels, which clearly increased upon cell exposure to 3-MA. Interestingly and consistent with the starvation data, among the three major cell organelles investigated, the effect of 3-MA appeared to be most pronounced for peroxisomes (Figure 6E). Taken together the data indicated that peroxisomes are degraded even under nutrient-sufficient conditions and at early exponential phase to considerable extent by constitutive autophagy.

#### DISCUSSION

Recently, several research groups independently published conclusive evidence that *Arabidopsis* peroxisomes are degraded by autophagy and that this process is important for quality control of peroxisomes (Farmer et al., 2013; Kim et al., 2013; Shibata et al., 2013; Yoshimoto et al., 2014). While *Arabidopsis* research benefits from public collections of knock-out mutants, which lack for other plant species, tobacco BY-2 cells offer a complementary model system with several advantages to study plant autophagy in general and pexophagy in particular. First, autophagy can easily be induced in heterotrophic suspension-cultured cells by omission of essential nutrients in the growth medium (Moriyasu and Ohsumi, 1996; Takatsuka et al., 2004). The uniform cell type further standardizes cellular effects. Second, pharmacological inhibitors of

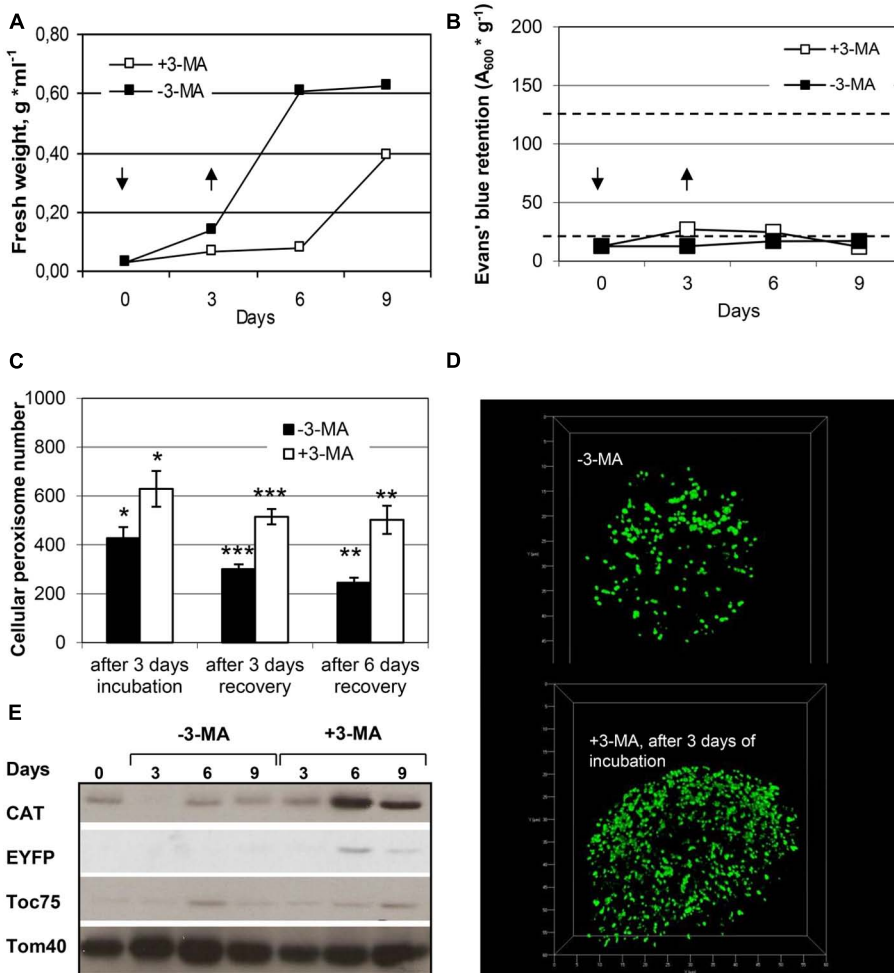


**FIGURE 6 | Quantification of peroxisome dynamics in BY-2 cells under standard growth conditions.** Tobacco BY-2 EYFP-SKL cells were cultivated under nutrient-rich standard growth conditions (3% sucrose) and in the absence or presence of 3-MA and analyzed for **(A)** fresh weight, **(B)** cell viability, **(C)** cellular peroxisome number (mean values of peroxisome numbers per cell  $\pm$  SE are shown; stars indicate a significant difference between -3-MA and +3-MA samples at the same timepoint: \*\*\* $p < 0.0001$ , \*\* $p < 0.001$ , \* $p < 0.05$ ) as determined from 3D-projections (examples shown in **D**), and **(E)** protein levels of

compartment-specific markers CAT (peroxisomes), Toc75 (plastids) and Tom40 (mitochondria). In the absence of 3-MA, the signals for CAT (3 days) and EYFP were below the detection limit in the given experiment. The amounts of protein loaded into each lane correspond to equal volumes of cell culture. Full cell viability (0% cell death) and complete cell death (100%) corresponded to 20 OD units  $g^{-1}$  and 125 OD units  $g^{-1}$ , respectively (dotted lines in **C**). Arrows indicate the time points of 3-MA application and removal by cell washing. Data from one representative experiment are shown.

autophagy that target key component of the autophagic machinery but are difficult to apply to entire *Arabidopsis* plants, are rapidly taken up by BY-2 cell lines and efficiently carry out their inhibitory functions. Third, the cellular peroxisome pool can be quantified relatively straight-forward in suspension-cultured cells. This analytical tool can be further explored in future quantitative studies of plant pexophagy addressing, for instance, which signal processes contribute to peroxisome turnover and which molecular players are involved (receptors, etc.). Last, stable transgenic tobacco cell lines with specific labeling of cell organelles by fluorescent markers can be generated.

Our investigations of peroxisome degradation are based on stable transgenic lines with fluorescently labeled peroxisomes expressing EYFP-SKL. Due to the very strong targeting signal

of hydroxypyruvate reductase, the reporter protein was targeted quantitatively to peroxisomes (Figure 1), thereby facilitating monitoring of peroxisomes with high microscopic and biochemical detection sensitivity. The high proteolytic stability of the  $\beta$ -barrel protein of GFP variants allowed autophagic pathway analysis until the very last stages in the vacuole (Figures 3 and 5) and quantitative determination of peroxisome degradation by EYFP immunoblotting analysis and cellular EYFP fluorescence. The reporter protein data were confirmed for two native plant peroxisomal marker proteins (CAT and ICL, Figures 2 and 6). The independent analytical methods complemented each other and allowed the underlying mechanism to be characterized as macroautophagy. The kinetics of protein accumulation differed slightly for three peroxisomal matrix proteins, and 3-MA-dependent protein accumulation was

most pronounced for CAT (**Figures 2C,D and 6E**). The data might suggest that particularly peroxisomes with a high content of CAT (possibly including oxidatively damaged CAT protein) are specifically prone to autophagic degradation, which needs to be investigated in greater detail in future studies. Kim et al. (2013) showed that even for two glyoxylate cycle enzymes, ICL and malate synthase, the kinetics of protein accumulation differed in mutants compromised in autophagy (*atg7-2* and *atg5-1*, Figure 2 in Kim et al., 2013).

Recent studies focused on autophagic degradation of peroxisomes (obsolete or damaged) in plant cells under normal conditions, i.e., in course of “constitutive,” or “basal,” autophagy (Inoue et al., 2006; Farmer et al., 2013; Kim et al., 2013; Shibata et al., 2013; Yoshimoto et al., 2014). They showed that constitutive autophagy is an important mechanism of the quality control of peroxisomes, which interacts with peroxisomal protein degradation by Lon2 protease in a tightly regulated manner (Farmer et al., 2013; Goto-Yamada et al., 2014a,b). Constitutive autophagy is active also in the absence of any stresses and is essential for plant survival (Inoue et al., 2006).

In our study we focused on degradation of peroxisomes during bulk autophagy-induced by carbohydrate starvation. Starvation of carbon (e.g., low light intensity) or nitrogen (insufficient nitrate and ammonium availability) are common abiotic stress conditions plants have to cope with in their natural environment. We demonstrate in this study that starvation-induced autophagy has a pronounced effect on peroxisome biology and induced pexophagy in BY-2 cells. Peroxisome degradation by autophagy was confirmed by several lines of evidence. First, the total number of cellular peroxisomes decreased particularly in the first phase of sucrose starvation (**Figure 5**). Second, this process was inhibited by 3-MA which has been previously described to block autophagy in BY-2 cells (Moriyasu and Ohsumi, 1996; Takatsuka et al., 2004; Moriyasu and Inoue, 2008). Even though 3-MA, which inhibits class I as well as class III phosphatidylinositol 3-kinases (Klionsky et al., 2008), is not fully specific to autophagy but also reported to inhibit, for instance, cell growth, multiple lines of evidence and indications obtained in former and this study strongly suggest that the major primary effect of 3-MA application on sucrose-starved BY-2 cells was the inhibition of autophagy including peroxisome degradation. Quantification of cellular peroxisome number by confocal microscopy provided solid evidence that 3-MA led to a significant increase in cellular peroxisome numbers and blocked peroxisome degradation in sucrose-deprived cells.

Third, upon application of inhibitors that block macroautophagy at specific stages such as autolysosome acidification and vesicle fusion with the vacuole (E-64, Yamada et al., 2005) and autophagic body degradation (ConcA), autolysosomes and autophagic bodies were shown to coincide with peroxisomes, strongly suggesting that the autolysosomes carried peroxisomes as autophagic cargo. Since acidotropic dyes such as MDC and LTR may also stain acidic organelles other than autolysosomes (Klionsky et al., 2012; Merkulova et al., 2014), our cytological studies do not allow conclusive identification of the acidic organelles as autolysosomes. More comprehensive cytological analyses, for instance, by labeling autophagosomes with a

fluorescent reporter attached to ATG8 need to extend this first study of peroxisome degradation in tobacco. Taking all data of this study together, conclusive evidence is provided that peroxisomes are degraded in sucrose-starved tobacco BY-2 cell by autophagy.

Investigations of peroxisome degradation in unicellular fungi and mammals focused on superfluous peroxisomes in the past. Since peroxisome proliferation can be easily induced by external stimuli (e.g., MeOH, fatty acids, clofibrate) in these organisms, the degradation of superfluous peroxisomes can be subsequently analyzed by removal of the chosen stimulus. In attempts to similarly induce peroxisome proliferation in tobacco BY-2 cells, we investigated the effects of various components such as fatty acids, detergents (Tween series), bezafibrate (a known peroxisome proliferator in mammalian cells), and ROS (e.g., H<sub>2</sub>O<sub>2</sub>) on peroxisome abundance. However, the stimuli were either not compatible with BY-2 cell viability or did not affect peroxisome abundance (data not shown). Besides, it remains unknown whether plant peroxisomes become superfluous under any physiological conditions.

The physiological function of constitutive autophagy is most likely the elimination and recycling of protein aggregates and dysfunctional organelles whose matrix enzymes and membrane lipids have been oxidatively and irreversibly damaged (Komatsu et al., 2007a). Consistent with these data, in BY-2 cells grown under nutrient-rich conditions, 3-MA caused a 1.5- to 2-fold accumulation of peroxisomes within 3 days (**Figure 6**). However, since steady-state levels of organelles are determined by three parameters, i.e., organelle biogenesis, organelle degradation and cell proliferation, the results are more difficult to interpret. Cell proliferation was differentially affected in control and 3-MA treated cells, as indicated by exponentially increasing FW of control cells and stagnant FW of 3-MA treated cells. Hence, continuous peroxisome proliferation in the absence of cell division might have caused an increase in cellular numbers of peroxisomes in MA-treated cells. More detailed analyses of cell and peroxisome proliferation are needed to decipher the underlying causes of the observed results.

The blockage of constitutive peroxisome degradation by 3-MA was further supported by immunobiochemical data. CAT protein strongly and EYFP-SKL moderately accumulated in 3-MA treated cells. This result strongly suggests that degradation of peroxisomes occurs by constitutive macroautophagy under standard growth conditions. Interestingly, 3-MA did not cause a comparable accumulation of marker proteins of other cellular compartments like plastids and mitochondria (**Figure 6E**). This suggests that the turnover rate of peroxisomes is highest amongst the major metabolic cell organelles. Since the total cellular protein content of peroxisomes is far lower than that of plastids, these results indicate that the function of peroxisome degradation is the elimination of dysfunctional organelles rather than recycling of proteins for cellular remodeling.

The need for pronounced peroxisome degradation under standard growth conditions can be rationalized by the organelle's oxidative metabolism. Xiong et al. (2007a,b) showed that ROS can induce macroautophagy in *Arabidopsis*. Macroautophagy-defective RNAi-AtATG18a transgenic plants were more sensitive to ROS and accumulated high levels of oxidized proteins due to

a lower rate of protein degradation, indicating that autophagy is involved in degrading oxidized proteins under both oxidative stress and normal growth conditions (Xiong et al., 2007a,b). Peroxisomes are a compartment of high ROS production by various metabolic pathways including photorespiration (Foyer and Noctor, 2003), fatty acid  $\beta$ -oxidation, polyamine and cofactor metabolism (Reumann, 2011), which might explain the especially high oxidative damage for these organelles also in heterotrophic BY-2 cells.

While starvation-induced peroxisome degradation is expected to target different peroxisome populations rather unspecifically, it is reasonable to hypothesize that constitutive peroxisome degradation specifically selects “old/senescence” and dysfunctional peroxisomes for elimination (Figure 4). Future studies need to address identification of the signal(s) emitted from dysfunctional and/or senescent peroxisomes and the components of signal transduction cascades activating constitutive autophagy under standard growth conditions. Hydrogen peroxide leaking from dysfunctional peroxisomes due to inactivation of oxidatively damaged CAT or reduced permeability of the peroxisomal membrane due to lipid peroxidation is the predicted candidate for the signaling molecule (Shibata et al., 2013; Goto-Yamada et al., 2014a,b). The mechanism responsible for specific labeling of dysfunctional peroxisomes might involve p62/SQSTM1, as demonstrated for mammalian cells (Kaniuk et al., 2007; Komatsu et al., 2007b; Pankiv et al., 2007; Kim et al., 2008).

In addition, several independent lines of indications emerged from this study that peroxisomes might be degraded, in addition to autophagy, by a complementary mechanism. First, even in the presence of 3-MA the average cellular peroxisome number steadily decreased under starvation conditions (Figure 5). Since relatively high inhibitor concentrations were used (5 mM) and 3-MA is not reported to be instable, it is unlikely that the inhibitory effect 3-MA ceased at advanced starvation stage. Furthermore, while peroxisome degradation continued (Figure 5), neither E-64 nor ConCA caused autolysosome or autophagic body accumulation, respectively, at this advanced stage of sucrose starvation (data not shown). Apparently, autophagosomes and autolysosomes were no longer formed on a larger scale. The activity of macroautophagy seemed to decline and the catabolic process be replaced by another degradation mechanism. Notably, the extent of cell death still remained rather low in the absence of 3-MA. At late stage of sucrose starvation, some peroxisomes appeared to disassemble directly in the cytosol. Future work needs to address the identity of this second non-autophagic degradation mechanism of peroxisomes.

## CONCLUSION

In conclusion, we demonstrated in the present study that (i) peroxisomes are continuously degraded in tobacco BY-2 cells not only under nutrient starvation but also under optimal growth conditions, (ii) that these two processes are mediated by the machinery and mechanism of autophagy, (iii) that the extent of constitutive peroxisome turnover is considerable and exceeds that of other cell organelles (plastids, mitochondria), and (iv) that a second mechanism is likely to act on top of autophagy at advanced stages of nutrient starvation and cell senescence. We established a new

model system for cell biological analyses of plant peroxisomes using tobacco BY-2 suspension-cultured cells. The system has been proven ideal for pharmacological and microscopic analyses, complements genetic studies in *Arabidopsis* and will assist in future advanced molecular analyses of plant pexophagy.

## ACKNOWLEDGMENTS

We are indebted to Beate Preitz (Department of Developmental Biology, University of Göttingen, Germany) and Dr. Kirill Demchenko (Komarov Botanical Institute, RAS, Saint Petersburg, Russia) for help in confocal microscopy. We are grateful to Dr. Anna Bulankina (Center for Molecular Physiology of the Brain and Department of Otolaryngology) for help in cell biology, to Dr. Corinna Thurow (Department of Molecular Biology and Physiology, both University of Göttingen, Germany) for assistance in BY-2 cell propagation and Dr. Flora Schuster (Institute of Molecular Biotechnology, RWTH Aachen, Germany) for help with the BY-2 cell transformation. The research was supported by funding from the Deutsche Forschungsgemeinschaft (DFG, grant number RE 1304/4-1 to Sigrun Reumann), and the Russian Foundation for Basic Research (project # 10-04-01186 to Olga V. Voitsekhskaja).

## SUPPLEMENTARY MATERIAL

The Supplementary Material for this article can be found online at: <http://www.frontiersin.org/journal/10.3389/fpls.2014.00629/abstract>

## REFERENCES

- An, G. (1985). High efficiency transformation of cultured tobacco cells. *Plant Physiol.* 79, 568–570. doi: 10.1104/pp.79.2.568
- Babujee, L., Wurtz, V., Ma, C., Lueder, F., Soni, P., Van Dorsselaer, A., et al. (2010). The proteome map of spinach leaf peroxisomes indicates partial compartmentalization of phylloquinone (vitamin K1) biosynthesis in plant peroxisomes. *J. Exp. Bot.* 61, 1441–1453. doi: 10.1093/jxb/erq014
- Bassham, D. C. (2007). Plant autophagy-more than a starvation response. *Curr. Opin. Plant Biol.* 10, 587–593. doi: 10.1016/j.pbi.2007.06.006
- Bassham, D. C. (2009). Function and regulation of macroautophagy in plants. *Biochim. Biophys. Acta* 1793, 1397–1403. doi: 10.1016/j.bbamcr.2009.01.001
- Contento, A. L., Xiong, Y., and Bassham, D. C. (2005). Visualization of autophagy in *Arabidopsis* using the fluorescent dye monodansylcadaverine and a GFP-AtATG8e fusion protein. *Plant J.* 42, 598–608. doi: 10.1111/j.1365-313X.2005.02396.x
- del Rio, L. A., Sandalio, L. M., Corpas, F. J., Palma, J. M., and Barroso, J. B. (2006). Reactive oxygen species and reactive nitrogen species in peroxisomes. Production, scavenging, and role in cell signaling. *Plant Physiol.* 141, 330–335. doi: 10.1104/pp.106.078204
- Dunn, W. A. Jr., Cregg, J. M., Kiel, J. A., Van Der Klei, I. J., Oku, M., Sakai, Y., et al. (2005). Pexophagy: the selective autophagy of peroxisomes. *Autophagy* 1, 75–83. doi: 10.4161/auto.1.2.1737
- Farmer, L. M., Rinaldi, M. A., Young, P. G., Danan, C. H., Burkhardt, S. E., and Bartel, B. (2013). Disrupting autophagy restores peroxisome function to an *Arabidopsis* lon2 mutant and reveals a role for the LON2 protease in peroxisomal matrix protein degradation. *Plant Cell* 25, 4085–4100. doi: 10.1105/tpc.113.113407
- Farre, J. C., and Subramani, S. (2004). Peroxisome turnover by micropexophagy: an autophagy-related process. *Trends Cell Biol.* 14, 515–523. doi: 10.1016/j.tcb.2004.07.014
- Foyer, C. H., and Noctor, G. (2003). Redox sensing and signalling associated with reactive oxygen in chloroplasts, peroxisomes and mitochondria. *Physiol. Plant.* 119, 355–364. doi: 10.1034/j.1399-3054.2003.00223.x
- Goto-Yamada, S., Mano, S., Nakamori, C., Kondo, M., Yamawaki, R., Kato, A., et al. (2014a). Chaperone and protease functions of LON protease 2 modulate the

- peroxisomal transition and degradation with autophagy. *Plant Cell Physiol.* 55, 482–496. doi: 10.1093/pcp/pcu017
- Goto-Yamada, S., Mano, S., Oikawa, K., Shibata, M., and Nishimura, M. (2014b). Interaction between chaperone and protease functions of LON2, and autophagy during the functional transition of peroxisomes. *Plant Signal. Behav.* 9:e28838. doi: 10.4161/psb.28838
- Graham, I. A. (2008). Seed storage oil mobilization. *Annu. Rev. Plant Biol.* 59, 115–142. doi: 10.1146/annurev.arplant.59.032607.092938
- Hayashi, M., and Nishimura, M. (2003). Entering a new era of research on plant peroxisomes. *Curr. Opin. Plant Biol.* 6, 577–582. doi: 10.1016/j.pbi.2003.09.012
- Hellens, R., Mullineaux, P., and Klee, H. (2000). A guide to *Agrobacterium* binary Ti vectors. *Trends Plant Sci.* 5, 446–451. doi: 10.1016/S1360-1385(00)01740-4
- Hu, J., Baker, A., Bartel, B., Linka, N., Mullen, R. T., Reumann, S., et al. (2012). Plant peroxisomes: biogenesis and function. *Plant Cell* 24, 2279–2303. doi: 10.1101/tpc.112.096586
- Inoue, Y., Suzuki, T., Hattori, M., Yoshimoto, K., Ohsumi, Y., and Moriyasu, Y. (2006). AtATG genes, homologs of yeast autophagy genes, are involved in constitutive autophagy in *Arabidopsis* root tip cells. *Plant Cell Physiol.* 47, 1641–1652. doi: 10.1093/pcp/pcl031
- Kaniuk, N. A., Kiraly, M., Bates, H., Vranic, M., Volchuk, A., and Brumell, J. H. (2007). Ubiquitinated-protein aggregates form in pancreatic beta-cells during diabetes-induced oxidative stress and are regulated by autophagy. *Diabetes Metab. Res. Rev.* 56, 930–939. doi: 10.2337/db06-1160
- Kaur, N., Reumann, S., and Hu, J. (2009). “Peroxisome biogenesis and function,” in *The Arabidopsis Book*, eds C. R. Somerville and E. M. Meyerowitz (Rockville, MD: The American Society of Plant Biologists), 1–41.
- Kim, J., Lee, H., Lee, H. N., Kim, S. H., Shin, K. D., and Chung, T. (2013). Autophagy-related proteins are required for degradation of peroxisomes in *Arabidopsis* hypocotyls during seedling growth. *Plant Cell* 25, 4956–4966. doi: 10.1101/tpc.113.117960
- Kim, J., Lee, H. N., and Chung, T. (2014). Plant cell remodeling by autophagy: switching peroxisomes for green life. *Autophagy* 10, 702–703. doi: 10.4161/auto.27953
- Kim, P. K., Hailey, D. W., Mullen, R. T., and Lippincott-Schwartz, J. (2008). Ubiquitin signals autophagic degradation of cytosolic proteins and peroxisomes. *Proc. Natl. Acad. Sci. U.S.A.* 105, 20567–20574. doi: 10.1073/pnas.081061105
- Klionsky, D. J., Abdalla, F. C., Abieliovich, H., Abraham, R. T., Acevedo-Arozena, A., Adeli, K., et al. (2012). Guidelines for the use and interpretation of assays for monitoring autophagy. *Autophagy* 8, 445–544. doi: 10.4161/auto.19496
- Klionsky, D. J., Abieliovich, H., Agostinis, P., Agrawal, D. K., Aliev, G., Askew, D. S., et al. (2008). Guidelines for the use and interpretation of assays for monitoring autophagy in higher eukaryotes. *Autophagy* 4, 151–175. doi: 10.4161/aut.0.5338
- Komatsu, M., Ueno, T., Waguri, S., Uchiyama, Y., Kominami, E., and Tanaka, K. (2007a). Constitutive autophagy: vital role in clearance of unfavorable proteins in neurons. *Cell Death Differ.* 14, 887–894.
- Komatsu, M., Waguri, S., Koike, M., Sou, Y. S., Ueno, T., Hara, T., et al. (2007b). Homeostatic levels of p62 control cytoplasmic inclusion body formation in autophagy-deficient mice. *Cell* 131, 1149–1163. doi: 10.1016/j.cell.2007.10.035
- Li, F., and Vierstra, R. D. (2012). Autophagy: a multifaceted intracellular system for bulk and selective recycling. *Trends Plant Sci.* 17, 526–537. doi: 10.1016/j.tplants.2012.05.006
- Liu, Y., and Bassham, D. C. (2012). Autophagy: pathways for self-eating in plant cells. *Annu. Rev. Plant Biol.* 63, 215–237. doi: 10.1146/annurev-arplant-042811-105441
- Lowry, O. H., Rosebrough, N. J., Farr, A. L., and Randall, R. J. (1951). Protein measurement with the Folin phenol reagent. *J. Biol. Chem.* 193, 265–275.
- Ma, C., Agrawal, G., and Subramani, S. (2011). Peroxisome assembly: matrix and membrane protein biogenesis. *J. Cell Biol.* 193, 7–16. doi: 10.1083/jcb.201010022
- Ma, C., and Reumann, S. (2008). Improved prediction of peroxisomal PTS1 proteins from genome sequences based on experimental subcellular targeting analyses as exemplified for protein kinases from *Arabidopsis*. *J. Exp. Bot.* 59, 3767–3779. doi: 10.1093/jxb/ern221
- Ma, C., and Subramani, S. (2009). Peroxisome matrix and membrane protein biogenesis. *IUBMB Life* 61, 713–722. doi: 10.1002/iub.196
- Merkulova, E. A., Guiobouleau, A., Naya, L., Masclaux-Daubresse, C., and Yoshimoto, K. (2014). Assessment and optimization of autophagy monitoring methods in *Arabidopsis* roots indicate direct fusion of autophagosomes with vacuoles. *Plant Cell Physiol.* 55, 715–726. doi: 10.1093/pcp/pcu041
- Moriyasu, Y., and Hillmer, S. (2000). “Autophagy and vacuole formation,” in *Vacuolar Compartments*, eds D. G. Robinson and J. C. Rogers (Sheffield: Sheffield Academic Press), 71–89.
- Moriyasu, Y., and Inoue, Y. (2008). Use of protease inhibitors for detecting autophagy in plants. *Methods Enzymol.* 451, 557–580. doi: 10.1016/S0076-6879(08)3232-1
- Moriyasu, Y., and Ohsumi, Y. (1996). Autophagy in tobacco suspension-cultured cells in response to sucrose starvation. *Plant Physiol.* 111, 1233–1241. doi: 10.1104/pp.111.4.1233
- Moschou, P. N., Sammartin, M., Andriopoulos, A. H., Rojo, E., Sanchez-Serrano, J. J., and Roubelakis-Angelakis, K. A. (2008). Bridging the gap between plant and mammalian polyamine catabolism: a novel peroxisomal polyamine oxidase responsible for a full back-conversion pathway in *Arabidopsis*. *Plant Physiol.* 147, 1845–1857. doi: 10.1104/pp.108.123802
- Palma, J. M., Corpas, F. J., and Del Rio, L. A. (2009). Proteome of plant peroxisomes: new perspectives on the role of these organelles in cell biology. *Proteomics* 9, 2301–2312. doi: 10.1002/pmic.200700732
- Pankiv, S., Clausen, T. H., Lamark, T., Brech, A., Bruun, J. A., Outzen, H., et al. (2007). p62/SQSTM1 binds directly to Atg8/LC3 to facilitate degradation of ubiquitininated protein aggregates by autophagy. *J. Biol. Chem.* 282, 24131–24145. doi: 10.1074/jbc.M702824200
- Reumann, S. (2011). Toward a definition of the complete proteome of plant peroxisomes: where experimental proteomics must be complemented by bioinformatics. *Proteomics* 11, 1764–1779. doi: 10.1002/pmic.201000681
- Reumann, S., Voitsekhoukaja, O., and Lillo, C. (2010). From signal transduction to autophagy of plant cell organelles: lessons from yeast and mammals and plant-specific features. *Protoplasma* 244, 233–256. doi: 10.1007/s00709-010-0190-0
- Reumann, S., and Weber, A. P. (2006). Plant peroxisomes respire in the light: some gaps of the photorespiratory C2 cycle have become filled – others remain. *Biochim. Biophys. Acta* 1763, 1496–1510. doi: 10.1016/j.bbamcr.2006.09.008
- Schiermeyer, A., Schinkel, H., Apel, S., Fischer, R., and Schillberg, S. (2005). Production of *Desmodus rotundus* salivary plasminogen activator alpha1 (DSPAalpha1) in tobacco is hampered by proteolysis. *Biotechnol. Bioeng.* 89, 848–858. doi: 10.1002/bit.20410
- Shibata, M., Oikawa, K., Yoshimoto, K., Kondo, M., Mano, S., Yamada, K., et al. (2013). Highly oxidized peroxisomes are selectively degraded via autophagy in *Arabidopsis*. *Plant Cell* 25, 4967–4983. doi: 10.1101/tpc.113.16947
- Stitt, M. (1984). “Fumarase,” in *Methods of Enzymatic Analysis*, 3rd Edn, ed. H. U. Bergmeyer (Weinheim: Verlag Chemie), 359–362.
- Stitt, M., Bulpin, P. V., and Ap Rees, T. (1978). Pathways of starch breakdown in photosynthetic tissues of *Pisum sativum*. *Biochem. Biophys. Acta* 544, 200–214. doi: 10.1016/0304-4165(78)90223-4
- Takatsuka, C., Inoue, Y., Matsuoka, K., and Moriyasu, Y. (2004). 3-methyladenine inhibits autophagy in tobacco culture cells under sucrose starvation conditions. *Plant Cell Physiol.* 45, 265–274. doi: 10.1093/pcp/pch031
- Thompson, A. R., Doelling, J. H., Suttangkakul, A., and Vierstra, R. D. (2005). Autophagic nutrient recycling in *Arabidopsis* directed by the ATG8 and ATG12 conjugation pathways. *Plant Physiol.* 138, 2097–2110. doi: 10.1104/pp.105.06073
- Thompson, A. R., and Vierstra, R. D. (2005). Autophagic recycling: lessons from yeast help define the process in plants. *Curr. Opin. Plant Biol.* 8, 165–173. doi: 10.1016/j.pbi.2005.01.013
- Toyooka, K., Moriyasu, Y., Goto, Y., Takeuchi, M., Fukuda, H., and Matsuoka, K. (2006). Protein aggregates are transported to vacuoles by a macroautophagic mechanism in nutrient-starved plant cells. *Autophagy* 2, 96–106. doi: 10.4161/auto.2.2.2366

- Wada, S., Ishida, H., Izumi, M., Yoshimoto, K., Ohsumi, Y., Mae, T., et al. (2009). Autophagy plays a role in chloroplast degradation during senescence in individually darkened leaves. *Plant Physiol.* 149, 885–893. doi: 10.1104/pp.108.130013
- Xiong, Y., Contento, A. L., and Bassham, D. C. (2007a). Disruption of autophagy results in constitutive oxidative stress in *Arabidopsis*. *Autophagy* 3, 257–258. doi: 10.4161/auto.3847
- Xiong, Y., Contento, A. L., Nguyen, P. Q., and Bassham, D. C. (2007b). Degradation of oxidized proteins by autophagy during oxidative stress in *Arabidopsis*. *Plant Physiol.* 143, 291–299. doi: 10.1104/pp.106.092106
- Yamada, K., Fuji, K., Shimada, T., Nishimura, M., and Hara-Nishimura, I. (2005). Endosomal proteases facilitate the fusion of endosomes with vacuoles at the final step of the endocytic pathway. *Plant J.* 41, 888–898. doi: 10.1111/j.1365-313X.2005.02349.x
- Yoshimoto, K., Shibata, M., Kondo, M., Oikawa, K., Sato, M., Toyooka, K., et al. (2014). Quality control of plant peroxisomes in organ specific manner via autophagy. *J. Cell Sci.* 127, 1161–1168. doi: 10.1242/jcs.139709

**Conflict of Interest Statement:** The authors declare that the research was conducted in the absence of any commercial or financial relationships that could be construed as a potential conflict of interest.

*Received: 16 May 2014; accepted: 23 October 2014; published online: 18 November 2014.*

*Citation: Voitsekhoukaja OV, Schiermeyer A and Reumann S (2014) Plant peroxisomes are degraded by starvation-induced and constitutive autophagy in tobacco BY-2 suspension-cultured cells. *Front. Plant Sci.* 5:629. doi: 10.3389/fpls.2014.00629*

*This article was submitted to Plant Cell Biology, a section of the journal Frontiers in Plant Science.*

*Copyright © 2014 Voitsekhoukaja, Schiermeyer and Reumann. This is an open-access article distributed under the terms of the Creative Commons Attribution License (CC BY). The use, distribution or reproduction in other forums is permitted, provided the original author(s) or licensor are credited and that the original publication in this journal is cited, in accordance with accepted academic practice. No use, distribution or reproduction is permitted which does not comply with these terms.*



# The emerging role of autophagy in peroxisome dynamics and lipid metabolism of phyllosphere microorganisms

Masahide Oku<sup>1</sup>, Yoshitaka Takano<sup>2</sup> and Yasuyoshi Sakai<sup>1,3 \*</sup>

<sup>1</sup> Division of Applied Life Sciences, Graduate School of Agriculture, Kyoto University, Kyoto, Japan

<sup>2</sup> Division of Applied Biosciences, Graduate School of Agriculture, Kyoto University, Kyoto, Japan

<sup>3</sup> Research Unit for Physiological Chemistry, Center for the Promotion of Interdisciplinary Education and Research, Kyoto University, Kyoto, Japan

## Edited by:

Jose Luis Crespo, Consejo Superior de Investigaciones Científicas, Spain

## Reviewed by:

Nuria Sanchez Coll, Centre for Research in Agricultural Genomics, Spain

Henri Batoko, Université Catholique de Louvain, Belgium

## \*Correspondence:

Yasuyoshi Sakai, Division of Applied Life Sciences, Graduate School of Agriculture, Kyoto University, Kitashirakawa-Oiwake, Sakyo-ku, Kyoto 606-8502, Japan  
e-mail: ysakai@kais.kyoto-u.ac.jp

Eukaryotic microorganisms resident in the phyllosphere (above-ground, plant-surface environments) undergo dynamic changes in nutrient conditions and adapt their metabolic pathways during proliferation or in the course of infection of host plants. Some of these metabolic switches are accomplished by regulation of organelle abundance. Recent studies have shown that autophagy plays a major role in reducing the organelle quantity, thereby contributing to the metabolic switch required for survival or virulence of the microorganisms in the phyllosphere. In this mini review the metabolic pathways in several phytopathogenic fungi and the non-infectious asporogenous yeast *Candida boidinii*, which involve lipid droplets and peroxisomes, are summarized. The physiological functions of Atg (Autophagy-related) proteins in these organisms are discussed in relation to the dynamics of these two important organelles.

**Keywords:** autophagy, lipid droplet, methylotrophic yeast, peroxisome, phyllosphere, phytopathogenic fungus

## INTRODUCTION

The phyllosphere has been evaluated as an ecological site for plant-microbe interaction, compared with the rhizosphere (Vorholt, 2012). However, dynamic environmental changes, i.e., light, heat, nutrient, plant immunity response, should affect the life style of microbes in the phyllosphere. Among the eukaryotic inhabitants, only plant-infectious fungi have been the subject of extensive studies based on their important influences on crop yields (Agrios, 2004; Dean et al., 2012). In general, asexual spores (conidia) of phytopathogenic fungi undergo sequential cellular differentiation on the plant-surface, i.e., conidia germinate and germ tubes of conidia differentiate into a specific cellular apparatus termed the appressorium for host invasion (Figure 1A). The process of differentiation requires induction/inactivation of specific metabolic pathways. In the following section of this mini review, we first introduce the melanin biosynthesis pathway, which is conserved among a subset of phytopathogenic fungi and is closely associated with the dynamics of lipid droplets and peroxisomes. Then several functional links between this biosynthetic pathway and autophagy are discussed.

Recent studies revealed that non-phytopathogenic eukaryotic microorganisms can also establish an inhabitation in the phyllosphere. One such example is the asporogenous methylotrophic yeast *Candida boidinii*, which can grow on methanol as a sole carbon and energy source (Kawaguchi et al., 2011). Although *Candida boidinii* could not form stress-resistant spores, this organism is often isolated from plant-surfaces, and was shown to proliferate on the leaves of growing *Arabidopsis thaliana*. Furthermore, phyllospheric growth depended on methanol, whose concentration fluctuated during the daily light-dark cycle. As a result of methanol fluctuation, *Candida boidinii* increased or decreased its quantity of peroxisomes. In the last section of this mini

review, the function of peroxisome-specific autophagy (termed pexophagy), which is vital for the decrease of peroxisome quantity and for the growth of this organism in the phyllosphere, is summarized.

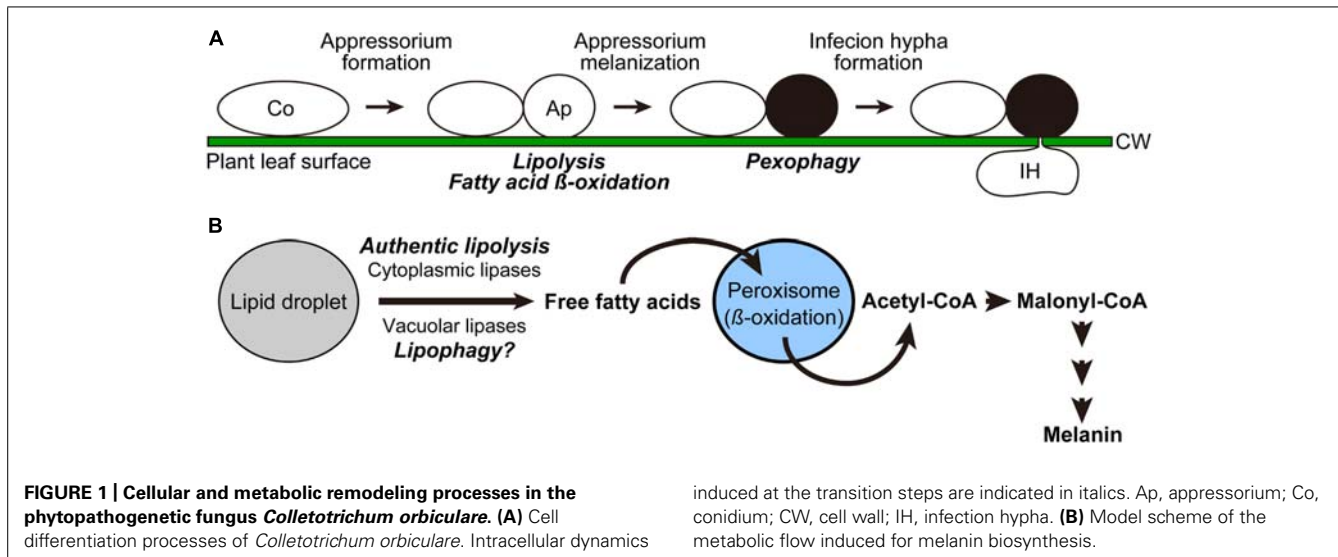
## PEROXISOME AND LIPID DROPLET DYNAMICS IN PHYTOPATHOGENIC FUNGI

### PEROXISOME AND LIPID DROPLET DYNAMICS FOR MELANIN BIOSYNTHESIS PATHWAY

Several genera of phytopathogenic fungi, including *Colletotrichum* and *Magnaporthe* species, develop appressoria pigmented with melanin for efficient infection of their host plants (Kubo and Furusawa, 1991). The melanin layer in the appressorial cell wall is thought to determine the correct penetration site because melanin is excluded from this site (Kubo and Furusawa, 1991). Melanin also provides the rigidity and selective permeability of the appressorial cell wall, and is considered to be responsible for generating the turgor pressure required for the appressorial penetration (Howard and Ferrari, 1989; Bechinger et al., 1999).

Since the precursor compound for melanin synthesis, malonyl-CoA, was found to be derived from acetyl-CoA in *Colletotrichum orbiculare* (Syn. *Colletotrichum lagenarium*; Asakura et al., 2012), robust biosynthesis of melanin in this organisms depends on mobilization of free fatty acids from lipid droplets, followed by the conversion of the liberated lipids into acetyl-CoA through the beta-oxidation pathway in peroxisomes (Figure 1B). Consistent with this, it was shown that functional assembly of peroxisomes was required for the formation of melanized appressoria as well as the pathogenicity of *Colletotrichum orbiculare* (Kimura et al., 2001).

Our recent study demonstrated that the liberation of fatty acids from lipid droplets (termed lipolysis) in the appressorium was



inhibited by blocking either the (1) beta-oxidation pathway, (2) conversion of acetyl-CoA to malonyl-CoA, or (3) consumption of malonyl-CoA by melanin biosynthesis (Asakura et al., 2012). This indicates that an intact melanin biosynthesis pathway is required for lipolysis (Figure 1B). Molecular details underlying this feedback regulation are not clear, but it is possible that the intermediates of the pathway, namely free fatty acids, acetyl-CoA, and/or malonyl-CoA, might act as signaling molecules to repress lipolysis, in order to avoid the deleterious effect called “lipotoxicity,” which results from excess accumulation of lipid substances, especially free fatty acids. In many experimental systems including yeast, the formation of lipid droplets is strongly suggested to contribute to the prevention of lipotoxicity by incorporating free fatty acids into the core contents of the organelle, or into neutral lipids (Eisenberg and Buttner, 2013).

The precise mechanism underlying the induction of lipolysis during the appressorium melanization has not been fully elucidated. An authentic definition of lipolysis solely refers to cleavage of neutral lipids inside lipid droplets by the action of cytoplasmic lipases (Zechner et al., 2012). In a mammalian experimental system, this reaction is known to be activated by the protein kinase A (PKA)-mediated signaling pathway (Holm, 2003), which is also known to be important for up-regulating the lipolysis activity and pathogenicity in several phytopathogenic fungi (*Magnaporthe oryzae* and *Colletotrichum orbiculare*; Thines et al., 2000; Yamauchi et al., 2004). Furthermore, a pioneering study on the morphological details of appressorium formation in *M. oryzae* demonstrated that lipid droplets are incorporated into the vacuolar portion of the cell and are degraded therein (Weber et al., 2001), which fits the fundamental criterion of lipid droplet autophagy (lipophagy). In this case, lipases inside the vacuole, not those in the cytoplasm, are thought to be responsible for the breakdown of neutral lipids, but they remain to be identified. Although the microautophagic process (a type of autophagy that includes direct engulfment of the target organelle by vacuolar/lysosomal membrane) was suggested to be involved in lipid droplet degradation in *Saccharomyces cerevisiae* (van Zutphen et al., 2014), little is known about the

molecular details of lipophagy, especially in terms of the mechanism targeting lipid droplets to the vacuole. Uncovering the factors functioning in lipophagy will be of great value for understanding how these different modes of lipolytic activities (authentic lipolysis and lipophagy) are utilized in phytopathogenic fungi.

### PEXOPHAGY REQUIRED FOR INFECTION OF *Colletotrichum orbiculare*

After formation of melanized appressoria in *Colletotrichum orbiculare*, the peroxisomes therein are subjected to degradation. Morphological experiments showed that the peroxisomes to be degraded were encapsulated by a membrane structure labeled with Atg8, and transferred into the lumen of the vacuole, showing a typical pattern of peroxisome-specific autophagy (pexophagy; Asakura et al., 2009). Consistent with this observation, the Atg26 protein, which was previously shown to be specifically required for pexophagy in the methylotrophic yeast *Pichia pastoris* (See next section; Oku et al., 2003), was found to be necessary for degradation of peroxisomes in the appressorium. Loss of Atg26 in *Colletotrichum orbiculare* abolished the functionality of the appressorium for the host plant invasion and thus impaired pathogenicity to the host. Notably, the appressorium formed by the *atg26* mutant strain was more resistant to hyper-osmotic shock than that formed by the wild-type strain, implying that pexophagy affects cell wall integrity or stiffness of the phytopathogenic apparatus for the process of penetration during the course of infection.

### PEROXISOME DYNAMICS IN THE METHYLOTROPHIC YEAST RESIDENT ON PLANT LEAVES

#### MOLECULAR MACHINERY OF PEXOPHAGY IN METHYLOTROPHIC YEASTS

A striking feature of methylotrophic yeasts is that they develop numerous peroxisomes that contain several primary enzymes in the methanol-metabolizing pathway, such as alcohol oxidase (Aod) and dihydroxyacetone synthase (Das), when these organisms are grown on methanol (Yurimoto et al., 2011). Owing to this property, the methylotrophic yeasts have been considered

to be good model organisms to study peroxisome dynamics, including pexophagy (Oku and Sakai, 2010).

Insights gained from these organisms include the molecular requirements for pexophagy of the so-called “core” Atg proteins for *de novo* membrane biogenesis (Yang and Klionsky, 2010), and the identification of several pexophagy-specific factors associated with these core proteins. One of the pexophagy-specific factors identified in *P. pastoris* is Atg26. This protein, encoding a sterol glucosyltransferase, was found to be required for degradation of methanol-induced peroxisomes (Nazarko et al., 2007), but to be dispensable for macroautophagy induced by nitrogen-source starvation (Oku et al., 2003). This protein was shown to act downstream of the phosphatidylinositol 4'-kinase (PI4K) signaling pathway, and was localized to the pre-autophagosomal structure (PAS; Yamashita et al., 2006). Another pexophagy-specific factor, Atg30, was identified as a receptor molecule on peroxisomes recognized by several core Atg proteins (Farre et al., 2008). The interactions between Atg30 and core Atg proteins (Atg8 and Atg11) were dependent on phosphorylation of two serine residues within Atg30 (Farre et al., 2013). By utilizing strains mutated in or devoid of these pexophagy-specific proteins, we are now able to reveal the physiological functions of pexophagy separately from the roles of general (bulk) autophagy.

## METHANOL METABOLISM AND AUTOPHAGY IN *Candida boidinii* REQUIRED FOR GROWTH ON PLANT LEAVES

Our recent study took advantage of the expression of a fluorescent protein (Venus) for the enhanced, quantitative detection of *Candida boidinii* cells inoculated on *A. thaliana* leaves (Kawaguchi et al., 2011). Through this technique we revealed that the inoculated *Candida boidinii* cells were able to proliferate on the leaf surface of plants grown in a chamber with illumination generating a daily light–dark cycle (Figure 2A). Growth was dependent on its methanol-metabolizing enzymes, Aod1 and Das1. In addition, methanol concentrations available to the organism on the plant leaves were also determined with the fluorescence intensity of Venus expressed under the regulation of a methanol-inducible promoter. Interestingly, dynamic oscillation of methanol concentration was observed on the surface of *A. thaliana* leaves during the daily light–dark cycle, with higher concentrations in the dark period (Figure 2B). In accordance with this oscillation, peroxisome abundance in the inoculated *Candida boidinii* cells was found to fluctuate as revealed by fluorescence microscopy of a peroxisome-targeted Venus: the organelle quantity increased in the dark period, and decreased in the light period (Figure 2B). We assume that the methanol-induced peroxisome serves as a storage organelle for proteins to replenish amino-acid pools

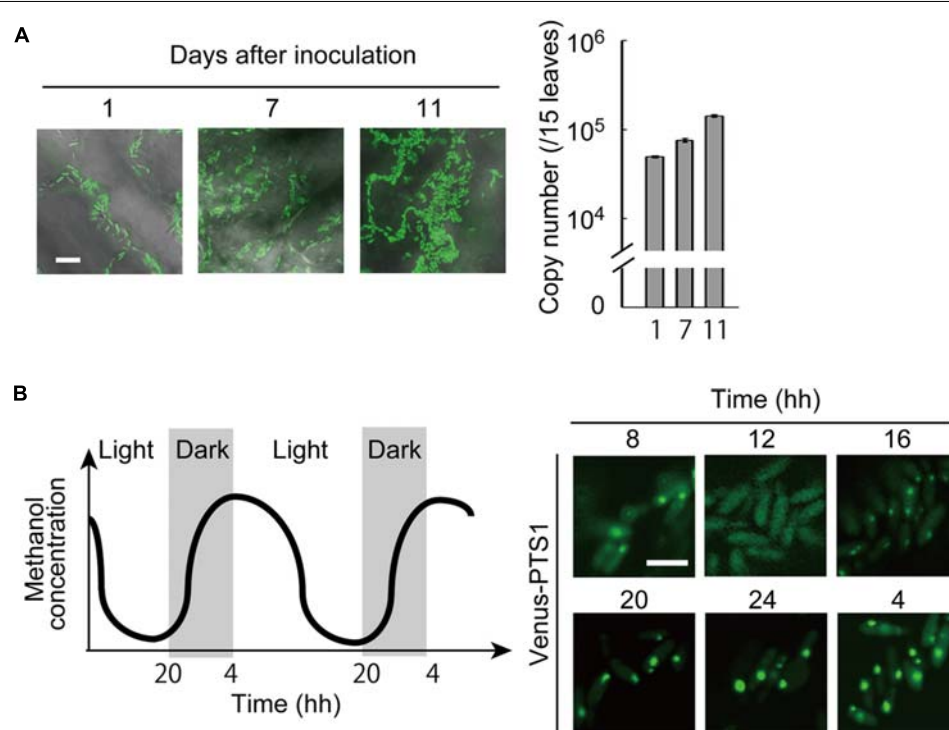


**FIGURE 2 | Peroxisome dynamics in the methylotrophic yeast *Candida boidinii* in the phyllosphere.** All of the experimental data were reconstructed from those in the study by Kawaguchi et al. (2011). (A) (Left) Microscopic images of the *Arabidopsis thaliana* leaf surface with fluorescent *Candida boidinii* cells. After inoculation with the yeast cells, the plant was grown for the designated number of days in a chamber equipped with an illumination system to generate a daily light–dark cycle. Bar, 10  $\mu$ m. (Right) Results of quantitative PCR using the plant leaf samples obtained after the

designated number of days after yeast inoculation. The copy numbers indicate those of the VENUS gene integrated in the genome of the inoculated *Candida boidinii* cells, and thus represent growth of the inoculated *Candida boidinii* cells. The error bars show standard deviations. (B) (Left) Schematic drawing of periodical changes in methanol concentrations on *A. thaliana* leaves. (Right) At the indicated times, peroxisomes in the *Candida boidinii* cells resident on *A. thaliana* leaves were visualized with Venus harboring a peroxisome targeting signal (PTS) 1. Bar, 5  $\mu$ m.

needed in the natural environment, in order for the immotile microorganism to survive until they obtain nutrients for further proliferation.

Since *Candida boidinii* possessed a homolog of *P. pastoris* Atg30 (the pexophagy-specific protein), we inoculated the *Cbatg30Δ* strain on plant leaves. The decrease in peroxisome quantity in the light period was suppressed by the loss of Atg30. Notably, this mutant strain exhibited a severe growth defect on plant leaves, similar to mutant strains incapable of methanol metabolism. The transport of Atg8 into the vacuole, a marker of general autophagy was detected in the inoculated *Candida boidinii* *Cbatg30Δ* strain, but not in the *Cbatg1Δ* strain, indicating that general autophagy occurs throughout the day. However, it is still unknown how autophagic activity and selectivity are regulated along the daily light–dark cycle.

## CONCLUDING REMARKS

Despite great advances in the understanding of the molecular mechanism of pexophagy, the physiological role of this selective autophagy had been an enigma for a long time, until the microorganisms were transferred from laboratory media to plant-surfaces or plant surface-mimicking environments. Likewise, the dynamics of lipid droplets is now an exciting topic of cell biology, and studies of eukaryotic microorganisms in the phyllosphere will give us profound insight into the physiological importance of organelle dynamics. Accumulating molecular information on the microorganisms in the phyllosphere will also be important for a better understanding of plant-microorganism interactions.

## ACKNOWLEDGMENTS

This work was supported by Advanced Low Carbon Technology Research and Development Program (ALCA, to Yasuyoshi Sakai) and Grant-in-Aid for Young Scientists (B) 24780100 (to Masahide Oku) from Japan Science and Technology Agency.

## REFERENCES

- Agrios, G. (2004). *Plant Pathology*, 5th Edn, Waltham, MA: Academic Press.
- Asakura, M., Ninomiya, S., Sugimoto, M., Oku, M., Yamashita, S., Okuno, T., et al. (2009). Atg26-mediated pexophagy is required for host invasion by the plant pathogenic fungus *Colletotrichum orbiculare*. *Plant Cell* 21, 1291–1304. doi: 10.1105/tpc.108.060996
- Asakura, M., Yoshino, K., Hill, A. M., Kubo, Y., Sakai, Y., and Takano, Y. (2012). Primary and secondary metabolism regulates lipolysis in appressoria of *Colletotrichum orbiculare*. *Fungal Genet. Biol.* 49, 967–975. doi: 10.1016/j.fgb.2012.08.009
- Bechinger, C., Giebel, K. F., Schnell, M., Leiderer, P., Deising, H. B., and Bastmeyer, M. (1999). Optical measurements of invasive forces exerted by appressoria of a plant pathogenic fungus. *Science* 285, 1896–1899. doi: 10.1126/science.285.5435.1896
- Dean, R., Van Kan, J. A., Pretorius, Z. A., Hammond-Kosack, K. E., Di Pietro, A., Spanu, P. D., et al. (2012). The Top 10 fungal pathogens in molecular plant pathology. *Mol. Plant Pathol.* 13, 414–430. doi: 10.1111/j.1364-3703.2011.00783.x
- Eisenberg, T., and Buttner, S. (2013). Lipids and cell death in yeast. *FEMS Yeast Res.* doi: 10.1111/1567-1364.12105 [Epub ahead of print].
- Farre, J. C., Burkenroad, A., Burnett, S. F., and Subramani, S. (2013). Phosphorylation of mitophagy and pexophagy receptors coordinates their interaction with Atg8 and Atg11. *EMBO Rep.* 14, 441–449. doi: 10.1038/embor.2013.40
- Farre, J. C., Manjithaya, R., Mathewson, R. D., and Subramani, S. (2008). PpAtg30 tags peroxisomes for turnover by selective autophagy. *Dev. Cell* 14, 365–376. doi: 10.1016/j.devcel.2007.12.011
- Holm, C. (2003). Molecular mechanisms regulating hormone-sensitive lipase and lipolysis. *Biochem. Soc. Trans.* 31, 1120–1124. doi: 10.1042/BST0311120
- Howard, R. J., and Ferrari, M. A. (1989). Role of melanin in appressorium function. *Exp. Mycol.* 13, 403–418. doi: 10.1016/0147-5975(89)90036-4
- Kawaguchi, K., Yurimoto, H., Oku, M., and Sakai, Y. (2011). Yeast methylotrophy and autophagy in a methanol-oscillating environment on growing *Arabidopsis thaliana* leaves. *PLoS ONE* 6:e25257. doi: 10.1371/journal.pone.0025257
- Kimura, A., Takano, Y., Furusawa, I., and Okuno, T. (2001). Peroxisomal metabolic function is required for appressorium-mediated plant infection by *Colletotrichum lagenarium*. *Plant Cell* 13, 1945–1957.
- Kubo, Y., and Furusawa, I. (1991). *The Fungal Spore and Disease Initiation in Plants and Animals*. New York: Plenum Publishing, 205–217. doi: 10.1007/978-1-4899-2635-7\_9
- Nazarko, T. Y., Polupanov, A. S., Manjithaya, R. R., Subramani, S., and Sibirny, A. A. (2007). The requirement of sterol glucoside for pexophagy in yeast is dependent on the species and nature of peroxisome inducers. *Mol. Biol. Cell* 18, 106–118. doi: 10.1091/mbc.E06-06-0554
- Oku, M., and Sakai, Y. (2010). Peroxisomes as dynamic organelles: autophagic degradation. *FEBS J.* 277, 3289–3294. doi: 10.1111/j.1742-4658.2010.07741.x
- Oku, M., Warnecke, D., Noda, T., Muller, F., Heinz, E., Mukaiyama, H., et al. (2003). Peroxisome degradation requires catalytically active sterol glucosyltransferase with a GRAM domain. *EMBO J.* 22, 3231–3241. doi: 10.1093/emboj/cdg331
- Thines, E., Weber, R. W., and Talbot, N. J. (2000). MAP kinase and protein kinase A-dependent mobilization of triacylglycerol and glycogen during appressorium turgor generation by *Magnaporthe grisea*. *Plant Cell* 12, 1703–1718.
- van Zutphen, T., Todde, V., De Boer, R., Kreim, M., Hofbauer, H. F., Wolinski, H., et al. (2014). Lipid droplet autophagy in the yeast *Saccharomyces cerevisiae*. *Mol. Biol. Cell* 25, 290–301. doi: 10.1091/mbc.E13-08-0448
- Vorholt, J. A. (2012). Microbial life in the phyllosphere. *Nat. Rev. Microbiol.* 10, 828–840. doi: 10.1038/nrmicro2910
- Weber, R. W., Wakley, G. E., Thines, E., and Talbot, N. J. (2001). The vacuole as central element of the lytic system and sink for lipid droplets in maturing appressoria of *Magnaporthe grisea*. *Protoplasma* 216, 101–112. doi: 10.1007/BF02680137
- Yamashita, S., Oku, M., Wasada, Y., Ano, Y., and Sakai, Y. (2006). PI4P-signaling pathway for the synthesis of a nascent membrane structure in selective autophagy. *J. Cell Biol.* 173, 709–717. doi: 10.1083/jcb.200512142
- Yamauchi, J., Takayanagi, N., Komeda, K., Takano, Y., and Okuno, T. (2004). cAMP-pKA signaling regulates multiple steps of fungal infection cooperatively with Cmk1 MAP kinase in *Colletotrichum lagenarium*. *Mol. Plant Microbe Interact.* 17, 1355–1365. doi: 10.1094/MPMI.2004.17.12.1355
- Yang, Z., and Klionsky, D. J. (2010). Mammalian autophagy: core molecular machinery and signaling regulation. *Curr. Opin. Cell Biol.* 22, 124–131. doi: 10.1016/j.ceb.2009.11.014
- Yurimoto, H., Oku, M., and Sakai, Y. (2011). Yeast methylotrophy: metabolism, gene regulation and peroxisome homeostasis. *Int. J. Microbiol.* 2011, 101298. doi: 10.1155/2011/101298
- Zechner, R., Zimmermann, R., Eichmann, T. O., Kohlwein, S. D., Haemmerle, G., Lass, A., et al. (2012). FAT SIGNALS—lipases and lipolysis in lipid metabolism and signaling. *Cell Metab.* 15, 279–291. doi: 10.1016/j.cmet.2011.12.018
- Conflict of Interest Statement:** The authors declare that the research was conducted in the absence of any commercial or financial relationships that could be construed as a potential conflict of interest.

Received: 27 January 2014; paper pending published: 17 February 2014; accepted: 21 February 2014; published online: 11 March 2014.

Citation: Oku M, Takano Y and Sakai Y (2014) The emerging role of autophagy in peroxisome dynamics and lipid metabolism of phyllosphere microorganisms. *Front. Plant Sci.* 5:81. doi: 10.3389/fpls.2014.00081

This article was submitted to Plant Cell Biology, a section of the journal Frontiers in Plant Science.

Copyright © 2014 Oku, Takano and Sakai. This is an open-access article distributed under the terms of the Creative Commons Attribution License (CC BY). The use, distribution or reproduction in other forums is permitted, provided the original author(s) or licensor are credited and that the original publication in this journal is cited, in accordance with accepted academic practice. No use, distribution or reproduction is permitted which does not comply with these terms.



# Involvement of autophagy in the direct ER to vacuole protein trafficking route in plants

**Simon Michaeli<sup>1</sup>, Tamar Avin-Wittenberg<sup>2</sup> and Gad Galili<sup>1\*</sup>**

<sup>1</sup> Department of Plant Sciences, The Weizmann Institute of Science, Rehovot, Israel

<sup>2</sup> Max-Planck-Institut für Molekulare Pflanzenphysiologie, Potsdam-Golm, Germany

**Edited by:**

Diane C. Bassham, Iowa State University, USA

**Reviewed by:**

Alessandro Vitale, National Research Council of Italy, Italy

Jan Zouhar, Universidad Politécnica de Madrid, Spain

Yule Liu, Tsinghua University, China

**\*Correspondence:**

Gad Galili, Department of Plant Sciences, The Weizmann Institute of Science, 234 Herzl Street, Rehovot 76100, Israel

e-mail: gad.galili@weizmann.ac.il

Trafficking of proteins from the endoplasmic reticulum (ER) to the vacuole is a fundamental process in plants, being involved both in vacuole biogenesis as well as with plant growth and response to environmental stresses. Although the canonical transport of cellular components from the ER to the vacuole includes the Golgi apparatus as an intermediate compartment, there are multiple lines of evidence that support the existence of a direct ER-to-vacuole, Golgi-independent, trafficking route in plants that uses the autophagy machinery. Plant autophagy was initially described by electron microscopy, visualizing cellular structures that are morphologically reminiscent of autophagosomes. In some of these reports these structures were shown to transport vacuole residing proteins, particularly seed storage proteins, directly from the ER to the vacuole. More recently, following the discovery of the proteins of the core autophagy machinery, molecular tools were implemented in deciphering the involvement of autophagy in this special trafficking route. Here we review the relatively older and more recent scientific observations, supporting the involvement of autophagy in the special cellular trafficking pathways of plants.

**Keywords:** plant autophagy, selective autophagy, plant vacuole, endoplasmic reticulum, seed storage proteins, golgi-independent trafficking, direct ER to vacuole, Atg8

## AUTOPHAGY AS AN ALTERNATIVE TRAFFICKING PATHWAY FOR PROTEINS DESTINED TO THE VACUOLE

Macroautophagy (termed hereafter simply autophagy) is a conserved cellular process that involves the sequestration of cytosolic components by a newly formed, double membrane vesicle termed autophagosome that is eventually directed to the cell's lytic compartment (lysosome in animals or vacuole in plants and fungi; Li and Vierstra, 2012; Liu and Bassham, 2012). This process was originally thought to be a process of stress and starvation-induced bulk-degradation of cytosolic components. Autophagy may however, also act selectively, specifically targeting malfunctioning organelles such as mitochondria (mitophagy) or peroxisomes (pexophagy), protein aggregates (aggrephagy), invading pathogens (xenophagy), and even specific proteins (Floyd et al., 2012; Li and Vierstra, 2012). Notably, selective autophagy was also reported to act in special trafficking routes, delivering vacuolar resident proteins to function in this organelle. This role of autophagy in biogenesis-mediating process is in contrast to the degradative nature classically associated with it. Currently, the best known autophagy-dependent trafficking route is the cytosol to vacuole targeting (Cvt) pathway of yeast (Scott et al., 1996). This pathway involves the trafficking of at least two hydrolases, aminopeptidase 1 (Ape1), and  $\alpha$ -manosidase (Ams1) from the cytosol into the vacuole. The Cvt pathway utilizes the core-autophagy machinery. The selectivity of this process is determined by Atg19 that attaches to the target proteins (Ape1 and Ams1) and can also bind Atg11 and Atg8 to mediate the formation of the Cvt vesicle (Lynch-Day and Klionsky, 2010). As will be further discussed here, analogous types of autophagy-dependent

trafficking routes may well exist also in plants, especially for the direct route between the endoplasmic reticulum (ER), and the vacuole, bypassing the Golgi apparatus (De Marchis et al., 2013).

## AN AUTOPHAGY-RESEMBLING, DIRECT ER-TO-VACUOLE, GOLGI-BYPASSING TRAFFICKING ROUTE OF SEED STORAGE PROTEINS

Maturing plant seeds synthesize massive amounts of storage proteins whose mobilization during germination provides an important metabolic boost during early germination. The seed storage proteins of most plant species are synthesized within the ER and are then transported to protein storage vacuoles (PSVs) where they are packed in highly condensed forms (Herman and Larkins, 1999; Vitale and Hinz, 2005). Yet, in contrast to most other secretory proteins, the seed storage proteins are synthesized in massive amounts and also naturally possess an aggregative nature making them insoluble material that is not fit to be transported in "classical" trafficking routes (Herman, 2008). These facts question the ability and capacity of the classical ER-Golgi-vacuole route to account for the transport of the entire bulk of storage proteins to storage vacuoles. Indeed, extensive microscopic evidence suggest that seed storage proteins are transported from the ER to the storage vacuole also by an alternative route, a special ER-vacuole trafficking (ERvt) route that bypasses the Golgi (Galili, 2004; Herman and Schmidt, 2004). This ERvt route, originally discovered using electron microscopy observations of storage proteins in developing wheat seeds (Levanony et al., 1992; Galili et al., 1993), begins by the aggregation of the storage proteins within the ER,

their subsequent budding from the ER to form special ER-derived PBs, and their internalization into the storage vacuoles by a process that strongly resembles autophagy (Hara-Nishimura et al., 1998; Robinson et al., 2005; Herman, 2008; Ibl and Stoger, 2011; Wang et al., 2011). Protein aggregation in the ER may also be the fate of non-storage proteins following stresses that hamper proper protein folding (a phenomenon known as ER-stress) resulting in the unfolded protein response (UPR; Howell, 2013). Recently it was shown that inducing ER stress in *Arabidopsis* results in the delivery of ER components, such as ER membrane decorated with ribosomes, to vacuoles via autophagy (Liu et al., 2012), further strengthening the possible involvement of autophagy in storage protein trafficking. Naturally, the ERvt autophagy is distinct from the classical non-selective starvation-induced autophagy by being selective to transport only storage proteins (**Figure 1**). Whether these two autophagy processes use the same or different machineries is an interesting issue that will be addressed further ahead in this review. The ERvt autophagy route appears to be dependent on the type of the storage proteins as well as the plant species and tissues where they are synthesized. The storage proteins of maize seeds accumulate entirely within ER-derived PBs. Surprisingly, expression of these storage proteins genes in transgenic tobacco plants resulted in their transport to the vacuole by autophagy (Hoffman et al., 1987). An analogous Golgi-bypass

route was further proposed for: (i) the transport of specific precursors of storage proteins from the ER to the vacuole via “precursor-accumulating” (PAC) bodies (Hara-Nishimura et al., 1998); (ii) the transport of germination-associated proteases, containing a C-terminal K/HDEL ER-retention signal, from the ER to the vacuole (this will be elaborated on in the next section); and (iii) the transport of storage proteins to the storage vacuole in aleurone cells of developing maize seeds (Reyes et al., 2011).

Reyes et al. (2011) presented data from *in vivo* imaging and electron tomography, suggesting that in maize seed aleurone cells, storage proteins are transported from the ER to PSVs using a special autophagic process. This process also appears to be similar to the ERvt process described in wheat (Levanony et al., 1992; Galili et al., 1993; Ibl and Stoger, 2011). Classically, the selection of cargo to be delivered by the autophagosome is mediated by binding of Atg8, residing on the growing autophagosome membrane, to the cargo protein or an adaptor protein linking the cargo to Atg8 (Li and Vierstra, 2012). Despite microscopic evidence suggesting the involvement of autophagy in storage protein transport, no co-localization of the maize seed storage proteins with Atg8 was observed in steady state microscopy images used in this report (Reyes et al., 2011). Reyes and associates claimed that the lack of co-localization might stem from the function of a non-canonical autophagy mechanism, not involving Atg8. Other, non-canonical (alternative) autophagic pathways may exist, as an Atg5/Atg7 independent autophagy was demonstrated in mammalian embryonic tissues (Nishida et al., 2009). However, another possibility could be a transient interaction between Atg8 and the potential cargo receptor proteins that might be localized on the surface of storage protein bodies. This may result in low co-localization frequency, which was possibly very difficult to detect by steady-state microscopic analysis. A similar observation was recently made in our group regarding the Atg8 interacting proteins, ATI1 and ATI2. *In vivo* interaction of Atg8f with either of these two proteins was detected, but co-localization was quite infrequent (Honig et al., 2012). Also, it is important to bear in mind that autophagy components are involved, not only in autophagosome biogenesis, but also in its transport to the vacuole, its fusion with the tonoplast and in the delivery of the autophagic-body into the vacuole lumen. Thus, evaluating the involvement of autophagy in any process must include each of these phases, usually by looking whether they are hampered in the background of autophagy deficient mutants (Klionsky et al., 2012).

## ERVT PATHWAYS TRANSPORTING GERMINATION AND DEFENSE-ASSOCIATED CYSTEINE PROTEASES TO THE VACUOLE

An ERvt route appears to be involved not only in the deposition of seed storage proteins inside PSVs during seed maturation, but also in their mobilization during early germination. Mobilization of the storage proteins during germination depends on the *de novo* synthesis of a family of cysteine proteases, which are inserted into the ER and are then transported to PSVs. Intriguingly, a number of these cysteine proteases contain a C-terminal K/HDEL signal, which classically functions in the retention of ER-resident

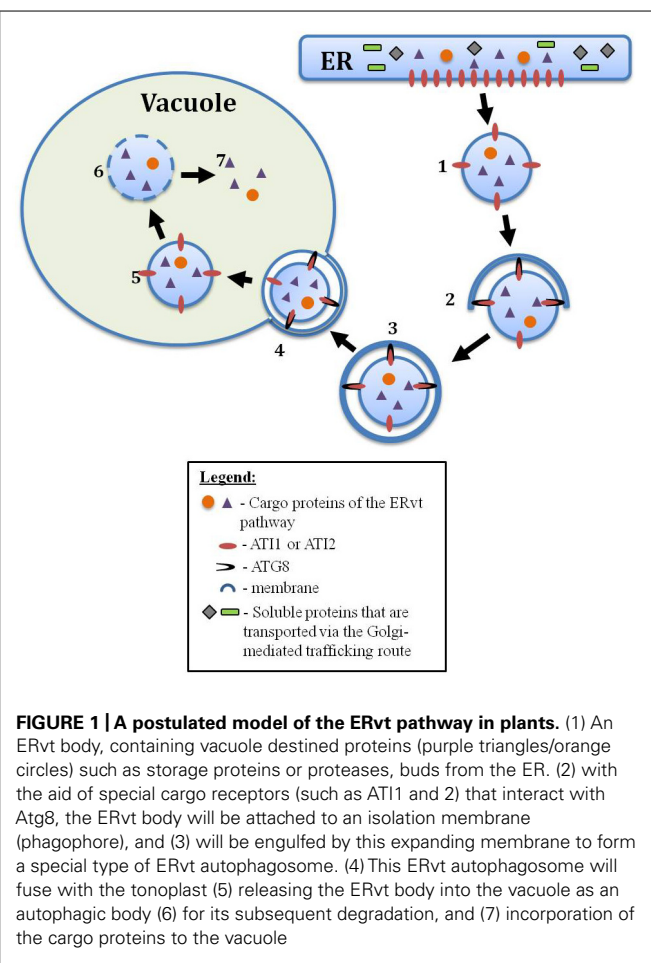


**FIGURE 1 | A postulated model of the ERvt pathway in plants.** (1) An ERvt body, containing vacuole destined proteins (purple triangles/orange circles) such as storage proteins or proteases, buds from the ER. (2) with the aid of special cargo receptors (such as ATI1 and 2) that interact with Atg8, the ERvt body will be attached to an isolation membrane (phagophore), and (3) will be engulfed by this expanding membrane to form a special type of ERvt autophagosome. (4) This ERvt autophagosome will fuse with the tonoplast (5) releasing the ERvt body into the vacuole as an autophagic body (6) for its subsequent degradation, and (7) incorporation of the cargo proteins to the vacuole

proteins within this organelle (Toyooka et al., 2000). Moreover, the K/HDEL signal appears to be essential for the trafficking of these cysteine proteases to the PSV because removal of this signal leads to their secretion (Okamoto et al., 2003). The nascent K/HDEL-containing cysteine proteases are transiently retained within the ER, enabling their deposition into special vesicles, called KDEL vesicles (KV), which bud directly from the ER and are then internalized into the vacuole (Toyooka et al., 2000). Notably, when expressed in the heterologous system of insect Sf-9 cells, the KDEL ER-retention sequence is post-translationally removed from this protein either within the ER or in a related compartment (Okamoto et al., 1999), implying that a similar mechanism of enzymatic removal of this ER-retention signal may also exist in plants and may be important for the transport of this protein to the vacuole.

Different cysteine proteases lacking a KDEL ER retention signal accumulate in a different organelle, namely, the spindle-shaped ER-body of *Arabidopsis* that is considered to be the largest ER-derived body in plants (Yamada et al., 2011). These cysteine proteases are the stress induced RD21 and  $\gamma$ -vacuolar processing enzyme (VPE) proteins. ER-bodies were seen fusing with the tonoplast following salt treatment mediating the delivery of RD21 and  $\gamma$ -VPE to the vacuole (Hayashi et al., 2001), thus defining another unique mode of ERvt. ER bodies are increasingly associated with defense against plant pests and fungi (Yamada et al., 2011). This illustrates that mobilization of proteins from the ER to the vacuole via ER bodies might be important for both biotic and abiotic stress tolerance. Notably, thus far no direct evidence linking autophagy with either KV or ER-body pathways have been reported.

### **SELECTIVE-AUTOPHAGY FACILITATING A STRESS-INDUCED, Atg8-MEDIATED, DIRECT ER-TO-VACUOLE TRAFFICKING**

Although the issue of the identity of the membrane donor for autophagosome biogenesis is controversial (Rubinsztein et al., 2012), the ER is considered one of the prominent candidates for this process (Hayashi-Nishino et al., 2009). Also, it is now recognized that following ER-stress, ER components are delivered for degradation via autophagy in both yeast and mammalian cells (Bernales et al., 2006; Ogata et al., 2006; Deegan et al., 2013). In this respect, plants are not different from other eukaryotes. Recently, the delivery of ER components, including ER-membrane decorated with ribosomes, was demonstrated to occur in plants cells following ER-stress (Liu et al., 2012). In this report, the accumulation of Atg8-positive bodies that co-localize with the ER marker, GFP-HDEL, was detected following ER-stress. Also, the presence of autophagic-bodies containing ER membrane was detected by electron-microscopy in vacuoles of ER-stressed plants. Finally, IRE1b, a special ER-stress sensor, was shown to be required for this autophagic process (Liu et al., 2012). Nevertheless, this most probably reflects the degradation of ER components and not the delivery of vacuole residing proteins that function in this organelle.

A support for the involvement of autophagy in the transport of functional cargo from the ER to the vacuole has recently been obtained, studying two novel, closely related, *Arabidopsis* proteins, termed Autophagy Interacting proteins one and two

(ATI1 and ATI2; Honig et al., 2012). Each of these proteins was shown to contain two consensus Atg8-binding motifs and also bind the *Arabidopsis* autophagy-associated Atg8f protein based on both the yeast 2-hybrid as well as the *in vivo* bimolecular fluorescence complementation (BiFC) approaches. Under normal growth conditions both ATI1 and ATI2 were localized to the ER. However, upon exposure to carbon starvation, the two proteins were incorporated into newly identified bodies that are not “classical” autophagosomes and are moving dynamically along the ER network. Subsequently, these ATI1 and two labeled bodies (ATI-bodies) are transported from the ER to the vacuole (Honig et al., 2012). These results provided the first hard-core evidence for the involvement of autophagy in the transport of cargo from the ER to the vacuole in plants. It also demonstrated that alternative pathways that involve autophagic components but are not “classical” autophagy do exist in plants. It was thus suggested that the ATI1 and ATI2 mediated transport from the ER might represent a pathway homologous to yeast Cvt, in that it mediates the transport of functional proteins to the vacuole, similarly to the route occurring in wheat (Li and Vierstra, 2012). A general model, depicting an ERvt body that originates from the ER and is delivered to the vacuole through the interaction of special cargo-receptors (such as ATI1 and ATI2) with Atg8, is presented in **Figure 1**.

The ability of autophagy to interact with components from other trafficking pathways and to deliver a variety of substrates directly to the vacuole was also recently demonstrated by the discovery of anthocyanin containing bodies that are labeled by both Atg8 and Exo70B1, a subunit of an exocyst complex (Kulich et al., 2013). Exocyst complexes are classically involved in the tethering of exocytosis-related vesicles to the plasma membrane, thus mediating their initial contact (Synek et al., 2014). Interestingly, significantly less mRFP-Atg8f positive bodies were found within vacuoles of Exo70B1 deficient plants compared to WT plants, implying for a direct role of Exo70B1 in the trafficking of anthocyanin autophagosomes to the vacuole (Kulich et al., 2013). Finally, it is important to mention also non-storage, lytic-vacuole residing proteins that were shown to reach the vacuole in a Golgi-independent manner. These are members of the tonoplast intrinsic protein (TIP) family (Gomez and Chrispeels, 1993; Rivera-Serrano et al., 2012) and vacuolar H<sup>+</sup>-driven ATPase subunits (VHA; Schumacher and Krebs, 2010). Although autophagy was not shown to be involved in TIPs trafficking, VHA-a subunits were recently utilized, among other markers, to monitor vacuole biogenesis in root meristematic cells, where autophagosome-like structures have been observed (Viotti et al., 2013) as will be discussed in the next section.

### **CONTRIBUTION OF MATERIAL FROM THE ER TO THE BIOGENESIS OF THE LYtic VACUOLE OCCURS THROUGH A GOLGI-BYPASSING TRAFFICKING ROUTE**

Autophagy was previously suggested to be involved in plant vacuole biogenesis (Marty, 1999) and it was also suggested that this is not the “classically” starvation induced autophagy, but rather a unique type of autophagy dedicated to the process of vacuole biogenesis (Yano et al., 2007). In animals, contribution of autophagy to replenish lysosome pool following starvation was

reported in rat kidney cells. This process, termed autophagic lysosome reformation (ALR), seems to be conserved in multiple animal species (Yu et al., 2010). Furthermore, the *Arabidopsis* deubiquitinating enzyme, AMSH1, a close homolog of AMSH3 that is essential for proper vacuole biogenesis (Isono et al., 2010), was shown to be necessary for proper autophagy (Katsiarimpas et al., 2013).

Recently, Viotti et al. (2013) demonstrated how the ER is the main membrane source for vacuole biogenesis in root meristematic cells. This contribution of membrane, sterol and specific protein pumps (vacuolar H<sup>+</sup>-PPase and the vacuolar H<sup>+</sup>-ATPase) occurs by a Golgi-bypassing trafficking route that seems homologous to ERvt described earlier. Also here, provacuoles that are considered precursors of the lytic vacuole displayed autophagosome-like structure of double or multilayered membranes (Viotti et al., 2013). Nonetheless, similarly to the report of storage proteins in maize aleurone cells (Reyes et al., 2011), ER-derived provacuoles were not labeled by Atg8 markers and their accumulation was not affected by *Atg2*, *Atg5*, or *Atg7* knockouts (Viotti et al., 2013). Thus, autophagy is probably not involved in the biogenesis of these provacuoles. Yet, it is possible that Atg8 transiently or rarely interacts with these provacuoles (as was demonstrated for ATI-bodies). Also, as already discussed, it is essential to test whether the delivery of cargo to vacuoles is occurring in *Atg* mutants before conclusions can be drawn regarding the involvement of autophagy (Klionsky et al., 2012). Though the authors showed the presence of provacuoles in *Atg* mutants, data regarding their trafficking to *Atg* mutant vacuoles was not presented (Viotti et al., 2013). Thus, currently it is not clear whether core-autophagy proteins are involved in provacuoles trafficking and vacuole biogenesis.

## CONCLUSION

There is no doubt that the trafficking pathways described here occur in plants and are distinct from the known Cvt pathway of yeast. The Cvt pathway delivers cargo from the cytoplasm to the vacuole while the plant pathways direct proteins from the ER to the vacuole. In addition, although the core-autophagy machinery is essential for the biogenesis of the Cvt vesicles, it does not seem to be essential for the biogenesis of the plant ERvt vesicles in plants. Nevertheless, the morphological resemblance of ERvt vesicles to autophagosomes, coupled with the involvement of Atg8 in such processes as described for the ATI-bodies, strongly suggests the involvement of autophagy in ERvt pathways in plants. Most probably this involvement is taking place in the transport of the ERvt vesicles to the vacuole following their autophagy-independent biogenesis (**Figure 1**). Yet, this hypothesis awaits clear evidences that can be supplied by further investigating both ATI-bodies in *Arabidopsis* and storage proteins trafficking in cereal seeds. This can be examined by evaluating whether these types of ERvt vesicles reach the vacuole in the background of classical autophagy deficient plants such as *Atg5*, *Atg7*, and *Atg4a4b*.

## ACKNOWLEDGMENTS

We thank Dr. Arik Honig for fruitful discussions. Our research was supported by grants from the Israel Science Foundation (grant No. 764/07), the J and R center for scientific research at the Weizmann

Institute of Science, and the Israeli Ministry of Agriculture. Gad Galili is an incumbent of the Bronfman Chair of Plant Science at the Weizmann Institute of Science.

## REFERENCES

- Bernales, S. N., McDonald, K. L., and Walter, P. (2006). Autophagy counterbalances endoplasmic reticulum expansion during the unfolded protein response. *PLoS Biol.* 4:e423. doi: 10.1371/journal.pbio.0040423
- Deegan, S., Saveljeva, S., Gorman, A., and Samali, A. (2013). Stress-induced self-cannibalism: on the regulation of autophagy by endoplasmic reticulum stress. *Cell. Mol. Life Sci.* 70, 2425–2441. doi: 10.1007/s00018-012-1173-4
- De Marchis, F., Bellucci, M., and Pompa, A. (2013). Unconventional pathways of secretory plant proteins from the endoplasmic reticulum to the vacuole bypassing the golgi complex. *Plant Signal. Behav.* 8, e25129. doi: 10.4161/psb.25129
- Floyd, B. E., Morriss, S. C., Macintosh, G. C., and Bassham, D. C. (2012). What to eat: evidence for selective autophagy in plants. *J. Integr. Plant Biol.* 54, 907–920. doi: 10.1111/j.1744-7909.2012.01178.x
- Galili, G. (2004). ER-derived compartments are formed by highly regulated processes and have special functions in plants. *Plant Physiol.* 136, 3411–3413. doi: 10.1104/pp.104.900125
- Galili, G., Altschuler, Y., and Levanony, H. (1993). Assembly and transport of seed storage proteins. *Trends Cell Biol.* 3, 437–442. doi: 10.1016/0962-8924(93)90033-W
- Gomez, L., and Chrispeels, M. J. (1993). Tonoplast and soluble vacuolar proteins are targeted by different mechanisms. *Plant Cell* 5, 1113–1124. doi: 10.1105/tpc.5.9.1113
- Hara-Nishimura, I., Shimada, T., Hatano, K., Takeuchi, Y., and Nishimura, M. (1998). Transport of storage proteins to protein storage vacuoles is mediated by large precursor-accumulating vesicles. *Plant Cell* 10, 825–836. doi: 10.1105/tpc.10.5.825
- Hayashi-Nishino, M., Fujita, N., Noda, T., Yamaguchi, A., Yoshimori, T., and Yamamoto, A. (2009). A subdomain of the endoplasmic reticulum forms a cradle for autophagosome formation. *Nat. Cell Biol.* 11, 1433–1437. doi: 10.1038/ncb1991
- Hayashi, Y., Yamada, K., Shimada, T., Matsushima, R., Nishizawa, N., Nishimura, M., et al. (2001). A proteinase-storing body that prepares for cell death or stresses in the epidermal cells of *Arabidopsis*. *Plant Cell Physiol.* 42, 894–899. doi: 10.1093/pcp/pce144
- Herman, E. M. (2008). Endoplasmic reticulum bodies: solving the insoluble. *Curr. Opin. Plant Biol.* 11, 672–679. doi: 10.1016/j.pbi.2008.08.004
- Herman, E. M., and Larkins, B. A. (1999). Protein storage bodies and vacuoles. *Plant Cell* 11, 601–613. doi: 10.1105/tpc.11.4.601
- Herman, E., and Schmidt, M. (2004). Endoplasmic reticulum to vacuole trafficking of endoplasmic reticulum bodies provides an alternate pathway for protein transfer to the vacuole. *Plant Physiol.* 136, 3440–3446. doi: 10.1104/pp.104.051722
- Hoffman, L. M., Donaldson, D. D., Bookland, R., Rashka, K., and Herman, E. M. (1987). Synthesis and protein body deposition of maize 15-kd zein in transgenic tobacco seeds. *EMBO J.* 6, 3213–3221.
- Honig, A., Avin-Wittenberg, T., Ufaz, S., and Galili, G. (2012). A new type of compartment, defined by plant-specific Atg8-interacting proteins, is induced upon exposure of *Arabidopsis* plants to carbon starvation. *Plant Cell* 24, 288–303. doi: 10.1105/tpc.111.093112
- Howell, S. H. (2013). Endoplasmic reticulum stress responses in plants. *Annu. Rev. Plant Biol.* 64, 477–499. doi: 10.1146/annurev-arplant-050312-120053
- Ibl, V., and Stoger, E. (2011). The formation, function and fate of protein storage compartments in seeds. *Protoplasma* 249, 379–392. doi: 10.1007/s00709-011-0288-z
- Isono, E., Katsiarimpas, A., Muller, I. K., Anzenberger, F., Stierhof, Y. D., Geldner, N., et al. (2010). The deubiquitinating enzyme AMSH3 is required for intracellular trafficking and vacuole biogenesis in *Arabidopsis thaliana*. *Plant Cell* 22, 1826–1837. doi: 10.1105/tpc.110.075952
- Katsiarimpas, A., Kalinowska, K., Anzenberger, F., Weis, C., Ostertag, M., Tsutsumi, C., et al. (2013). The deubiquitinating enzyme AMSH1 and the ESCRT-III subunit VPS21 are required for autophagic degradation in *Arabidopsis*. *Plant Cell* 25, 2236–2252. doi: 10.1105/tpc.113.113399

- Klionsky, D. J., Abdalla, F. C., Abeliovich, H., Abraham, R. T., Acevedo-Arozena, A., Adeli, K., et al. (2012). Guidelines for the use and interpretation of assays for monitoring autophagy. *Autophagy* 8, 445–544. doi: 10.4161/auto.19496
- Kulich, I., Peèenková, T., Sekereš, J., Smetana, O., Fendrych, M., Foissner, I., et al. (2013). *Arabidopsis* exocyst subcomplex containing subunit EXO70B1 is involved in autophagy-related transport to the vacuole. *Traffic* 14, 1155–1165. doi: 10.1111/tra.12101
- Levanony, H., Rubin, R., Altschuler, Y., and Galili, G. (1992). Evidence for a novel route of wheat storage proteins to vacuoles. *J. Cell Biol.* 119, 1117–1128. doi: 10.1083/jcb.119.5.1117
- Li, F., and Vierstra, R. D. (2012). Autophagy: a multifaceted intracellular system for bulk and selective recycling. *Trends Plant Sci.* 17, 526–537. doi: 10.1016/j.tplants.2012.05.006
- Liu, Y., and Bassham, D. C. (2012). Autophagy: pathways for self-eating in plant cells. *Annu. Rev. Plant Biol.* 63, 215–237. doi: 10.1146/annurev-arplant-042811-105441
- Liu, Y., Burgos, J. S., Deng, Y., Srivastava, R., Howell, S. H., and Bassham, D. C. (2012). Degradation of the endoplasmic reticulum by autophagy during endoplasmic reticulum stress in *Arabidopsis*. *Plant Cell* 24, 4635–4651. doi: 10.1105/tpc.112.101535
- Lynch-Day, M. A., and Klionsky, D. J. (2010). The Cvt pathway as a model for selective autophagy. *FEBS Lett.* 584, 1359–1366. doi: 10.1016/j.febslet.2010.02.013
- Marty, F. (1999). Plant vacuoles. *Plant Cell* 11, 587–600.
- Nishida, Y., Arakawa, S., Fujitani, K., Yamaguchi, H., Mizuta, T., Kanaseki, T., et al. (2009). Discovery of Atg5/Atg7-independent alternative macroautophagy. *Nature* 461, 654–658. doi: 10.1038/nature08455
- Ogata, M., Hino, S.-I., Saito, A., Morikawa, K., Kondo, S., Kanemoto, S., et al. (2006). Autophagy is activated for cell survival after endoplasmic reticulum stress. *Mol. Cell. Biol.* 26, 9220–9231. doi: 10.1128/mcb.01453-06
- Okamoto, T., Shimada, T., Hara-Nishimura, I., Nishimura, M., and Minamikawa, T. (2003). C-terminal KDEL sequence of a KDEL-tailed cysteine proteinase (sulphydryl-endopeptidase) is involved in formation of KDEL vesicle and in efficient vacuolar transport of sulphydryl-endopeptidase. *Plant Physiol.* 132, 1892–1900. doi: 10.1104/pp.103.021147
- Okamoto, T., Minamikawa, T., Edward, G., Vakharia, V., and Herman, E. (1999). Posttranslational removal of the carboxyl-terminal KDEL of the cysteine protease SH-EP occurs prior to maturation of the enzyme. *J. Biol. Chem.* 274, 11390–11398. doi: 10.1074/jbc.274.16.11390
- Reyes, F. C., Chung, T., Holding, D., Jung, R., Vierstra, R., and Otegui, M. S. (2011). Delivery of prolamins to the protein storage vacuole in maize aleurone cells. *Plant Cell* 23, 769–784. doi: 10.1105/tpc.110.082156
- Rivera-Serrano, E. E., Rodriguez-Welsh, M. F., Hicks, G. R., and Rojas-Pierce, M. (2012). A small molecule inhibitor partitions two distinct pathways for trafficking of tonoplast intrinsic proteins in *Arabidopsis*. *PLoS ONE* 7:e44735. doi: 10.1371/journal.pone.0044735
- Robinson, D. G., Oliviusson, P., and Hinz, G. (2005). Protein sorting to the storage vacuoles of plants: a critical appraisal. *Traffic* 6, 615–625. doi: 10.1111/j.1600-0854.2005.00303.x
- Rubinsztein, D. C., Shpilka, T., and Elazar, Z. (2012). Mechanisms of autophagosome biogenesis. *Curr. Biol.* 22, R29–R34. doi: 10.1016/j.cub.2011.11.034
- Schumacher, K., and Krebs, M. (2010). The V-ATPase: small cargo, large effects. *Curr. Opin. Plant Biol.* 13, 724–730. doi: 10.1016/j.pbi.2010.07.003
- Scott, S. V., Hefner-Gravink, A., Morano, K. A., Noda, T., Ohsumi, Y., and Klionsky, D. J. (1996). Cytoplasm-to-vacuole targeting and autophagy employ the same machinery to deliver proteins to the yeast vacuole. *Proc. Natl. Acad. Sci. U.S.A.* 93, 12304–12308. doi: 10.1073/pnas.93.22.12304
- Synek, L., Sekeres, J., and Zarsky, V. (2014). The exocyst at the interface between cytoskeleton and membranes in eukaryotic cells. *Front. Plant Sci.* 4:543. doi: 10.3389/fpls.2013.00543
- Toyooka, K., Okamoto, T., and Minamikawa, T. (2000). Mass transport of pro-form of a KDEL-tailed cysteine proteinase (Sh-EP) to protein storage vacuoles by endoplasmic reticulum derived vesicle is involved in protein mobilization in germinating seeds. *J. Cell Biol.* 148, 453–464. doi: 10.1083/jcb.148.3.453
- Viotti, C., Krüger, F., Krebs, M., Neubert, C., Fink, F., Lupanga, U., et al. (2013). The endoplasmic reticulum is the main membrane source for biogenesis of the lytic vacuole in *Arabidopsis*. *Plant Cell* 25, 3434–3449. doi: 10.1105/tpc.113.114827
- Vitale, A., and Hinz, G. (2005). Sorting of proteins to storage vacuoles: how many mechanisms? *Trends Plant Sci.* 10, 316–323. doi: 10.1016/j.tplants.2005.05.001
- Wang, H., Rogers, J. C., and Jiang, L. (2011). Plant RMR proteins: unique vacuolar sorting receptors that couple ligand sorting with membrane internalization. *FEBS J.* 278, 59–68. doi: 10.1111/j.1742-4658.2010.07923.x
- Yamada, K., Hara-Nishimura, I., and Nishimura, M. (2011). Unique defense strategy by the endoplasmic reticulum body in plants. *Plant Cell Physiol.* 52, 2039–2049. doi: 10.1093/pcp/pcr156
- Yano, K., Hattori, M., and Moriyasu, Y. (2007). A novel type of autophagy occurs together with vacuole genesis in miniprotoplasts prepared from tobacco culture cells. *Autophagy* 3, 215–221.
- Yu, L., McPhee, C. K., Zheng, L., Mardones, G. A., Rong, Y., Peng, J., et al. (2010). Termination of autophagy and reformation of lysosomes regulated by mTOR. *Nature* 465, 942–946. doi: 10.1038/nature09076

**Conflict of Interest Statement:** The authors declare that the research was conducted in the absence of any commercial or financial relationships that could be construed as a potential conflict of interest.

Received: 17 February 2014; paper pending published: 03 March 2014; accepted: 21 March 2014; published online: 08 April 2014.

Citation: Michaeli S, Avin-Wittenberg T and Galili G (2014) Involvement of autophagy in the direct ER to vacuole protein trafficking route in plants. *Front. Plant Sci.* 5:134. doi: 10.3389/fpls.2014.00134

This article was submitted to Plant Cell Biology, a section of the journal Frontiers in Plant Science.

Copyright © 2014 Michaeli, Avin-Wittenberg and Galili. This is an open-access article distributed under the terms of the Creative Commons Attribution License (CC BY). The use, distribution or reproduction in other forums is permitted, provided the original author(s) or licensor are credited and that the original publication in this journal is cited, in accordance with accepted academic practice. No use, distribution or reproduction is permitted which does not comply with these terms.



# Selective autophagy of non-ubiquitylated targets in plants: looking for cognate receptor/adaptor proteins

Vasko Veljanovski and Henri Batoko\*

Institut des Sciences de la Vie, Université Catholique de Louvain, Louvain-la-Neuve, Belgium

**Edited by:**

Diane C. Bassham, Iowa State University, USA

**Reviewed by:**

Alessandro Vitale, National Research Council of Italy, Italy

Jianping Hu, Michigan State University, USA

**\*Correspondence:**

Henri Batoko, Institut des Sciences de la Vie, Université Catholique de Louvain, Croix du Sud 4–5, L70714 1348, Louvain-la-Neuve, Belgium  
e-mail: henri.batoko@uclouvain.be

Cellular homeostasis is essential for the physiology of eukaryotic cells. Eukaryotic cells, including plant cells, utilize two main pathways to adjust the level of cytoplasmic components, namely the proteasomal and the lysosomal/vacuolar pathways. Macroautophagy is a lysosomal/vacuolar pathway which, until recently, was thought to be non-specific and a bulk degradation process. However, selective autophagy which can be activated in the cell under various physiological conditions, involves the specific degradation of defined macromolecules or organelles by a conserved molecular mechanism. For this process to be efficient, the mechanisms underlying the recognition and selection of the cargo to be engulfed by the double membrane autophagosome are critical, and not yet well understood. Ubiquitin (poly-ubiquitin) conjugation to the target appears to be a conserved ligand mechanism in many types of selective autophagy, and defined receptors/adaptors recognizing and regulating the autophagosomal capture of the ubiquitylated target have been characterized. However, non-proteinaceous and non-ubiquitylated cargoes are also selectively degraded by this pathway. This ubiquitin-independent selective autophagic pathway also involves receptor and/or adaptor proteins linking the cargo to the autophagic machinery. Some of these receptor/adaptor proteins including accessory autophagy-related (Atg) and non-Atg proteins have been described in yeast and animal cells but not yet in plants. In this review we discuss the ubiquitin-independent cargo selection mechanisms in selective autophagy degradation of organelles and macromolecules and speculate on potential plant receptor/adaptor proteins.

**Keywords:** selective autophagy cargo receptor, non-ubiquitylated cargo, plant cell, TSPO protein, porphyrins

## DIVERSITY OF TYPES AND TARGETS FOR SELECTIVE AUTOPHAGY

Following his discovery of the lysosome in rat hepatic cells in 1955, the Belgian cytologist and biochemist Christian de Duve, the 1974 Nobel Prize laureate in Physiology or Medicine, coined the term “autophagy” in 1963. This term describes morphologically a process whereby living eukaryotic cells achieve the degradation of their own constituent through a vesicular encapsulation of a portion of their cytoplasm and its degradation in the lysosome/vacuole. Although describing what currently is known as *sensu stricto* non-selective macroautophagy, De Duve and Wattiaux (1966) acknowledged the possibility that this degradation process can be selective, targeting defined cellular structures as opposed to a random and bulk degradation of a portion of the cytoplasm. Macroautophagy (hereafter referred to as autophagy) is an evolutionarily conserved catabolic process allowing eukaryotic cells to recycle nutrients and biosynthetic monomers, and mitigate cellular damage during stressful physiological conditions (Yorimitsu and Klionsky, 2005; Mizushima et al., 2011; Liu and Bassham, 2012). Previously thought to be essentially a non-selective bulk degradation process, within the last decade or so it has been well documented that this complex and highly regulated pathway comes in two main types, non-selective and selective autophagy (Pankiv et al., 2007; Sandoval et al., 2008; Lynch-Day and Klionsky, 2010; Johansen

and Lamark, 2011; Levine et al., 2011). One of the distinctive features of autophagy is the *de novo* formation of a double membrane vesicle called an autophagosome, which can fuse with the lysosome/vacuole delivering its content/cargo and membrane constituents for degradation by acidic hydrolases (Mizushima et al., 2011; Klionsky et al., 2012). The formation of an autophagosome is a hierarchical, regulated, and complex series of events involving initiation, elongation, closure, and maturation steps (Thumm et al., 1994; Klionsky et al., 2003; Mizushima et al., 2011; Feng et al., 2014). These steps are marshaled by the coordinated action of four autophagy-related (Atg) protein complexes including a protein kinase complex (Atg1 complex), a lipid kinase complex (Atg6 complex), an ubiquitin-like conjugation complex (Atg5–12–16 complex), and a cycling vesicular complex (Atg9 complex). Out of the 38 Atg gene products described to date in eukaryotic cells, about 15 or so are involved in the activity of these complexes and are known to be conserved through evolution, hence they are considered as core autophagic genes. Both the non-selective and selective autophagic pathways appear to use basically the same core molecular machinery (Behrends et al., 2010; Lamb et al., 2013). Cell type-specific selective autophagy pathways such as (i) the biosynthetic cytoplasm-to-vacuole targeting (Cvt) of defined enzyme precursors in yeast (Klionsky et al., 1992; Lynch-Day and Klionsky, 2010), (ii) the chaperone-mediated autophagy and variants targeting defined

motif-containing soluble proteins in mammalian cells, and (iii) various forms of selective microautophagy (Cuervo and Wong, 2014), have not yet been described in plant cells and will not be discussed here. However, selective autophagy is a conserved mechanism in higher eukaryotes, playing a vital physiological role in proteostasis, cell growth, and development. The expanding list of endogenous substrates for this pathway includes organelles such as mitochondria (mitophagy), peroxisomes (pexophagy), chloroplasts (chlorophagy), endoplasmic reticulum (ER; reticulophagy), ribosomes (ribophagy), intracellular pathogens (xenophagy), individual proteins or their aggregates, and non-proteinaceous targets such as lipid droplets or harmful molecules. Selective autophagy is not only critical in the clearance of damaged, superfluous, or dysfunctional cellular structures but also in regulating key molecular mechanisms such as small RNA metabolism, iron utilization by the cell, or antigen presentation to name a few (Crotzer and Blum, 2009; Kirkin et al., 2009; Gibbings et al., 2012; Gump et al., 2013; Mancias et al., 2014). However, the machinery that promotes and regulates selective autophagy is largely unknown, and more so in plant cells for which experimental evidence of this pathway are quite recent and limited.

Selective sequestration and segregation of autophagic targets/cargo from other cellular structures has been observed and characterized both in yeast and mammals. It was only recently that similar observations have been made in plants. Recognition of a given target by a cognate receptor requires a defined ligand or structural feature on the target. A common molecular determinant recognized by selective autophagy receptors in animal cells is conjugated ubiquitin (Rogov et al., 2014). The conjugated ubiquitin on the cargo is bound by receptors of the sequestosome-1-like family such as the modular p62/sequestosome-1 or neighbor of breast cancer 1 (NBR1). Sequestosome-1-like receptors are involved or required for organelles and protein aggregates selective autophagy in mammals (Rogov et al., 2014). Related sequestosome-1-like proteins in plants are functional hybrids (with respect to their modular domains) of both mammalian p62 and NBR1, and may be involved in the clearance of soluble protein aggregates by selective autophagy (Svenning et al., 2011; Zientara-Rytter et al., 2011; Zhou et al., 2013). This important family of receptors links the target to the autophagy machinery either directly or via an adaptor protein by interacting with membrane-bound Atg8 family members. However, there is no sequestosome-1-like protein in yeast, and in higher eukaryotes, organelles and other non-proteinaceous targets of selective autophagy are also recognized through other molecular features. In addition, some sequestosome 1-like proteins in mammals such as Optineurin, which is involved in xenophagy, can also target protein aggregates in an ubiquitin-independent manner (Korac et al., 2013).

In addition to the common fundamental and unresolved question of the membrane source for the formation of the corresponding autophagosome, how individual endogenous substrates for selective autophagy are recognized and targeted for degradation is paramount for our understanding of the molecular mechanisms and the biological roles of this pathway. Recent findings suggest that the expanding repertoire

of cargo for selective autophagy parallels structurally diverse cognate receptor/adaptor proteins responsible for the recognition and recruitment of the cargo into the autophagosome. We will discuss the recognition and selection processes during mitophagy, pexophagy, and reticulophagy characterized in different cell types including plant cells, and elaborate on the scavenging of porphyrins through the selective autophagic pathway which has also been recently described in plants. Because the molecular mechanism of chloroplast degradation through selective autophagy is not yet clear, we will not discuss chlorophagy.

## MITOPHAGY

Dysfunctional mitochondria are tightly controlled in eukaryotic cells. For instance, oxidative stress within mammalian mitochondria up to a certain level can generate the disposal of oxidized proteins through a vesicular trafficking pathway from the mitochondria to the lysosome (Soubannier et al., 2012; McLelland et al., 2014). This specific pathway is regulated by an E3 ubiquitin ligase, Parkin, and the phosphatase and tensin homologue-induced putative kinase protein 1, PINK1. More damaged mitochondria are degraded by selective autophagy in eukaryotic cells. Parkin and PINK1 are also involved in ubiquitin-dependent selective autophagy of dysfunctional mitochondria. However, selective degradation of dysfunctional mitochondria in yeast is regulated by Atg32, a mitochondrial outer membrane protein (Kanki et al., 2009; Okamoto et al., 2009). Atg32 is a 60 kDa protein anchored to the mitochondrial membrane through a C-terminal transmembrane span. Atg32 connects the mitochondria to the autophagosome machinery by interacting sequentially with the coiled-coil domain-containing adaptor protein Atg11 and the ubiquitin-like protein Atg8. Both Atg11 and Atg32 interact with Atg8 through the so-called Atg8-family interacting motif (AIM, also known as the LC3-interacting region (LIR) in animal proteins). The core consensus of AIM and LIR is W/Y/FxxL/V/I (single amino acid code where x stands for any amino acid; Birgisdottir et al., 2013; Rogov et al., 2014). Structural evidence suggests that the Atg8-like protein contains an aromatic pocket and an aliphatic pocket accommodating the structural determinants of the core AIM/LIR sequence (Noda et al., 2008). It is not yet clear whether Atg32/Atg11 interact with phosphatidylethanolamine-conjugated Atg8 (Atg8-PE, membrane-bound) or soluble Atg8. There is no Atg32 homologue in animal cells, but 3 structurally unrelated mitochondrial outer membrane proteins function as mitophagy receptors. Nix is required for mitochondrial clearance during erythrocyte maturation (Sandoval et al., 2008; Youle and Narendra, 2011) and Bnip3 induces both mitochondria and ER removal by selective autophagy (Zhang et al., 2012). Both proteins are homologous and share the BCL2 homology 3 (BH3) domain and interact with Atg8-family members through an N-terminal LIR (WveL). FUN14 domain-containing 1 (FUNDC1) is a mitochondrial outer membrane protein acting as a receptor of hypoxia-induced mitophagy (Liu et al., 2012b). FUNDC1 is membrane-anchored through 3 transmembrane spans and the cytoplasmic N-terminus contains a LIR (YevL). In contrast to Nix and Bnip3, binding of FUNDC1 to Atg8-family members (specifically LC3B) is promoted by phosphorylation of the aromatic residue of the LIR motif (Y<sup>P</sup>evL).

The kinase responsible for this modification has not yet been identified. Neither Atg32 nor the mammalian mitophagy receptors have homologues in plants. However, an Atg11-related protein (single locus At4g30790) was recently characterized in *Arabidopsis* and elegantly shown to be required for senescence-induced mitophagy in plants (Li et al., 2014). Interestingly, the *Arabidopsis* Atg11-related protein structurally resembles the mammalian RB1-inducible coiled-coil protein 1 (RB1CC1) also known as FIP200 (FAK-family interacting protein of 200 kDa), with an Atg17 functional domain (IPR007240) at the N-terminus and an Atg11 functional domain (IPR19460) at the C-terminus. FIP200 is known to be the functional equivalent of Atg17 in animals, interacting with the Atg1-related kinases and the accessory protein Atg101 during autophagosome formation (Feng et al., 2014). It may be that the structural composition of the Atg1 complex is identical in plant and mammalian cells. Atg17 also acts as an adaptor/scaffold protein during pexophagy in *Pichia pastoris* (Farré et al., 2008). It is not yet clear whether the Atg17 domain in the plant protein is functional. It would be interesting to identify potential interacting partners of the Atg11-domain of the plant protein using mitochondrial outer membrane proteins as bait.

### PEXOPHAGY

The maintenance and turnover of peroxisomes are important for plant development and growth under normal conditions or subjected to (a)biotic stress (Farmer et al., 2013; Hackenberg et al., 2013; Kim et al., 2013; Shibata et al., 2013; Yoshimoto et al., 2014). Marked accumulation of peroxisomes as aggregates were observed in autophagy-deficient *Arabidopsis* mutants (affected in the core autophagy genes; Shibata et al., 2013; Yoshimoto et al., 2014). The peroxisome unusual positioning (Peup) 1, 2, and 4 alleles were shown to be identical to the autophagy core genes Atg2, Atg18a, and Atg7, respectively (Shibata et al., 2013). Interestingly, as compared to control plants, the accumulation of peroxisomes in autophagy-deficient plants was cell type-dependent, since this cellular phenotype was present in leaves but not in roots (Yoshimoto et al., 2014). Further study indicated that the uncleared peroxisomes in leaf cells contained increased levels of catalase, a known substrate for selective autophagy (Yu et al., 2006). In an *Arabidopsis* atg5 mutant grown under normal conditions, catalase levels increased eightfold in leaves but the catalase levels remained unaffected in root tissues. In plants, it seems that catalase acts upstream of immunity-triggered autophagy. The reaction of catalase with reactive oxygen species (ROS) allows catalase to act as a molecular link between ROS and the promotion of autophagy-dependent death (Hackenberg et al., 2013; Shibata et al., 2013). Intriguingly, isolated leaf peroxisomes do not show a substantial increase in ubiquitylated proteins after immuno-electron microscopy using anti-ubiquitin, suggesting that the aggregated peroxisomes are not cleared by an ubiquitin-dependent mechanism (Yoshimoto et al., 2014). Atg36 and Atg30 are receptors for pexophagy in *Saccharomyces cerevisiae* and *P. pastoris*, respectively (Farré et al., 2013). Both proteins are recruited to peroxisomes by the peroxisomal membrane protein Pex3, and contain AIM and bind to Atg8-family members. Phosphorylation of the pexophagy receptor proteins at the vicinity of their

AIM also regulates their interaction with Atg11 or Atg17, and enhances their affinity for Atg8 (Farré et al., 2013). To date, no related counterparts of Atg36 or Atg30 have been described in plants.

### RETICULOPHAGY

Secreted proteins are synthesized in the ER and this organelle is also the site of stringent quality control for the correct folding and quaternary structure of proteins in eukaryotic cells. For instance, misfolded polytopic membrane proteins are targeted for ER-associated degradation (ERAD). Protein misfolding can arise for example as a consequence of cellular stress or mutation in the primary structure of the polypeptide. A recent work in mammalian cells showed that the ER-associated HSP40 chaperone JB12 participates in partitioning mutant conformers of the gonadotropin releasing hormone receptor (GnRHR), a G-protein-coupled receptor, between ERAD and what was coined the ER quality control autophagy pathway (Houck et al., 2014). This selective autophagy pathway degrades the E90K-GnRHR mutant form which is ERAD-resistant. Interaction between ER-associated HSP40s and the vacuolar protein sorting 34 complex may allow the selective autophagy degradation of ERAD-resistant membrane proteins from the ER (Houck et al., 2014).

Experimental evidence was provided recently that plant cells also use reticulophagy as a response to ER stress (Liu et al., 2012a). Chemical ER stress agents-triggered reticulophagy requires the ER stress sensor inositol-requiring enzyme-1b (IRE1b).

In addition, an ER-to-vacuole pathway was also described in plant cells, and this pathway is regulated by the putative cargo receptors *Arabidopsis thaliana* Atg8-interacting proteins ATI1 and ATI2, which are unique to plants (Honig et al., 2012). ATI1 and ATI2 bind Atg8-family members via their conserved AIM WqVL, and could help segregate specific cargo molecules from the ER for their transport and degradation in the vacuole, although none has been identified yet.

### HEME AND AtTSPO DETOXIFICATION

We recently showed that plant cells can scavenge toxic free heme in the cytoplasm through the autophagic pathway (Vanhee et al., 2011). In contrast to other higher eukaryotes, heme biosynthesis, and heme oxygenase (ER-localized in mammalian cells) which is responsible for heme degradation, are localized in plant plastids. Abiotic stress transiently up-regulates heme biosynthesis (required for the activity of ROS scavengers) and simultaneously induces the expression of the polytopic TSPO-related membrane protein AtTSPO (*Arabidopsis thaliana* Translocator-related protein). Because heme functions not only as a prosthetic group for a myriad of proteins scattered throughout the cell but also as a regulatory signaling molecule (Severance and Hamza, 2009), this suggests that “free” heme is present albeit transiently in the cell. We showed that the ER-Golgi-localized AtTSPO (Guillaumot et al., 2009) binds heme *in vivo* and the complex is recruited to the autophagosome through an AIM present in AtTSPO (Vanhee et al., 2011). Constitutive expression of AtTSPO is toxic to plant and yeast (*S. cerevisiae*, devoid of TSPO-related protein) cells. When expressed as a fluorescent fusion, AtTSPO accumulates in autophagic

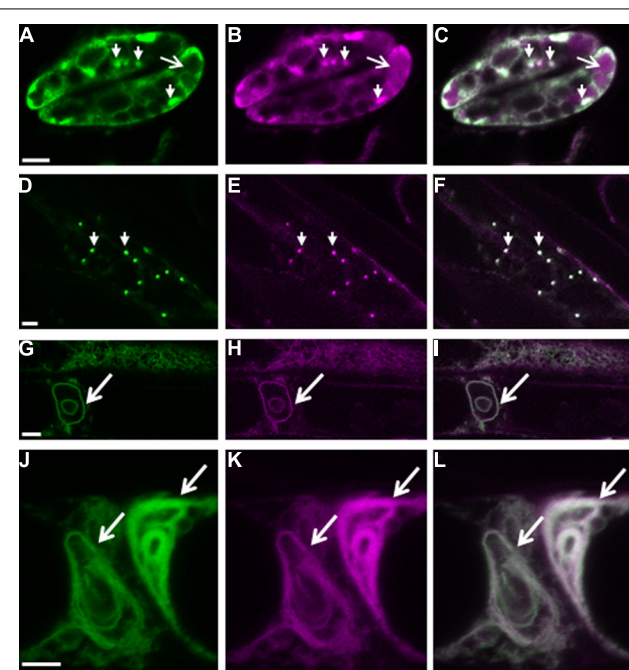


**FIGURE 1 | Autophagy-dependent degradation of AtTSPO.** Confocal images of a mCherry-GFP-AtTSPO fusion stably expressed constitutively in transgenic *Arabidopsis thaliana*; the green signal represents GFP fluorescence, magenta mCherry fluorescence, and the overlapping signal is shown as white in the merge images. Arrowheads in panels **A–C** indicate Golgi stacks in guard cells, and the arrow highlights mCherry fluorescence (but not GFP) in the vacuole. Panels **D–F** show imaging of the fluorescent chimera in a root cell, and the arrowheads indicate Golgi stacks. Panels **G–I** show the formation of autophagy bodies (arrow) in root cells after Concanamycin A treatment. Panels **J–L** show complex entangled membranes of autophagy bodies after Concanamycin A treatment. Scale bar is 5  $\mu$ m in **A–I**, and 2  $\mu$ m in **J–L**.

bodies after concanamycin A treatment (**Figure 1**), suggesting an active degradation of the protein through the autophagic pathway. Mammalian TSPO proteins are encoded by essential genes indicating a functional divergence with seed plant TSPOs. AtTSPO can oligomerize and seems to function as an authentic autophagy receptor at least for toxic porphyrins in the plant cell.

### FORMATION AND MATURATION OF SELECTIVE AUTOPHAGOSOMES IN PLANT CELLS

Where and how selective autophagosomes are initiated in the plant cell is still not clear. Hypothetically, the autophagy machinery could be recruited on the cargo by the receptor-Atg8 complex to promote phagophore nucleation. The elongated double membrane could then close and engulf the cargo. Alternatively, the receptor-cargo complex could recruit a preformed phagophore/initial membrane (**Figure 2A**). The latter supposes the presence of preformed phagophores, which are probably initiated to sustain basic non-specific autophagy (Liu and Bassham, 2012). Autophagosomes can be rapidly induced in the cell; therefore, the cell must have the capacity to mobilize a substantial amount of membrane to create these double membrane structures (Lamb et al., 2013). Many studies in mammalian cells and in yeast to some extent favor the ER and ER-mitochondrial contact sites as the most common origin of autophagosomal membranes, although other evidence suggests that several cellular compartments including the Golgi, the plasma membrane, endosome, and mitochondria contribute to the expansion of the nascent phagophore (Lamb et al., 2013; Puri et al., 2013). Recent molecular evidence also points to the ER as the structure initiating autophagosomes in the plant cell (Zhuang et al., 2013). ER-bound selective autophagy receptors such ATI1 and ATI2 could nucleate the formation of specialized autophagosomes

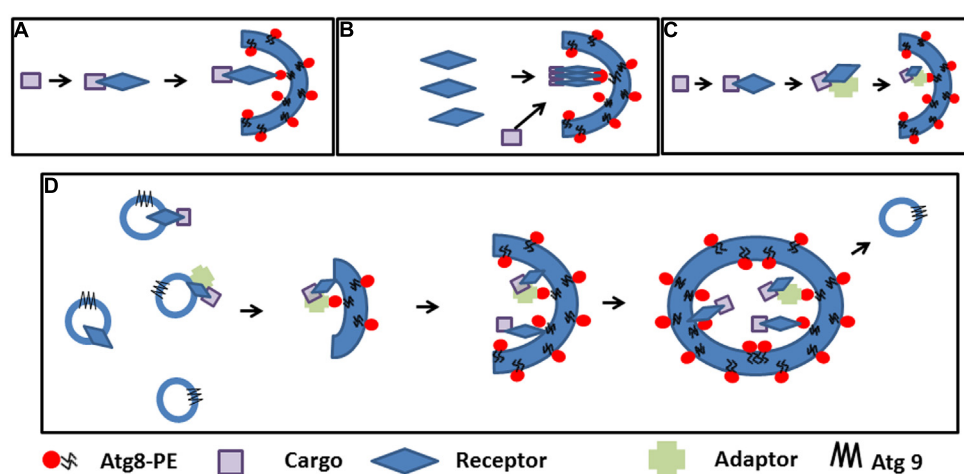


**FIGURE 2 | Cargo selection and speculative autophagosome formation during selective autophagy.** **(A)** The cargo is recognized by the receptor and the complex recruits pre-existing phagophores by receptor-Atg8 interaction. **(B)** First polymeric autophagy receptors are recruited in the phagophore through Atg8 interaction followed by the cargo. **(C)** The cargo is recognized by the receptor and the complex

binds an adaptor before recruiting pre-existing phagophores through Atg8 interactions. **(D)** Interaction between the receptor, the cargo (with or without an adaptor protein) nucleates the initiation of the phagophore and recruit the autophagy machinery; elongation of the phagophore and concentration of the cargo is achieved through Atg9-containing cycling vesicles

after interacting with Atg8-PE and contributing to the assembly of molecular platforms on which the selective autophagosomes are formed. In yeast, Atg8-PE conjugation to various membranes occurs constantly and independently of autophagy-inducing stimuli (Kirisako et al., 2000; Nair et al., 2012). Recent evidence suggests that Atg-family members recruited by selective autophagy receptors to the cargo directly engage regulatory and core autophagy proteins, potentially priming the site of autophagosome formation (Rogov et al., 2014). Concentration of the cargo may require oligomerization of the receptor, and adaptor or scaffold protein-containing AIM may help bridge the complex to membrane-bound Atg8 (**Figures 2B,C**). The elongation step is then regulated in part by cycling Atg9-containing vesicles that supply the required membrane lipids, but also additional receptor-cargo complexes and regulatory components (Lamb et al., 2013; **Figure 2D**). The subcellular localization and trafficking of the polytopic membrane protein Atg9 are not yet known in plants. It is tempting to speculate that membrane bound receptors such as AtTSPO linked to their cargo could be enriched in the autophagosomal membrane through vesicular transport mediated by Atg9.

## CONCLUDING REMARKS AND PERSPECTIVES

The repertoire of targets for selective autophagy is expanding quite fast, and so is the list of individual cognate receptor/adaptor involved in their recognition. The mechanism of recognition involves specific ligands (such as ubiquitin or others) or structural patterns on the target. The receptor proteins characterized so far suggest non-overlapping roles of the cargo receptors for the same target and an intriguing lack of evolutionary conservation, complicating the *in silico* search for potential candidates. A functional AIM is not an indication of potential cargo receptor function, as a plethora of proteins including autophagic substrates and regulators contain AIMs. Some cargo receptors also contain functional atypical AIM/LIR without the canonical aromatic residue (von Muhlinen et al., 2012). In addition, Atg5 plays a crucial role in selective autophagosome formation and Atg5-binding proteins are emerging selective autophagy receptors.

## ACKNOWLEDGMENTS

We apologize to colleagues whose work could not be cited herein because of space limitation. This work was supported by the Belgian National Fund for Scientific Research (FNRS) and the “Communauté française de Belgique-ACTIONS de Recherche Concertées.” Henri Batoko is a research associate of the FNRS.

## REFERENCES

- Behrends, C., Sowa, M. E., Gygi, S. P., and Harper, J. W. (2010). Network organization of the human autophagy system. *Nature* 466, 68–76. doi: 10.1038/nature09204
- Birgisdottir, Á. B., Lamark, T., and Johansen, T. (2013). The LIR motif – crucial for selective autophagy. *J. Cell Sci.* 126, 3237–3247. doi: 10.1242/jcs.126128
- Crotzer, V. L., and Blum, J. S. (2009). Autophagy and its role in MHC-mediated antigen presentation. *J. Immunol.* 182, 3335–3341. doi: 10.4049/jimmunol.0803458
- Cuervo, A. M., and Wong, E. (2014). Chaperone-mediated autophagy: roles in disease and aging. *Cell Res.* 24, 92–104. doi: 10.1038/cr.2013.153
- De Duve, C., and Wattiaux, R. (1966). Functions of lysosomes. *Annu. Rev. Physiol.* 28, 435–492. doi: 10.1146/annurev.ph.28.030166.002251
- Farmer, L. M., Rinaldi, M. A., Young, P. G., Danan, C. H., Burkhardt, S. E., and Bartel, B. (2013). Disrupting autophagy restores peroxisome function to an *Arabidopsis* lon2 mutant and reveals a role for the LON2 protease in peroxisomal matrix protein degradation. *Plant Cell* 25, 4085–4100. doi: 10.1105/tpc.113.113407
- Farré, J. C., Burkenroad, A., Burnett, S. F., and Subramani, S. (2013). Phosphorylation of mitophagy and pexophagy receptors coordinates their interaction with Atg8 and Atg11. *EMBO Rep.* 14, 441–449. doi: 10.1038/embor.2013.40
- Farré, J. C., Manjithaya, R., Mathewson, R. D., and Subramani, S. (2008). PpAtg30 tags peroxisomes for turnover by selective autophagy. *Dev. Cell* 14, 365–376. doi: 10.1016/j.devcel.2007.12.011
- Feng, Y., He, D., Yao, Z., and Klionsky, D. J. (2014). The machinery of macroautophagy. *Cell Res.* 24, 24–41. doi: 10.1038/cr.2013.168
- Gibbings, D., Mostowy, S., Jay, F., Schwab, Y., Cossart, P., and Voinnet, O. (2012). Selective autophagy degrades DICER and AGO2 and regulates miRNA activity. *Nat. Cell Biol.* 14, 1314–1321. doi: 10.1038/ncb2611
- Guillaumot, D., Guillou, S., Deplanque, T., Vanhee, C., Gumi, C., Masquelier, D., et al. (2009). The *Arabidopsis* TSPO-related protein is a stress and abscisic acid-regulated, endoplasmic reticulum-Golgi-localized membrane protein. *Plant J.* 60, 242–256. doi: 10.1111/j.1365-313X.2009.03950.x
- Gump, J. M., Staskiewicz, L., Morgan, M. J., Banberg, A., Riches, D. W. H., and Thorburn, A. (2013). Autophagy variation within a cell population determines cell fate through selective degradation of Fap-1. *Nat. Cell Biol.* 16, 47–54. doi: 10.1038/ncb2886
- Hackenberg, T., Juul, T., Auzina, A., Gwizdz, S., Malolepszy, A., Van Der Kelen, K., et al. (2013). Catalase and NO CATALASE ACTIVITY1 promote autophagy-dependent cell death in *Arabidopsis*. *Plant Cell* 25, 4616–4626. doi: 10.1105/tpc.113.117192
- Honig, A., Avin-Wittenberg, T., Ufaz, S., and Galili, G. (2012). A new type of compartment, defined by plant-specific Atg8-interacting proteins, is induced upon exposure of *Arabidopsis* plants to carbon starvation. *Plant Cell* 24, 288–303. doi: 10.1105/tpc.111.09312
- Houck, S. A., Ren, H. Y., Madden, V. J., Bonner, J. N., Conlin, M. P., Janovick, J. A., et al. (2014). Quality control autophagy degrades soluble ERAD-resistant conformers of the misfolded membrane protein GnRHR. *Mol. Cell* 54, 166–179. doi: 10.1016/j.molcel.2014.02.025
- Johansen, T., and Lamark, T. (2011). Selective autophagy mediated by autophagic adapter proteins. *Autophagy* 7, 279–296. doi: 10.4161/auto.7.3.14487
- Kanki, T., Wang, K., Cao, Y., Baba, M., and Klionsky, D. J. (2009). Atg32 is a mitochondrial protein that confers selectivity during mitophagy. *Dev. Cell* 17, 98–109. doi: 10.1016/j.devcel.2009.06.014
- Kim, J., Lee, H., Lee, H. N., Kim, S., Shin, K., and Chung, T. (2013). Autophagy-related proteins are required for degradation of peroxisomes in *Arabidopsis* hypocotyls during seedling growth. *Plant Cell* 25, 4956–4966. doi: 10.1105/tpc.113.117960
- Kirisako, T., Ichimura, Y., Okada, H., Kabeya, Y., Mizushima, N., Yoshimori, T., et al. (2000). The reversible modification regulates the membrane-binding state of Apg8/Aut7 essential for autophagy and the cytoplasm to vacuole targeting pathway. *J. Cell Biol.* 151, 263–276. doi: 10.1083/jcb.151.2.263
- Kirkin, V., McEwan, D. G., Novak, I., and Dikic, I. (2009). A role for ubiquitin in selective autophagy. *Mol. Cell* 34, 259–269. doi: 10.1016/j.molcel.2009.04.026
- Klionsky, D. J., Abdalla, F. C., Abieliovich, H., Abraham, R. T., Acevedo-Arozena, A., Adeli, K., et al. (2012). Guidelines for the use and interpretation of assays for monitoring autophagy. *Autophagy* 8, 445–544. doi: 10.4161/auto.19496
- Klionsky, D. J., Cregg, J. M., Dunn, W. A. Jr., Emr, S. D., Sakai, Y., Sandoval, I. V., et al. (2003). A unified nomenclature for yeast autophagy-related genes. *Dev. Cell* 5, 539–545. doi: 10.1016/S1534-5807(03)00296-X
- Klionsky, D. J., Cueva, R., and Yaver, D. S. (1992). Aminopeptidase I of *Saccharomyces cerevisiae* is localized to the vacuole independent of the secretory pathway. *J. Cell Biol.* 119, 287–299. doi: 10.1083/jcb.119.2.287
- Korac, J., Schaeffer, V., Kovacevic, I., Clement, A. M., Jungblut, B., Behl, C., et al. (2013). Ubiquitin-independent function of optineurin in autophagic clearance of protein aggregates. *J. Cell Sci.* 126, 580–592. doi: 10.1242/jcs.114926
- Lamb, C. A., Yoshimori, T., and Tooze, S. A. (2013). The autophagosome: origins unknown, biogenesis complex. *Nat. Rev. Mol. Cell Biol.* 14, 759–774. doi: 10.1038/nrm3696

- Levine, B., Mizushima, N., and Virgin, H. W. (2011). Autophagy in immunity and inflammation. *Nature* 469, 323–335. doi: 10.1038/nature09782
- Li, F., Chung, T., and Vierstra, R. D. (2014). AUTOPHAGY-RELATED11 plays a critical role in general autophagy- and senescence-induced mitophagy in *Arabidopsis*. *Plant Cell* 26, 788–807. doi: 10.1105/tpc.113.120014
- Liu, Y., and Bassham, D. C. (2012). Autophagy: pathways for self-eating in plant cells. *Annu. Rev. Plant Biol.* 63, 215–237. doi: 10.1146/annurev-arplant-042811-105441
- Liu, Y., Burgos, J. S., Deng, Y., Srivastava, R., Howell, S. H., and Bassham, D. C. (2012a). Degradation of the endoplasmic reticulum by autophagy during endoplasmic reticulum stress in *Arabidopsis*. *Plant Cell* 24, 4635–4651. doi: 10.1105/tpc.112.101535
- Liu, L., Feng, D., Chen, G., Chen, M., Zheng, Q., Song, P., et al. (2012b). Mitochondrial outer-membrane protein FUNDC1 mediates hypoxia-induced mitophagy in mammalian cells. *Nat. Cell Biol.* 14, 177–185. doi: 10.1038/ncb2422
- Lynch-Day, M. A., and Klionsky, D. J. (2010). The Cvt pathway as a model for selective autophagy. *FEBS Lett.* 584, 1359–1366. doi: 10.1016/j.febslet.2010.02.013
- Mancias, J. D., Wang, X., Gygi, S. P., Harper, J. W., and Kimmelman, A. C. (2014). Quantitative proteomics identifies NCOA4 as the cargo receptor mediating ferritinophagy. *Nature* 7498, 105–109. doi: 10.1038/nature13148
- McLellan, G.-L., Soubannier, V., Chen, C. X., McBride, H. M., and Fon, E. A. (2014). Parkin and PINK1 function in a vesicular trafficking pathway regulating mitochondrial quality control. *EMBO J.* 33, 282–295. doi: 10.1002/embo.201385902
- Mizushima, N., Yoshimori, T., and Ohsumi, Y. (2011). The role of Atg proteins in autophagosome formation. *Annu. Rev. Cell Dev. Biol.* 27, 107–132. doi: 10.1146/annurev-cellbio-092910-154005
- Nair, U., Yen, W. L., Mari, M., Cao, Y., Xie, Z., Baba, M., et al. (2012). A role for Atg8-PE deconjugation in autophagosome biogenesis. *Autophagy* 8, 780–793. doi: 10.4161/auto.19385
- Noda, N. N., Kumeta, H., Nakatogawa, H., Satoo, K., Adachi, W., Ishii, J., et al. (2008). Structural basis of target recognition by Atg8/LC3 during selective autophagy. *Genes Cells* 13, 1211–1218. doi: 10.1111/j.1365-2443.2008.01238.x
- Okamoto, K., Kondo-Okamoto, N., and Ohsumi, Y. (2009). Mitochondria-anchored receptor Atg32 mediates degradation of mitochondria via selective autophagy. *Dev. Cell* 17, 87–97. doi: 10.1016/j.devcel.2009.06.013
- Pankiv, S., Clausen, T. H., Lamark, T., Brech, A., Bruun, J. A., Outzen, H., et al. (2007). p62/SQSTM1 binds directly to Atg8/LC3 to facilitate degradation of ubiquitinated protein aggregates by autophagy. *J. Biol. Chem.* 282, 24131–24145. doi: 10.1074/jbc.M702824200
- Puri, C., Renna, M., Bento, C. F., Moreau, K., and Rubinsztein, D. C. (2013). Diverse autophagosome membrane sources coalesce in recycling endosomes. *Cell* 154, 1285–1299. doi: 10.1016/j.cell.2013.08.044
- Rogov, V., Dötsch, V., Johansen, T., and Kirkin, V. (2014). Interactions between autophagy receptors and ubiquitin-like proteins form the molecular basis for selective autophagy. *Mol. Cell* 53, 167–178. doi: 10.1016/j.molcel.2013.12.014
- Sandoval, H., Thiagarajan, P., Dasgupta, S. K., Schumacher, A., Prchal, J. T., Chen, M., et al. (2008). Essential role for Nix in autophagic maturation of erythroid cells. *Nature* 454, 232–235. doi: 10.1038/nature07006
- Severance, S., and Hamza, I. (2009). Trafficking of heme and porphyrins in metazoa. *Chem. Rev.* 109, 4596–4616. doi: 10.1021/cr9001116
- Shibata, M., Oikawa, K., Yoshimoto, K., Kondo, M., Mano, S., Yamada, K., et al. (2013). Highly oxidized peroxisomes are selectively degraded via autophagy in *Arabidopsis*. *Plant Cell* 25, 4967–4983. doi: 10.1105/tpc.113.116947
- Soubannier, V., Rippstein, P., Kaufman, B. A., Shoubridge, E. A., and McBride, H. M. (2012). Reconstitution of mitochondria derived vesicle formation demonstrates selective enrichment of oxidized cargo. *PLoS ONE* 7:e52830. doi: 10.1371/journal.pone.0052830
- Svenning, S., Lamark, T., Krause, K., and Johansen, T. (2011). Plant NBR1 is a selective autophagy substrate and a functional hybrid of the mammalian autophagic adapters NBR1 and p62/SQSTM1. *Autophagy* 7, 993–1010. doi: 10.4161/auto.7.9.16389
- Thumm, M., Egner, R., Koch, B., Schlumpberger, M., Straub, M., Veenhuis, M., et al. (1994). Isolation of autophagocytosis mutants of *Saccharomyces cerevisiae*. *FEBS Lett.* 349, 275–280. doi: 10.1016/0014-5793(94)00672-5
- Vanhee, C., Zapotocny, G., Masquelier, D., Ghislain, M., and Batoko, H. (2011). The *Arabidopsis* multistress regulator TSPO is a heme binding membrane protein and a potential scavenger of porphyrins via an autophagy-dependent degradation mechanism. *Plant Cell* 23, 785–805. doi: 10.1105/tpc.110.081570
- von Muhlinen, N., Akutsu, M., Ravenhill, B. J., Foeglein, Å., Bloor, S., Rutherford, T. J., et al. (2012). LC3C, bound selectively by a noncanonical LIR motif in NDP52, is required for antibacterial autophagy. *Mol. Cell* 48, 329–342. doi: 10.1016/j.molcel.2012.08.024
- Yorimitsu, T., and Klionsky, D. J. (2005). Autophagy: molecular machinery for self-eating. *Cell Death Differ.* 12, 1542–1552. doi: 10.1038/sj.cdd.4401765
- Yoshimoto, K., Shibata, M., Kondo, M., Oikawa, K., Sato, M., Toyooka, K., et al. (2014). Organ-specific quality control of plant peroxisomes is mediated by autophagy. *J. Cell Sci.* 127, 1161–1168. doi: 10.1242/jcs.139709
- Youle, R. J., and Narendra, D. P. (2011). Mechanisms of mitophagy. *Nat. Rev. Mol. Cell Biol.* 12, 9–14. doi: 10.1038/nrm3028
- Yu, L., Wan, F., Dutta, S., Welsh, S., Liu, Z., Freundt, E., et al. (2006). Autophagic programmed cell death by selective catalase degradation. *Proc. Natl. Acad. Sci. U.S.A.* 103, 4952–4957. doi: 10.1073/pnas.0511288103
- Zientara-Rytter, K., Lukomska, J., Moniuszko, G., Gwozdecki, R., Surowiecki, P., Lewandowska, M., et al. (2011). Identification and functional analysis of Joka2, a tobacco member of the family of selective autophagy cargo receptors. *Autophagy* 7, 1145–1158. doi: 10.4161/auto.7.10.16617
- Zhang, J., Loyd, M. R., Randall, M. S., Waddell, M. B., Kriwacki, R. W., and Ney, P. A. (2012). A short linear motif in BNIP3L (NIX) mediates mitochondrial clearance in reticulocytes. *Autophagy* 8, 1325–1332. doi: 10.4161/auto.20764
- Zhou, J., Wang, J., Cheng, Y., Chi, Y.-J., Fan, B., Yu, J.-Q., et al. (2013). NBR1-mediated selective autophagy targets insoluble ubiquitinylated protein aggregates in plant stress responses. *PLoS Genet.* 9:e1003196. doi: 10.1371/journal.pgen.1003196
- Zhuang, X., Wang, H., Lam, S. K., Gao, C., Wang, X., Cai, Y., et al. (2013). A BAR-domain protein SH3P2, which binds to phosphatidylinositol 3-phosphate and ATG8, regulates autophagosome formation in *Arabidopsis*. *Plant Cell* 25, 4596–4615. doi: 10.1105/tpc.113.118307

**Conflict of Interest Statement:** The authors declare that the research was conducted in the absence of any commercial or financial relationship that could be construed as a potential conflict of interest.

*Received: 29 April 2014; paper pending published: 13 May 2014; accepted: 10 June 2014; published online: 25 June 2014.*

*Citation: Veljanovski V and Batoko H (2014) Selective autophagy of non-ubiquitylated targets in plants: looking for cognate receptor/adaptor proteins. Front. Plant Sci. 5:308. doi: 10.3389/fpls.2014.00308*

*This article was submitted to Plant Cell Biology, a section of the journal Frontiers in Plant Science.*

*Copyright © 2014 Veljanovski and Batoko. This is an open-access article distributed under the terms of the Creative Commons Attribution License (CC BY). The use, distribution or reproduction in other forums is permitted, provided the original author(s) or licensor are credited and that the original publication in this journal is cited, in accordance with accepted academic practice. No use, distribution or reproduction is permitted which does not comply with these terms.*



# When RNA and protein degradation pathways meet

**Benoît Derrien<sup>1</sup> and Pascal Genschik<sup>1,2 \*</sup>**

<sup>1</sup> Centre National de la Recherche Scientifique, Institut de Biologie Moléculaire des Plantes, Unité Propre de Recherche 2357, Conventionné avec l'Université de Strasbourg, Strasbourg, France

<sup>2</sup> Laboratoire de Biochimie et Physiologie Moléculaire des Plantes, Institut de Biologie Intégrative des Plantes 'Claude Grignon', UMR CNRS/INRA/SupAgro/UM2, Montpellier Cedex, France

**Edited by:**

Jose Luis Crespo, Consejo Superior de Investigaciones Científicas, Spain

**Reviewed by:**

Christian Luschnig, University of Natural Resources and Life Sciences, Austria

Sergey Morozov, Moscow State University, Russia

**\*Correspondence:**

Pascal Genschik, Centre National de la Recherche Scientifique, Institut de Biologie Moléculaire des Plantes, Unité Propre de Recherche 2357, Conventionné avec l'Université de Strasbourg, 67084 Strasbourg, France  
e-mail: pascal.genschik@ibmp-cnrs.unistra.fr

RNA silencing has become a major focus of molecular and biomedical research in the last decade. This mechanism, which is conserved in most eukaryotes, has been extensively studied and is associated to various pathways implicated in the regulation of development, in the control of transposition events, heterochromatin maintenance and also playing a role in defense against viruses. Despite of its importance, the regulation of the RNA silencing machinery itself remains still poorly explored. Recently several reports in both plants and metazoans revealed that key components of RNA silencing, such as RNA-induced silencing complex component ARGONAUTE proteins, but also the endonuclease Dicer are subjected to proteasomal and autophagic pathways. Here we will review these post-translational proteolytic regulations with a special emphasis on plant research and also discuss their functional relevance.

**Keywords:** RNA silencing, RISC, ubiquitin, autophagy, virus, proteasome

## A GLIMPSE IN THE RNA SILENCING PATHWAYS

RNA silencing involves processing of double stranded (dsRNA) by the enzyme Dicer, into small RNAs, 21–25 nucleotides in length called small interfering RNAs (siRNAs; reviewed in (Ghildiyal and Zamore, 2009; Voinnet, 2009; Krol et al., 2010)). One of the two strands of each RNA fragment is then incorporated into a protein complex called RNA induced silencing complex (RISC) that invariably contains a member of the highly conserved ARGONAUTE protein (AGO) family. Once integrated into the RISC, siRNAs will base-pair to their target mRNA and induce their cleavage. The process of RNA interference (RNAi) is widely used for functional genomics and has also practical applications in therapeutics and agriculture. Most importantly, RNA silencing mediates resistance to exogenous pathogenic nucleic acids. Thus, important functions for small RNAs have emerged in the study of host-pathogen interactions and the most compelling illustration of the role of RNA silencing in defense is provided in the case of viral infections in plants, invertebrates and also more recently mammals, where populations of siRNAs are produced in infected cells directly by processing dsRNA molecules derived from the viral genome (Ding, 2010; Maillard et al., 2013). These viral-derived siRNAs are then incorporated into an antiviral RISC and turned back onto viral RNAs to trigger their degradation.

RNA silencing also regulates the expression of protein-coding genes. In this process, an important source of endogenous dsRNAs are primary transcripts of RNA-coding genes called pri-miRNAs which are processed, in the nucleus of metazoan cells, to 70-nucleotide stem-loop pre-miRNAs by the RNase III enzyme Drosha (Siomi and Siomi, 2010). After their export to the cytoplasm, pre-microRNAs are further processed via Dicer

or Dicer-like (DCL) enzymes to produce miRNA duplexes. Plant genomes do not encode Drosha homologs, and all miRNA biogenesis steps at least in *Arabidopsis* are carried out by one of the four DCL proteins (Rogers and Chen, 2013). The microRNA (miRNA) duplex is separated, and one strand is selected as the 21-nucleotide mature miRNAs, whereas the other strand is degraded. Mature miRNAs are integrated into RISC complexes that repress the expression of one or more target mRNAs with complementary sequence by inhibiting mRNA translation or inducing their degradation. Thus miRNAs are predicted to regulate the expression of hundreds of mRNAs suggesting that they can regulate a significant proportion of the transcriptome (Leung and Sharp, 2010). Notably it has recently been shown that miRNAs are also subjected to turnover through degradation mechanisms implying both 3'-5' and 5'-3' exoribonucleases, adding another layer of complexity (Ramachandran and Chen, 2008; Chatterjee and Grosshans, 2009; Ruegger and Grosshans, 2012).

## REGULATION OF THE RNA SILENCING MACHINERY BY AUTOPHAGY

While the biogenesis and the function of small RNAs have been extensively studied in various biological processes across many organisms, less attention was paid on the regulation of the RNA silencing machinery itself. As indicated above, AGOs are core components of the RISC (Hutvágner and Simard, 2008; Vaucheret, 2008; Voinnet, 2009). These proteins have undergone a high degree of gene duplication in metazoans and plants, counting 8 and 10 genes in humans and *Arabidopsis*, respectively. Genetic and biochemical analyses revealed that *Arabidopsis* AGO1 plays a central role in both miRNA and si-mediated RNA silencing (Mi et al., 2008; Takeda et al., 2008). Based on its key role as effectors

in RNA silencing, it is expected that AGO1 protein abundance must be strictly regulated, most likely at multiple levels. Hence, either an increase or a decrease in AGO1 protein content leads to significant effects on plant development (Vaucheret et al., 2004, 2006). The most studied and best-understood mechanism controlling AGO1 homeostasis is its negative regulation by miRNA168 (Vaucheret et al., 2006; Mallory and Vaucheret, 2009). In this pathway, the miRNA miR168 represses AGO1 transcript in an AGO1-dependant manner. Besides AGO1, other elements of the RNA silencing machinery, like DCL1 or AGO2 are also regulated via specific miRNAs, respectively, miR162 and miR403 (Xie et al., 2003; Allen et al., 2005). However, it became evident that AGO1 is also regulated at the post-translational level and in particular at the level of its stability.

The first evidence of selective AGO1 protein turnover was in the context of plant-viral interactions. *Arabidopsis* AGO1 is not only involved in the miRNA pathway, but together with AGO2 mediates antiviral defense (Alvarado and Scholthof, 2011). As a counter defense, viruses have elaborated various strategies to avoid silencing by expressing Viral Suppressors of RNA silencing (VSRs) proteins (Pumplin and Voinnet, 2013). Interestingly, it was found that certain VSRs, called P0 proteins from Poleroviruses, promote the degradation of AGO1 and thus presumably could impair RNA-based anti-viral immunity (Baumberger et al., 2007; Bortolamiol et al., 2007). This mechanism is conserved and was extended to VSRs of other viruses (Chiu et al., 2010; Fusaro et al., 2012). Interestingly, it was shown that P0 acts upstream of AGO1 loading and thus would prevent the formation of RISC (Csorba et al., 2010). This is supported by the fact that newly synthesized AGO1 after transient expression in tobacco leaves is subjected to P0-mediated destruction while endogenous AGO1 pre-assembled complex is P0-resistant. At the molecular level, viral P0 VSRs encode F-box proteins (Pazhouhandeh et al., 2006) that hijack the host SKP1-Cullin1-F-box protein (SCF) ubiquitin-protein ligase (E3) to promote ubiquitylation, which serves as a signal for degradation. This post-translational modification (PTM) regulates a broad range of physiologically and developmentally controlled processes in all eukaryotes (Ciechanover et al., 2000; Smalle and Vierstra, 2004). Because ubiquitylation of target proteins by SCF-type complexes most often leads to their proteasomal degradation, it was a surprise to find that the degradation of AGO1 by P0 was insensitive to inhibition of the proteasome (Baumberger et al., 2007). The mystery of AGO1 degradation pathway by the SCF<sup>P0</sup> E3 ligase was, however, solved when it was reported that this process is mediated by autophagy (Derrien et al., 2012). Although recent studies already indicate a function of ubiquitylation in autophagy (McEwan and Dikic, 2011), this finding was nevertheless intriguing with respect to the presumed high selectivity of the P0-mediated ubiquitylation process, as degradation by autophagy is generally believed to be unspecific, even taking into account “selective autophagy” destroying protein aggregates and organelles.

Because viruses usually hijack host cell machineries, it was conceivable that AGO1 protein turnover by autophagy may also occur in a P0-independent context. Hence, this prediction was confirmed when it was shown that mutations affecting

miRNA biogenesis and/or accumulation and thus disturbing RISC assembly, also result in AGO1 degradation by autophagy (Derrien et al., 2012). This finding, however, raises the question of which is the endogenous ubiquitin-protein ligase (E3) that promotes ubiquitylation of AGO1 in a non-viral context. Notably *Arabidopsis* genome encodes several classes of E3s that are the key factors defining substrate specificity and among them more than 700 hundred F-box proteins (Vierstra, 2009). One good candidate to fulfill such a function is the *Arabidopsis* F-box protein FBW2 (Earley et al., 2010). FBW2 was identified by a genetic suppressor screen of a null allele of SQUINT (SQN), encoding a Cyclophilin-40 chaperon, a positive regulator of AGO1 activity. While FBW2 loss-of-function mutants do not exhibit an increase in AGO1 protein level, most likely because of the miR168-dependent feedback mechanism regulating AGO1 expression (Vaucheret et al., 2006), FBW2 overexpression significantly reduces AGO1 protein content (Earley et al., 2010). Interestingly, the proteasome inhibitor MG132 was also unable to block the FBW2-mediated degradation of AGO1, a situation reminiscent to the viral SCF<sup>P0</sup> complex. At present it remains unclear whether FBW2 mediates AGO1 destruction by autophagy similarly to viral P0 (**Figure 1**), with which FBW2 does not share any significant sequence similarity beside an F-box motif.

Notably AGO1 is not the only *Arabidopsis* AGO so tightly regulated at the post-translational level. Thus, at least in transient expression assays in tobacco leaves, P0 is also able to mediate the degradation of AGO2, AGO4-6, and AGO9 (Baumberger et al., 2007). Whether those AGOs are targeted by the endogenous SCF<sup>FBW2</sup> is presently unknown, thought some of them have already been identified as ubiquitylated by proteomic approaches (Maor et al., 2007; Kim et al., 2013).

Is autophagy-mediated regulation of AGO proteins specific to the green lineage? The answer is no and several findings suggest that the fate of the animal RNA silencing machinery shares some striking similarities with plants. Previous studies already reported that in mammals, AGO proteins are regulated at the post-translational level. For instance, in human cells, AGO2 (the only mammalian AGO producing RNA cleavage) is both hydroxylated and phosphorylated (Qi et al., 2008; Zeng et al., 2008). In particular hydroxylation was shown to influence both AGO2 subcellular localisation and stability, although the biological significance of this modification is still unclear.

Significant molecular insights on the post-translational control of metazoan AGO proteins emerged only recently. First it has been shown that the molecular chaperone HSP90 is required for the stability of mammalian AGO1 and AGO2 (Johnston et al., 2010). Thus inhibition of HSP90 function by geldanamycin triggered the degradation of both AGOs, an effect that could be alleviated, at least partially, by the proteasome inhibitor MG132. Interestingly, HSP90 does not bind AGO2 complexes that contain miRNAs and was therefore proposed to act upstream of RISC action indicating already that it is RNA-free AGO2 that is degraded in this pathway (Johnston et al., 2010). However, the first ubiquitin E3 ligase proposed to control mammalian AGO2 stability was the mouse Trim domain containing protein mLIN41 (Rybak et al., 2009). This protein is preferentially expressed in

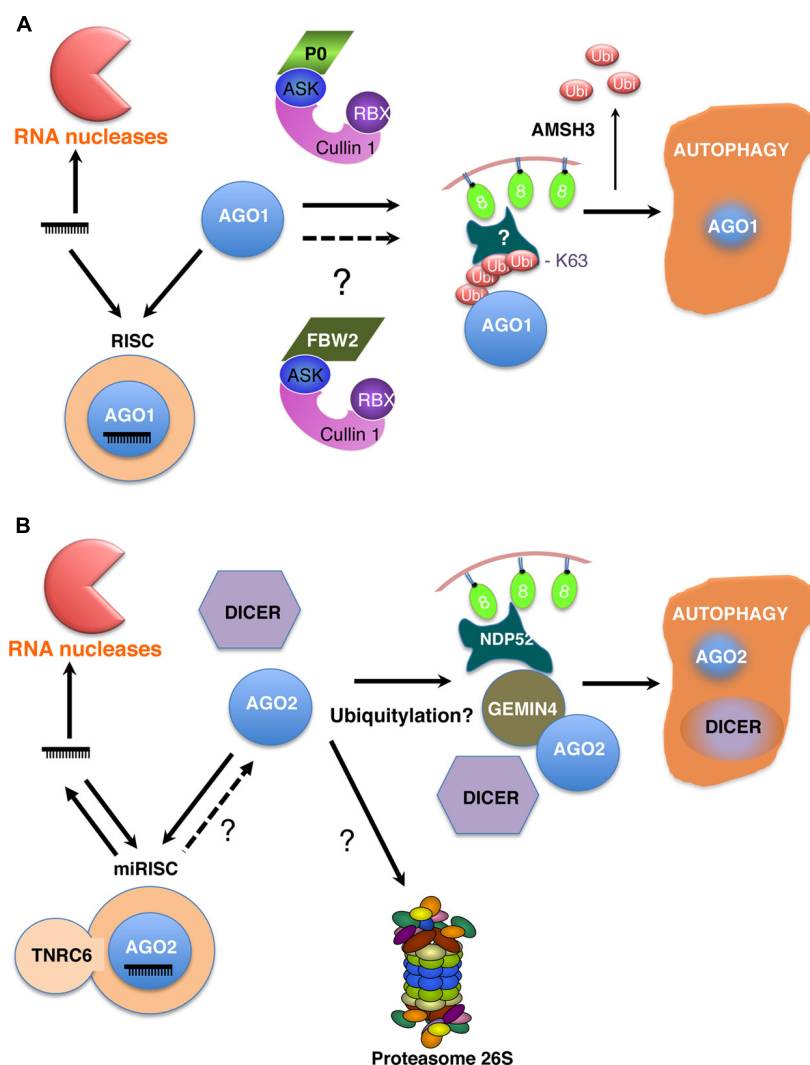


**FIGURE 1 | Models for the turnover of AGO proteins in *Arabidopsis* (A) and mammalian cells (B).** Different levels of regulation operate on the homeostasis of RISCs. First, the steady-state levels of microRNAs are regulated by degradation processes involving different ribonucleases (RNases) acting either 3'-5' or 5'-3'. Thus microRNAs most likely are in competition for AGO binding. Recent evidences essentially from metazoans indicate that at least some microRNAs can be released from RISCs, explaining their short half-lives. However, not only microRNAs but also AGO proteins are degraded. Thus in both plants and animal cells, it is now clearly established that AGO proteins are degraded by autophagy in an RNA free form prior RISC assembly. This mechanism also co-degrades other

components of the silencing machinery such as DICER in mammals (B). In *Arabidopsis*, the polerovirus protein P0 assembles an SCF<sup>P0</sup> ubiquitin ligase to ubiquitylate AGO1 or an AGO1 associated protein (A). Viral P0-mediated AGO1 degradation by autophagy also requires the deubiquitylating enzyme AMSH3. However, the identity of endogenous ubiquitin ligases involved in this process have not yet been unambiguously identified. The role of ubiquitylation in the turnover of human AGO2 is at present unclear but requires GEMIN4 and NDP52 (B). Finally, whether upon guide RNA dissociation AGO2 would become accessible to autophagy and the role of the proteasome in AGOs degradation are other still open questions.

several stem cell niches and participates in the control of stem cell maintenance. mLin41 physically interacts with AGO2 through its coiled-coil domain and promotes AGO2 ubiquitylation *in vitro* and *in vivo* through its RING and B-Box domains, all located in the Trim domain. Moreover, the ectopic overexpression of mLin41 reduced the level of endogenous Ago2 in embryonic carcinoma cells and this effect was attenuated by inhibition of the proteasome with MG132. However, more recent studies put into question the control of AGO2 stability by mLin41 (Chang et al., 2012; Chen et al., 2012). In particular, it was shown that

mLin41 promotes neuronal progenitor cell maintenance through FGF signaling by ubiquitylation of Shc SH2-binding protein 1 (SHCBP1), but not via the regulation of AGO2 stability (Chen et al., 2012).

While the turnover of AGO2 by the mLin41-proteasome pathway will need further investigations, the degradation of Argonautes proteins by the autophagy pathway turned out to be conserved across kingdoms (Figure 1). Hence it was shown that both DICER and AGO2 levels increased in HeLa cells treated with chemical inhibitors known to block autophagy and in siRNA-depleted

cells for different component of the autophagy pathway, such as ATG5, ATG6, ATG7 or NDP52 (Gibbings et al., 2012). Of particular interest was NDP52, a known autophagy receptor, which confers some cargo selectivity typically by recognizing conjugated ubiquitin (Rogov et al., 2014). At present the mechanism by how NDP52 recognizes AGO2 and DICER is unclear, but GEMIN4, a component of the multi-protein SMN (survival of motor neuron) complex, is required in this process eventually by interacting with both NDP52 and AGO2. Whether AGO2 ubiquitylation is a prerequisite to be directed to autophagy is unknown. In contrast DICER might be recruited by a mechanism independent of GEMIN4. Moreover similar to plant AGO1 decay (Csorba et al., 2010), mammalian AGO2 autophagy-mediated degradation occurs upstream of the formation of miRISC (Gibbings et al., 2012).

This novel paradigm of the post-translational control of the RNA silencing machinery exhibits nevertheless some variations. Hence in *Caenorhabditis elegans*, the Ago homologs ALG-1 and ALG-2 accumulate into aggregates in autophagy mutants only under certain stress conditions and the role of selective autophagy in their regulation under normal physiological conditions is presently unclear (Zhang and Zhang, 2013). Instead, AIN-1, a homolog of mammalian GW182/TNRC6 that interacts with AGO and mediates silencing, is clearly degraded by autophagy (Zhang and Zhang, 2013). AIN-1 colocalizes with SQST-1, the homolog of mammalian p62 that acts as a receptor for autophagic degradation of ubiquitylated protein aggregates and also directly interacts with Atg8/LC3 contributing to cargo specificity. This mechanism seems also to involve EPG-7 a scaffold protein linking cargo-receptor complexes with the autophagic assembly machinery (Lin et al., 2013). The putative role of ubiquitylation in the mechanism of AIN-1 destruction will nevertheless need further investigations.

## SOME PERSPECTIVES

It is clear that more work is required to better understand post-translational regulations of AGOs in both plants and metazoans. Moreover in plants, it will also be important to characterize the different protein complexes containing AGOs and their subcellular locations. We already know that plant AGO1 is present in both low and high molecular protein complexes that co-fractionate with small RNAs (Baumberger and Baulcombe, 2005; Qi et al., 2005; Csorba et al., 2010). Whether these multi-protein complexes resemble those identified in mammals (Filipowicz et al., 2008) remains, however, to be established. Moreover, evidence of two distinct cellular pools of AGO1 (siRNA versus miRNA loaded AGO1) RISCs was also recently established (Schott et al., 2012). In addition, in *Arabidopsis*, at least a fraction of AGO1 is also associated to membranes and isoprenoid biosynthesis which is important for membrane protein localization and trafficking, is required for miRNA function (Brodersen et al., 2012). Mammalian AGO2 was already known to bind to cellular membranes, most likely as a component of RISC (Cikaluk et al., 1999). AGO proteins are therefore present in cells as various pools representing likely different functional states. How are these different AGO protein pools regulated at the post-translational level and what is the impact of these regulations on RNAi function are major questions that will have to be solved.

Concerning the process of AGOs degradation by autophagy, an important issue will be to clarify the role of ubiquitylation. In plants, immunoprecipitation assays revealed an enrichment of polyubiquitin conjugates of AGO1 and/or an AGO1-associated protein and MLN-4924, a drug that inhibits the activity of cullin-RING ubiquitin ligases, impaired P0-dependant AGO1 degradation in *Arabidopsis* (Derrien et al., 2012). In mammals, AGO2 or one of its associated protein was also found ubiquitylated in cells treated with siRNAs to deplete autophagy activity (Gibbings et al., 2012). Notably, ubiquitin contains seven internal lysine residues and all can serve as conjugation sites to build up poly-ubiquitin chains that depending on their topologies can direct the substrate to the 26S proteasome or to the autophagy pathway (Grabbe et al., 2011; McEwan and Dikic, 2011). Therefore future experiments should reveal the identity of endogenous ubiquitin E3 ligases involved in this process, where and how they recognize AGOs or other associated proteins, the topology of the polyubiquitin chains that are generated and how these chains will be selected by the autophagy pathway.

Notably, at present we cannot rule out the possibility that the 26S proteasome also plays important functions in controlling the homeostasis of the RNA silencing machinery, as both proteolytic pathways may coexist, eventually in different cell types or specific developmental contexts. For instance, several studies incriminate the proteasome in controlling the stability of *Drosophila* and mammalian AGO effector proteins (Johnston et al., 2010; Smibert et al., 2013). Also in plants, the silencing suppressor protein P25 of *Potato virus X* (PVX) triggers AGO1 destabilization by the proteasome (Chiu et al., 2010). The mechanism by which this is achieved is unknown, but P25 might recruit a still unknown endogenous ubiquitin ligase complex to achieve such a function. Moreover, the Double-stranded RNA Binding protein (DRB4) that interacts with DCL4, one of the four Dicer-like proteins present in *Arabidopsis*, is also degraded by the proteasome after being recognized by the APC/C (anaphase promoting complex or cyclosome), a master ubiquitin protein ligase that usually targets cell cycle regulatory proteins (Marrocco et al., 2012). Thus to understand the contribution of proteasomal degradation versus the autophagy pathway in fine-tuning components of the RNA silencing machinery needs further investigations, both in metazoans and plants.

Finally, the most interesting question is what could be the physiological function(s) of these proteolytic pathways? The current model indicates that the stability of AGO proteins depends on miRNA biogenesis and thus unloaded AGOs are unstable (Derrien et al., 2012; Martinez and Gregory, 2013; Smibert et al., 2013). If AGO proteins are degraded essentially prior RISC assembly (Csorba et al., 2010; Johnston et al., 2010; Gibbings et al., 2012), the key regulatory step would be at the level of small RNA production that would compete for binding of available AGOs. In such a scenario, the P0 proteins from poleroviruses would destroy AGO1 at an early step to prevent viral siRNAs produced during infection to be incorporated into novel RISCs and this would compromise antiviral RNA silencing. However, what is the fate of AGO proteins once part of small RNA programmed RISCs? In mammals the half-life of Ago2 bound to small RNAs seems rather stable, at least under normal grow conditions (Johnston

et al., 2010). Similarly, a half-life of 2–3 days of AGO1 RISCs was estimated in plants (Csorba et al., 2010). However, recent findings revealed that target RNAs could destabilize the interaction between human Ago2 and their corresponding guide RNAs, indicating that at least some RISCs can be unloaded (De et al., 2013). Such a dynamic loading and unloading mechanism might not only allow reprogramming of Ago2 by novel guide RNAs, but might also expose the protein to cellular degradation machineries such as the autophagy pathway. If this holds true, what would be the functional relevance of this degradation on RISC homeostasis and reprogramming?

## ACKNOWLEDGMENTS

“This work has been published under the framework of the LABEX: ANR-10-LABX-0036\_NETRNA and benefits from a funding from the state managed by the French National Research Agency as part of the Investments for the future program” and from the European Research Council under the European Union’s Seventh Framework Program (FP7/2007-2013)/ERC grant agreement n° [338904].

## REFERENCES

- Allen, E., Xie, Z., Gustafson, A. M., and Carrington, J. C. (2005). microRNA-directed phasing during trans-acting siRNA biogenesis in plants. *Cell* 121, 207–221. doi: 10.1016/j.cell.2005.04.004
- Alvarado, V. Y., and Scholthof, H. B. (2011). AGO2: a new argonaute compromising plant virus accumulation. *Front. Plant Sci.* 2:112. doi: 10.3389/fpls.2011.00112
- Baumberger, N., and Baulcombe, D. C. (2005). *Arabidopsis* ARGONAUTE1 is an RNA slicer that selectively recruits microRNAs and short interfering RNAs. *Proc. Natl. Acad. Sci. U.S.A.* 102, 11928–11933. doi: 10.1073/pnas.0505461102
- Baumberger, N., Tsai, C.-H., Lie, M., Havecker, E., and Baulcombe, D. C. (2007). The *Poлерovirus* silencing suppressor P0 targets ARGONAUTE proteins for degradation. *Curr. Biol.* 17, 1609–1614. doi: 10.1016/j.cub.2007.08.039
- Bortlamoli, D., Pazhouhandeh, M., Marrocco, K., Genschik, P., and Ziegler-Graff, V. (2007). The *Poлерovirus* F box protein P0 targets ARGONAUTE1 to suppress RNA silencing. *Curr. Biol.* 17, 1615–1621. doi: 10.1016/j.cub.2007.07.061
- Brodersen, P., Sakvarelidze-Achard, L., Schaller, H., Khafif, M., Schott, G., Bendahmane, A., et al. (2012). Isoprenoid biosynthesis is required for miRNA function and affects membrane association of ARGONAUTE 1 in *Arabidopsis*. *Proc. Natl. Acad. Sci. U.S.A.* 109, 1778–1783. doi: 10.1073/pnas.1112500109
- Chang, H.-M., Martinez, N. J., Thornton, J. E., Hagan, J. P., Nguyen, K. D., and Gregory, R. I. (2012). Trim71 cooperates with microRNAs to repress Cdkn1a expression and promote embryonic stem cell proliferation. *Nat. Commun.* 3, 923. doi: 10.1038/ncomms1909
- Chatterjee, S., and Grosshans, H. (2009). Active turnover modulates mature microRNA activity in *Caenorhabditis elegans*. *Nature* 461, 546–549. doi: 10.1038/nature08349
- Chen, J., Lai, F., and Niswander, L. (2012). The ubiquitin ligase mLin41 temporally promotes neural progenitor cell maintenance through FGF signaling. *Genes Dev.* 26, 803–815. doi: 10.1101/gad.187641.112
- Chiu, M.-H., Chen, I.-H., Baulcombe, D. C., and Tsai, C.-H. (2010). The silencing suppressor P25 of Potato virus X interacts with Argonaute1 and mediates its degradation through the proteasome pathway. *Mol. Plant Pathol.* 11, 641–649. doi: 10.1111/j.1364-3703.2010.00634.x
- Ciechanover, A., Orian, A., and Schwartz, A. L. (2000). Ubiquitin-mediated proteolysis: biological regulation via destruction. *Bioessays* 22, 442–451. doi: 10.1002/(SICI)1521-1878(200005)22:5<442::AID-BIES6>3.0.CO;2-Q
- Cikaluk, D. E., Tahbaz, N., Hendricks, L. C., DiMattia, G. E., Hansen, D., Pilgrim, D., et al. (1999). GERp95, a membrane-associated protein that belongs to a family of proteins involved in stem cell differentiation. *Mol. Biol. Cell* 10, 3357–3372. doi: 10.1091/mbc.10.10.3357
- Csorba, T., Lózsa, R., Hutvágner, G., and Burgýán, J. (2010). *Poлерovirus* protein P0 prevents the assembly of small RNA-containing RISC complexes and leads to degradation of ARGONAUTE1. *Plant J.* 62, 463–472. doi: 10.1111/j.1365-313X.2010.04163.x
- De, N., Young, L., Lau, P.-W., Meissner, N.-C., Morrissey, D. V., and MacRae, I. J. (2013). Highly complementary target RNAs promote release of guide RNAs from human Argonaute2. *Mol. Cell* 50, 344–355. doi: 10.1016/j.molcel.2013.04.001
- Derrien, B., Baumberger, N., Schepetilnikov, M., Viotti, C., De Cillia, J., Ziegler-Graff, V., et al. (2012). Degradation of the antiviral component ARGONAUTE1 by the autophagy pathway. *Proc. Natl. Acad. Sci. U.S.A.* 109, 15942–15946. doi: 10.1073/pnas.1209487109
- Ding, S.-W. (2010). RNA-based antiviral immunity. *Nat. Rev. Immunol.* 10, 632–644. doi: 10.1038/nri2824
- Earley, K., Smith, M., Weber, R., Gregory, B., and Poethig, R. (2010). An endogenous F-box protein regulates ARGONAUTE1 in *Arabidopsis thaliana*. *Silence* 1, 15. doi: 10.1186/1758-907X-1-15
- Filipowicz, W., Bhattacharyya, S. N., and Sonenberg, N. (2008). Mechanisms of post-transcriptional regulation by microRNAs: are the answers in sight? *Nat. Rev. Genet.* 9, 102–114. doi: 10.1038/nrg2290
- Fusaro, A. F., Correa, R. L., Nakasugi, K., Jackson, C., Kawchuk, L., Vaslin, M. F. S., et al. (2012). The *Enamovirus* P0 protein is a silencing suppressor which inhibits local and systemic RNA silencing through AGO1 degradation. *Virology* 426, 178–187. doi: 10.1016/j.virol.2012.01.026
- Ghildiyal, M., and Zamore, P. D. (2009). Small silencing RNAs: an expanding universe. *Nat. Rev. Genet.* 10, 94–108. doi: 10.1038/nrg2504
- Gibbings, D., Mostowy, S., Jay, F., Schwab, Y., Cossart, P., and Voinnet, O. (2012). Selective autophagy degrades DICER and AGO2 and regulates miRNA activity. *Nat. Cell Biol.* 14, 1314–1321. doi: 10.1038/ncb2611
- Grabbe, C., Husnjak, K., and Dikic, I. (2011). The spatial and temporal organization of ubiquitin networks. *Nat. Rev. Mol. Cell Biol.* 12, 295–307. doi: 10.1038/nrm3099
- Hutvágner, G., and Simard, M. J. (2008). Argonaute proteins: key players in RNA silencing. *Nat. Rev. Mol. Cell Biol.* 9, 22–32. doi: 10.1038/nrm2321
- Johnston, M., Geoffroy, M.-C., Sobala, A., Hay, R., and Hutvágner, G. (2010). HSP90 protein stabilizes unloaded argonaute complexes and microscopic P-bodies in human cells. *Mol. Biol. Cell* 21, 1462–1469. doi: 10.1091/mbc.E09-10-0885
- Kim, D.-Y., Scalf, M., Smith, L. M., and Vierstra, R. D. (2013). Advanced proteomic analyses yield a deep catalog of ubiquitylation targets in *Arabidopsis*. *Plant Cell* 25, 1523–1540. doi: 10.1105/tpc.112.108613
- Krol, J., Loedige, I., and Filipowicz, W. (2010). The widespread regulation of microRNA biogenesis, function and decay. *Nat. Rev. Genet.* 11, 597–610. doi: 10.1038/nrg2843
- Leung, A. K. L., and Sharp, P. A. (2010). MicroRNA functions in stress responses. *Mol. Cell* 40, 205–215. doi: 10.1016/j.molcel.2010.09.027
- Lin, L., Yang, P., Huang, X., Zhang, H., Lu, Q., and Zhang, H. (2013). The scaffold protein EPG-7 links cargo-receptor complexes with the autophagic assembly machinery. *J. Cell Biol.* 201, 113–129. doi: 10.1083/jcb.201209098
- Maillard, P. V., Ciaudo, C., Marchais, A., Li, Y., Jay, F., Ding, S. W., et al. (2013). Antiviral RNA interference in mammalian cells. *Science* 342, 235–238. doi: 10.1126/science.1241930
- Mallory, A. C., and Vaucheret, H. (2009). ARGONAUTE 1 homeostasis invokes the coordinate action of the microRNA and siRNA pathways. *EMBO Rep.* 10, 521–526. doi: 10.1038/embor.2009.32
- Maor, R., Jones, A., Nühse, T. S., Studholme, D. J., Peck, S. C., and Shirasu, K. (2007). Multidimensional protein identification technology (MudPIT) analysis of ubiquitinated proteins in plants. *Mol. Cell Proteomics* 6, 601–610. doi: 10.1074/mcp.M600408-MCP200
- Marrocco, K., Criqui, M.-C., Zervudacki, J., Schott, G., Eisler, H., Parnet, A., et al. (2012). APC/C-mediated degradation of dsRNA-binding protein 4 (DRB4) involved in RNA silencing. *PLoS ONE* 7:e35173. doi: 10.1371/journal.pone.0035173

- Martinez, N. J., and Gregory, R. I. (2013). Argonaute2 expression is post-transcriptionally coupled to microRNA abundance. *RNA* 19, 605–612. doi: 10.1261/rna.036434.112
- McEwan, D. G., and Dikic, I. (2011). The three musketeers of autophagy: phosphorylation, ubiquitylation and acetylation. *Trends Cell Biol.* 21, 195–201. doi: 10.1016/j.tcb.2010.12.006
- Mi, S., Cai, T., Hu, Y., Chen, Y., Hodges, E., Ni, F., et al. (2008). Sorting of small RNAs into *Arabidopsis* argonaute complexes is directed by the 5' terminal nucleotide. *Cell* 133, 116–127. doi: 10.1016/j.cell.2008.02.034
- Pazhouhandeh, M., Dieterle, M., Marrocco, K., Lechner, E., Berry, B., Brault, V., et al. (2006). F-box-like domain in the *Poletovirus* protein P0 is required for silencing suppressor function. *Proc. Natl. Acad. Sci. U.S.A.* 103, 1994–1999. doi: 10.1073/pnas.0510784103
- Pumplin, N., and Voinnet, O. (2013). RNA silencing suppression by plant pathogens: defense, counter-defense and counter-counter-defense. *Nat. Rev. Microbiol.* 11, 745–760. doi: 10.1038/nrmicro3120
- Qi, H. H., Ongusara, P. P., Myllyharju, J., Cheng, D., Pakkanen, O., Shi, Y., et al. (2008). Prolyl 4-hydroxylation regulates Argonaute 2 stability. *Nature* 455, 421–424. doi: 10.1038/nature07186
- Qi, Y., Denli, A. M., and Hannon, G. J. (2005). Biochemical specialization within *Arabidopsis* RNA silencing pathways. *Mol. Cell* 19, 421–428. doi: 10.1016/j.molcel.2005.06.014
- Ramachandran, V., and Chen, X. (2008). Degradation of microRNAs by a family of exoribonucleases in *Arabidopsis*. *Science* 321, 1490–1492. doi: 10.1126/science.1163728
- Rogers, K., and Chen, X. (2013). Biogenesis, turnover, and mode of action of plant microRNAs. *Plant Cell* 25, 2383–2399. doi: 10.1105/tpc.113.113159
- Rogov, V., Dötsch, V., Johansen, T., and Kirkin, V. (2014). Interactions between autophagy receptors and Ubiquitin-like proteins form the molecular basis for selective autophagy. *Mol. Cell* 53, 167–178. doi: 10.1016/j.molcel.2013.12.014
- Rüegger, S., and Grosshans, H. (2012). MicroRNA turnover: when, how, and why. *Trends Biochem. Sci.* 37, 436–446. doi: 10.1016/j.tibs.2012.07.002
- Rybak, A., Fuchs, H., Hadian, K., Smirnova, L., Wulczyn, E. A., Michel, G., et al. (2009). The let-7 target gene mouse lin-41 is a stem cell specific E3 ubiquitin ligase for the miRNA pathway protein Ago2. *Nat. Cell Biol.* 11, 1411–1420. doi: 10.1038/ncb1987
- Schott, G., Mari-Ordonez, A., Himber, C., Alioua, A., Voinnet, O., and Dunoyer, P. (2012). Differential effects of viral silencing suppressors on siRNA and miRNA loading support the existence of two distinct cellular pools of ARGONAUTE1. *EMBO J.* 31, 2553–2565. doi: 10.1038/emboj.2012.92
- Siomi, H., and Siomi, M. C. (2010). Post-transcriptional regulation of microRNA biogenesis in animals. *Mol. Cell* 38, 323–332. doi: 10.1016/j.molcel.2010.03.013
- Smalle, J., and Vierstra, R. D. (2004). The ubiquitin 26S proteasome proteolytic pathway. *Annu. Rev. Plant Biol.* 55, 555–590. doi: 10.1146/annurev.arplant.55.031903.141801
- Smibert, P., Yang, J.-S., Azzam, G., Liu, J.-L., and Lai, E. C. (2013). Homeostatic control of Argonaute stability by microRNA availability. *Nat. Struct. Mol. Biol.* 20, 789–795. doi: 10.1038/nsmb.2606
- Takeda, A., Iwasaki, S., Watanabe, T., Utsumi, M., and Watanabe, Y. (2008). The mechanism selecting the guide strand from small RNA duplexes is different among argonaute proteins. *Plant Cell Physiol.* 49, 493–500. doi: 10.1093/pcp/pcn043
- Vaucheret, H. (2008). Plant ARGONAUTES. *Trends Plant Sci.* 13, 350–358. doi: 10.1016/j.tplants.2008.04.007
- Vaucheret, H., Mallory, A. C., and Bartel, D. P. (2006). AGO1 homeostasis entails coexpression of MIR168 and AGO1 and preferential stabilization of miR168 by AGO1. *Mol. Cell* 22, 129–136. doi: 10.1016/j.molcel.2006.03.011
- Vaucheret, H., Vazquez, F., Crété, P., and Bartel, D. P. (2004). The action of ARGONAUTE1 in the miRNA pathway and its regulation by the miRNA pathway are crucial for plant development. *Genes Dev.* 18, 1187–1197. doi: 10.1101/gad.1201404
- Vierstra, R. D. (2009). The ubiquitin-26S proteasome system at the nexus of plant biology. *Nat. Rev. Mol. Cell Biol.* 10, 385–397. doi: 10.1038/nrm2688
- Voinnet, O. (2009). Origin, biogenesis, and activity of plant microRNAs. *Cell* 136, 669–687. doi: 10.1016/j.cell.2009.01.046
- Xie, Z., Kasschau, K. D., and Carrington, J. C. (2003). Negative feedback regulation of Dicer-like1 in *Arabidopsis* by microRNA-guided mRNA degradation. *Curr. Biol.* 13, 784–789. doi: 10.1016/S0960-9822(03)00281-1
- Zeng, Y., Sankala, H., Zhang, X., and Graves, P. R. (2008). Phosphorylation of Argonaute 2 at serine-387 facilitates its localization to processing bodies. *Biochem. J.* 413, 429–436. doi: 10.1042/BJ20080599
- Zhang, P., and Zhang, H. (2013). Autophagy modulates miRNA-mediated gene silencing and selectively degrades AIN-1/GW182 in *C. elegans*. *EMBO Rep.* 14, 568–576. doi: 10.1038/embor.2013.53

**Conflict of Interest Statement:** The authors declare that the research was conducted in the absence of any commercial or financial relationships that could be construed as a potential conflict of interest.

*Received: 26 February 2014; paper pending published: 17 March 2014; accepted: 07 April 2014; published online: 23 April 2014.*

*Citation: Derrien B and Genschik P (2014) When RNA and protein degradation pathways meet. *Front. Plant Sci.* 5:161. doi: 10.3389/fpls.2014.00161*

*This article was submitted to Plant Cell Biology, a section of the journal *Frontiers in Plant Science*.*

*Copyright © 2014 Derrien and Genschik. This is an open-access article distributed under the terms of the Creative Commons Attribution License (CC BY). The use, distribution or reproduction in other forums is permitted, provided the original author(s) or licensor are credited and that the original publication in this journal is cited, in accordance with accepted academic practice. No use, distribution or reproduction is permitted which does not comply with these terms.*



# Autophagy-like processes are involved in lipid droplet degradation in *Auxenochlorella protothecoides* during the heterotrophy-autotrophy transition

Li Zhao, Junbiao Dai \* and Qingyu Wu \*

MOE Key Laboratory of Bioinformatics, School of Life Sciences, Tsinghua University, Beijing, China

**Edited by:**

Jose Luis Crespo, Consejo Superior de Investigaciones Científicas, Spain

**Reviewed by:**

Ursula Goodenough, Washington University, USA

Maria Esther Perez-Perez, CNRS, France

**\*Correspondence:**

Junbiao Dai, MOE Key Laboratory of Bioinformatics, Center for Epigenetics and Chromatin, School of Life Sciences, Tsinghua University, Biotechnology Building 2-305, Beijing 100084, China  
e-mail: jbdai@tsinghua.edu.cn;

Qingyu Wu, MOE Key Laboratory of Bioinformatics, School of Life Sciences, Tsinghua University, Biotechnology Building 2-302, Beijing 100084, China  
e-mail: qingyu@mail.tsinghua.edu.cn

Autophagy is a cellular degradation process that recycles cytoplasmic components in eukaryotes. Although intensively studied in yeast, plants, and mammals, autophagy in microalgae is not well understood. *Auxenochlorella protothecoides* is a green microalga that has the ability to grow either autotrophically when under light or heterotrophically when in media containing glucose. The two growth modes are inter-convertible and transition between them is accompanied by drastic changes in morphology and cellular composition; however, the mechanisms underlying these changes are unknown. In this study, we identified autophagy-related genes and characterized their roles in the degradation of lipid droplets during the heterotrophy-to-autotrophy (HA) transition in *A. protothecoides*. Most of the proteins constituting the eukaryotic "core machinery" were conserved in *A. protothecoides*. Two proteins, Atg4 and Atg8, were further investigated. *A. protothecoides* ATG4 was cloned from a cDNA library and expressed within yeast, and was able to functionally restore the autophagy pathway in *atg4Δ* yeast during nitrogen starvation. Furthermore, Atg8, which displayed high sequence identity with its yeast homolog, was able to conjugate to phosphatidylethanolamine (PE) *in vitro* and was recruited to the phagophore assembly site in yeast. We also identified a C-terminal glycine residue, G118, that was the cleavage site for Atg4. Finally, we used confocal and transmission electron microscopy to reveal that autophagic-like vacuoles were detectable in algal cells during the HA transition. Our data suggested that the lipid droplets in heterotrophic cells were engulfed directly by the autophagic-like vacuole instead of via autophagosomes.

**Keywords:** Atg8, Atg4, autophagic vacuole, lipid droplet, microalgae

## INTRODUCTION

All organisms need to adjust their growth and metabolic status according to changes in environmental and nutritional cues. Some organisms, named mixotrophs, have the ability to grow either autotrophically via photosynthesis or heterotrophically by utilizing organic carbon sources directly from the environment. Consequently, mixotroph cells display dramatic differences in their morphology and cellular composition under the two growth conditions. *Auxenochlorella protothecoides*, a free-living unicellular alga, grows under autotrophic conditions by forming a large cup-shaped chloroplast within the cell, and the cell largely consists of proteins and carbohydrates (Lu et al., 2013). When switched to heterotrophic conditions (limited nitrogen and abundant glucose), *A. protothecoides* grows rapidly and accumulates large amounts of lipid (>50% of dry cell weight). This lipid has been harnessed for the production of biofuel (Miao and Wu, 2006; Xiong et al., 2010; Lu et al., 2013). The two different growth modes are inter-convertible, and completely depend upon nutrient availability in the growth medium. *A. protothecoides* therefore provides a good model for the study of biogenesis and degradation of chloroplasts and the lipid body.

Autophagy is one of the two major degradative systems that eukaryotes employ for quality control of proteins and organelles (Lilienbaum, 2013). Three types of autophagy have been described so far: macroautophagy, microautophagy, and chaperone-mediated autophagy (CMA) (Mizushima, 2007). Autophagy has been intensively investigated in diverse organisms from the fungal, animal, and plant kingdoms and a large number of AuTophaGy-related (ATG) genes have been discovered (Tsukada and Ohsumi, 1993; Hanaoka et al., 2002; Yang and Klionsky, 2009; Xia et al., 2011). Studies on these ATG genes suggest that the core machinery of autophagy is highly conserved in eukaryotes (Meijer et al., 2007; Xia and Klionsky, 2007; Yang and Klionsky, 2009; Mizushima and Komatsu, 2011; Liu and Bassham, 2012).

Recently, several studies suggested that autophagy participates in the degradation of lipid droplets (LDs) (Singh et al., 2009; Kurusu et al., 2014; van Zutphen et al., 2014). LDs are well-defined organelles, delimited by a single protein-associated membrane, that mainly contain lipid esters, i.e., triacylglycerols (TAGs) and cholesteryl esters (Fujimoto and Parton, 2011). LDs are found in most cell types, including yeast, plant seeds, and adipocytes,

but the lipid content is highly variable. In addition to the lipid storage function, LDs are involved in lipid metabolism and homeostasis, and have been implicated in several metabolic diseases. Singh et al. (2009) showed that LDs in mouse hepatocytes were degraded by macrolipophagy (the formation of autolipophagosomes and their delivery to the lysosomes). Similar processes were also reported in plants and fungi. For example, autophagy-deficient mutants in rice exhibited delayed pollen maturation and male sterility as a result of blocked degradation of LDs in tapetum cells (Kurusu et al., 2014). In addition, autophagosome-like double membrane structures and vacuole-enclosed lipid droplets were observed during pollen maturation (Kurusu et al., 2014). In yeast cultured with oleic acid media and in *Magnaporthe grisea* during appressorium development, LDs were taken up by vacuoles in a process resembling microautophagy (Weber et al., 2001; van Zutphen et al., 2014).

Studies on autophagy in microalgae remain limited to date. A few recent studies presented the ultrastructure of autophagic-like vacuoles in some cells. Examined cells include *Dunaliella primolecta* in stationary phase, a photosynthesis-deficient mutant of *Chlamydomonas reinhardtii*, *Micrasterias denticulata* under salt or cadmium sulfate stress, *Dunaliella viridis* during nitrogen starvation, and the diatom *Cyclotella meneghiniana* treated with chlorinated benzenes or chromium (Eyden, 1975; Sicko-Goad et al., 1989; Lazinsky and Sicko-Goad, 1990; Inwood et al., 2008; Affenzeller et al., 2009; Jimenez et al., 2009; Andosch et al., 2012). In addition, *C. reinhardtii* Atg8 (CrAtg8) was identified and used as a specific marker for monitoring autophagy (Perez-Perez et al., 2010, 2012). Furthermore, we previously examined sequenced microalgae genomes and located most of the ATG-related genes described in other organisms. This suggests that the eukaryotic autophagy pathway may be conserved within these ancient unicellular organisms (Jiang et al., 2012).

In this study, we employed genomic analysis to identify ATG genes in *A. protothecoides*. We then conducted genetic and biochemical characterization of two of the autophagy-related genes in the Atg8-conjugating pathway (*ApATG8* and *ApATG4*). In addition, we demonstrated that autophagy was involved in the heterotroph-to-autotroph (HA) transition and provided evidence that lipid droplets in heterotrophic cells were degraded by the central vacuole in autophagy-like processes.

## MATERIALS AND METHODS

### ALGA STRAIN AND GROWTH CONDITIONS

*Auxenochlorella protothecoides* sp.0710 was originally obtained from the Culture Collection of Alga at the University of Texas (Austin, USA). The culture media and methods of autotrophic and heterotrophic cells were performed as described by Xiong et al. (2010). For induction of the heterotrophy-autotrophy (HA) transition, cells were cultivated in heterotrophic media containing 30 g/l glucose, 2 g/l yeast extract and 0.1 g/l glycine for 7 days and were then transformed into the autotrophic media supplied with light and aseptic air. The glucose and yeast extract were depleted and the glycine was added at the concentration of 5 g/L in autotrophic media.

### IDENTIFICATION OF *ApATG8* AND *ApATG4*

The gene sequence annotations of *ApATG8* and *ApATG4* from whole genome data were confirmed using CD-search on NCBI. The multiple sequence alignment and 3D structure prediction were performed using Jalview and Swiss-model, respectively. Alignment of the 3D structure was constructed by PyMOL and phylogenetic analysis was conducted by MEGA4.

### RNA EXTRACTION AND REVERSE TRANSCRIPTION

Seven-day-old heterotrophic liquid culture (10 ml;  $\sim 1.8 \times 10^8$  cells/ml) was harvested and frozen in liquid nitrogen for 20 min. Cells were powdered using a mortar and pestle with a liquid nitrogen bath. Total RNA was extracted using Trizol (Invitrogen). For genomic DNA removal,  $\sim 1 \mu\text{g}$  total RNA was treated in a 10  $\mu\text{l}$  reaction containing DNaseI, buffer with MgCl<sub>2</sub> and nuclease-free water at 37°C for 30 min. The reaction was stopped with the addition of 1  $\mu\text{l}$  of 50 mM EDTA and incubation at 65°C for 10 min. Reverse transcription was performed using a first strand cDNA synthesis kit (Fermentas). Genomic DNA-free template RNA (0.1  $\mu\text{g}$ ) was added to a 20  $\mu\text{l}$  reaction containing buffer, oligo(dT)<sub>18</sub> primers, RNase inhibitor, dNTP mix, and reverse transcriptase. The reaction was incubated at 42°C for 60 min and terminated by incubation at 70°C for 5 min.

### FUNCTIONAL COMPLEMENTATION OF *ApAtg4* IN YEAST

The ORF of *ApATG4* was inserted into the vector pRS415 under the yeast *ADH1* promoter. The construct was transformed into yeast (BY4741 MAT $\alpha$  his3Δ1 leu2Δ0 met15Δ0 ura3Δ0 *atg4*::KanMX4 pRS316 [GFP-*ATG8* URA3]) using a standard lithium acetate protocol. Transformants were cultured in SC-uracil-leucine medium to log-phase and stained with FM4-64 for 30 min at 30°C. Cells were chased in the same medium for 1 h at 30°C and then transformed into SD (-N) medium for 4 h. Cells were harvested after nitrogen starvation and observed using a confocal microscope (Leica TCS SP5) with GFP and TRITC filters.

### CLEAVAGE ASSAY OF *ApAtg8* BY Atg4

Three different forms of the ApAtg8 protein [wild type, glycine to alanine mutant (G118A), and glycine deletion mutant (ΔG118)] were fused to the N-terminal of GFP. Coding sequences were linked by overlapping extension PCR and the fusion constructs were inserted into vector pRS415 under the *GAL10* promoter with an N-terminal polyhistidine tag. The construct was transformed into a yeast *atg8* mutant (BY4741 MAT $\alpha$  his3Δ1 leu2Δ0 met15Δ0 ura3Δ0 *atg8*::KanMX4) and expression was induced with 2% galactose for 2 h. Yeast cells were subjected to immunoblot with anti-His antibody. For the *in vitro* cleavage assay, the ApAtg8-GFP, ApAtg4, and ScAtg4 sequences were cloned into vector pET21b and expressed in *E. coli*. Cells were homogenized by sonication. The reaction was conducted as previously described (Kirisako et al., 2000). The processing of ApAtg8 was detected by western blot using anti-GFP antibody.

### IN VITRO LIPIDATION OF Atg8

Phospholipids for liposome preparation were purchased from Avanti Polar Lipids. Lipid mixtures consisting of 1-palmitoyl-2-oleylphosphatidylcholine (POPC; 80%) and

dioleoylphosphatidylethanolamine (DOPE; 20%) were prepared from stocks dissolved in chloroform. After transfer to a glass tube, the mixture was dried to a thin film under a stream of nitrogen. Samples were dried further in a desiccator under vacuum for more than 6 h to remove the traces of organic solvent. The resulting lipid film was hydrated in a buffer consisting of 20 mM Tris-HCl (pH 7.5) and 150 mM NaCl at room temperature for 1 h to produce large multilamellar vesicles (MLVs). MLV suspensions were then disrupted by several freeze-thaw cycles (A single freeze-thaw cycle consisted of freezing for 3 min at liquid nitrogen temperature ( $-196^{\circ}\text{C}$ ) and thawing for 3 min in a water bath at  $42^{\circ}\text{C}$ ). The lipid suspension was then extruded through two polycarbonate membranes (Whatman) of 400 nm pore size using the Avanti Mini-Extruder at room temperature. Liposomes were stored at  $4^{\circ}\text{C}$ .

*In vitro* lipidation of Atg8 was conducted using purified Atg3, Atg5, Atg7, Atg8, Atg12, and liposomes. The ApAtg8 protein was purified using HIS-Select Nickel Affinity Gel (Sigma). Reactions were performed as previously described (Ichimura et al., 2004). To distinguish Atg8 and Atg8-PE, the reaction products were subjected to 13.5% urea-SDS-PAGE and stained with Coomassie blue.

#### CO-LOCALIZATION OF Atg8 WITH Ape1

GFP-ApATG8 and Ape1-mCherry were inserted into pRS416 and pRS415, respectively, under the control of the *ADH1* promoter. Yeast *atg8 $\Delta$*  cells were co-transformed with these two plasmids. Transformants were cultured to log-phase in SC-uracil-leucine medium at  $30^{\circ}\text{C}$ , washed three times, and resuspended in SC-uracil-leucine medium containing 0.2  $\mu\text{g}/\text{ml}$  rapamycin for 1 h at  $30^{\circ}\text{C}$ . Cells were harvested and observed using a Zeiss710META microscope using eGFP and mCherry filters.

#### MONODANSYLCADAVERINE AND NILE RED STAINING

For monodansylcadaverine and Nile red staining, algal cells were harvested and washed with 100 mM PBS (pH6.8) three times. Cells were stained for 10 min with 0.5 mM monodansylcadaverine dissolved in water (Sigma-Aldrich) at room temperature or with 1  $\mu\text{g}/\text{ml}$  Nile red dissolved in DMSO (Genmed Scientifics) at  $37^{\circ}\text{C}$ . Cells were then washed with PBS three times to remove excess fluorescent dyes. Cells were observed using a Zeiss710META microscope with dansylcadaverine, Nile red, and chlorophyll A filters. The MDC-incorporated structures were excited at 405 nm and detected at 451–539 nm. Fluorescence intensity was measured using ImageJ. The original images of HA cells stained with MDC were transformed into 8-bit images and cellular regions were outlined using the threshold tools of ImageJ. Integrated density (IntDen) and area were measured. The final average fluorescent intensity per cell was calculated as IntDen/Area. Approximately 100 cells were measured.

#### DETERMINATION OF TOTAL LIPID AND CHLOROPHYLL CONTENT IN ALGAL CELLS

Algal cells were harvested, washed twice with distilled water, and lyophilized. Lipid in algal powder was transesterified into biodiesel with sulfuric acid and then measured using gas chromatography as previously described (Xiong et al., 2010). For

chlorophyll analysis, algal powder was boiled in DMF (N, N-dimethylformamide) (Amresco) for 5 min for chlorophyll extraction, followed by measurement of OD<sub>663</sub> and OD<sub>645</sub> using UV/visible spectrophotometry (Pharmacia Biotech Ultrospec 2000, Sweden) as described previously (Xiong et al., 2010).

#### TRANSMISSION ELECTRON MICROSCOPY

*A. protothecoides* cells were fixed in 2.5% glutaraldehyde (pH6.8) for 12 h at  $4^{\circ}\text{C}$ . Samples were prepared as described by Jiang et al. (2012). Cells were imaged using a transmission electron microscope (Hitachi, Japan).

#### RESULTS

##### MOST OF THE CORE PROTEIN MACHINERY FOR AUTOPHAGY IS CONSERVED IN *A. PROTOTHECOIDES*

Recently, we generated the complete genome sequence of *A. protothecoides* (Gao et al., 2014) and identified several hypothetical genes that were annotated as homologs of ATG genes. Next, we conducted a genome-wide protein BLAST analysis using yeast ATG proteins as query sequences. Each identified candidate was subjected to the CD-search at the National Center for Biotechnology Information (NCBI) data bank to confirm the presence of conserved autophagy protein domains. Eventually, we found that most of the identified autophagy-related genes (12 of 17) could be assigned to one of the core machineries that participated in different stages of autophagy. The assigned core machineries included membrane initiation, elongation, closure, and fusion with vacuoles, suggesting that *A. protothecoides* possessed the molecular components needed for autophagy induction. Unlike plants, only a single copy of each ATG gene was identified in the *A. protothecoides* genome. As shown in Figure 1, most of the putative genes had moderate but substantial identities (20–80%) with the yeast homologs. All the identified proteins contained conserved ATG domains (data not shown). Notably, all of the components of the Atg8-conjugating pathway (Atg8, Atg4, Atg5, Atg7, Atg3, and Atg12) were identified in the *A. protothecoides* genome, suggesting that the pathway was likely to be active in this alga.

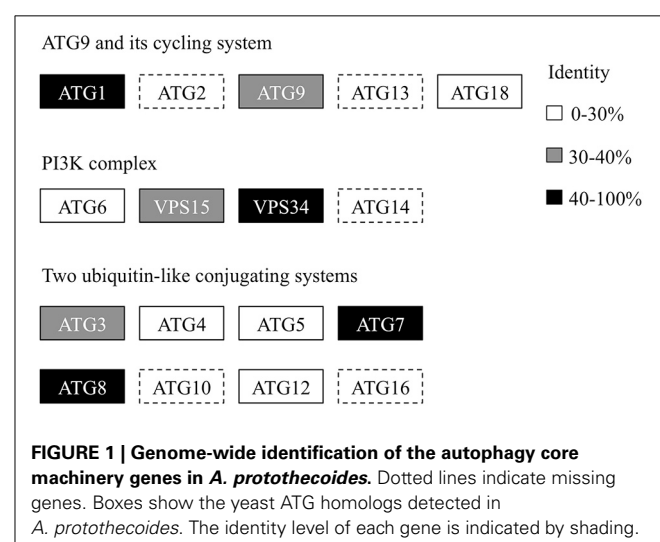


**FIGURE 1 | Genome-wide identification of the autophagy core machinery genes in *A. protothecoides*.** Dotted lines indicate missing genes. Boxes show the yeast ATG homologs detected in *A. protothecoides*. The identity level of each gene is indicated by shading.

## IDENTIFICATION OF ApAtg8 AND ApAtg4

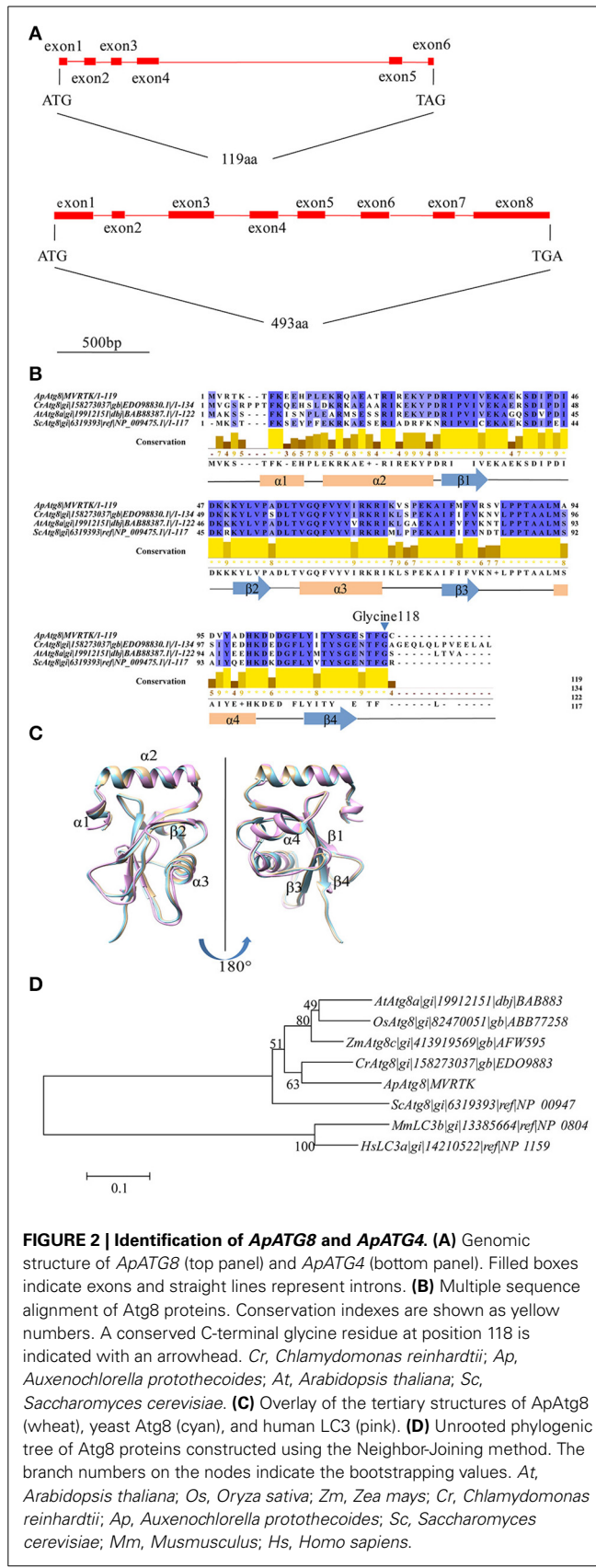
To investigate whether an active autophagy pathway was present in *A. protothecoides*, we focused on characterization of two key components: *ApATG4* and *ApATG8*. The putative *ApATG8* and *ApATG4* genes were amplified from a cDNA library using gene-specific primers (Supplementary Table 1) and were cloned and sequenced. DNA sequence alignments between the cloned cDNA and the genomic DNA (gDNA) sequence revealed the gene structures of *ApATG8* and *ApATG4* (Figure 2A). The *ApATG8* gene spanned approximately 2 kb of the genome and contained 6 exons and 5 introns. The *ApATG4* gene was about 2.6 kb in length and had 8 exons and 7 introns. These gene structures closely resembled the structures of the plant homologs. The ApAtg8 protein also had a considerable degree of identity (~73%) with the yeast homolog. Several C-terminal Atg8 protein sequences from *A. protothecoides* and model organisms were aligned (Figure 2B). This analysis indicated that the C-terminal glycine residue of Atg8 at position 118, which is modified by Atg4 during autophagy induction, was conserved. The predicted ApAtg8 protein structure contained four  $\alpha$ -helices and four  $\beta$ -sheets and was consistent with the reported secondary structures of the yeast and human homologs. The predicted tertiary structure of ApAtg8, which consisted of an N-terminal  $\alpha$ -helix domain and a C-terminal ubiquitin-like core (Figure 2C), was similar to yeast Atg8 (resolved by NMR) and human LC3 (resolved by crystallization). Phylogenetic analysis of Atg8 proteins from *A. protothecoides* and model organisms indicated that ApAtg8 had the closest relationship to Atg8 from *C. reinhardtii*, which corresponded to the 16S rRNA phylogeny (Figure 2D). Taken together, these data indicate that Atg8 is conserved between eukaryotes.

## ApAtg4 CAN FUNCTIONALLY REPLACE Atg4 IN YEAST

To confirm the function of the ApAtg4 protein, a complementation experiment was conducted in yeast. GFP-Atg8 was used as a marker of autophagy. The ApAtg4 protein was expressed in a yeast strain containing GFP-tagged Atg8 and a complete deletion of *ATG4* (*atg4 $\Delta$* ). As shown in the top panel of Figure 3, Atg8 was not processed or translocated to the vacuole upon nitrogen starvation when an empty vector was supplied (i.e., no ApAtg4). Localization of GFP-tagged Atg8 was restored upon expression of yeast Atg4 from a plasmid containing *ScATG4* (middle panel). Localization of GFP-tagged Atg8 was similarly restored when *ApATG4* was expressed (bottom panel). This indicated that ApAtg4 could functionally replace yeast Atg4 and restore the autophagy pathway under conditions of nitrogen starvation. ApAtg4 is therefore the homolog of yeast Atg4 and the two proteins probably perform similar functions during autophagy in their respective organisms.

## ApAtg8 IS CLEAVED BY Atg4 PROTEASE IN VITRO AND IN VIVO

ApAtg4 functioned as a protease and was able to functionally replace yeast Atg4. We therefore hypothesized that ApAtg8 would be processed by cleavage at the C-terminal glycine residue as in yeast Atg4. As mentioned above, a highly conserved glycine residue was located at amino acid position 118 (G118) of ApAtg8,



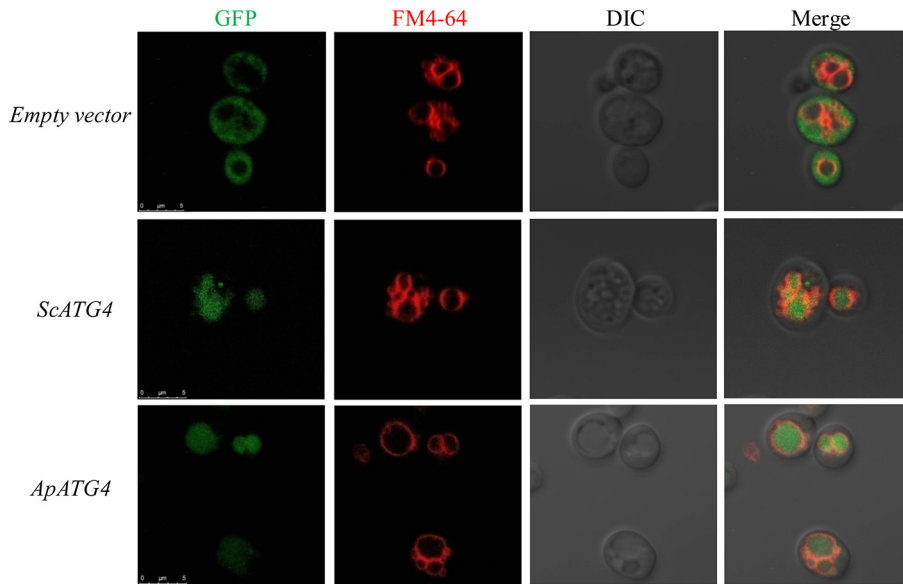


**FIGURE 3 | Functional complementation of ApAtg4 in *atg4* mutant yeast.** *ApATG4* cDNA was cloned and expressed in a yeast *atg4* mutant in a GFP-Atg8 background. The yeast *ATG4* (*ScATG4*) and the empty vector were used as positive and negative controls, respectively.

Log-phase cells were transformed into nitrogen starvation SD (-N) medium for 4 h. The yeast vacuolar membrane was stained by FM4-64. DIC, Differential interference contrast microscopy images. Scale bar, 5  $\mu$ m.

and this was the likely target site for Atg4. To test this possibility, we constructed a reporter protein by fusing ApAtg8 with an N-terminal polyhistidine tag and a C-terminal GFP tag. In addition, plasmids were generated containing one of two mutant *ApATG8* genes, one of which encoded a glycine to alanine substitution (G118A) and one of which encoded a glycine deletion ( $\Delta$ G118) (Figure 4A). Fusion proteins and Atg4 from yeast (*ScAtg4*) and *A. protothecoides* (ApAtg4) were expressed in *E. coli*. An *in vitro* Atg8 cleavage assay was performed by mixing the whole-cell extracts from Atg8-expressing bacteria with whole-cell extracts from bacteria expressing ScAtg4, ApAtg4, or empty vector. Western blots were performed using anti-GFP antibody to detect free GFP (Figure 4B). Minimal free GFP was observed in the absence of Atg4. Free GFP was observed in increasing amounts with time when ApAtg8-GFP was incubated with Atg4 from yeast or *A. protothecoides*. The amount of ApAtg8-GFP fusion protein decreased concurrently. Liberation of free GFP did not occur when mutated ApAtg8-GFP (G118A or  $\Delta$ G118) was incubated with ApAtg4, indicating that cleavage of ApAtg8-GFP by Atg4 was dependent on ApAtg8 G118.

Next, we assessed whether Atg4 could cleave ApAtg8 *in vivo*. Fusion constructs were transformed and expressed in a yeast *atg4 $\Delta$*  strain and western analysis with anti-HIS antibody was used to identify free ApAtg8 protein. As shown in Figure 4C, ApAtg8-GFP was cleaved upon activation of autophagy by nitrogen starvation and a fragment of ~18 kDa was generated. This fragment size corresponded with the size of ApAtg8 protein. Mutant proteins containing either G118A or  $\Delta$ G118 could not be processed. This indicated that, as with the *in vitro* analysis, G118 was essential for cleavage of ApAtg8. Cleavage was also completely abrogated in *atg4 $\Delta$*  yeast, which indicated that Atg4 was

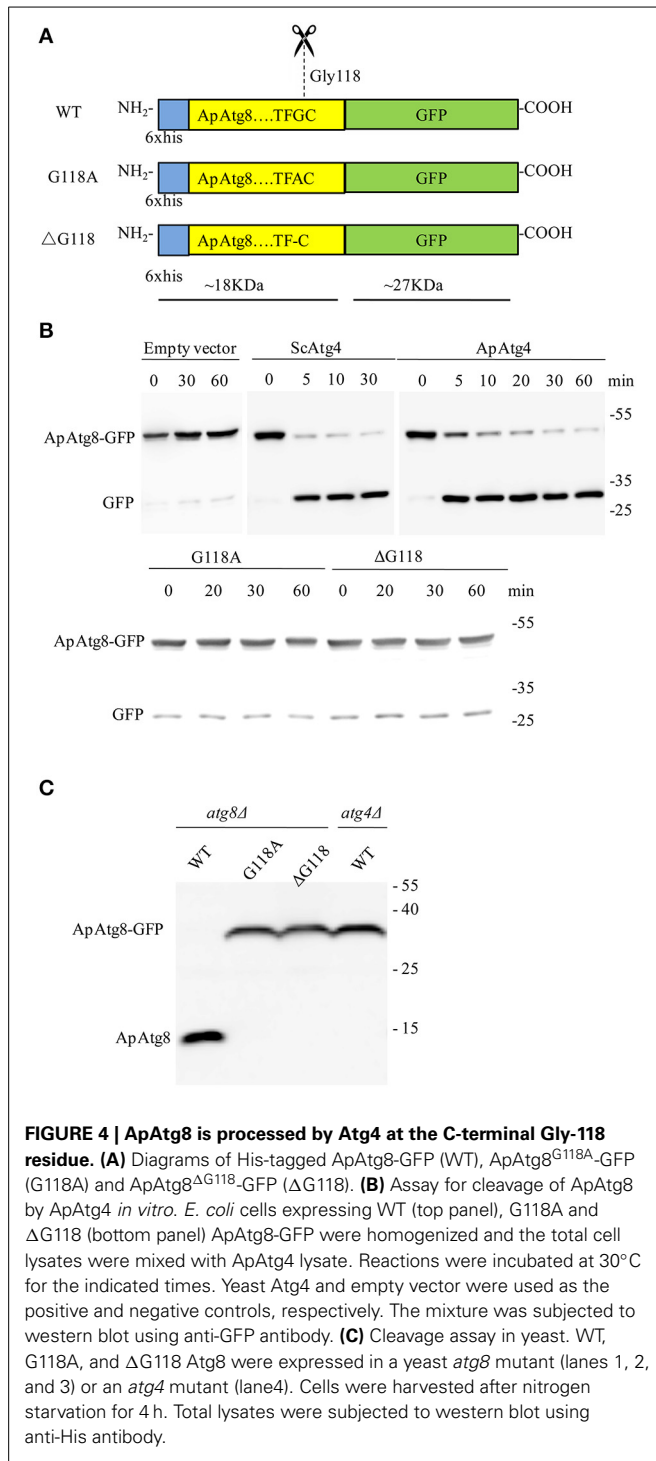
also essential for processing of ApAtg8. Taken together, our data indicate that ApAtg8 can be cleaved by Atg4 *in vitro* and *in vivo*, and that Atg4 and ApAtg8 G118 are both necessary for processing.

#### ApAtg8 CAN BE CONJUGATED TO PHOSPHATIDYLETHANOLAMINE IN VITRO

After processing, Atg8 is conjugated to phosphatidylethanolamine (PE) in a process crucial for autophagosome formation known as Atg8 lipidation. The Atg8 conjugation system was reconstituted *in vitro* using purified ATG proteins and liposomes to provide an experimental environment to assess ApAtg8 lipidation. Purified ApAtg8<sup>G118</sup>, with C-terminal glycine exposed, was added to a reaction system containing purified yeast Atg7, Atg3, Atg5-Atg12, and 20% PE liposomes. Yeast Atg8<sup>G116</sup> was used as a positive control and ApAtg8<sup>C119</sup> (no exposed C-terminal glycine) was used as a negative control. Urea-SDS-PAGE showed that the nascent form of ApAtg8 was detected as a single ~16 kDa fragment, as expected (Figure 5). A faster-migrating fragment, representing lipidated Atg8, was observed after incubation with ApAtg8<sup>G118</sup> or yeast Atg8<sup>G116</sup> for 15 min. No lipidation was detected when the terminal glycine was masked (ApAtg8<sup>C119</sup>). We therefore concluded that ApAtg8 could be conjugated to PE and that the conserved glycine at position mediated conjugation.

#### ApAtg8 CAN BE RECRUITED TO THE PHAGOPHORE ASSEMBLY SITE IN YEAST

After lipidation, Atg8 is recruited to the phagophore assembly site (PAS), where the core autophagy machinery was assembled. In yeast, Ape1 is recruited to PAS and is then transported to the vacuole for maturation by the cytoplasm to vacuole targeting



pathway (CVT). We wished to determine whether ApAtg8 could be recruited to PAS. Ape1 co-localizes with Atg8 in yeast (van der Vaart et al., 2010) and we therefore examined co-localization of Ape1 and ApAtg8. GFP-labeled ApAtg8 and mCherry-labeled Ape1 were expressed in yeast cells and examined by fluorescence microscopy. GFP-alone was observed as diffuse green fluorescence and Ape1-mCherry was seen as spherical dots. As with yeast Atg8-GFP, ApAtg8-GFP formed punctate structures and

co-localized with Ape1 after rapamycin treatment (Figure 6), indicating that ApAtg8 localized to the PAS during induction of autophagy in yeast.

#### DEGRADATION OF LIPID BODIES AND BIOGENESIS OF THE PHOTOSYNTHETIC SYSTEM DURING THE HA TRANSITION

We examined the morphological and biochemical component changes that occurred during the *A. protothecoides* HA transition. Algal cells were cultivated in heterotrophic media for 7 days, harvested, and used to inoculate autotrophic media (high nitrogen, glucose deprivation). Cells were stained for lipid using Nile red and were examined by confocal microscopy (Figure 7A). Large lipid bodies occupying more than half of the entire cellular space were typically found in heterotrophic cells at the initiation of the HA transition. The lipid bodies subsequently shrank in size and chlorophyll auto-fluorescence emerged during the first 24 h of adaptation to light. Assembly of chloroplastic structures was completed within 72 h. Cup-shaped or spherical chloroplasts were dominant, which suggested that the photosynthetic system was completely reconstructed. Analysis of total cellular lipid and chlorophyll contents confirmed the degradation of lipid and biosynthesis of chlorophyll. The lipid content gradually decreased from ~80% (w/w) at the initiation of the HA transition to 10% (w/w) after 72 h cultivation in autotrophic media. During the same time period, chlorophyll content increased to greater than 30 mg/g dry cell weight (Figure 7B).

#### AUTOPHAGY INDUCTION DURING THE HA TRANSITION IN *A. PROTOTHECOIDES*

To investigate whether autophagy is involved in the HA transition, cells at different time points were monitored using monodansylcadaverine (MDC), a fluorescent dye that stains the autophagic structures *in vivo* (Biederick et al., 1995; Munafò and Colombo, 2001; Contento et al., 2005). Single-dye labeling samples were tested to ensure that bleed-through signal between filters did not occur (data not shown). The intensity of the MDC fluorescent signal increased >5-fold between 0 and 36/48 h (Figure 8A). Several MDC-labeled spherical structures were found in close proximity to the chloroplast envelope (Figures 8B,C). These mobile structures were probably autophagic bodies located randomly in the *A. protothecoides* vacuole. Cells containing MDC-labeled structures were quantitated, and numbers of MDC-positive cells rose during the 48 h after the shift to autotrophic growth. Approximately 15-fold more MDC-positive cells were found at 48 h than at 0 h (Figure 8D; \**p* < 0.03, \*\**p* < 0.01).

To further confirm the presence of autophagic-like vacuoles in *A. protothecoides* during the HA transition, transmission electron microscopy was used to investigate ultrastructural changes within algal cells during transition. As shown in Figure 9A, the lipid bodies and starch granules that had accumulated in heterotrophic cells were degraded and the cup-shaped chloroplast was regenerated during the HA transition. This was consistent with the confocal microscopy observations. Autotrophic cells utilized plastoglobuli for lipid storage in chloroplasts (Figure 9A, white arrows). Electron-dense spherical structures and single-membrane-bound vesicles (~0.3–1 μm in diameter) that resembled autophagic bodies were typically detected in the vacuoles

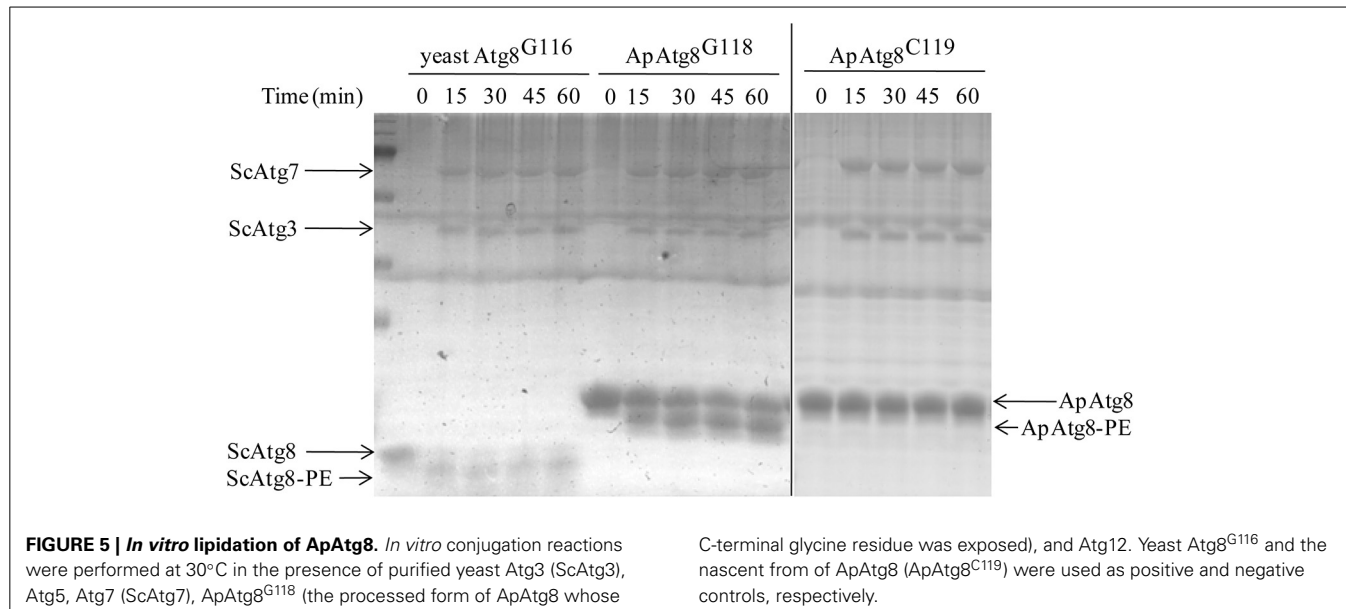


**FIGURE 5 |** *In vitro* lipidation of ApAtg8. *In vitro* conjugation reactions were performed at 30°C in the presence of purified yeast Atg3 (ScAtg3), Atg5, Atg7 (ScAtg7), ApAtg8<sup>G118</sup> (the processed form of ApAtg8 whose

C-terminal glycine residue was exposed), and Atg12. Yeast Atg8<sup>G116</sup> and the nascent form of ApAtg8 (ApAtg8<sup>C119</sup>) were used as positive and negative controls, respectively.

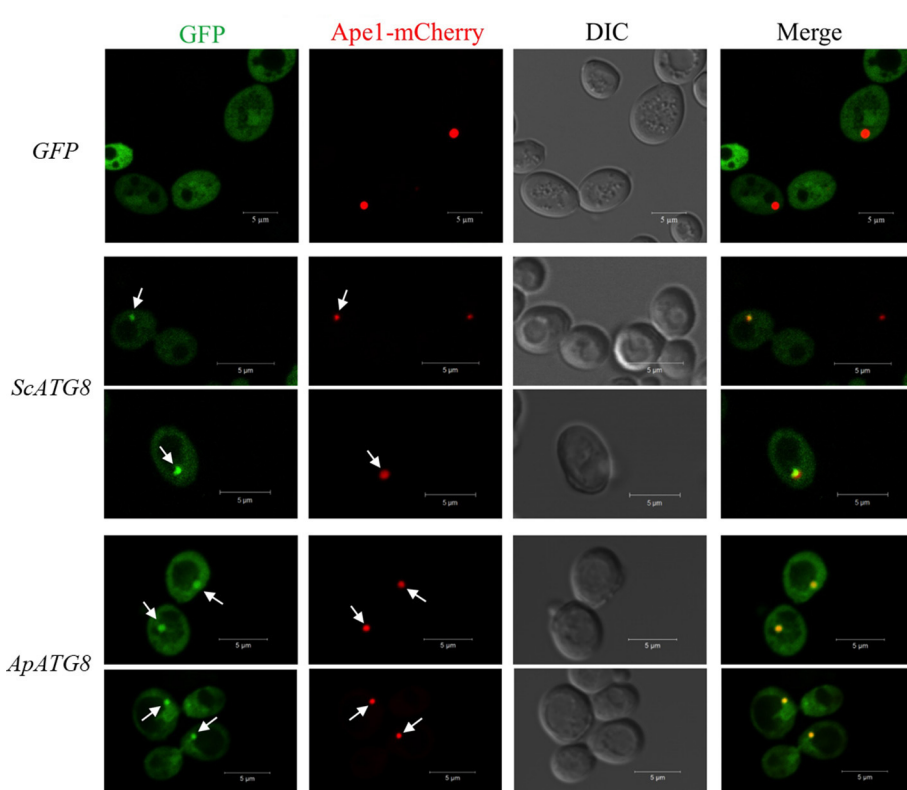


**FIGURE 6 |** ApAtg8 co-localizes with Ape1 at the PAS. ApATG8 cDNA was expressed in *atg8Δ* yeast. Yeast ATG8 (*ScATG8*) and the empty vector were used as positive and negative controls, respectively. Cells in log-phase were shifted to SC-uracil-leucine

medium containing 0.2 μg/ml rapamycin for 1 h. Arrows indicate the punctate structures where GFP-Atg8 and Ape1-mCherry co-localize. DIC, Differential interference contrast microscopy images. Scale bar, 5 μm.

of HA cells subjected to autotrophic growth for 36 and 48 h but were absent within cells exposed to 0 h of light (Figures 9A,B). Smaller autophagic vacuoles generated within one single cell early in the HA transition subsequently fused into one large autophagic

vacuole (Figure 9A). These data suggest that autophagy was induced during the HA transition. Instead of the large lipid bodies observed in the heterotrophic cells at 0 h, a number of small lipid droplets (LDs) were seen in the proximity of the central

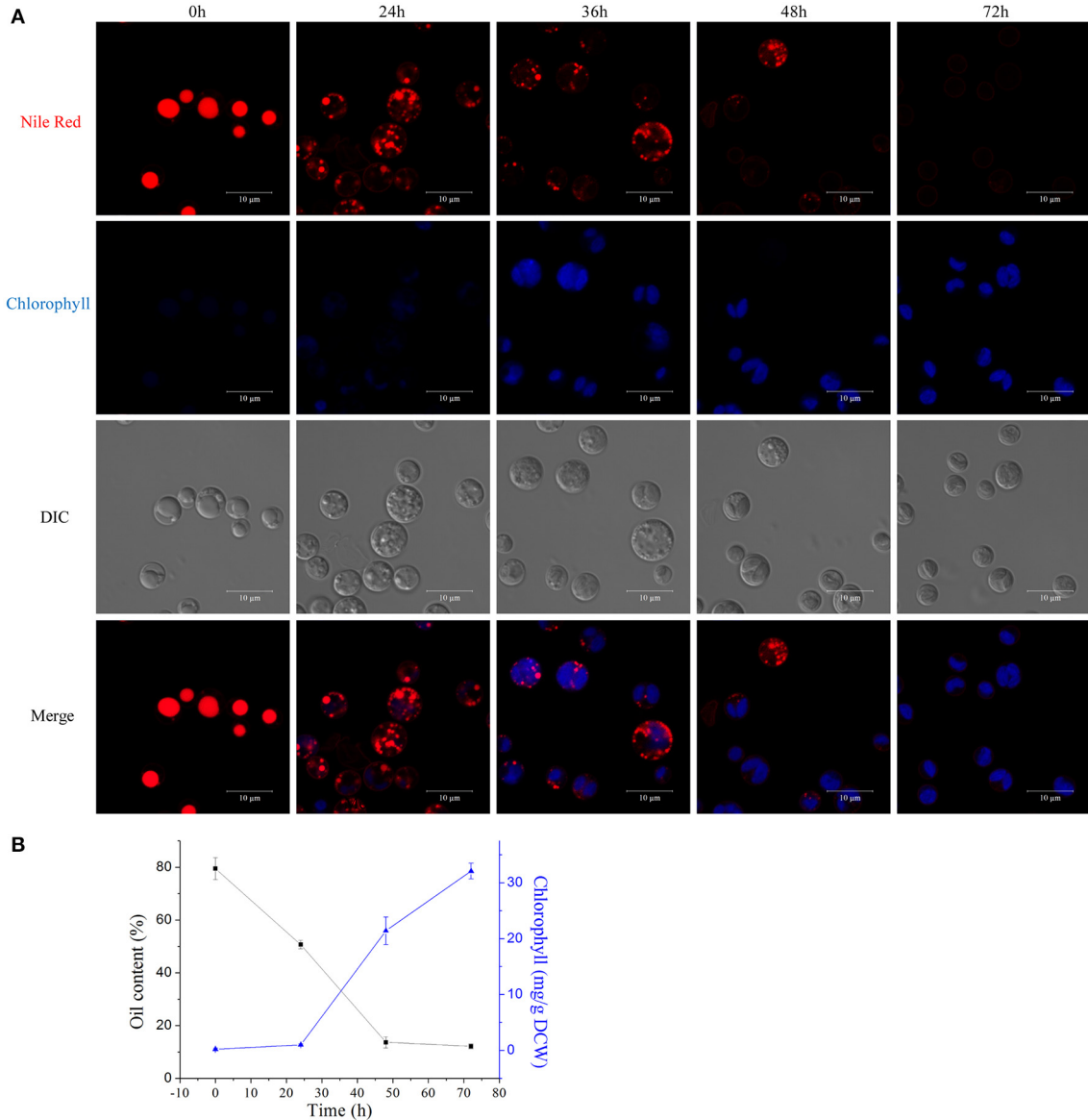


**FIGURE 7 | Degradation of lipids and biogenesis of chloroplasts during the HA transition. (A)** Confocal microscopy images of algal cells during the HA transition. Cells were cultivated in heterotrophic medium for 7 days and then transferred into autotrophic medium for 3 days. LDs were stained using

Nile red and chlorophyll auto-fluorescence is shown as a pseudo-color image in blue. DIC, Differential interference contrast microscopy images. Scale bar, 10 μm. **(B)** Determination of total lipid and chlorophyll contents of HA cells. Closed black square, lipid content; closed blue triangles, chlorophyll content.

vacuole during the HA transition. These LDs, which were delimited by a single membrane, tended to be internalized by the larger (1.5 μm diameter) autophagic vacuole (Figures 9C–E). The different stages of LD internalization by autophagic vacuoles are shown in Figures 9F–I. A minority of LDs that were relatively large partially extruded into the autophagic vacuole (Figure 9G). Figures 9H,I show LDs completely engulfed by autophagic vacuoles. To further confirm the autophagic degradation of lipid bodies in *A. protothecoides* during HA transition, cells were double-labeled with Nile red and MDC and examined with confocal microscopy. Lipid bodies in a number of cells exposed to light for 24–36 h co-localized with MDC-labeled structures,

demonstrating that the dense bodies within vacuoles were likely to be LDs (Supplementary Figure 1). No double membrane structures consistent with lipophagy were detected, indicating that the degradation of LDs during HA transition in *A. protothecoides* was probably a microautophagy-like process.

## DISCUSSION

Autotrophic and heterotrophic *A. protothecoides* undergo different growth patterns that result in diverse subcellular structures and chemical composition (Miao and Wu, 2006; Xiong et al., 2010; Lu et al., 2013). The majority of the cellular space in heterotrophic cells comprises large lipid droplets (~1–2 μm) and

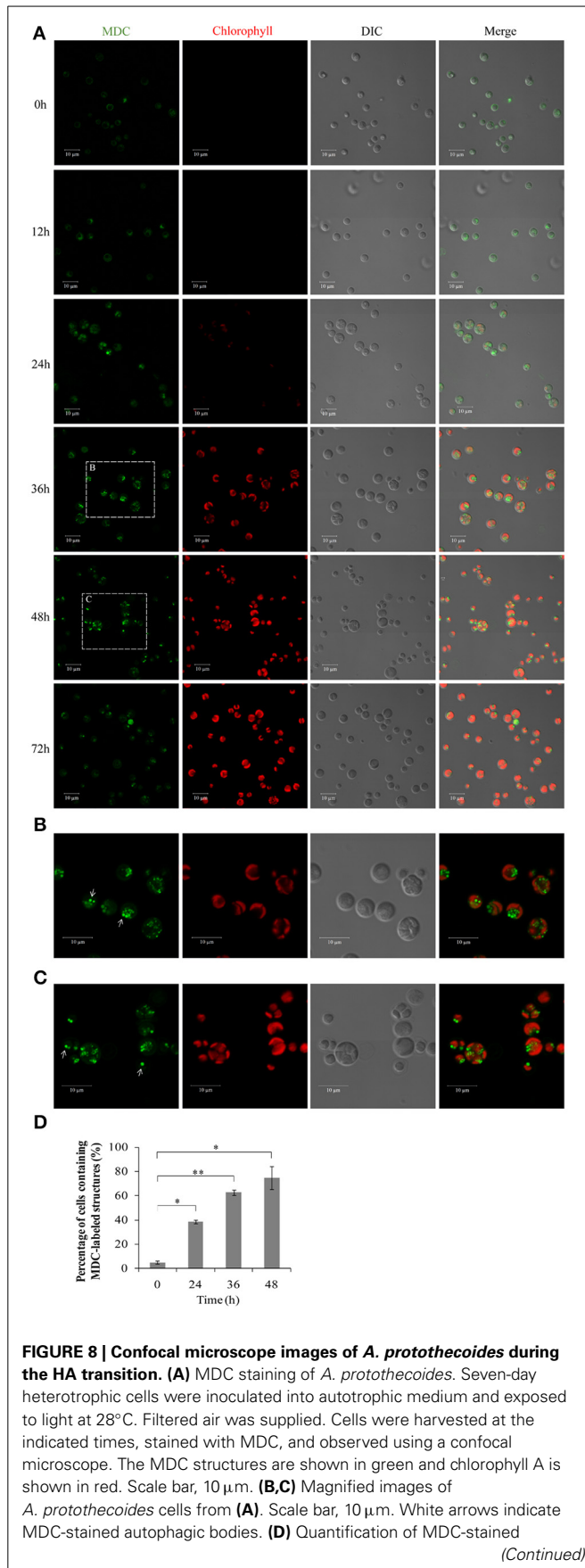


**FIGURE 8 | Confocal microscope images of *A. protothecoides* during the HA transition. (A)** MDC staining of *A. protothecoides*. Seven-day heterotrophic cells were inoculated into autotrophic medium and exposed to light at 28°C. Filtered air was supplied. Cells were harvested at the indicated times, stained with MDC, and observed using a confocal microscope. The MDC structures are shown in green and chlorophyll A is shown in red. Scale bar, 10 μm. **(B,C)** Magnified images of *A. protothecoides* cells from (A). Scale bar, 10 μm. White arrows indicate MDC-stained autophagic bodies. **(D)** Quantification of MDC-stained

#### FIGURE 8 | Continued

structures. More than 100 cells were counted each time and the percentage of cells containing MDC-labeled structures was calculated. Error bars represent standard error from two independent experiments. Student's *t*-test was used to determine significant differences (\**P* < 0.03, \*\**P* < 0.01).

starch granules and photosynthetic chloroplasts are completely absent. The neutral lipid content varies greatly between heterotrophic (above 50%) and autotrophic (~10%) cells. Algal cells have the ability to undergo HA transition, in which lipid droplets and starch granules diminish and the large cup-shaped chloroplast is regenerated. However, the mechanisms underlying the HA transition remain obscure. In this study, we demonstrated that autophagy-related genes in the ATG8-conjugating pathway were conserved in *A. protothecoides*. We also showed that an autophagy-like process was involved in the degradation of LDs during the HA transition. *A. protothecoides* may therefore serve as a useful study model for the metabolism and dynamics of lipid droplets and chloroplasts.

#### CONSERVATION OF AUTOPHAGY-RELATED GENES IN *A. PROTOTHECOIDES*

Previous studies revealed that autophagy-related pathways evolved in eukaryotes for the chambered-protease degradation of proteins and organelles (Hughes and Rusten, 2007). *A. protothecoides* is a eukaryotic green alga derived from primary endosymbiosis (Keeling et al., 2005). In this study, we performed a genome-wide *in silico* study of the autophagy machinery in *A. protothecoides* and provided evidence for the existence of most autophagy-related genes. This is consistent with our previous survey of autophagy-related genes in seven different microalgae (Jiang et al., 2012). These data suggest that autophagy is an evolutionarily ancient process.

We failed to identify several core autophagy components (Figure 1). As canonical autophagy genes were mainly identified in model organisms, such as yeast, one possible explanation is that the related autophagy pathways might not exist in *A. protothecoides*. Alternatively, these components may lack sufficient sequence conservation with their yeast counterparts to allow identification. Finally, some species-specific autophagy factors or pathways may exist that would compensate for the missing canonical components. In support of the last hypothesis, recent genetic screens of autophagy-deficient mutants in *Caenorhabditis elegans* reveal several uncharacterized metazoan-specific genes required for macroautophagy, including *epg-2*, *-3*, *-4*, and *-5* (Tian et al., 2010). Further investigation will be required to test this possibility.

#### HOW DO LIPID BODIES IN HETEROPTROPHIC ALGAL CELLS DEGRADE?

Previous studies reveal that LDs perform functions other than lipid storage. LDs are dynamic multifunctional organelles that are involved in various physiological pathways, including membrane synthesis, viral replication, protein degradation, and energy production (Walther and Farese, 2012). Disorders in the metabolism of LDs, particularly those involving excessive LD storage in mammalian tissues, are related to several diseases such as diabetes and

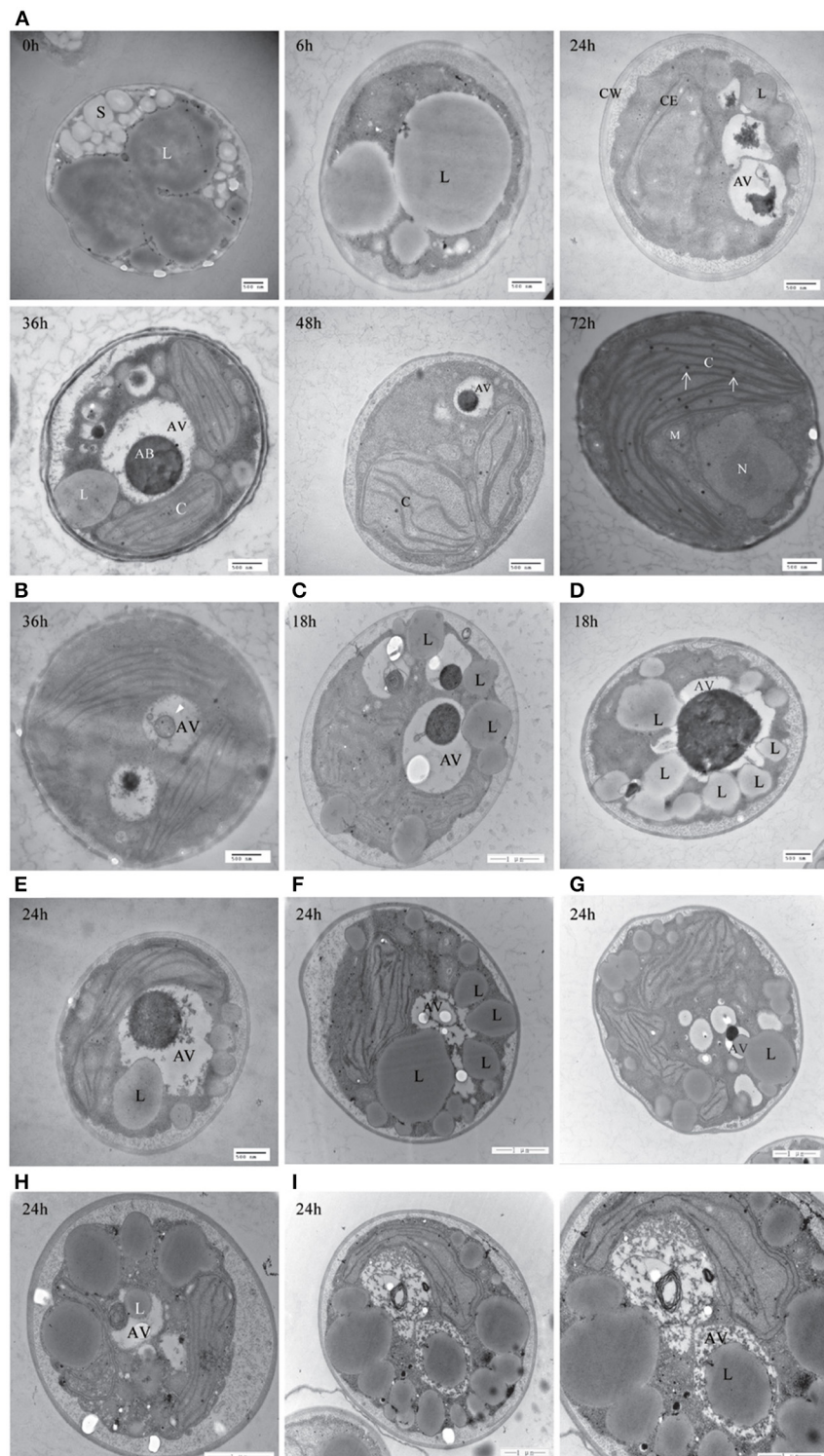


**FIGURE 9 | Transmission electron microscope (TEM) images of *A. protothecoides* during the HA transition. (A)** Heterotrophic cells were resuspended in autotrophic medium for the indicated time and then processed for TEM. C, chloroplast; CE, chloroplast envelope; CW, cell wall; S, starch granules; L, lipid bodies; AV, autophagic vacuoles; AB, autophagic bodies; M, mitochondria; N, nuclear. White arrows indicate plastoglobuli in

chloroplasts. **(B)** Representative ultrastructure of autophagic vacuoles in HA cells after 36 h cultivation in autotrophic media. Single-membrane-bound vesicles (white arrowhead) were detected within the vacuoles of HA cells. **(C–I)** Different stages of internalization of the small scattered LDs by autophagic vacuoles in *A. protothecoides* exposed to light for 18 or 24 h during the HA transition. L, lipid bodies; AV, autophagic vacuoles.

atherosclerosis. LDs are hydrolyzed in a process called lipolysis by a series of cytosolic lipases such as adipose triglyceride lipase (ATGL), hormone sensitive lipase (HSL) in mammals, and Tg13&Tg14 in yeast (Fujimoto and Parton, 2011). More recently, autophagy is shown to contribute to the breakdown of LDs for the maintenance of lipid homeostasis in mouse liver, plant seeds, and fungi (Singh et al., 2009; Kurusu et al., 2014; van Zutphen et al., 2014).

In this study, we found that LDs were directly sequestered by the *A. protothecoides* vacuole during the HA transition. This occurred via a microautophagy-resembling pathway that involved the protrusion of the vacuolar membrane rather than engulfment by double membrane structures such as autophagosomes. However, the vacuole was not large enough to entirely engulf the lipid bodies during early stages of HA transition. TEM images suggested that the cells might adopt two strategies to break down large LDs. The first step involves lipolysis, in which the large lipid bodies are disintegrated by LD-resident TAG lipases into many small-sized LDs. Alternatively, a portion of the large lipid bodies might protrude into the autophagic vacuole, be pinched off into the vacuolar lumen, and then be hydrolyzed by vacuolar lipase. The partial sequestration of organelles by the autophagic vacuole in yeast has been described previously for piecemeal microautophagy of the nucleus (PMN) (Roberts et al., 2003). In the second step, small LDs could be integrally incorporated into the central vacuole for autophagy degradation by inward invagination. This resembles lipid autophagy in yeast and is distinct from lipid metabolism in mammalian cells and plant seeds. The lipolysis and microautophagy pathways are therefore delicately orchestrated in *A. protothecoides* during the HA transition to satisfy the demands of lipid metabolism and energy supply.

#### WHAT INDUCES AUTOPHAGY DURING THE HA TRANSITION?

Due to the inclusion of glucose, the heterotrophic cultivation medium used for *A. protothecoides* is relatively nutritious compared to the medium used for autotrophic growth. As a result, cells probably undergo carbon starvation upon transfer into glucose-free autotrophic media during the delay before a functioning chloroplast is established. Carbon starvation may serve as an inducer to trigger autophagy in a similar manner to the classic nitrogen starvation signal found in other organisms. Autophagy could be induced in *A. protothecoides* during the HA transition to allow cells to generate enough energy to propagate and to rebuild the photosynthetic machinery. Similar phenomena have been reported in other systems such as tobacco BY-2 cells and *Arabidopsis* suspension cells during sucrose starvation (Takatsuka et al., 2004; Rose et al., 2006). However, no evidence linking autophagy to lipid degradation was presented in those studies.

#### ACKNOWLEDGMENTS

We are grateful to Cong Yi for providing the yeast strains, Shaojin Zhang for providing purified yeast ATG proteins and liposomes, Jingjing Tong for suggestions and assistance in experiments and Diane C. Bassham for helpful discussion and critical comments. This work was supported by NSFC project 31370282 and 41030210, MOST project 2011BAD14B05 and 2014AA02200

to Qingyu Wu and by Tsinghua University Initiative Scientific Research Program 2012Z08128 to Junbiao Dai.

#### SUPPLEMENTARY MATERIAL

The Supplementary Material for this article can be found online at: <http://www.frontiersin.org/journal/10.3389/fpls.2014.00400/abstract>

#### REFERENCES

- Affenzeller, M. J., Darchshouri, A., Andosch, A., Lutz, C., and Lutz-Meindl, U. (2009). Salt stress-induced cell death in the unicellular green alga *Micrasterias denticulata*. *J. Exp. Bot.* 60, 939–954. doi: 10.1093/jxb/ern348
- Andosch, A., Affenzeller, M. J., Lütz, C., and Lütz-Meindl, U. (2012). A freshwater green alga under cadmium stress: ameliorating calcium effects on ultrastructure and photosynthesis in the unicellular model *Micrasterias*. *J. Plant Physiol.* 169, 1489–1500. doi: 10.1016/j.jplph.2012.06.002
- Biederbick, A., Kern, H. F., and Elsasser, H. P. (1995). Monodansylcadaverine (MDC) is a specific *in vivo* marker for autophagic vacuoles. *Eur. J. Cell Biol.* 66, 3–14.
- Contento, A. L., Xiong, Y., and Bassham, D. C. (2005). Visualization of autophagy in *Arabidopsis* using the fluorescent dye monodansylcadaverine and a GFP-AtATG8e fusion protein. *Plant J.* 42, 598–608. doi: 10.1111/j.1365-313X.2005.02396.x
- Eyden, B. P. (1975). Light and electron microscope study of *Dunaliella pri-molesta* butcher (*Volvocida*). *J. Protozool.* 22, 336–344. doi: 10.1111/j.1550-7408.1975.tb05183.x
- Fujimoto, T., and Parton, R. G. (2011). Not just fat: the structure and function of the lipid droplet. *Cold Spring Harb. Perspect. Biol.* 3:a004838. doi: 10.1101/cshperspect.a004838
- Gao, C., Wang, Y., Shen, Y., Yan, D., He, X., Dai, J., et al. (2014). Oil accumulation mechanisms of the oleaginous microalgae *Chlorella protothecoides* revealed-through its genome, transcriptomes and proteomes. *BMC Genomics* 15:582–595. doi: 10.1186/1471-2164-15-582
- Hanaoka, H., Noda, T., Shirano, Y., Kato, T., Hayashi, H., Shibata, D., et al. (2002). Leaf senescence and starvation-induced chlorosis are accelerated by the disruption of an *Arabidopsis* autophagy gene. *Plant Physiol.* 129, 1181–1193. doi: 10.1104/pp.011024
- Hughes, T., and Rusten, T. E. (2007). Origin and evolution of self-consumption: autophagy. *Adv. Exp. Med. Biol.* 607, 111–118. doi: 10.1007/978-0-387-74021-8\_9
- Ichimura, Y., Imamura, Y., Emoto, K., Umeda, M., Noda, T., and Ohsumi, Y. (2004). *In vivo* and *in vitro* reconstitution of Atg8 conjugation essential for autophagy. *J. Biol. Chem.* 279, 40584–40592. doi: 10.1074/jbc.M405860200
- Inwood, W., Yoshihara, C., Zalpuri, R., Kim, K. S., and Kustu, S. (2008). The ultrastructure of a *Chlamydomonas reinhardtii* mutant strain lacking phytoene synthase resembles that of a colorless alga. *Mol. Plant* 1, 925–937. doi: 10.1093/mp/ssn046
- Jiang, Q., Zhao, L., Dai, J. B., and Wu, Q. Y. (2012). Analysis of autophagy genes in microalgae: *Chlorella* as a potential model to study mechanism of autophagy. *PLoS ONE* 7:e41826. doi: 10.1371/journal.pone.0041826
- Jimenez, C., Capasso, J. M., Edelstein, C. L., Rivard, C. J., Lucia, S., Breusegem, S., et al. (2009). Different ways to die: cell death modes of the unicellular chlorophyte *Dunaliella viridis* exposed to various environmental stresses are mediated by the caspase-like activity DEVDase. *J. Exp. Bot.* 60, 815–828. doi: 10.1093/jxb/ern330
- Keeling, P. G., Burger, G., Durnford, D. G., Lang, B. F., Lee, R. W., Pearlman, R. E., et al. (2005). The tree of eukaryotes. *Trends Ecol. Evol.* 20, 670–676. doi: 10.1016/j.tree.2005.09.005
- Kirisako, T., Ichimura, Y., Okada, H., Kabeya, Y., Mizushima, N., Yoshimori, T., et al. (2000). The reversible modification regulates the membrane-binding state of Atg8/Aut7 essential for autophagy and the cytoplasm to vacuole targeting pathway. *J. Cell Biol.* 151, 263–275. doi: 10.1083/jcb.151.2.263
- Kurusu, T., Koyano, T., Hanamata, S., Kubo, T., Noguchi, Y., Yagi, C., et al. (2014). OsATG7 is required for autophagy-dependent lipid metabolism in rice postmeiotic anther development. *Autophagy* 10, 878–888. doi: 10.4161/auto.28279

- Lazinsky, D., and Sicko-Goad, L. (1990). Morphometric analysis of phosphate and chromium interactions in *Cyclotella meneghiniana*. *Aquat. Toxicol.* 16, 127–140. doi: 10.1016/0166-445X(90)90082-Z
- Lilienbaum, A. (2013). Relationship between the proteasomal system and autophagy. *Int. J. Biochem. Mol. Biol.* 4, 1–26.
- Liu, Y., and Bassham, D. C. (2012). Autophagy: pathways for self-eating in plant cells. *Annu. Rev. Plant Biol.* 63, 215–237. doi: 10.1146/annurev-arplant-042811-105441
- Lu, Y., Dai, J. B., and Wu, Q. (2013). Photosynthesis-fermentation hybrid system to produce lipid feedstock for algal biofuel. *Environ. Technol.* 34, 1869–1876. doi: 10.1080/09593330.2013.824011
- Meijer, W. H., van der Klei, I. J., Veenhuis, M., and Kiel, J. A. K. W. (2007). ATG genes involved in non-selective autophagy are conserved from yeast to man, but the selective Cvt and pexophagy pathways also require organism-specific genes. *Autophagy* 3, 106–116. doi: 10.4161/auto.3595
- Miao, X. L., and Wu, Q. Y. (2006). Biodiesel production from heterotrophic microalgal oil. *Bioresour. Technol.* 97, 841–876. doi: 10.1016/j.biortech.2005.04.008
- Mizushima, N. (2007). Autophagy: process and function. *Gene Dev.* 21, 2861–2873. doi: 10.1101/gad.1599207
- Mizushima, N., and Komatsu, M. (2011). Autophagy: renovation of cells and tissues. *Cell* 147, 728–741. doi: 10.1016/j.cell.2011.10.026
- Munafo, D. B., and Colombo, M. I. (2001). A novel assay to study autophagy: regulation of autophagosome vacuole size by amino acid deprivation. *J. Cell Sci.* 114, 3619–3629.
- Perez-Perez, M. E., Couso, I., and Crespo, J. L. (2012). Carotenoid deficiency triggers autophagy in the model green alga *Chlamydomonas reinhardtii*. *Autophagy* 8, 376–388. doi: 10.4161/auto.18864
- Perez-Perez, M. E., Florencio, F. J., and Crespo, J. L. (2010). Inhibition of target of rapamycin signaling and stress activate autophagy in *Chlamydomonas reinhardtii*. *Plant Physiol.* 152, 1874–1888. doi: 10.1104/pp.109.152520
- Roberts, P., Moshitch-Moshkovitz, S., Kvam, E., O'Toole, E., Winey, M., and Goldfarb, D. S. (2003). Piecemeal microautophagy of nucleus in *Saccharomyces cerevisiae*. *Mol. Biol. Cell* 14, 129–141. doi: 10.1091/mbc.E02-08-0483
- Rose, T. L., Bonneau, L., Der, C., Marty-Mazars, D., and Marty, F. (2006). Starvation-induced expression of autophagy-related genes in *Arabidopsis*. *Biol. Cell* 98, 53–67. doi: 10.1042/BC20040516
- Sicko-Goad, L., Evans, M. S., Lazinsky, D., Hall, J., and Simmons, M. S. (1989). Effects of chlorinated benzenes on diatom fatty acid composition and quantitative morphology. IV. Pentachlorobenzene and comparison with trichlorobenzeneisomers. *Arch. Environ. Contam. Toxicol.* 18, 656–668. doi: 10.1007/BF01225004
- Singh, R., Kaushik, S., Wang, Y. J., Xiang, Y. Q., Novak, I., Komatsu, M., et al. (2009). Autophagy regulates lipid metabolism. *Nature* 458, 1131–1135. doi: 10.1038/nature07976
- Takatsuka, C., Inoue, Y., Matsuoka, K., and Moriyasu, Y. (2004). 3-Methyladenine inhibits autophagy in tobacco culture cells under sucrose starvation conditions. *Plant Cell Physiol.* 45, 265–274. doi: 10.1093/pcp/pch031
- Tian, T., Li, Z. P., Hu, W. Q., Ren, H. Y., Tian, E., Zhao, Y., et al. (2010). *C. elegans* screen identifies autophagy genes specific to multicellular organisms. *Cell* 141, 1042–1055. doi: 10.1016/j.cell.2010.04.034
- Tsukada, M., and Ohsumi, Y. (1993). Isolation and characterization of autophagy-defective mutants of *Saccharomyces cerevisiae*. *FEBS Lett.* 333, 169–174. doi: 10.1016/0014-5793(93)80398-E
- van der Vaart, A., Griffith, J., and Reggiori, F. (2010). Exit from the golgi is required for the expansion of the autophagosomal phagophore in yeast *Saccharomyces cerevisiae*. *Mol. Biol. Cell* 21, 2270–2284. doi: 10.1091/mbc.E09-04-0345
- van Zutphen, T., Todde, V., der Boer, R., Kreim, M., Hofbauer, H. F., Wolinski, H., et al. (2014). Lipid droplet autophagy in the yeast *Saccharomyces cerevisiae*. *Mol. Biol. Cell* 25, 290–301. doi: 10.1091/mbc.E13-08-0448
- Walther, T. C., and Farese, R. V. Jr. (2012). Lipid droplets and cellular lipid metabolism. *Annu. Rev. Biochem.* 81, 687–714. doi: 10.1146/annurev-biochem-11009-102430
- Weber, R. W., Wakley, G. E., Thines, E., and Talbot, N. J. (2001). The vacuole as central element of the lytic system and sink for lipid droplets in maturing appressoria of *Magnaporthe grisea*. *Protoplasma* 216, 101–112. doi: 10.1007/BF02680137
- Xia, K. F., Liu, T., Ouyang, J., Wang, R., Fan, T., and Zhang, M. Y. (2011). Genome-wide identification, classification, and expression analysis of autophagy-associated gene homologs in rice (*Oryza sativa L.*). *DNA Res.* 18, 363–377. doi: 10.1093/dnares/dsr024
- Xia, Z. P., and Klionsky, D. J. (2007). Autophagosome formation: core machinery and adaptations. *Nat. Cell Biol.* 9, 1102–1109. doi: 10.1038/ncb1007-1102
- Xiong, W., Gao, C. F., Yan, D., Wu, C., and Wu, Q. Y. (2010). Double CO<sub>2</sub> fixation in photosynthesis-fermentation model enhances algal lipid synthesis for biodiesel production. *Bioresour. Technol.* 101, 2287–2293. doi: 10.1016/j.biortech.2009.11.041
- Yang, Z. F., and Klionsky, D. J. (2009). An overview of the molecular mechanism of autophagy. *Curr. Top. Microbiol. Immunol.* 335, 1–32. doi: 10.1007/978-3-642-00302-8\_1

**Conflict of Interest Statement:** The authors declare that the research was conducted in the absence of any commercial or financial relationships that could be construed as a potential conflict of interest.

Received: 04 June 2014; accepted: 28 July 2014; published online: 14 August 2014.

Citation: Zhao L, Dai J and Wu Q (2014) Autophagy-like processes are involved in lipid droplet degradation in *Auxenochlorella protothecoides* during the heterotrophy-autotrophy transition. *Front. Plant Sci.* 5:400. doi: 10.3389/fpls.2014.00400

This article was submitted to Plant Cell Biology, a section of the journal *Frontiers in Plant Science*.

Copyright © 2014 Zhao, Dai and Wu. This is an open-access article distributed under the terms of the Creative Commons Attribution License (CC BY). The use, distribution or reproduction in other forums is permitted, provided the original author(s) or licensor are credited and that the original publication in this journal is cited, in accordance with accepted academic practice. No use, distribution or reproduction is permitted which does not comply with these terms.



# Roles of autophagy in male reproductive development in plants

Shigeru Hanamata<sup>1,2†</sup>, Takamitsu Kurusu<sup>1,3,4 \*†</sup> and Kazuyuki Kuchitsu<sup>1,4 \*</sup>

<sup>1</sup> Department of Applied Biological Science, Tokyo University of Science, Noda, Japan

<sup>2</sup> Department of Integrated Biosciences, University of Tokyo, Kashiwa, Japan

<sup>3</sup> School of Bioscience and Biotechnology, Tokyo University of Technology, Hachioji, Japan

<sup>4</sup> Research Institute for Science and Technology, Tokyo University of Science, Noda, Japan

**Edited by:**

Diane C. Bassham, Iowa State University, USA

**Reviewed by:**

Byung-Ho Kang, University of Florida, USA

Beatrice Satiat-Jeunemaitre, Centre National de la Recherche Scientifique, France

**\*Correspondence:**

Kazuyuki Kuchitsu, Department of Applied Biological Science, Tokyo University of Science, 2641 Yamazaki, Noda, Chiba 278-8510, Japan  
e-mail: kuchitsu@rs.noda.tus.ac.jp;  
Takamitsu Kurusu, School of Bioscience and Biotechnology, Tokyo University of Technology, 1404-1 Kataura, Hachioji, Tokyo 192-0982, Japan  
e-mail: kurusutkmt@stf.teu.ac.jp

<sup>†</sup> Shigeru Hanamata and Takamitsu Kurusu have contributed equally to this work.

## INTRODUCTION

Reproductive development, both in animals and plants, is accompanied by drastic changes in metabolism for plentiful supply of nutrients and thus requires its appropriate regulation. In flowering plants, the anther exhibits a four-layered structure composed of the epidermis, endothecium, middle layer, and tapetum. Of these layers, the tapetum provides metabolites and nutrients to pollen grains, microspores, and the pollen coat during their development (Ariizumi and Toriyama, 2011). Tapetum contains triacylglycerol (TAG)-containing lipid bodies, which supply essential lipid components during pollen maturation (Li-Beisson et al., 2010; Murphy, 2012). Recent transcriptomic and bioinformatic analyses have suggested some factors that play roles in regulating lipid metabolism in the anther including a receptor-like kinase, proteases, cell wall-degrading enzymes, cytochrome P450 as well as lipid transfer proteins (Wang et al., 2008; Huang et al., 2009).

Autophagy is an evolutionarily conserved system for degradation and recycling of nutrients (Li and Vierstra, 2012). Intracellular components are enveloped by autophagosomal membranes and fused with the vacuoles/lysosomes, in which they are broken down by lytic enzymes. In animals, this process has recently been suggested to be involved in lipid droplet degradation, and defects in lipid autophagy (lipophagy) have been linked to

Autophagy, a major catabolic pathway in eukaryotic cells, is essential in development, maintenance of cellular homeostasis, immunity and programmed cell death (PCD) in multicellular organisms. In plant cells, autophagy plays roles in recycling of proteins and metabolites including lipids, and is involved in many physiological processes such as abiotic and biotic stress responses. However, its roles during reproductive development had remained poorly understood. Quantitative live cell imaging techniques for the autophagic flux and genetic studies in several plant species have recently revealed significant roles of autophagy in developmental processes, regulation of PCD and lipid metabolism. We here review the novel roles of autophagic fluxes in plant cells, and discuss their possible significance in PCD and metabolic regulation, with particular focus on male reproductive development during the pollen maturation.

**Keywords:** autophagic flux, male reproductive development, programmed cell death, tapetum, rice

important metabolic disorders such as fatty liver, obesity, and atherosclerosis (Dong and Czaja, 2011; Liu and Czaja, 2012). In many eukaryotes, autophagy is required for normal development, e.g., for dauer development in nematodes and preimplantation in mice (Tsukamoto et al., 2008; Melendez and Levine, 2009; Mizushima and Komatsu, 2011). In plants, autophagy has been suggested to be involved in seed development and germination, photomorphogenesis, chloroplast maturation, mineral nutrition, hormonal responses, pathogen resistance, stress protection, senescence, and fertile floret development under nutrient-limiting conditions (Ghiglione et al., 2008; Ishida et al., 2008; Chung et al., 2009). However, autophagy-defective *Arabidopsis* mutants exhibit normal life cycles, and little is known on the roles of autophagy during reproductive development in plants (Yoshimoto, 2012).

Programmed cell death (PCD), a genetically regulated form of cell suicide, plays vital roles in numerous physiological and developmental processes in multicellular organisms (Bozhkov and Lam, 2011; Fuchs and Steller, 2011; Teng et al., 2011). In plants, PCD is essential in various stress responses such as innate immunity against pathogen attack, and development including xylogenesis, pollen maturation, leaf senescence, seed germination, and embryogenesis (Pennell and Lamb, 1997). In angiosperms, cells in numerous reproductive organs undergo PCD during

reproductive development, e.g., synergids, the anther tapetum, non-functional megasporangia, the endosperm, the reproductive primordium, style transmitting tissues, abortive pollens, and antipodal cells (Greenberg, 1996; Pennell and Lamb, 1997; Wei et al., 2002). Homologs of many apoptosis-related genes in animals are not found in plants, and hence, it has been postulated that plants have evolved their own PCD mechanisms (Higaki et al., 2011; Li et al., 2011).

Autophagy is also involved in animal PCD (Shimizu et al., 2004; Tsujimoto and Shimizu, 2005), and has also been suggested to play critical roles in leaf senescence, a developmental PCD specific in plants (Ishida et al., 2008; Van Doorn and Woltering, 2010). Recent studies have shown that tapetal PCD, which plays extremely important roles in fertility, is regulated by a transcriptional network, reactive oxygen species (ROS) as well as activation of proteolytic enzymes in several plant species (Phan et al., 2011; Ma et al., 2012; Niu et al., 2013; Xie et al., 2014).

In this review, we describe temporal changes in autophagic flux that occur in tapetal cells and discuss the relationships between these changes and tapetal degeneration or metabolic regulation, with particular emphasis on plant anther development.

## ROLES OF AUTOPHAGY IN RICE ANTER DEVELOPMENT AND POSSIBLE TAPETAL DEGRADATION DURING POLLEN MATURATION

The rice autophagy-defective mutants, *Osatg7* and *Osatg9*, show complete sporophytic male sterility and limited anther dehiscence under normal growth conditions, suggesting that autophagy is crucial in reproductive development in rice (Kurusu et al., 2014).

Pollens of the autophagy-defective mutants are premature due to the significant defects in the anther during pollen maturation, while those of the heterozygous plants are normal and mature as the wild type, and the pollination of wild-type stigmas with the heterozygous pollens resulted in normal fertility. These findings indicate that parental tissue or organ defects cause the immature pollen phenotype displayed by the autophagy-defective mutants.

During pollen development, the tapetum provides metabolites and nutrients to pollen grains and microspores. Autophagosome-like structures, including dense globular bodies enclosed within the vacuoles, are detected in the tapetum during the uninucleate stage (Kurusu et al., 2014). On the other hand, the cytoplasm of the autophagy-defective mutants contained basically no autophagosome-like structures, indicating that autophagy is induced at the uninucleate stage in postmeiotic tapetum cells of rice and may be involved in the catabolism of intracellular components such as plastids and lipid bodies during pollen maturation (Kurusu et al., 2014; **Figures 1A–D**).

As pollens develop, the tapetum is broken down to provide nutrients, metabolites, and sporopollenin precursors to the developing microspores. Defects in tapetal degradation can result in the development of abnormal pollen coats and grains, leading to severe male sterility (Ku et al., 2003; Li et al., 2006; Zhang et al., 2008; Ariizumi and Toriyama, 2011). During tapetal degradation, which is tightly regulated, the characteristic features of PCD such as chromatin condensation, cell shrinkage, endoplasmic reticulum swelling, mitochondrial persistence (Rogers et al., 2005) and nuclear fragmentation (Wang et al., 1999; Vardar and Unal, 2012) are observed.

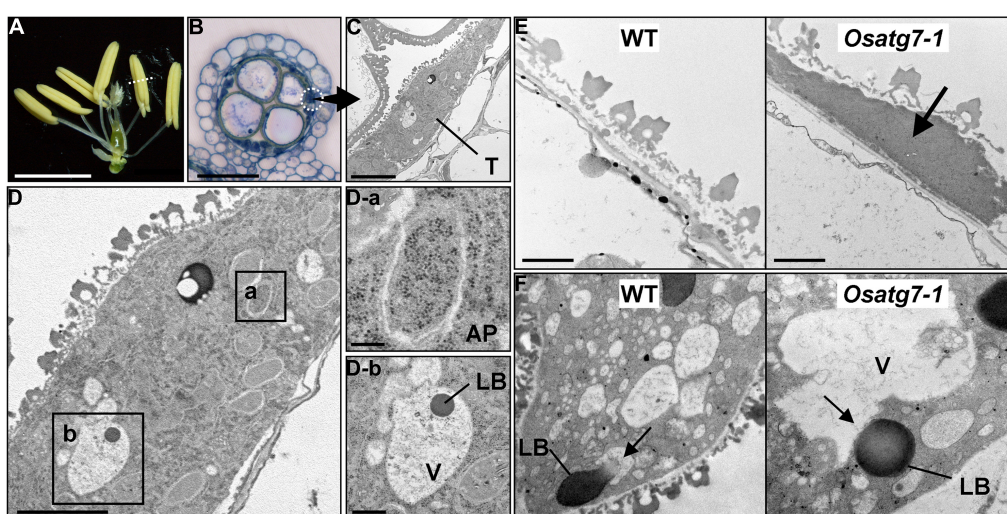


**FIGURE 1 |** Rice autophagy-defective mutants exhibit sporophytic male sterility, and autophagic degradation within tapetal cells is essential for postmeiotic anther development. **(A)** Anthers in the wild-type at the uninucleate stage. Scale bar: 3 mm. **(B)** Transverse sections of wild-type anthers stained with hematoxylin at the uninucleate stage. Scale bar: 50  $\mu$ m. **(C,D)** Autophagosome-like structures and lipid bodies enclosed within the vacuoles detected in postmeiotic tapetum cells during pollen development are depicted. Scale bars: 5  $\mu$ m **(C,D)** and 1  $\mu$ m **(D-a,b)**.

**(E)** Potential role of autophagy in tapetal degradation and programmed cell death in rice. Tapetal ultrastructure of the wild-type and the *Osatg7-1* mutant at the flowering stage. Scale bar: 1  $\mu$ m. Arrows indicate the tapetal cell layers. **(F)** Lipid bodies directly fuse with the vacuoles at the uninucleate stage in the rice tapetum. Scale bar: 1  $\mu$ m. AP, autophagosome; LB, lipid body; V, vacuole; T, tapetum. Arrows indicate the vacuoles fused with lipid bodies in the wild-type (WT). Similar structure was not observed in the *Osatg7-1* mutant.

Appropriate temporal regulation of tapetal PCD is vital for normal pollen development. The signal initiating tapetal PCD has been suggested to be first produced during the tetrad stage (Kawanabe et al., 2006). Gibberellin controls tapetum degradation (Cheng et al., 2004; Aya et al., 2009). A delay in tapetal breakdown and a switch from PCD to necrosis in the tapeta were observed in an *ms1* mutant (Vizcay-Barrena and Wilson, 2006). Pollen wall deposition and the subsequent microspore degeneration failed in a rice mutant in which tapetal degeneration and PCD was retarded (Li et al., 2006, 2011; Zhang et al., 2008).

The rice *Osatg7-1* mutant was found to exhibit reduced anther dehiscence, which may contribute to its sterility (Kurusu et al., 2014). Furthermore, the *Osatg7-1* mutant exhibits a dense thin layer of tapetal tissue that came into contact with the orbicules, which is not observed in the wild-type even at the flowering stage (**Figure 1E**), suggesting that whilst the tapetal cell layer of the wild-type is completely degraded, its remnants remain in the mutant (Kurusu et al., 2014). As well as apoptosis, autophagy also plays a role in PCD and cell degeneration in animals (Shimizu et al., 2004; Tsujimoto and Shimizu, 2005).

Autophagic cell death typically involves the formation of double-membrane autophagosomes within the dying cells, which act to remove cell debris (Gump and Thorburn, 2011). Furthermore, a study examining metamorphosis in *Drosophila melanogaster* found that the destruction of the salivary glands and digestive tract during the latter process were controlled via significant increase in autophagic activity before and during the cell death (Melendez and Neufeld, 2008). Taken together, autophagy may contribute to tapetal breakdown in rice.

Proper timing of tapetal PCD is tightly controlled by an evolutionarily conserved transcriptional network mediated by several key transcription factors (e.g., MYB, MADS families) in *Arabidopsis* and rice. Some proteolytic enzymes including cystein proteases, which play roles in PCD, are often targets of the tapetal transcriptional network (Li et al., 2006; Phan et al., 2011; Niu et al., 2013), suggesting possible involvement of the proteases in the execution of tapetal PCD.

Possible involvement of ROS production has also been suggested to play a role in tapetal PCD. Characteristic ROS accumulation is shown in rice anthers, which was abolished in *mads3* mutant, in which tapetal PCD occurs prematurely (Hu et al., 2011). NADPH oxidase/respiratory burst oxidase homolog (Rboh)-mediated ROS production has recently been suggested to be essential for tapetal PCD progression and pollen development in *Arabidopsis* (Xie et al., 2014). Expression of Rbohs is also regulated by the transcriptional network regulating the tapetal PCD (Xie et al., 2014). Autophagy-deficient mutants of *Arabidopsis* such as *atg5* have been shown to over-accumulate ROS in leaves (Yoshimoto et al., 2009). The potential role of autophagy in the regulation of the tapetal transcriptional network as well as ROS signaling is an important topic for future research.

Dynamic reorganization of the vacuoles mediated by actin microfilament has been suggested to play a critical role in executing various PCD in plants (Higaki et al., 2007, 2011). During the tetrad stage, abnormal vacuolization in the tapetum can lead to inappropriate tapetal PCD, resulting in male sterility (Wan et al., 2010).

Tapetal vacuoles have been suggested to provide enzymes capable of degrading the tetrad wall, which are subsequently secreted into the anther locules (Wu and Yang, 2005). These findings indicate that tapetal vacuoles play significant roles in anther development and PCD. In the tapeta of *Lathyrus undulatus* L., the vacuolar membrane ruptures and the vacuole collapses at the vacuolated microspore stage, resulting in the release of hydrolytic enzymes and the subsequent destruction of cellular components (Vardar and Unal, 2012). Vacuolar processing enzyme (VPE) is expressed in *Arabidopsis* anther (Hatsugai et al., 2006), suggesting that VPE-mediated proteolysis may be involved in tapetal PCD. Dynamics of the vacuole and autophagy during tapetal PCD should be elucidated in various species in order to understand the molecular mechanisms responsible for autophagy-mediated PCD and its physiological significance in reproductive development in plants.

## ROLES OF AUTOPHAGY IN THE REGULATION OF LIPID METABOLISM AND NUTRIENT SUPPLY FROM THE TAPETUM TO DEVELOPING MICROSPORES

During pollen maturation, lipid bodies containing triacyl glycerols (TAGs) in the tapetum are necessary as a supplier of lipid components (Li-Beisson et al., 2010; Murphy, 2012). However, regulation of lipid metabolism including lipid remodeling remains largely unknown.

Lipophagy; i.e., the autophagic catabolism of lipids, is a selective form of autophagy targeting intracellular lipids. In animals, lipophagy is involved in the breakdown of lipid droplets (Dong and Czaja, 2011), and some important metabolic disorders such as atherosclerosis, fatty liver, and obesity have been found to be associated with defective lipophagy (Dong and Czaja, 2011; Liu and Czaja, 2012).

Lipid bodies enclosed in the vacuoles are detected in rice tapetum cells. Lipid body-like structures in the cytoplasm at the bicellular stage are more abundant in the autophagy-defective mutant than the wild type. A lipidomic analysis of the mutant anthers indicated impaired phosphatidylcholine (PC) editing and lipid desaturation during pollen maturation. These results suggest that in rice anthers, tapetal autophagy is involved in breakdown of lipid bodies and regulation of lipid metabolism, especially Lands cycle-mediated PC editing and desaturation, which affect pollen maturation including pollen coat formation (Kurusu et al., 2014). These findings highlight the significance of autophagy-mediated regulation of lipid metabolism in development. Autophagy is also involved in turnover of peroxisomes (Honig et al., 2012; Shibata et al., 2013; Yoshimoto et al., 2014), which play a role in the regulation lipid metabolism/turnover (Linka and Esser, 2012). The potential role of autophagy in the regulation of lipid metabolism is an important topic for future research.

Since autophagy-defective *Arabidopsis* mutants complete their own life cycles (Yoshimoto, 2012), autophagy may not play a critical role in the regulation of anther development in *Arabidopsis*. The most significant difference of the tapetum between dicots and monocots is that dicots have tapetosomes that possess ER-derived vesicles and lipid droplets for delivery to the pollen surface (Hsieh and Huang, 2007), while monocots do not form lipidic tapetosomes in tapetal cells. Moreover, many cereals including rice and a vast majority of other plants contain the secretory-type

tapetum. Their tapetum produces the orbicules termed Ubsisch bodies that mainly transport tapetum-derived sporopollenin precursors to developing microspores. However, no such Ubsisch bodies have been identified in *Brassicaceae* including *Arabidopsis*. A family of lipid transfer proteins is one of the candidates for delivery of sporopollenin precursors from tapetum cells to the developing microspores (Ariizumi and Toriyama, 2011). It may suggest a critical difference in the development of lipidic components in the pollen grains between rice and *Arabidopsis*. In fact, the structures and components of pollen coat are quite different between cereals and *Brassicaceae* (Wilson and Zhang, 2009; Ariizumi and Toriyama, 2011). Detailed imaging analyses of various tapetum developmental stages under environmental stress conditions in the *Arabidopsis* mutants may clarify a novel mechanism for autophagy-mediated PCD and its physiological significance in *Arabidopsis*.

Several types of autophagy-related pathways have been observed in plant and yeast cells. In macroautophagy and the cytoplasm-to-vacuole transport (CVT) pathway, double-membrane structure in the cytoplasm fuses with the vacuole. *Arabidopsis* roots exhibit macroautophagy, in which autophagosomes directly fuse with the vacuoles (Merkulova et al., 2014). On the other hand, in cultured tobacco cells, treatment with E-64c induced the accumulation of autolysosome-like structures around the nucleus, suggesting an alternative autophagic pathway than the macroautophagy (Moriyasu and Ohsumi, 1996). Microautophagy involving invagination of the vacuolar membrane has also been observed (Toooka and Matsuoka, 2006), however, its dynamics are largely unknown in most plant cells. These results imply that there exist multiple autophagic pathways specific to each cell type, species and tissue in plants.

In rice tapetal cells, lipid bodies directly fuse with the vacuoles at the uninucleate stage, which is distinct from macro- or microautophagy and dependent on *OsATG7* (Figure 1F). Further characterization of the dynamics of lipid bodies in the tapetum in various developmental stages in other plant species including *Arabidopsis* along with genetic analyses may reveal a novel function of autophagy related to lipid metabolism and its physiological significance during postmeiotic anther development.

## CONCLUDING REMARKS AND FUTURE PERSPECTIVES

The GFP-ATG8 fusion protein has been shown as a useful marker to monitor the whole process of autophagy in animals and fungi (Klionsky et al., 2007). A tandem fluorescent protein-tagged ATG8 (RFP-YFP-ATG8)-based non-invasive and semi-quantitative monitoring technique for autophagic flux has recently established in tobacco BY-2 cells (Hanamata et al., 2013). A further advantage of this method is that the autophagic activity of the cells can be quantitatively monitored by simply measuring the fluorescence of cell suspension without using inhibitors such as concanamycin A, a vacuolar H<sup>+</sup>-ATPase inhibitor. Moreover, turnover and degradation of an autophagy-specific cargo protein cytochrome *b5* fused with the photoconvertible fluorescent protein Kikume Green-Red (KikGR) has recently been monitored as a useful marker for autophagic flux in tobacco BY-2 cells (Tasaki et al., 2014). These technical advances in combination with genetic analyses may be useful to characterize

environmentally induced autophagy in various specific tissues including tapetum, and reveal novel aspects of autophagy in PCD in plants.

Autophagy is rapidly activated in response to various stimuli as well as developmental processes to induce dynamic reorganization of cytoplasmic components and is involved in the regulation of a wide range of physiological functions in plants. The duration, frequency, amplitude, and selectivity of autophagy seem to affect the specificity of autophagic signaling. Recent studies on ATG proteins have revealed their complex structures, diversity, and regulatory mechanisms, and the identification of ATG8-interacting proteins that recruit specific cargo to the enveloping phagophore sheds new light in the selectivity of autophagy *in planta*. For future studies, more information on autophagy-mediated signaling events including downstream effectors and signaling cascades is required to better understand their roles. In addition, genetic studies in many plant species and molecular characterization of their associated molecules are necessary to understand their functions.

## ACKNOWLEDGMENTS

This study was supported, in part, by Grants-in-Aid for Scientific Research on Priority Area Nos. 21117516 and 23117718 and Grants-in-Aid for Scientific Research B Nos. 19370023 and 23380027 to Kazuyuki Kuchitsu from MEXT, Japan.

## REFERENCES

- Ariizumi, T., and Toriyama, K. (2011). Genetic regulation of sporopollenin synthesis and pollen exine development. *Annu. Rev. Plant Biol.* 62, 437–460. doi: 10.1146/annurev-arplant-042809-112312
- Aya, K., Ueguchi-Tanaka, M., Kondo, M., Hamada, K., Yano, K., Nishimura, M., et al. (2009). Gibberellin modulates anther development in rice via the transcriptional regulation of GAMYB. *Plant Cell* 21, 1453–1472. doi: 10.1105/tpc.108.062935
- Bozhkov, P. V., and Lam, E. (2011). Green death: revealing programmed cell death in plants. *Cell Death Differ.* 18, 1239–1240. doi: 10.1038/cdd.2011.86
- Cheng, H., Qin, L., Lee, S., Fu, X., Richards, D. E., Cao, D., et al. (2004). Gibberellin regulates *Arabidopsis* floral development via suppression of DELLA protein function. *Development* 131, 1055–1064. doi: 10.1242/dev.00992
- Chung, T., Suttangkakul, A., and Vierstra, R. D. (2009). The ATG autophagic conjugation system in maize: ATG transcripts and abundance of the ATG8-lipid adduct are regulated by development and nutrient availability. *Plant Physiol.* 149, 220–234. doi: 10.1104/pp.108.126714
- Dong, H., and Czaja, M. J. (2011). Regulation of lipid droplets by autophagy. *Trends Endocrinol. Metab.* 22, 234–240. doi: 10.1016/j.tem.2011.02.003
- Fuchs, Y., and Steller, H. (2011). Programmed cell death in animal development and disease. *Cell* 147, 742–758. doi: 10.1016/j.cell.2011.10.033
- Ghiglione, H. O., Gonzalez, F. G., Serrago, R., Maldonado, S. B., Chilcott, C., Cura, J. A., et al. (2008). Autophagy regulated by day length determines the number of fertile florets in wheat. *Plant J.* 55, 1010–1024. doi: 10.1111/j.1365-313X.2008.03570.x
- Greenberg, J. T. (1996). Programmed cell death: a way of life for plants. *Proc. Natl. Acad. Sci. U.S.A.* 93, 12094–12097. doi: 10.1073/pnas.93.22.12094
- Gump, J. M., and Thorburn, A. (2011). Autophagy and apoptosis: what is the connection? *Trends Cell Biol.* 21, 387–392. doi: 10.1016/j.tcb.2011.03.007
- Hanamata, S., Kurusu, T., Okada, M., Suda, A., Kawamura, K., Tsukada, E., et al. (2013). In vivo imaging and quantitative monitoring of autophagic flux in tobacco BY-2 cells. *Plant Signal. Behav.* 8:e22510. doi: 10.4161/psb.22510
- Hatsugai, N., Kuroyanagi, M., Nishimura, M., and Hara-Nishimura, I. (2006). A cellular suicide strategy of plants: vacuole-mediated cell death. *Apoptosis* 11, 905–911. doi: 10.1007/s10495-006-6601-1
- Higaki, T., Goh, T., Hayashi, T., Kutsuna, N., Kadota, Y., Hasezawa, S., et al. (2007). Elicitor-induced cytoskeletal rearrangement relates to vacuolar dynamics and

- execution of cell death: in vivo imaging of hypersensitive cell death in tobacco BY-2 cells. *Plant Cell Physiol.* 48, 1414–1425. doi: 10.1093/pcp/pcm109
- Higaki, T., Kurusu, T., Hasezawa, S., and Kuchitsu, K. (2011). Dynamic intracellular reorganization of cytoskeletons and the vacuole in defense responses and hypersensitive cell death in plants. *J. Plant Res.* 124, 315–324. doi: 10.1007/s10265-011-0408-z
- Honig, A., Avin-Wittenberg, T., Ufaz, S., and Galili, G. (2012). A new type of compartment, defined by plant-specific Atg8-interacting proteins, is induced upon exposure of *Arabidopsis* plants to carbon starvation. *Plant Cell* 24, 288–303. doi: 10.1105/tpc.111.093112
- Hsieh, K., and Huang, A. H. (2007). Tapetosomes in *Brassica* tapetum accumulate endoplasmic reticulum-derived flavonoids and alkanes for delivery to the pollen surface. *Plant Cell* 19, 582–596. doi: 10.1105/tpc.106.049049
- Hu, L., Liang, W., Yin, C., Cui, X., Zong, J., Wang, X., et al. (2011). Rice MADS3 regulates ROS homeostasis during late anther development. *Plant Cell* 23, 515–533. doi: 10.1105/tpc.110.074369
- Huang, M. D., Wei, F. J., Wu, C. C., Hsing, Y. I., and Huang, A. H. (2009). Analyses of advanced rice anther transcriptomes reveal global tapetum secretory functions and potential proteins for lipid exine formation. *Plant Physiol.* 149, 694–707. doi: 10.1104/pp.108.131128
- Ishida, H., Yoshimoto, K., Izumi, M., Reisen, D., Yano, Y., Makino, A., et al. (2008). Mobilization of rubisco and stroma-localized fluorescent proteins of chloroplasts to the vacuole by an ATG gene-dependent autophagic process. *Plant Physiol.* 148, 142–155. doi: 10.1104/pp.108.122770
- Kawanabe, T., Ariizumi, T., Kawai-Yamada, M., Uchimiya, H., and Toriyama, K. (2006). Abolition of the tapetum suicide program ruins microsporogenesis. *Plant Cell Physiol.* 47, 784–787. doi: 10.1093/pcp/pcj039
- Klionsky, D. J., Cuervo, A. M., and Seglen, P. O. (2007). Methods for monitoring autophagy from yeast to human. *Autophagy* 3, 181–206. doi: 10.4161/auto.3678
- Ku, S. J., Yoon, H., Suh, H. S., and Chung, Y. Y. (2003). Male-sterility of thermosensitive genic male-sterile rice is associated with premature programmed cell death of the tapetum. *Planta* 217, 559–565. doi: 10.1007/s00425-003-1030-7
- Kurusu, T., Koyano, T., Hanamata, S., Kubo, T., Noguchi, Y., Yagi, C., et al. (2014). OsATG7 is required for autophagy-dependent lipid metabolism in rice postmeiotic anther development. *Autophagy* 10, 878–888. doi: 10.4161/auto.28279
- Li-Besson, Y., Shorrosh, B., Beisson, F., Andersson, M. X., Arondel, V., Bates, P. D., et al. (2010). Acyl-lipid metabolism. *Arabidopsis Book* 8:e0133. doi: 10.1199/tab.0133
- Li, F., and Vierstra, R. D. (2012). Autophagy: a multifaceted intracellular system for bulk and selective recycling. *Trends Plant Sci.* 17, 526–537. doi: 10.1016/j.tplants.2012.05.006
- Li, N., Zhang, D. S., Liu, H. S., Yin, C. S., Li, X. X., Liang, W. Q., et al. (2006). The rice tapetum degeneration retardation gene is required for tapetum degradation and anther development. *Plant Cell* 18, 2999–3014. doi: 10.1105/tpc.106.044107
- Li, X., Gao, X., Wei, Y., Deng, L., Ouyang, Y., Chen, G., et al. (2011). Rice APOPTOSIS INHIBITOR5 coupled with two DEAD-box adenosine 5'-triphosphate-dependent RNA helicases regulates tapetum degeneration. *Plant Cell* 23, 1416–1434. doi: 10.1105/tpc.110.082636
- Linka, N., and Esser, C. (2012). Transport proteins regulate the flux of metabolites and cofactors across the membrane of plant peroxisomes. *Front. Plant Sci.* 3:3. doi: 10.3389/fpls.2012.00003
- Liu, K., and Czaja, M. J. (2012). Regulation of lipid stores and metabolism by lipophagy. *Cell Death Differ.* 20, 3–11. doi: 10.1038/cdd.2012.63
- Ma, X., Feng, B., and Ma, H. (2012). AMS-dependent and independent regulation of anther transcriptome and comparison with those affected by other *Arabidopsis* anther genes. *BMC Plant Biol.* 12:23. doi: 10.1186/1471-2229-12-23
- Melendez, A., and Levine, B. (2009). “Autophagy in *C. elegans*,” in *WormBook*, eds J. M. Kramer, D. C. Moerman, and The *C. elegans* Research Community. Available at: <http://www.wormbook.org/>
- Melendez, A., and Neufeld, T. P. (2008). The cell biology of autophagy in metazoans: a developing story. *Development* 135, 2347–2360. doi: 10.1242/dev.016105
- Merkulova, E. A., Guiboileau, A., Naya, L., Masclaux-Daubresse, C., and Yoshimoto, K. (2014). Assessment and optimization of autophagy monitoring methods in *Arabidopsis* roots indicate direct fusion of autophagosomes with vacuoles. *Plant Cell Physiol.* 55, 715–726. doi: 10.1093/pcp/pcu041
- Mizushima, N., and Komatsu, M. (2011). Autophagy: renovation of cells and tissues. *Cell* 147, 728–741. doi: 10.1016/j.cell.2011.10.026
- Moriyasu, Y., and Ohsumi, Y. (1996). Autophagy in tobacco suspension-cultured cells in response to sucrose starvation. *Plant Physiol.* 111, 1233–1241.
- Murphy, D. J. (2012). The dynamic roles of intracellular lipid droplets: from archaea to mammals. *Protoplasma* 249, 541–585. doi: 10.1007/s00709-011-0329-7
- Niu, N., Liang, W., Yang, X., Jin, W., Wilson, Z. A., Hu, J., et al. (2013). EAT1 promotes tapetal cell death by regulating aspartic proteases during male reproductive development in rice. *Nat. Commun.* 4:1445. doi: 10.1038/ncomms2396
- Pennell, R. I., and Lamb, C. (1997). Programmed cell death in plants. *Plant Cell* 9, 1157–1168. doi: 10.1105/tpc.9.7.1157
- Phan, H. A., Iacuone, S., Li, S. F., and Parish, R. W. (2011). The MYB80 transcription factor is required for pollen development and the regulation of tapetal programmed cell death in *Arabidopsis thaliana*. *Plant Cell* 23, 2209–2224. doi: 10.1105/tpc.110.082651
- Rogers, L. A., Dubos, C., Surman, C., Willment, J., Cullis, I. F., Mansfield, S. D., et al. (2005). Comparison of lignin deposition in three ectopic lignification mutants. *New Phytol.* 168, 123–140. doi: 10.1111/j.1469-8137.2005.01496.x
- Shibata, M., Oikawa, K., Yoshimoto, K., Kondo, M., Mano, S., Yamada, K., et al. (2013). Highly oxidized peroxisomes are selectively degraded via autophagy in *Arabidopsis*. *Plant Cell* 25, 4967–4983. doi: 10.1105/tpc.113.116947
- Shimizu, S., Kanaseki, T., Mizushima, N., Mizuta, T., Arakawa-Kobayashi, S., Thompson, C. B., et al. (2004). Role of Bcl-2 family proteins in a non-apoptotic programmed cell death dependent on autophagy genes. *Nat. Cell Biol.* 6, 1221–1228. doi: 10.1038/ncb1192
- Tasaki, M., Asatuma, S., and Matsuoka, M. (2014). Monitoring protein turnover during phosphate starvation-dependent autophagic degradation using a photoconvertible fluorescent protein aggregate in tobacco BY-2 cells. *Front. Plant Sci.* 5:172. doi: 10.3389/fpls.2014.00172
- Teng, X., Cheng, W. C., Qi, B., Yu, T. X., Ramachandran, K., Boersma, M. D., et al. (2011). Gene-dependent cell death in yeast. *Cell Death Dis.* 2:e188. doi: 10.1038/cddis.2011.72
- Toyooka, K., and Matsuoka, K. (2006). “Autophagy and non-classical vacuolar targeting in tobacco BY-2 cells,” in *Biotechnology in Agriculture and Forestry*, Vol. 58, eds T. Nagata, K. Matsuoka, and D. Inze (Berlin: Springer-Verlag), 167–180.
- Tsujimoto, Y., and Shimizu, S. (2005). Another way to die: autophagic programmed cell death. *Cell Death Differ.* 12(Suppl. 2), 1528–1534. doi: 10.1038/sj.cdd.4401777
- Tsukamoto, S., Kuma, A., Murakami, M., Kishi, C., Yamamoto, A., and Mizushima, N. (2008). Autophagy is essential for preimplantation development of mouse embryos. *Science* 321, 117–120. doi: 10.1126/science.1154822
- Van Doorn, W. G., and Woltering, E. J. (2010). What about the role of autophagy in PCD? *Trends Plant Sci.* 15, 361–362. doi: 10.1016/j.tplants.2010.04.009
- Vardar, F., and Unal, M. (2012). Ultrastructural aspects and programmed cell death in the tapetal cells of *Lathyrus undulatus* Boiss. *Acta Biol. Hung.* 63, 52–66. doi: 10.1556/ABiol.63.2012.1.5
- Vizcay-Barrena, G., and Wilson, Z. A. (2006). Altered tapetal PCD and pollen wall development in the *Arabidopsis ms1* mutant. *J. Exp. Bot.* 57, 2709–2717. doi: 10.1093/jxb/erl032
- Wan, L., Xia, X., Hong, D., Li, J., and Yang, G. (2010). Abnormal vacuolization of the tapetum during the tetrad stage is associated with male sterility in the recessive genic male sterile *Brassica napus* L. Line 9012A. *J. Plant Biol.* 53, 121–133. doi: 10.1007/s12374-009-9095-x
- Wang, M., Hoekstra, S., Van Bergen, S., Lamers, G. E., Oppedijk, B. J., Van Der Heijden, M. W., et al. (1999). Apoptosis in developing anthers and the role of ABA in this process during androgenesis in *Hordeum vulgare* L. *Plant Mol. Biol.* 39, 489–501. doi: 10.1023/A:1006198431596
- Wang, Y., Wu, H., and Yang, M. (2008). Microscopy and bioinformatic analyses of lipid metabolism implicate a sporophytic signaling network supporting pollen development in *Arabidopsis*. *Mol. Plant* 1, 667–674. doi: 10.1093/mp/ssn027
- Wei, C. X., Lan, S. Y., and Xu, Z. X. (2002). Ultrastructural features of nucleus degradation during programmed cell death of starch endosperm cells in rice. *Acta Bot. Sin.* 44, 1396–1402.
- Wilson, Z. A., and Zhang, D. B. (2009). From *Arabidopsis* to rice: pathways in pollen development. *J. Exp. Bot.* 60, 1479–1492. doi: 10.1093/jxb/erp095
- Wu, H., and Yang, M. (2005). Reduction in vacuolar volume in the tapetal cells coincides with conclusion of the tetrad stage in *Arabidopsis thaliana*. *Sex. Plant Reprod.* 18, 173–178. doi: 10.1007/s00497-005-0010-4
- Xie, H. T., Wan, Z. Y., Li, S., and Zhang, Y. (2014). Spatiotemporal production of reactive oxygen species by NADPH Oxidase is critical for tapetal programmed

- cell death and pollen development in *Arabidopsis*. *Plant Cell* 26, 2007–2023. doi: 10.1105/tpc.114.125427
- Yoshimoto, K. (2012). Beginning to understand autophagy, an intracellular self-degradation system in plants. *Plant Cell Physiol.* 53, 1355–1365. doi: 10.1093/pcp/pcs099
- Yoshimoto, K., Jikumaru, Y., Kamiya, Y., Kusano, M., Consonni, C., Panstruga, R., et al. (2009). Autophagy negatively regulates cell death by controlling NPR1-dependent salicylic acid signaling during senescence and the innate immune response in *Arabidopsis*. *Plant Cell* 21, 2914–2927. doi: 10.1105/tpc.109.068635
- Yoshimoto, K., Shibata, M., Kondo, M., Oikawa, K., Sato, M., Toyooka, K., et al. (2014). Organ-specific quality control of plant peroxisomes is mediated by autophagy. *J. Cell Sci.* 127, 1161–1168. doi: 10.1242/jcs.139709
- Zhang, D. S., Liang, W. Q., Yuan, Z., Li, N., Shi, J., Wang, J., et al. (2008). Tapetum degeneration retardation is critical for aliphatic metabolism and gene regulation during rice pollen development. *Mol. Plant* 1, 599–610. doi: 10.1093/mp/ssn028

**Conflict of Interest Statement:** The authors declare that the research was conducted in the absence of any commercial or financial relationships that could be construed as a potential conflict of interest.

*Received: 27 May 2014; accepted: 23 August 2014; published online: 15 September 2014.*

*Citation: Hanamata S, Kurusu T and Kuchitsu K (2014) Roles of autophagy in male reproductive development in plants. Front. Plant Sci. 5:457. doi: 10.3389/fpls.2014.00457*

*This article was submitted to Plant Cell Biology, a section of the journal Frontiers in Plant Science.*

*Copyright © 2014 Hanamata, Kurusu and Kuchitsu. This is an open-access article distributed under the terms of the Creative Commons Attribution License (CC BY). The use, distribution or reproduction in other forums is permitted, provided the original author(s) or licensor are credited and that the original publication in this journal is cited, in accordance with accepted academic practice. No use, distribution or reproduction is permitted which does not comply with these terms.*



# Functions of autophagy in plant carbon and nitrogen metabolism

Chenxia Ren<sup>†</sup>, Jingfang Liu<sup>†</sup> and Qingqiu Gong\*

Tianjin Key Laboratory of Protein Science and Department of Plant Biology and Ecology, College of Life Sciences, Nankai University, Tianjin, China

**Edited by:**

Jose Luis Crespo, Consejo Superior de Investigaciones Científicas, Spain

**Reviewed by:**

Viktor Zarsky, Charles University, Czech Republic

Celine Masclaux-Daubresse, Institut National de la Recherche Agronomique, France

**\*Correspondence:**

Qingqiu Gong, Tianjin Key Laboratory of Protein Science and Department of Plant Biology and Ecology, A513 Biology Station, College of Life Sciences, Nankai University, 94 Weijin Road, Nankai District, Tianjin 300071, China

e-mail: gongq2@gmail.com

<sup>†</sup>Chenxia Ren and Jingfang Liu have contributed equally to this work.

Carbon and nitrogen are essential components for plant growth. Although models of plant carbon and nitrogen metabolisms have long been established, certain gaps remain unfilled, such as how plants are able to maintain a flexible nocturnal starch turnover capacity over various light cycles, or how nitrogen remobilization is achieved during the reproductive growth stage. Recent advances in plant autophagy have shed light on such questions. Not only does autophagy contribute to starch degradation at night, but it participates in the degradation of chloroplast proteins and even chloroplasts after prolonged carbon starvation, thus help maintain the free amino acid pool and provide substrate for respiration. The induction of autophagy under these conditions may involve transcriptional regulation. Large-scale transcriptome analyses revealed that *ATG8e* belongs to a core carbon signaling response shared by *Arabidopsis* accessions, and the transcription of *Arabidopsis ATG7* is tightly co-regulated with genes functioning in chlorophyll degradation and leaf senescence. In the reproductive phase, autophagy is essential for bulk degradation of leaf proteins, thus contributes to nitrogen use efficiency (NUE) both under normal and low-nitrogen conditions.

**Keywords:** autophagy, carbon, nitrogen, chloroplast, starch

## INTRODUCTION

Eukaryotic cells carry out autophagy to clean up the house and keep fit (Yang and Klionsky, 2010). The hallmark of autophagy is the formation of a double-membrane vesicle, the autophagosome, and its subsequent fusion with the lysosome or the lytic vacuole (Mizushima et al., 2011). The cargoes inside the autophagosome are then degraded; free amino acids are released back into the cytosol (Mizushima et al., 2011). Conserved from yeasts to plants, this bulk degradation pathway is highly efficient in turning over proteins and organelles, and has an essential role in maintaining free amino acid pools upon starvation (Onodera and Ohsumi, 2005; Thompson and Vierstra, 2005). Defects in autophagy compromises plant vitality and disease resistance mostly in a salicylic acid signaling-dependent way (Liu et al., 2005; Yoshimoto et al., 2009; Lai et al., 2011; Lenz et al., 2011; Wang et al., 2011). Autophagy mutants are generally sensitive towards abiotic stresses (Liu et al., 2009; Zhou et al., 2013), have lower levels of anthocyanin biosynthesis (Masclaux-Daubresse et al., 2014), and produce less seeds than the wild-type (Hanaoka et al., 2002; Guiboileau et al., 2012).

Studies over the past 15 years have successfully defined the autophagy process in plants (Liu and Bassham, 2012; Li and Vierstra, 2012). Nearly all core machinery AuTophagy (ATG) proteins identified based on their sequence homology to the yeast and mammalian homologs (Xie and Klionsky, 2007). Molecular functions of the plant ATGs have been verified both through *in vivo*, genetic and physiological studies (Liu and Bassham, 2012; Li and Vierstra, 2012) and *in vitro* reconstitution (Fujioka

et al., 2008). The basic mechanisms of plant autophagy now have been confirmed to be similar to those of yeasts and animals.

Moreover, plant-specific, autophagy-related genes and functions have been discovered (Ishida et al., 2008; Wada et al., 2009; Izumi et al., 2010, 2013; Honig et al., 2012; Ono et al., 2013; Wang et al., 2013). Through these findings, a unique link between autophagy and plant carbon status can be seen. Also different from the yeast, plant autophagy genes are regulated not only post-transcriptionally (Suttangkakul et al., 2011; Li et al., 2014), but transcriptionally. Recent studies have also revealed a function for autophagy in nitrogen remobilization (Guiboileau et al., 2012, 2013; Xia et al., 2012), thus pointing out a new direction for the study of plant nitrogen metabolism and yield formation. More details are discussed hereafter.

## TRANSCRIPTION OF PLANT ATG GENES ARE REGULATED BY CARBON AND NITROGEN STATUS

Most yeast ATG genes are not regulated transcriptionally. For instance, upon nitrogen starvation, only *ATG8* and *ATG14* are promptly and significantly induced (Kirisako et al., 1999; Chan et al., 2001). In contrast, many plant ATG genes are transcriptionally regulated. The mRNA levels of rice ATG genes have been reported to be strongly regulated by nitrogen level, abiotic stresses, and hormones (Xia et al., 2011). Sucrose starvation induced waves of expression of core machinery ATG genes in *Arabidopsis* suspension culture (Rose et al., 2006). In tobacco leaves, transcript levels of several ATG genes are elevated during the night (Wang et al., 2013). Furthermore, transcription of individual *ATG8* and *ATG18*

genes is regulated differently upon carbon and nitrogen starvation, and further exhibits tissue-specificity (Yoshimoto et al., 2004; Xiong et al., 2005; Xia et al., 2012).

More importantly, large-scale analyses have suggested the possible involvement of certain *ATG* genes in plant carbon metabolism and signaling. *ATG8e* was identified as one of 26 genes that constitute a robust core of a carbon signaling response shared by a large number of *Arabidopsis* accessions (Sulpice et al., 2009). In a graphical Gaussian model (GGM) constructed over 2000 *Arabidopsis* Affymetrix gene chips which captures only very strong correlations in transcript levels (Ma et al., 2007), several *ATG* genes emerged as hubs of sub-networks (**Figure 1**). For instance, *ATG7*, encoding the E1-like activating enzyme for both *ATG8* and *ATG12* conjugation, is surrounded by key regulators and marker genes of leaf senescence such as *MYB2*, *AtNAP*, *SAG12*, and *NYE1* (**Figure 1**). According to the guilty by association rule, *ATG7* is likely a hub during plant senescence, when carbon is used for leaf energy and nitrogen gets remobilized (Diaz et al., 2008). Clearly, compared with unicellular eukaryotes, higher plants have extended the regulatory repertoire to better adapt to the changing environment and to efficiently allocate essential resources throughout their lifespan.

### AUTOPHAGY PARTICIPATES IN STARCH BREAKDOWN

The diurnal cycle has a great impact on the life of a plant. During the day, the plant fixes carbon; at night, remobilization of starch supports respiration and growth. An intriguing fact about starch breakdown is that the rate can be adjusted to suit a range of day lengths, always with little left by dawn (Smith and Stitt, 2007), thus enabling the plant to maintain a maximum growth rate possible. Genetic and biochemical studies have established the starch degradation pathway (Stitt and Zeeman, 2012), and regulation of starch degradation has been shown to be circadian rhythm-dependent (Graf et al., 2010). Nevertheless, new questions have been raised, such as what exactly the clock signals are and how they are integrated with the

information on the remaining amount of starch (Stitt and Zeeman, 2012).

The newly reported, autophagy-dependent starch degradation pathway has shed some light on the questions (Wang et al., 2013). Several core machinery *ATG* genes are transcriptionally regulated by the diurnal cycle (Wang et al., 2013). The number of autophagosomes gets higher before dusk, and goes back to normal by dawn. In contrast to the wild-type, several *atg* mutants have starch left on their plates in the morning (Wang et al., 2013). Interestingly, the starch granules that are transported into the vacuole by autophagosomes are much smaller than the remaining ones in the chloroplast, suggesting that the autophagy-dependent pathway might be a complement to the classic degradation pathway (Wang et al., 2013).

### AUTOPHAGY IS INDUCED BY LEAF CARBON DEFICIENCY TO MAINTAIN ENERGY LEVELS

The chloroplast is not only the site for photosynthesis, but stocks 75–80% of total leaf nitrogen (Makino and Osmond, 1991). Transcriptome analyses showed that, when a plant is severely challenged by stresses, suppression of chloroplast activities and activation of protein turnover pathways (including autophagy) both happen at the same time (Gong et al., 2005; Ma et al., 2006). During leaf senescence, not only proteins inside the chloroplast but also pieces of chloroplast are recycled (Hortensteiner and Feller, 2002; Otegui et al., 2005; Martinez et al., 2008a). Whether such degradation involves autophagy has unsurprisingly become a hot topic in recent years.

Anyone who has worked with protoplasts may have noticed that, after kept in the dark for a prolonged period of time, chloroplasts within a single mesophyll protoplast become less in number and smaller in size (Contento et al., 2005). Although chloroplast protein turnover have been studied extensively (Hortensteiner, 2006; Martinez et al., 2008b), recently identified autophagy-dependent chloroplast protein degradation further advanced our

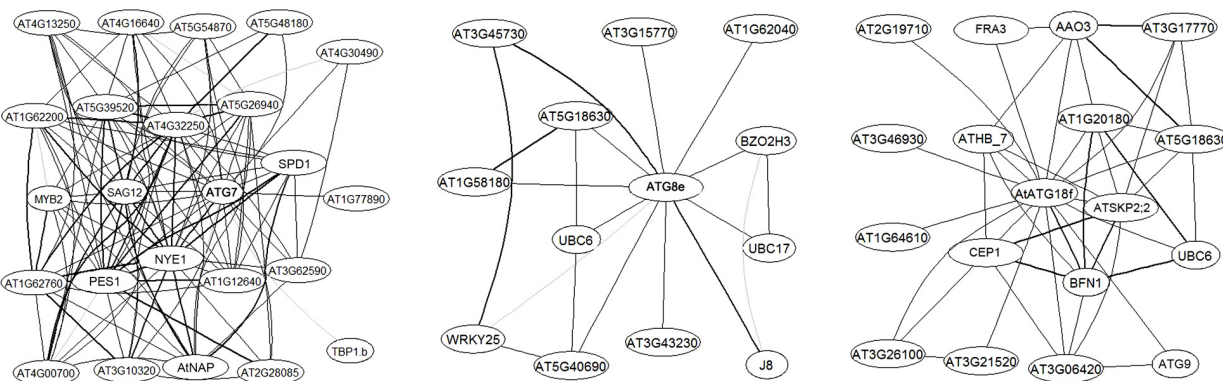


**FIGURE 1 |** At*ATG7*, At*ATG8e*, and At*ATG18f* are hubs in *Arabidopsis* transcriptional networks. The network was built as described in Ma et al. (2007). Sub-networks centered on the *ATG* genes with a maximum of two steps are extracted from the expanded network. Genes are labeled with their

primary gene symbols (TAIR10) wherever possible. AGI numbers are provided otherwise. Edges, i.e., links between nodes, represent co-expression. Correlation levels are represented by the width of the lines, with the boldest lines indicating top 20% correlation values.

understanding of the process, as reviewed recently (Ishida et al., 2014). After dark treatment (combined with vacuolar H<sup>+</sup>-ATPase inhibitor Concanamycin A), *Arabidopsis* mesophyll cells accumulate RuBisCO-containing bodies (RCBs) and structures containing pieces of chloroplasts in the lytic vacuole, whereas in *atg4a atg4b-1* double mutants neither can be seen (Ishida et al., 2008; Wada et al., 2009). Consistently, the number of chloroplasts is not reduced in *atg4a atg4b-1* mesophyll cells after prolonged carbon starvation, and the size of chloroplasts is only partially reduced (Wada et al., 2009). RCBs also appeared to be more sensitive to carbon starvation than to nitrogen starvation, and by adding carbohydrates to the culture, accumulation of RCBs is inhibited (Izumi et al., 2010). Furthermore, starchless mutants *pgm1-1* and *adg1-1* accumulate more RCBs than the wild-type, whereas less RCBs can be seen in starch-excess mutants *sex1-1* and *mex1-3*, suggesting that this specific form of plant autophagy may be controlled by starch levels (Izumi et al., 2010). Finally, in the latest report by Izumi et al. (2013) autophagy was suggested to contribute to the maintenance of the free amino acid pool during carbon starvation, thus providing energy source for respiration.

### AUTOPHAGY CONTRIBUTES TO NITROGEN REMOBILIZATION AND SEED PRODUCTION

Nitrogen is an essential element for plants. To turn soil nitrogen into macromolecules such as amino acids, nucleic acids, and chlorophyll, nitrogen uptake, assimilation, translocation, and remobilization must be coordinately executed by the plant (Masclaux-Daubresse et al., 2010; Xu et al., 2012; Avila-Ospina et al., 2014). Recent studies have illuminated the functions of plant autophagy in nitrogen remobilization both under starvation conditions and during normal growth phases.

Nitrogen starvation has been used by yeast, animal, and plant researchers as a standard procedure to induce autophagy. The *Arabidopsis* autophagy mutants, such as *atg5*, *atg10*, *atg13a* *atg13b*, and *ATG18a RNAi*, are all less tolerant to nitrogen limitation compared to the wild-type (Thompson et al., 2005; Xiong et al., 2005; Phillips et al., 2008; Suttangkakul et al., 2011), confirming a role for autophagy in nitrogen recycling. Consistently, over-expression of *GmATG8c*, an ATG8 homolog from soybean, confers tolerance towards nitrogen limitation both in soybean calli and in transgenic *Arabidopsis* (Xia et al., 2012).

After a transition from vegetative phase into reproductive phase, a plant produces seeds to complete its life cycle. At this stage, leaves generally have started to senesce, and nitrogen source obtained from uptake and assimilation is usually not enough to support seed development (Lim et al., 2007). Leaf nitrogen remobilization thus becomes a critical step during seed maturation (Masclaux-Daubresse et al., 2010).

Guiboileau et al. (2012) discovered that, in several *atg* mutants and RNAi plants, nitrogen use efficiency (NUE), represented by the nitrogen harvest index (NHI): Harvest index (HI) ratio, is lower than that of the wild-type both at the nitrogen-rich condition (+N) and over nitrogen limitation (-N). The lower NUE was shown to be independent of seed productivity (Guiboileau et al., 2012). They also demonstrated that the lower

NUE of *atg* mutants is due to a defect of nitrogen remobilization leading to the accumulation of undigested soluble proteins in their leaves (Guiboileau et al., 2013). Similarly, using transgenic *Arabidopsis* lines carrying 35S:*GmATG8c*, we found that the transgenic lines with higher levels of autophagy have comparable nitrogen concentrations to the wild-type at -N condition, yet maintain a higher biomass at both +N and -N conditions, and enter the reproductive phase earlier to produce more branches and more siliques at +N condition (Xia et al., 2012). Upon seed maturation, the transgenic lines also had slightly but significantly more seeds in each silique, however, the 1000 grain weight stays unchanged (Xia et al., 2012). These results indicate that a higher level of autophagy can better facilitate the flux of nitrogen from source to sink, thus enabling more flower production and subsequent seed setting. Taken together, autophagy can be considered as an essential factor in nitrogen remobilization.

### PERSPECTIVES

So far, studies have elucidated many basic molecular mechanisms and physiological and pathological consequences of autophagy in plants. The relationships between autophagy and plant carbon and nitrogen metabolism have started to be revealed. It can be expected that in the coming years, more interesting and fundamental researches will emerge to solve more existing problems in plant cell biology and plant metabolism. For instance, is there a common set of transcription regulators for the induction of plant ATG genes? Construction of higher-order gene regulatory networks will certainly be useful. Can the newly identified role of autophagy in starch degradation be integrated into the classic model of nocturnal starch turnover? The core machinery genes are generally controlled by the circadian rhythm; however, are they directly linked to the yet unidentified clock signals? Both mathematical modeling and well-planned screening may help answer these questions. Finally, the interaction between carbon and nitrogen has always been a vital topic in plant metabolism and signaling, and autophagy now appears to have a leading role (Guiboileau et al., 2013). The detailed molecular mechanism behind the link still waits to be explored. Given the importance of autophagy in maintaining cell homeostasis and plant vitality, future discoveries will not only advance our understanding in plant autophagy, but also surely be applicable in crop improvement.

### ACKNOWLEDGMENTS

We apologize to colleagues whose works are not cited due to space limitations. We thank Dr. Zhiping Xie for critical reading of the manuscript. Research in Gong lab is supported by the National Key Basic Research Program of China (2011CB910100), the Tianjin Research Program of Applied Basic and Cutting-edge Technologies (No. 11JCZDJC16400), and the Fundamental Research Funds for the Central Universities.

### REFERENCES

- Avila-Ospina, L., Moison, M., Yoshimoto, K., and Masclaux-Daubresse, C. (2014). Autophagy, plant senescence, and nutrient recycling. *J. Exp. Bot.* doi: 10.1093/jxb/eru039 [Epub ahead of print].

- Chan, T. F., Bertram, P. G., Ai, W., and Zheng, X. F. (2001). Regulation of APG14 expression by the GATA-type transcription factor Gln3p. *J. Biol. Chem.* 276, 6463–6467. doi: 10.1074/jbc.M008162200
- Contento, A. L., Xiong, Y., and Bassham, D. C. (2005). Visualization of autophagy in Arabidopsis using the fluorescent dye monodansylcadaverine and a GFP-AtATG8e fusion protein. *Plant J.* 42, 598–608. doi: 10.1111/j.1365-313X.2005.02396.x
- Diaz, C., Lemaitre, T., Christ, A., Azzopardi, M., Kato, Y., Sato, F., et al. (2008). Nitrogen recycling and remobilization are differentially controlled by leaf senescence and development stage in Arabidopsis under low nitrogen nutrition. *Plant Physiol.* 147, 1437–1449. doi: 10.1104/pp.108.119040
- Fujioka, Y., Noda, N. N., Fujii, K., Yoshimoto, K., Ohsumi, Y., and Inagaki, F. (2008). In vitro reconstitution of plant Atg8 and Atg12 conjugation systems essential for autophagy. *J. Biol. Chem.* 283, 1921–1928. doi: 10.1074/jbc.M706214200
- Gong, Q., Li, P., Ma, S., Indu Rupassara, S., and Bohnert, H. J. (2005). Salinity stress adaptation competence in the extremophile *Thellungiella halophila* in comparison with its relative *Arabidopsis thaliana*. *Plant J.* 44, 826–839. doi: 10.1111/j.1365-313X.2005.02587.x
- Graf, A., Schlereth, A., Stitt, M., and Smith, A. M. (2010). Circadian control of carbohydrate availability for growth in Arabidopsis plants at night. *Proc. Natl. Acad. Sci. U.S.A.* 107, 9458–9463. doi: 10.1073/pnas.0914299107
- Guiboulein, A., Avila-Ospina, L., Yoshimoto, K., Soulay, F., Azzopardi, M., Marmande, A., et al. (2013). Physiological and metabolic consequences of autophagy deficiency for the management of nitrogen and protein resources in *Arabidopsis* leaves depending on nitrate availability. *New Phytol.* 199, 683–694. doi: 10.1111/nph.12307
- Guiboulein, A., Yoshimoto, K., Soulay, F., Bataille, M. P., Avice, J. C., and Masclaux-Daubresse, C. (2012). Autophagy machinery controls nitrogen remobilization at the whole-plant level under both limiting and ample nitrate conditions in Arabidopsis. *New Phytol.* 194, 732–740. doi: 10.1111/j.1469-8137.2012.04084.x
- Hanaoka, H., Noda, T., Shirano, Y., Kato, T., Hayashi, H., Shibata, D., et al. (2002). Leaf senescence and starvation-induced chlorosis are accelerated by the disruption of an *Arabidopsis* autophagy gene. *Plant Physiol.* 129, 1181–1193. doi: 10.1104/pp.011024
- Honig, A., Avin-Wittenberg, T., Ufaz, S., and Galili, G. (2012). A new type of compartment, defined by plant-specific Atg8-interacting proteins, is induced upon exposure of *Arabidopsis* plants to carbon starvation. *Plant Cell* 24, 288–303. doi: 10.1105/tpc.111.093112
- Hortensteiner, S. (2006). Chlorophyll degradation during senescence. *Annu. Rev. Plant Biol.* 57, 55–77. doi: 10.1146/annurev.arplant.57.032905.105212
- Hortensteiner, S., and Feller, U. (2002). Nitrogen metabolism and remobilization during senescence. *J. Exp. Bot.* 53, 927–937. doi: 10.1093/jexbot/53.370.927
- Ishida, H., Izumi, M., Wada, S., and Makino, A. (2014). Roles of autophagy in chloroplast recycling. *Biochim. Biophys. Acta* 1837, 512–521. doi: 10.1016/j.bbabiobio.2013.11.009
- Ishida, H., Yoshimoto, K., Izumi, M., Reisen, D., Yano, Y., Makino, A., et al. (2008). Mobilization of rubisco and stroma-localized fluorescent proteins of chloroplasts to the vacuole by an ATG gene-dependent autophagic process. *Plant Physiol.* 148, 142–155. doi: 10.1104/pp.108.122770
- Izumi, M., Hidema, J., Makino, A., and Ishida, H. (2013). Autophagy contributes to nighttime energy availability for growth in *Arabidopsis*. *Plant Physiol.* 161, 1682–1693. doi: 10.1104/pp.113.215632
- Izumi, M., Wada, S., Makino, A., and Ishida, H. (2010). The autophagic degradation of chloroplasts via rubisco-containing bodies is specifically linked to leaf carbon status but not nitrogen status in *Arabidopsis*. *Plant Physiol.* 154, 1196–1209. doi: 10.1104/pp.110.158519
- Kirisako, T., Baba, M., Ishihara, N., Miyazawa, K., Ohsumi, M., Yoshimori, T., et al. (1999). Formation process of autophagosome is traced with Apg8/Aut7p in yeast. *J. Cell Biol.* 147, 435–446. doi: 10.1083/jcb.147.2.435
- Lai, Z., Wang, F., Zheng, Z., Fan, B., and Chen, Z. (2011). A critical role of autophagy in plant resistance to necrotrophic fungal pathogens. *Plant J.* 66, 953–968. doi: 10.1111/j.1365-313X.2011.04553.x
- Lenz, H. D., Haller, E., Melzer, E., Kober, K., Wurster, K., Stahl, M., et al. (2011). Autophagy differentially controls plant basal immunity to biotrophic and necrotrophic pathogens. *Plant J.* 66, 818–830. doi: 10.1111/j.1365-313X.2011.04546.x
- Li, F., Chung, T., and Vierstra, R. D. (2014). AUTOPHAGY-RELATED11 plays a critical role in general autophagy- and senescence-induced mitophagy in *Arabidopsis*. *Plant Cell* 26, 788–807. doi: 10.1105/tpc.113.120014
- Li, F., and Vierstra, R. D. (2012). Autophagy: a multifaceted intracellular system for bulk and selective recycling. *Trends Plant Sci.* 17, 526–537. doi: 10.1016/j.tplants.2012.05.006
- Lim, P. O., Kim, H. J., and Nam, H. G. (2007). Leaf senescence. *Annu. Rev. Plant Biol.* 58, 115–136. doi: 10.1146/annurev.applant.57.032905.105316
- Liu, Y., and Bassham, D. C. (2012). Autophagy: pathways for self-eating in plant cells. *Annu. Rev. Plant Biol.* 63, 215–237. doi: 10.1146/annurev.applant-042811-105441
- Liu, Y., Schiff, M., Czymbek, K., Talloczy, Z., Levine, B., and Dinesh-Kumar, S. P. (2005). Autophagy regulates programmed cell death during the plant innate immune response. *Cell* 121, 567–577. doi: 10.1016/j.cell.2005.03.007
- Liu, Y., Xiong, Y., and Bassham, D. C. (2009). Autophagy is required for tolerance of drought and salt stress in plants. *Autophagy* 5, 954–963. doi: 10.4161/auto.5.7.9290
- Ma, S., Gong, Q., and Bohnert, H. J. (2006). Dissecting salt stress pathways. *J. Exp. Bot.* 57, 1097–1107. doi: 10.1093/jxb/erj098
- Ma, S., Gong, Q., and Bohnert, H. J. (2007). An *Arabidopsis* gene network based on the graphical Gaussian model. *Genome Res.* 17, 1614–1625. doi: 10.1101/gr.691120
- Makino, A., and Osmond, B. (1991). Effects of nitrogen nutrition on nitrogen partitioning between chloroplasts and mitochondria in pea and wheat. *Plant Physiol.* 96, 355–362. doi: 10.1104/pp.96.2.355
- Martinez, D. E., Costa, M. L., Gomez, F. M., Otegui, M. S., and Guiamet, J. J. (2008a). “Senescence-associated vacuoles” are involved in the degradation of chloroplast proteins in tobacco leaves. *Plant J.* 56, 196–206. doi: 10.1111/j.1365-313X.2008.03585.x
- Martinez, D. E., Costa, M. L., and Guiamet, J. J. (2008b). Senescence-associated degradation of chloroplast proteins inside and outside the organelle. *Plant Biol.* 10(Suppl. 1), 15–22. doi: 10.1111/j.1438-8677.2008.00089.x
- Masclaux-Daubresse, C., Clement, G., Anne, P., Routaboul, J. M., Guiboulein, A., Soulay, F., et al. (2014). Stitching together the multiple dimensions of autophagy using metabolomics and transcriptomics reveals impacts on metabolism, development, and plant responses to the environment in *Arabidopsis*. *Plant cell* doi: 10.1105/tpc.114.124677 [Epub ahead of print].
- Masclaux-Daubresse, C., Daniel-Vedele, F., Dechorganat, J., Chardon, F., Gaufichon, L., and Suzuki, A. (2010). Nitrogen uptake, assimilation and remobilization in plants: challenges for sustainable and productive agriculture. *Ann. Bot.* 105, 1141–1157. doi: 10.1093/aob/mcq028
- Mizushima, N., Yoshimori, T., and Ohsumi, Y. (2011). The role of Atg proteins in autophagosome formation. *Annu. Rev. Cell Dev. Biol.* 27, 107–132. doi: 10.1146/annurev-cellbio-092910-154005
- Ono, Y., Wada, S., Izumi, M., Makino, A., and Ishida, H. (2013). Evidence for contribution of autophagy to rubisco degradation during leaf senescence in *Arabidopsis thaliana*. *Plant Cell Environ.* 36, 1147–1159. doi: 10.1111/pce.12049
- Onodera, J., and Ohsumi, Y. (2005). Autophagy is required for maintenance of amino acid levels and protein synthesis under nitrogen starvation. *J. Biol. Chem.* 280, 31582–31586. doi: 10.1074/jbc.M506736200
- Otegui, M. S., Noh, Y. S., Martinez, D. E., Vila Petroff, M. G., Staehelin, L. A., Amasino, R. M., et al. (2005). Senescence-associated vacuoles with intense proteolytic activity develop in leaves of *Arabidopsis* and soybean. *Plant J.* 41, 831–844. doi: 10.1111/j.1365-313X.2005.02346.x
- Phillips, A. R., Suttangkakul, A., and Vierstra, R. D. (2008). The ATG12-conjugating enzyme ATG10 Is essential for autophagic vesicle formation in *Arabidopsis thaliana*. *Genetics* 178, 1339–1353. doi: 10.1534/genetics.107.086199
- Rose, T. L., Bonneau, L., Der, C., Marty-Mazars, D., and Marty, F. (2006). Starvation-induced expression of autophagy-related genes in *Arabidopsis*. *Biol. Cell* 98, 53–67. doi: 10.1042/BC20040516

- Smith, A. M., and Stitt, M. (2007). Coordination of carbon supply and plant growth. *Plant Cell Environ.* 30, 1126–1149. doi: 10.1111/j.1365-3040.2007.01708.x
- Stitt, M., and Zeeman, S. C. (2012). Starch turnover: pathways, regulation and role in growth. *Curr. Opin. Plant Biol.* 15, 282–292. doi: 10.1016/j.pbi.2012.03.016
- Sulpice, R., Pyl, E. T., Ishihara, H., Trenkamp, S., Steinath, M., Witucka-Wall, H., et al. (2009). Starch as a major integrator in the regulation of plant growth. *Proc. Natl. Acad. Sci. U.S.A.* 106, 10348–10353. doi: 10.1073/pnas.0903478106
- Suttangkakul, A., Li, F., Chung, T., and Vierstra, R. D. (2011). The ATG1/ATG13 protein kinase complex is both a regulator and a target of autophagic recycling in *Arabidopsis*. *Plant Cell* 23, 3761–3779. doi: 10.1105/tpc.111.090993
- Thompson, A. R., Doelling, J. H., Suttangkakul, A., and Vierstra, R. D. (2005). Autophagic nutrient recycling in *Arabidopsis* directed by the ATG8 and ATG12 conjugation pathways. *Plant Physiol.* 138, 2097–2110. doi: 10.1104/pp.105.060673
- Thompson, A. R., and Vierstra, R. D. (2005). Autophagic recycling: lessons from yeast help define the process in plants. *Curr. Opin. Plant Biol.* 8, 165–173. doi: 10.1016/j.pbi.2005.01.013
- Wada, S., Ishida, H., Izumi, M., Yoshimoto, K., Ohsumi, Y., Mae, T., et al. (2009). Autophagy plays a role in chloroplast degradation during senescence in individually darkened leaves. *Plant Physiol.* 149, 885–893. doi: 10.1104/pp.108.130013
- Wang, Y., Nishimura, M. T., Zhao, T., and Tang, D. (2011). ATG2, an autophagy-related protein, negatively affects powdery mildew resistance and mildew-induced cell death in *Arabidopsis*. *Plant J.* 68, 74–87. doi: 10.1111/j.1365-313X.2011.04669.x
- Wang, Y., Yu, B., Zhao, J., Guo, J., Li, Y., Han, S., et al. (2013). Autophagy contributes to leaf starch degradation. *Plant Cell* 25, 1383–1399. doi: 10.1105/tpc.112.108993
- Xia, K., Liu, T., Ouyang, J., Wang, R., Fan, T., and Zhang, M. (2011). Genome-wide identification, classification, and expression analysis of autophagy-associated gene homologues in rice (*Oryza sativa* L.). *DNA Res.* 18, 363–377. doi: 10.1093/dnarecs/dsr024
- Xia, T., Xiao, D., Liu, D., Chai, W., Gong, Q., and Wang, N. N. (2012). Heterologous expression of ATG8c from soybean confers tolerance to nitrogen deficiency and increases yield in *Arabidopsis*. *PLoS ONE* 7:e37217. doi: 10.1371/journal.pone.0037217
- Xie, Z., and Klionsky, D. J. (2007). Autophagosome formation: core machinery and adaptations. *Nat. Cell Biol.* 9, 1102–1109. doi: 10.1038/ncb1007-1102
- Xiong, Y., Contento, A. L., and Bassham, D. C. (2005). AtATG18a is required for the formation of autophagosomes during nutrient stress and senescence in *Arabidopsis thaliana*. *Plant J.* 42, 535–546. doi: 10.1111/j.1365-313X.2005.02397.x
- Xu, G., Fan, X., and Miller, A. J. (2012). Plant nitrogen assimilation and use efficiency. *Annu. Rev. Plant Biol.* 63, 153–182. doi: 10.1146/annurev-arplant-042811-105532
- Yang, Z., and Klionsky, D. J. (2010). Eaten alive: a history of macroautophagy. *Nat. Cell Biol.* 12, 814–822. doi: 10.1038/ncb0910-814
- Yoshimoto, K., Hanaoka, H., Sato, S., Kato, T., Tabata, S., Noda, T., et al. (2004). Processing of ATG8s, ubiquitin-like proteins, and their deconjugation by ATG4s are essential for plant autophagy. *Plant Cell* 16, 2967–2983. doi: 10.1105/tpc.104.025395
- Yoshimoto, K., Jikumaru, Y., Kamiya, Y., Kusano, M., Consonni, C., Panstruga, R., et al. (2009). Autophagy negatively regulates cell death by controlling NPR1-dependent salicylic acid signaling during senescence and the innate immune response in *Arabidopsis*. *Plant Cell* 21, 2914–2927. doi: 10.1105/tpc.109.068635
- Zhou, J., Wang, J., Cheng, Y., Chi, Y. J., Fan, B., Yu, J. Q., et al. (2013). NBR1-mediated selective autophagy targets insoluble ubiquitinated protein aggregates in plant stress responses. *PLoS Genet.* 9:e1003196. doi: 10.1371/journal.pgen.1003196

**Conflict of Interest Statement:** The authors declare that the research was conducted in the absence of any commercial or financial relationships that could be construed as a potential conflict of interest.

Received: 24 April 2014; accepted: 09 June 2014; published online: 24 June 2014.

Citation: Ren C, Liu J and Gong Q (2014) Functions of autophagy in plant carbon and nitrogen metabolism. *Front. Plant Sci.* 5:301. doi: 10.3389/fpls.2014.00301

This article was submitted to Plant Cell Biology, a section of the journal *Frontiers in Plant Science*.

Copyright © 2014 Ren, Liu and Gong. This is an open-access article distributed under the terms of the Creative Commons Attribution License (CC BY). The use, distribution or reproduction in other forums is permitted, provided the original author(s) or licensor are credited and that the original publication in this journal is cited, in accordance with accepted academic practice. No use, distribution or reproduction is permitted which does not comply with these terms.